ENGINEERING RESEARCH INSTITUTE
UNIVERSITY OF MICHIGAN
ANN ARBOR

SUBJECT REPORT

LOCAL RATES OF MASS TRANSFER IN A PACKED BED OF SPHERES, WITH ORIFICE ENTRY OF AIR

(John C.)

J. C. BRIER
S. W. CHURCHILL
F. N. DAWSON
C. M. THATCHER

Project M985

DEPARTMENT OF THE NAVY, BUREAU OF ORDNANCE
CONTRACT NOrd 12109

September, 1954

ensn

UMR0556

PREFACE

It was the purpose of this investigation to make experimental measurements of local rates of mass transfer in a packed bed, and to determine the effects on these rates of position within the bed, gas flow rate, pellet diameter, and velocity perturbations at the entrance to the bed. In the absence of precedent work of this kind, considerable work of a preliminary nature was required before any data could be taken, and the complete program involved the following stages:

1. Design and construction of equipment to supply to a cylindrical bed of random-packed spheres, a gas stream of controlled temperature, pressure, and composition.

2. Development of a technique for the experimental determination of the variation of mass-transfer rates with position in the bed, for any given conditions of flow rate, pellet diameter, and entrance geometry.

3. Experimental determination of the variation of mass-transfer rates with position as a function of the other variables.

4. Correlation and interpretation of the experimental results.

More than 3000 experimental runs were needed to provide the data for meaningful correlations, and the task would have been almost impossible without the assistance of the following people: J. S. Berray, E. D. Blum, L. D. Boddy, A. H. Bonnell, D. L. Engibous, P. G. Friedman, A. D. Gowans, D. J. Groff, H. D. Hall, R. C. Hannenberg, W. P. Hegarty, L. Kaufman, R. W. Kruggel, C. F. Lombard, D. A. Maron, A. E. Molini, A. S. Nicholas, D. A. Olson, E. T. Sherman, J. M. VandenBoegaerde, C. E. Wise, and I. Zwiebel.

ABSTRACT

Local rates of mass transfer in a packed bed were determined by measuring the loss in weight of individual spherical pellets of p-dibromobenzene, carefully positioned in an otherwise inert bed of spheres through which a stream of air was passed.

The tests were made in a cylindrical bed 4 inches in diameter, measurements being made to within 1/32 inch from the wall, with packing diameters of 1/8, 1/4, and 1/2 inch, and covered a Reynolds number range of $150 < D_pG/\mu < 7000$. Measurememts were also made with the air entering the bed though 1- and 2-inch orifices, to determine the effect of the resulting velocity perturbations on mass-transfer rates.

The experimental equipment consisted of an air-supply system capable of supplying air at a temperature of approximately 80°F and at rates ranging from 10 to 120 standard cubic feet per minute, and a packed test section which could be quickly detached from the air-supply line to facilitate the loading and recovery of the active pellets.

Measured weight losses were first corrected for minor fluctuations in air temperature and for the loss attributable to exposure to the atmosphere during the loading and recovery operations, and were then converted to mass-transfer rates by introducing the surface area of the pellets and the running time over which the weight loss was incurred.

Within the scope of the investigation, it was found that local rates of mass transfer in a packed bed could be correlated by the general equation

$$k'/G' \times 10^6 = B\left(\frac{D_pG}{\mu}\right)^m \quad , \qquad (1)$$

where k' is the transfer rate in pound-mols per square foot of surface per hour, G is the superficial mass velocity (prime denotes molal units), D_p is the packing diameter, μ the viscosity of air, and B and m generally depend on position within the bed and orifice diameter, but are independent of air flow rate and packing diameter.

When no orifice was used, entrance effects were observed only in the first 1/2 inch of bed depth, where the transfer rates were slightly higher than elsewhere. The rates were found to be independent of radius at all depths, however.

With an orifice across the entrance to the bed, the exponent in Equation (1) is independent of orifice diameter and position in the bed, and is equal to -0.35. B, on the other hand, varies with both of these parameters. Transfer rates as much as 300 percent higher than elsewhere were observed in the vicinity of the orifice, but the perturbations created by the orifice are completely dissipated at a bed depth of approximately 2 inches.

The nature of the data does not permit direct comparison with the results of previous investigations of overall mass-transfer rates in packed beds. By making certain assumptions, however, a limited comparison is possible and indicates that the present correlation may be high by a factor of approximately two. Despite this lack of agreement, the relative effects of pellet diameter, air flow rate, position in the bed, and orifice diameter on local rates of mass transfer are believed to be correctly delineated.

TABLE OF CONTENTS

TABLE OF CONTENTS (Continued)

LIST OF TABLES

LIST OF FIGURES

LIST OF APPENDICES

INTRODUCTION

During the past decade, considerable progress has been made in the development of quantitative correlations for the prediction of pressure drop and heat- and mass-transfer rates in packed beds. The interest in this field is a natural outgrowth of the increased use of packed beds in engineering operations and processes of many types. Absorption, fixed-bed catalytic reaction, heating and cooling, leaching, and fluid mixing, for example, are fields in which packed beds are already being used to advantage, and new applications will naturally result as a broader understanding of the pertinent principles is attained.

The transfer of mass and heat in packed beds is of major interest in most of these applications, and pertinent data have been accumulated and correlated by many research investigators. In general, the studies in this field have been concerned with overall properties, i.e., the bed has been considered as an integral unit of equipment and transfer rates have been studied from the overall viewpoint.

Many of the problems involved in the commercial application of packed beds have been overcome through the use of such overall rate data. There are, however, other problems which can never be resolved without supplementary information regarding local or point conditions within such beds. The overall approach cannot, for example, predict the location of hot-spots in a fixed-bed catalytic reactor.

Thus, there is a definite need for data on local heat- and mass-transfer rates in packed beds, and the present work was undertaken with the objective of making direct measurement of such rates.

This is by no means the first attempt to obtain information regarding local conditions in packed beds. Other things being equal, the local transfer rate should be a function only of the local velocity, and for many years a flat velocity profile, i.e., a uniform mass flow rate across the bed, was generally assumed as being both reasonable and also affording mathematical relationships which could be easily handled. Recently, however, several investigators have attempted to determine experimentally actual velocity profiles in packed beds, and to use their results to predict transfer-rate profiles. Unfortunately, most of this work has been of a qualitative nature, and even at best it provides only an indirect insight into the phenomena of mass and heat transfer. The present work should, therefore, be a worthwhile contribution to available knowledge of the behavior of packed beds.

In this work, local mass-transfer rates in packed beds were determined by measuring the loss in weight of individual spherical pellets of p-dibromobenzene, carefully positioned in an otherwise inert bed of spheres through which a stream of air was passed. The tests were made in a cylindrical bed 4 inches in diameter with spheres having diameters of 1/8, 1/4, and 1/2 inch, and covered a reasonable range of Reynolds number (D_pG/μ). Measurements were made at enough positions

in the bed to permit the mapping of local mass-transfer rates at all points.

Particular attention was given to entrance effects in these studies, and the results are therefore applicable even to very thin beds made up of only a few layers of pellets. In addition to determining mass-transfer rates in the first few layers of pellets in a bed whose surface was completely exposed to the entering air stream, measurements were also made with the air entering the bed through an orifice, to determine the effect of the resulting local velocity perturbations on mass-transfer rates. Orifice diameters of 1 and 2 inches were used in this phase of the work.

The experimental data and correlations are presented in this report, and the results are interpreted in terms of present-day mass-transfer theory. The equipment and experimental procedure are described in detail, as is the method of processing and correlating the data. Conclusions relative to the effect of position in the bed, pellet diameter, air flow rate, and velocity perturbations at the entrance to the bed on local mass-transfer rates in packed beds are drawn and discussed. Insofar as the analogy between heat and mass transfer is valid, these conclusions should be equally applicable to heat-transfer work.

REVIEW OF PREVIOUS WORK

Although no previous work directly paralleled the present investigation has been reported in the literature, many studies have been made which are pertinent to some extent. These previous studies can be roughly divided into two categories: those concerned with overall rather than local mass-transfer rates for packed beds, and those concerned with point conditions but which did not include a quantitative investigation of mass-transfer rates as such.

Before discussing any of the work done in the first of these categories, it is advisable to review briefly the development of the basic correlations for mass-transfer data, derived for the most part from studies of mass transfer from isolated surfaces or in open tubes.

The fundamental rate equation for molecular diffusion was stated as early as 1855 by Fick (22), and may be expressed in the form

$$\frac{N_v}{A} = - D \left(\frac{\partial c_v}{\partial x}\right) \quad , \qquad (1)$$

where D is the coefficient of diffusion. For molecular diffusion of one gas through another, the equation can be expressed in a modified form originally derived by Maxwell (45) and Stefan (64) and later by Colburn and Hougen (16):

$$\frac{N_v}{A} = - \frac{D_G P}{RTp_g} \left(\frac{\partial p_v}{\partial x} \right) \qquad (2)$$

Although this equation is still used to describe molecular diffusion, it has become customary in modern work to make use of a dimensionless mass-transfer factor, j, to characterize total diffusion, which includes eddy or turbulent transfer as well as molecular processes. The development of this concept was an outgrowth of the analogy between heat transfer and fluid friction originally suggested by Reynolds (57) and later improved by Prandtl (53) and Taylor (66). Colburn (15) extended the development of the analogy and proposed the use of a transfer factor, j, to parallel the use of the friction factor, f, in pressure-drop calculations. The transfer factor was related to the heat-transfer coefficient by the equation

$$j = \frac{h}{C_p G} \left(\frac{C_p \mu}{k} \right)^{2/3} , \qquad (3)$$

and for turbulent flow conditions it was proposed that j be equal to f/2, making it a function only of the Reynolds number, DG/μ .

Previously, Colburn had also extended the analogy between heat transfer and fluid friction to include mass transfer (14), and with the development of the j-factor for heat transfer, he then sought to obtain a similar factor for use in mass-transfer work. The relationship finally proposed by Chilton and Colburn (10) was

$$j = \frac{k_g p_{gf}}{G/M_m} \left(\frac{\mu}{\rho D_G}\right)^{2/3}, \qquad (4)$$

where again, for turbulent flow conditions, j was set equal to f/2, making the factor for mass transfer identically equal to that for heat transfer.

Colburn selected the exponent 2/3 for the Prandtl number in Equation 3 as being an average value of exponents recommended in the correlations of several earlier investigators (17, 31, 50, 62). This exponent was merely carried over to the Schmidt number in the development of the j-factor for mass transfer, without any supporting experimental evidence. Since then, however, the use of the 2/3 exponent has been confirmed by Linton and Sherwood (41) from tests covering a wide range of Schmidt number. Gaffney and Drew more recently correlated similar data with an exponent of 0.58 (25), while Bedingfield and Drew used an exponent of 0.56 to correlate their data for single cylinders (5). However, the exponent of 2/3 has been generally accepted by most investigators.

It should be re-emphasized that all the original data supporting the use of the j-factor in the correlation of mass-transfer data were obtained from experiments with single, isolated surfaces or in open tubes, and it remained to be shown that the proposed method of correlation could also be applied to mass transfer in packed beds. As a matter of fact, Colburn's original development of the j-factor was also based entirely on gas-phase data, but McCune and Wilhelm (48) and

Hobson and Thodos (32) have recently shown the factor to be equally applicable to transfer in liquids.

An alternate method of correlation specifically applicable to packed-bed data was proposed by Chilton and Colburn in 1935 (11), and has found some acceptance. It was their suggestion that the difficulty of separation in a packed distillation or absorption column be expressed as a number of "transfer units", equivalent to the number of theoretical plates used in plate-column calculations. Column efficiency is correspondingly expressed as the "height of a transfer unit", paralleling the "height equivalent to a theoretical plate" in plate columns. The height of a transfer unit is, of course, equal to the total column height divided by the number of transfer units, and was defined by the equation

$$H.T.U. = \frac{H}{n} = \frac{G}{k_g a M_m p_{gf}} = \frac{1}{ja}\left(\frac{\mu}{\rho D_G}\right)^{2/3} \qquad (5)$$

From the indicated relationship between the height of a transfer unit and the j-factor, it can be seen that for any given system H.T.U. will also be a function of Reynolds number only.

The study of transfer processes as specifically encountered in packed beds undoubtedly received its greatest impetus from the work of Gamson, Thodos, and Hougen in 1943 (27). In their experiments, spherical and cylindrical solid pellets of various materials, densities, and sizes were soaked in distilled water, drained and rolled in cheesecloth

to remove loose surface water, placed on a tray to form a bed of from 1 to 2-1/2 inches in thickness, and weighed. Air was then blown through the bed while the inlet and outlet temperature and humidity were recorded, and the tray was reweighed at the end of the run. Since the running time covered only a fraction of the constant-rate drying period, the mass-transfer rate could be calculated from the total weight loss and the running time, and could be verified by the humidity and temperature data. Further, since the process was adiabatic and since the total resistance to mass and heat transfer was in the gas film alone, the gas-film transfer coefficients for both heat and mass transfer could be evaluated.

When the j-factor for mass transfer, j_d, was plotted against the Reynolds number, D_pG/μ, on log-log paper, most of the data were correlated within ± 4 per cent by a straight line,

$$j_d = 0.989 \left(\frac{D_pG}{\mu}\right)^{-0.41} \qquad (6)$$

for Reynolds numbers above 350. Below this value, the data deviated progressively from the correlation, and in view of the analogy between transfer phenomena and fluid friction, the deviation was attributed to the transition from turbulent to laminar flow. Experimental difficulties prevented the accumulation of data at Reynolds numbers below 100, but it was proposed that in the laminar flow region j_d be correlated by the equation

$$j_d = 16.8 \left(\frac{D_p G}{\mu}\right)^{-1} , \qquad (7)$$

the exponent on the Reynolds number being taken from the analogy with fluid friction in the laminar region as proposed by Colburn (14). Data taken at Reynolds numbers below 350 bracketed a smooth curve connecting the line of Equation 6 with that of Equation 7, which it joined at $D_p G/\mu = 40$.

A similar correlation was obtained for the j-factor for heat transfer, the corresponding equations being

$$j_h = 1.064 \left(\frac{D_p G}{\mu}\right)^{-0.41} \qquad (8)$$

for Reynolds numbers above 350, and

$$j_h = 18.1 \left(\frac{D_p G}{\mu}\right)^{-1} \qquad (9)$$

for Reynolds numbers below 40. It was noted that j_h and j_d were not quite identical as had been hypothesized by Chilton and Colburn (10), but that they did bear a constant ratio to each other: $j_h/j_d = 1.076$. However, there is some question as to whether the measured wet-bulb temperature is truly equal to the temperature at the pellet surface, as was assumed in arriving at this ratio, and its validity is therefore somewhat in doubt.

It will be noted that the pellet diameter was used as the characteristic length in the Reynolds number in these correlations, and this practice permitted the use of the

same correlation for all pellet sizes. Further, by defining an equivalent diameter for the cylindrical pellets equal to the diameter of a sphere having the same surface area, the data for cylindrical shapes were also brought into agreement with the correlation.

Using the same technique as Gamson et al., Wilke and Hougen (67) later obtained additional data at lower Reynolds numbers and recommended the equation

$$j_d = 1.82\left(\frac{D_p G}{\mu}\right)^{-0.51} \qquad (10)$$

for Reynolds numbers below 350. The critical Reynolds number of 350 was retained from the earlier work to facilitate comparison of the correlations, but it was noted that a plot of j_d versus $D_p G/\mu$ on log-log paper actually yielded a single continuous curve over the range $50 < D_p G/\mu < 5{,}000$.

Ergun, in an excellent resumé and critique of most of the significant studies of mass-transfer rates in packed beds (20), notes that because the technique used by Gamson, Wilke, et al., involved the removal of capillary moisture, "it is expected that the interfacial surface area between the gas stream and the liquid was different from the geometric surface area of the solids on which the calculation of the transfer coefficients were based." He also calls attention to the relatively shallow beds used in the experiments, and suggests that a rather undefinable void volume and possible entrance and exit effects may also detract from the validity

of the data. The latter criticism is to be discussed further in the light of the findings of the present work.

Studies along the same general lines as those conducted by Gamson et al. were carried out at about the same time but independently by Hurt (36), who used a similar technique in investigating the humidification of air over water-wetted pellets of silica gel. Other experiments were concerned with the adsorption of water from moist air by particles of silica gel and by particles coated with phosphorous pentoxide, and with the evaporation of naphthalene pellets and flakes into air and hydrogen. In contrast to the findings of Gamson et al., Hurt was unable to correlate data from particles of different sizes with a single curve, although Ergun (20) noted later that a log-log plot of $H.T.U./D_p$ versus D_pG/μ would bring the data for different sizes into a single straight line. At the same time, however, Ergun calls attention to significant discrepancies in the values used by Hurt for the Schmidt number and for the vapor pressure of naphthalene, and states that a different set of vapor pressure data, for example, would materially alter Hurt's results.

In an extension of the work by Gamson et al., and using the same method, Taecker and Hougen studied mass-transfer rates from Raschig rings, partition rings, and Berl saddles (65). With an effective particle diameter equal to $\sqrt{A_p/\pi}$, where A_p is the surface area of a particle, the data were correlated by the equations

$$j_d = 1.251 \left(\frac{D_p G}{\mu}\right)^{-0.41} \qquad (11)$$

for $D_p G/\mu > 620$, and

$$j_d = 2.24 \left(\frac{D_p G}{\mu}\right)^{-0.51} \qquad (12)$$

for $D_p G/\mu < 620$. A significant separation between each of the three sets of data for rings, for saddles, and for cylinders and spheres suggests that the use of an effective particle diameter based on the surface area was not adequate to account for the variation in particle shape.

Mass transfer in solid-liquid systems was studied by McCune and Wilhelm (48) by dissolving 2-naphthol pellets in a water stream. Spherical pellets of three different diameters were used in a 4-inch-diameter bed. The data were correlated by the equations

$$j_d = 0.687 \left(\frac{D_p G}{\mu}\right)^{-0.327} \qquad (13)$$

for $D_p G/\mu > 120$, and

$$j_d = 1.625 \left(\frac{D_p G}{\mu}\right)^{-0.507} \qquad (14)$$

for $D_p G/\mu < 120$, and are in fair agreement with those of Gamson et al. Except for its use as the characteristic length in the Reynolds number, no effect of pellet diameter was observed in these studies.

Resnick and White (56) were primarily interested in mass transfer in fluidized beds, but also reported some data from fixed beds. Air, hydrogen, and carbon dioxide were blown through beds of naphthalene granules, over a Reynolds number range of from 0.8 to 30, and the data were correlated empirically by plotting $j_d/D_p^{1.5}$ versus D_pG/μ. Plotted in this manner, the data for all particle sizes were correlated by a single straight line, the equation for which was not reported but which appears to be

$$j_d/D_p^{1.5} = 0.19 \left(\frac{D_pG}{\mu}\right)^{-0.279} \qquad (15)$$

where D_p is in millimeters. When j_d was directly plotted versus D_pG/μ, a separate line was obtained for each particle size, as was the case with Hurt's data (36). However, the two sets of data were inconsistent in other respects, which may be attributable to the deficiencies in Hurt's data already noted or, as Ergun points out (20), to the fact that Resnick and White really did not obtain enough fixed-bed data to yield a correlation having any statistical significance.

Good agreement with the data of Gamson, Wilke, et al. (27, 67) has been reported by Hobson and Thodos (32), who passed water through a bed of cellite pellets soaked with a saturated solution of water in either isobutyl alcohol or methyl ethyl ketone and measured the effluent concentration. These new data and those of Gamson, Wilke, et al., were correlated by the equation

$$\log j_d = 0.7683 - 0.9175 \log \frac{D_p G}{\mu} + 0.0817 \left(\log \frac{D_p G}{\mu}\right)^2, \qquad (16)$$

in which particle diameter appears only in the Reynolds number. Transfer rates were calculated by plotting the variable effluent concentration versus time and extrapolating back to zero time, when the pellets were presumably completely wetted. In view of the fact that the extrapolation of curved lines could lead to significant errors, this procedure was later questioned by Gaffney and Drew (25), who also wondered about the initial presence of excess solution on the surface of the pellets.

These objections were eliminated in subsequent work by Hobson and Thodos (33), in which additional data pertaining to mass transfer across gas films at Reynolds numbers in the range 20-300 were obtained using a modified technique. The liquids studied were n-butanol, n-dodecane, n-octane, toluene, and water, while hydrogen, nitrogen, carbon dioxide, and air were used as gases. Both the new and old data, plus that of Gamson et al. (27) and of McCune and Wilhelm (48) were correlated by the equations

$$j_d = 1.30 \left(\frac{D_p G}{\mu}\right)^{-0.45} \qquad (17)$$

for $D_p G/\mu > 150$, and

$$j_d = 10 \left(\frac{D_p G}{\mu}\right)^{-1} \qquad (18)$$

for $D_p G/\mu < 50$.

A thorough investigation of transfer rates between organic solvents and pellets of solid organic acids was conducted by Gaffney and Drew (25). To cover a wide range of Schmidt number, three solvent-acid combinations were used: acetone and succinic acid, benzene and salicylic acid, and n-butanol and succinic acid. The data were correlated by plotting (H.T.U.)$a/Sc^{0.58}$ versus $D_pG/\mu\epsilon$, and are in excellent agreement with those of McCune and Wilhelm (48). The data were fitted by a curved line for which no equation was given, and subsequent data reported by Ishino and Otake (38) for pellets of benzoic acid dissolving in water could also be correlated by this line.

To facilitate comparison of the Gaffney-Drew data with those of others, Ergun (20) suggests that the former can be approximately represented by the equations

$$j_d' = 0.290 \left(\frac{D_pG}{\mu\epsilon}\right)^{-0.254} \qquad (19)$$

for $D_pG/\mu\epsilon > 200$, and

$$j_d' = 1.97 \left(\frac{D_pG}{\mu\epsilon}\right)^{-0.613} \qquad (20)$$

for $D_pG/\mu\epsilon < 200$, where

$$j_d' = \frac{S_c^{0.58}}{a(HTU)} = \frac{k_g M_m p_{gf}}{G} \left(\frac{\mu}{\rho D_G}\right)^{0.58}$$

Gaffney and Drew note that their correlation is significantly poorer if the usual exponent of 2/3 is used on the Schmidt number.

Shulman and DeGouff (63) blew air through beds of Raschig rings made of naphthalene and correlated their data with the equation

$$j_d = 1.07 \left(\frac{G\sqrt{A_p}}{\mu} \right)^{-0.41} \qquad (21)$$

for $G\sqrt{A_p}/\mu > 400$. The data are in agreement with those of Taecker and Hougen (65), but by the same token are not comparable with data for cylindrical and spherical shapes.

Water was passed through fixed and fluidized beds of benzoic acid pellets by Evans and Gerald (21), who found that the line

$$j_d = 1.48 \left(\frac{D_p G}{\mu} \right)^{-0.52} \qquad (22)$$

fit their data for fixed beds, all taken at $D_p G/\mu < 70$.

In addition to the investigators who collected and correlated mass-transfer data for packed beds, there are several authors who have sought improved correlations by reworking the data of others. Much of this work has been aimed at developing correlations applicable to both packed beds and open tubes on the one hand and to both fixed and fluidized beds on the other. A brief review of such correlations, insofar as they apply to fixed beds, is pertinent to the present work and is given in the paragraphs which follow.

A theoretical study of the relationship between mass transfer in open tubes and that in packed beds was made by Pratt (54), who recommended the introduction of the fractional

void space, ϵ , into the Reynolds number: $D_pG/\mu\epsilon$. Use of this modified Reynolds number does not appear to result in any significant improvement in the agreement among the data of Gamson et al. (27), Wilke and Hougen (67), Taecker and Hougen (65), and Hobson and Thodos (32). It will be noted, however, that Gaffney and Drew chose to use the same modified Reynolds number in correlating their data (25).

Kaufman and Thodos (39) reworked the data of Gamson et al. for cylinders (27) and that of Taecker and Hougen (65) for Raschig rings, partition rings, and Berl saddles, in an attempt to resolve these data to those for spheres. The resolution was accomplished by the empirical calculation of effective particle diameters for each of the various shapes and by introducing a "critical area factor", f_A, into the j-factor. The area factors for each of the shapes were also determined empirically.

Similar shape factors were also evolved by Gamson (26), who chose to introduce them into the denominator of the Reynolds number for theoretical reasons. The use of empirical effective particle diameters was avoided by using $6G/a\mu$, equal to $D_pG/\mu(1 - \epsilon)$ for spheres, in place of the usual Reynolds number. In a further modification, he was able to correlate some fluidized bed data with that for fixed beds by including the term $(1 - \epsilon)^{-0.2}$ in the j-factor, and his final correlations then became

$$j_d = 1.46 \left(\frac{6G}{a\phi\mu}\right)^{-0.41} (1 - \epsilon)^{0.2} \qquad (23)$$

for $6G/a\phi\mu > 100$, and

$$j_d = 17 \left(\frac{6G}{a\varphi\mu}\right)^{-1} (1 - \epsilon)^{0.2} \qquad (24)$$

for $6G/a\varphi\mu < 10$, where φ is the shape factor given empirically for various shapes, and was found to differ slightly from the corresponding factors recommended by Kaufman and Thodos (39).

In his comprehensive analysis of mass-transfer phenomena in packed beds, Ergun (20) suggests that the concept of hydraulic radius requires that a modified Reynolds number equal to $D_pG/\mu(1 - \epsilon)$ be used if the analogy between mass transfer and fluid friction is to be preserved, and this modification is in agreement with that proposed by Gamson (26). A new mass-transfer factor, J, is also proposed, and is equal to the old factor, j, times $6\epsilon(Sc)^{1/3}$. On the basis of his earlier analysis of pressure drop data (19) and the presumed analogy between mass transfer and fluid friction, Ergun proposes the correlation

$$J = 150\,(Re')^{-1} + 1.75 \quad , \qquad (25)$$

where $Re' = D_pG/\mu(1 - \epsilon)$.

The data of McCune and Wilhelm (48), Hobson and Thodos (32), and Gaffney and Drew (25), all for liquid streams, are shown to be fairly well correlated by this equation, but the attempt to apply it to gas-phase data was not successful. As has been noted previously, Ergun calls attention to deficiencies and uncertainties in these latter data, but also

states that the Chilton-Colburn j-factor and hence the J-factor used in Equation 25 are strictly applicable only to systems in which there is no mixing along the length of the tube, a questionable assumption in the case of gas flow. Indeed, Ergun's analysis of Hurt's data (36) indicates complete longitudinal mixing in his experiments, and it is presumed that similar conditions existed to an unknown degree in the other gaseous systems.

Two recent investigators have found it convenient to use the modified Reynolds number as proposed by Gamson and Ergun, perhaps because their primary concern was with fluidized rather than fixed beds. In any event, the data of Hsu (34), obtained by passing carbon tetrachloride through a bed of activated charcoal, were found to be in satisfaction with Gamson's correlation, while Chu et al. (12), recommended the use of the equations

$$j_d = 1.77\ (Re')^{-0.44} \tag{26}$$

for $30 > Re' > 5000$, and

$$j_d = 5.7\ (Re')^{-0.78} \tag{27}$$

for $1 > Re' > 30$, where $Re' = D_p G/\mu\ (1 - \epsilon)$, to correlate their data obtained by passing air through a bed of inert pellets coated with naphthalene. The correlation is shown to fit the data of Gamson et al. (27), Wilke and Hougen (67), Hobson and Thodos (32), McCune and Wilhelm (48), and Gaffney

and Drew (25), with the inclusion of suitable area factors in the modified Reynolds number for the data on non-spherical particles.

In an analysis of the problem of mass transfer in packed beds made from a somewhat different angle, Ranz (55) relates the transfer from spheres in a packed bed to the transfer from single spheres. Data for single spheres are plotted as $k_g D_p p_{gf}/D_G$ versus $(D_p G/\mu)(\mu/\rho D_G)^{2/3}$, and are displaced laterally from the packed bed data of Gamson et al. (27) by a constant factor of approximately 10, i.e., the transfer rate in a bed can be predicted from the correlation for single spheres by entering the plot at an abscissa approximately 10 times that calculated for the packed bed.

On the basis of the relationship advanced by Ranz, it is perhaps pertinent to mention some of the studies made of mass transfer for single particles, since at least the slope of the line correlating the data from such studies should be in agreement with slopes obtained in correlating packed bed data. Such is apparently the case: for the correlation of data on evaporation from a cylinder transverse to a fluid stream, Powell (52) used a slope of -0.5, Maisel and Sherwood (44) a slope of -0.43, and Bedingfield and Drew (5) a slope of -0.4.

As was noted at the outset of this review, all the foregoing studies have been concerned with overall mass-transfer rates in packed beds, as opposed to point conditions within the bed. It was also pointed out that other

studies were concerned with point conditions, but that they did not include a quantitative investigation of mass transfer as such. Previous work done in this latter category will be reviewed in the paragraphs which follow.

It will be noted that the major share of the studies of point conditions in packed beds were concerned with the velocity distribution. The pertinence of such investigations lies in the fact that mass-transfer rates have already been shown to be a function of velocity as embodied in the Reynolds number. Although superficial mass velocities, based on the cross-sectional area of the empty bed, are almost universally used in packed bed correlations, a fixed ratio between the superficial velocity and actual point velocities has been tacitly assumed in most work. Indeed, the use of a modified Reynolds number equal to $D_pG/\mu\epsilon$ in the correlation proposed by Gaffney and Drew (25) was occasioned by the belief that mass-transfer rates should more properly be functions of the interstitial velocity.

The earliest work of interest from the standpoint of point conditions within a packed bed was that of Mayo, Hunter, and Nash (46), who were primarily interested in determining the extent to which packing surfaces were wetted in a packed absorption column. The measurements were made by passing a red dye solution through a bed of paper rings, made of paper strips wrapped to give double thickness so that only one side of the strip was exposed. The fractional area of the rings which became colored was determined by

the rather unique method of cutting apart the dyed and undyed sections of each strip and weighing the separate piles of scraps. In conjunction with their other findings, Mayo et al. reported noting a greater degree of wetting in the layers of rings near the entrance to the bed, and also more wetting near the tube wall than at the center of the bed.

These indications of higher porosity at the wall were also present in photographs of packed beds made by Furnas (24) and Graton and Fraser (29), and suggested that higher velocities might also be encountered at the wall. That such is the actual case was confirmed by Saunders and Ford (58), who made measurements with a movable Pitot tube just beyond the outlet of a packed bed of spheres. Although their readings were found to be somewhat erratic owing to jets of air from the interstices, they reported a uniform mean velocity across the bed except in an annulus within about one sphere diameter from the wall, where it was about 50 per cent higher.

A more detailed study of the velocity distribution in packed beds has been made by Smith and co-workers (49, 61), who also reported higher velocities near the wall. In their experiments, circular hot-wire anemometers of various diameters were centered over the outlet end of a packed bed, and the variation of velocity with radius was thereby determined. The velocity was found to be lower both at the center of the bed and at the wall, reaching a maximum value at a point about 7/10 of the distance from the center to the wall, where velocities up to 100 percent greater than those at the

center were observed. In the later work (61), it was indicated that the maxima were actually located at a distance of approximately one pellet diameter from the pipe wall, regardless of pipe or pellet size.

Other conclusions reached on the basis of these experiments were: (1) for 1/2-inch spheres in a 4-inch pipe, velocity profiles were unchanged for bed depths of from 3 to 23 inches, but the profiles gradually approach that observed in an empty pipe as bed thicknesses are successively decreased below 3 inches; (2) the ratio of point velocities to the average velocity is independent of total flow rate; (3) the divergence from a flat velocity profile increases as packing size increases and as pipe size decreases; and (4) the larger the pipe, the more uniform the velocity.

Velocity profiles were also obtained in earlier work by Kinney (40), who made his measurements with a Pitot tube driven down into the charge in a blast furnace. In contrast to the findings of Smith et al., Kinney found the maximum velocity at the center in two of the four radial planes investigated, although wall velocities were slightly higher than those at the center in the two other planes. Because of the marked difference in bed size and packing, however, these results are hardly comparable to those of Smith. On the other hand, Kinney also made some preliminary tests in a bed 16 inches in diameter packed with 1- to 2-inch limestone particles, and found the velocity to increase with distance from the center of the bed, although no data were

taken near the wall. Also interesting in his conclusion that "the area available for flow of gas in a bed of broken solids is not the area as determined by voids but only a part thereof."

Arthur et al. (4) also reported higher gas flow along the wall of a packed bed, on the basis of findings from five different types of experiments: (a) the exit stream from a packed bed was separated into central and annular portions and the two flow rates were measured; (b) hydrogen sulfide was passed through a bed of coppered charcoal, and the bed was then divided into central and annular portions and the degree of adsorption in each section was determined; (c) sulfur dioxide was passed through a bed of silica gel colored with alkaline phenolphthalein and the location of the initial color change in the layer of granules at the bed exit was observed; (d) sulfur dioxide was passed through a bed of coppered charcoal, and the location of the first color change on strips of litmus paper placed across the tube immediately beyond the bed was observed; and (e) the rate of temperature rise at various radial positions was noted in a charcoal bed through which either sulfur dioxide or hydrogen sulfide was blown. It was concluded that the velocity distribution is very sensitive to the detailed pressure conditions both above and below the bed, but that there is always an excess flow rate along the wall of the bed, the maximum rate being observed in the region slightly removed from the wall.

The colorimetric methods of Arthur et al. were used earlier by Saunders and Wild (59) and by Hughes (35). Saunders and Wild passed a chlorine-air mixture through a glass-walled bed of marble chips impregnated with potassium iodide, and took photographs of the advancing front of sorption at intervals. Unfortunately, their work was concerned with flow distribution in blast furnaces, and in all cases the gas entered the bed through a slotted grate which protruded into the bed. Further, their observations of velocity distribution were confined to the region immediately adjacent to the grate, and no information regarding radial velocity profiles was obtained.

The work of Hughes (35) is of particular interest inasmuch as it included a study of flow into a packed bed through a small orifice. The technique used was similar to that of Saunders and Wild, except that the marble chips were treated with lead acetate and a mixture of hydrogen sulfide and air then used for the gas. For a bed of 20-30 mesh particles, Hughes observed that the flow of gas at relatively low velocities from a small orifice produced a hemispherical wave front emanating at the orifice, and also noted that "the gas velocity may be varied considerably with little effect on the wave front produced." He was aware that preferential flow along the glass front of his bed might give misleading results, but reported that later work showed the wall effect to be surprisingly small.

When 3/16- to 1/4-inch chips were used in the bed, Hughes' results were significantly different. Under these conditions the wave front was observed to spread horizontally to the full width of the bed at a distance of only 3/4 of an inch into the bed, and then advance through the bed as an almost horizontal line.

Aerov and Umnik (1) passed a mixture of hydrogen sulfide and air through pellets treated with lead acetate until darkening was first noted in the exit layer of pellets, and then removed successive thin layers of the bed and observed the degree of blackening in each layer. The velocity of the gas near the wall was found to be 30 to 70 per cent higher than that at the center of the bed. Similar work had been done earlier by Chernyshev et al. (9) using iodine vapor and starch pellets, but no data pertaining to velocity distribution were reported.

Further indication of higher velocities at the wall is reported by Schuler et al. (60), who found a radial variation in the effective thermal conductivity of a packed bed which was consistent with the velocity profiles obtained by Smith et al. (49, 61).

On the other hand, Coberly and Marshall (13) concluded that velocities are uniform across a packed bed, on the basis of hot-wire anemometer readings taken at the bed exit. Since the anemometer was placed very close to the exit layer of pellets, the data were widely scattered due to the presence of interstitial jets of gas, but no

significant trend away from a flat profile was noted, either in shallow (1.25-inch) or deep beds.

The analogy between heat and mass transfer suggests that information pertinent to the present work might also be found in reports of heat-transfer studies. Such studies have been almost entirely concerned with overall rates, although measurements have been made of temperature profiles in packed beds during heating and cooling (3,8,13,30,42,43). Despite the local nature of such measurements, they are still applicable only to the problem of overall heat transfer between the flowing fluid and the walls of the bed, and are of no use whatsoever in analyzing local transfer rates between the fluid and individual particles in the bed.

GENERAL EXPERIMENTAL METHOD

It is significant that the effects of local turbulence in the interstitial spaces in packed beds are not to be deduced from most of the work done by previous investigators. Smith, et al. (49, 61), for example, recorded rapidly fluctuating readings in preliminary work when their hot-wire anemometers were placed close to the exit layer of pellets in the bed, but elected to make the bulk of their measurements with the anemometers located farther downstream, where such fluctuations were no longer present. In the same regard, the work of Arthur, et al. (4), and all the other colorimetric work may be conclusive as far as average velocities are concerned, but leaves the question of the fluctuations in velocity associated with turbulence unresolved.

The significance of local turbulence to transfer phenomena in packed beds should be apparent, since it is actually the local velocity near the interface of each pellet in the bed, rather than any average velocity in the direction of main flow, which affects transfer rates. Indeed, if high velocities at the tube wall go hand in hand with higher porosity, it would seem that the interstitial space along the wall would be less tortuous, and that local turbulences might be reduced accordingly. This could be the explanation for the discrepancies between the results obtained by Smith et al. (49, 61) and those of Coberly and Marshall (13). Although the latter merely state that their anemometer readings were made "very close" to the exit layer of pellets, it may

be that they actually recorded transient velocity effects as well as the main-stream velocity component. In any event, it is entirely conceivable that radial variations in the average velocity in the main-stream direction are of little significance in either heat- or mass-transfer phenomena.

Actual measurement of true interstitial velocities in a packed bed was given some consideration at the outset of the present investigation, but was rejected in view of the many experimental difficulties involved. The use of a hot-wire anemometer would presumably be involved, and the wire itself would occupy a significant fraction of the interstitial space under study. Further, it seemed apparent that an individual pellet surrounded by interstitial space having a completely undefinable shape would have its surface exposed simultaneously to many different levels of velocity, all bearing an extremely uncertain relationship to the anemometer readings. Finally, it was realized that a knowledge of the flow characteristics within a packed bed would be useful primarily for its bearing on problems involving transfer phenomena, and that the measurement of actual local transfer rates would be a much more direct approach to the ultimate problem.

Local rates of heat transfer in a packed bed could conceivably be measured, and this approach was also considered and rejected at the outset of the present work. Such an approach would require the quantitative measurement of heat flux to a particle in a packed bed, an almost impossible

task for the particle sizes of interest, as well as the accurate determination of the temperature difference between the particle surface and the adjacent fluid stream. The latter problem is almost as formidable as the former, in view of evidence that such temperature differences are extremely small (3, 8).

In contrast to the difficulties inherent in the measurement of either local heat-transfer rates or true local velocities, the determination of local rates of mass transfer could be accomplished by relatively simple and direct methods, and this approach to the problem was therefore selected. After a review of the literature and consideration of several methods by which meaningful data might be obtained, it was decided that the most suitable technique would be to pass a liquid or gas through an inert bed containing carefully positioned soluble or volatile solid pellets, and to determine mass-transfer rates by measuring the loss in weight of the active pellets. Since the effect of fluid properties was not a major concern, water and air were obvious choices and air was arbitrarily selected.

The choice of a suitable volatile solid was based on the following criteria: (1) the volatility should not be so high as to result in inordinately large weight losses during the packing and recovery operations, when the pellets would be exposed to the atmosphere; (2) the volatility should not be so low as to require inconveniently long running times to obtain measurable weight losses; (3) the specific gravity

should be as high as possible, so that measurable weight losses would be accompanied by a minimal change in pellet volume and surface area; and (4) inter-granular cohesion should be good in order to permit the pressing of pellets of various sizes, preferably without the addition of a binder. Naphthalene, camphor, p-dichlorobenzene, and p-dibromobenzene were considered and subjected to preliminary tests, and p-dibromobenzene was finally selected as best meeting the requirements.

In summary, then, the experimental method used in this investigation involved the careful positioning of preweighed individual pellets of p-dibromobenzene in an otherwise inert bed, blowing air through the bed, recovering and reweighing the active pellets, and calculating mass-transfer rates from the loss in weight as a function of position in the bed, air flow rate, pellet diameter, and geometry at the entrance to the bed, i.e., air entry through an orifice as compared with unimpeded entry over the entire cross-section. This technique proved to be completely satisfactory for the study of local transfer rates in a packed bed, and is to be commended to anyone interested in conducting similar studies.

EXPERIMENTAL APPARATUS AND EQUIPMENT

The basic apparatus required to produce a measurable loss in weight of individual pellets of p-dibromobenzene in an otherwise inert bed through which a stream of air is passed is relatively simple. Broadly speaking, the only requirements are a controllable air supply system, a test section affording easy access, and the necessary instrumentation. As a result of preliminary tests, however, it became apparent that the problem of equipment design was by no means that simple, and an apparatus comprising the following units was eventually developed and found to be suitable:

1) A motor-driven blower with suitable controls.

2) A finned-tube heater-cooler to permit regulation of the temperature of the air entering the test section.

3) A calming section to insure against an abnormal velocity profile at the entrance to the test section.

4) A test section which was clamped in place during actual runs, but which could be swung aside to facilitate the introduction and recovery of the active p-dibromobenzene pellets.

5) A mercury manometer for measuring the pressure drop across the packed test section.

6) Chromel-alumel thermocouples and a potentiometer for the measurement of temperatures in the bed.

7) A rotameter for measuring air flow rates.

Auxiliary equipment such as orifice plates, glass beads, p-dibromobenzene pellets, radius and depth gauges, weighing bottles, and an analytical balance completed the requirements.

The entire apparatus is shown schematically in Figure 1, and most of the components can also be seen in Figures 2-4. A detailed description of each of the components of the apparatus is presented in the sub-headed paragraphs which follow.

Air Supply System

Motor and blower. Atmospheric air was drawn directly into the inlet of a two-lobe rotary blower, which was driven by a General Electric 7.5-horsepower 230-volt shunt-wound DC motor, Model No. 5B294A14. Since the blower was obtained from Navy surplus and was apparently a special design, no exact specifications can be given, other than that it was built by the Sutorbilt Corporation and appeared to be similar to their blower No. 5-M, which has a displacement of 0.18 cubic feet of air per revolution and a rated capacity of 115 cubic feet per minute at a discharge head of 4.9 pounds per square inch.

With a belt drive, major changes in the operating range of the blower could be effected by changing the diameter of either of the two sheaves. For closer control, the speed of the motor could be regulated by means of a rheostat in the field circuit as well as by introducing resistance

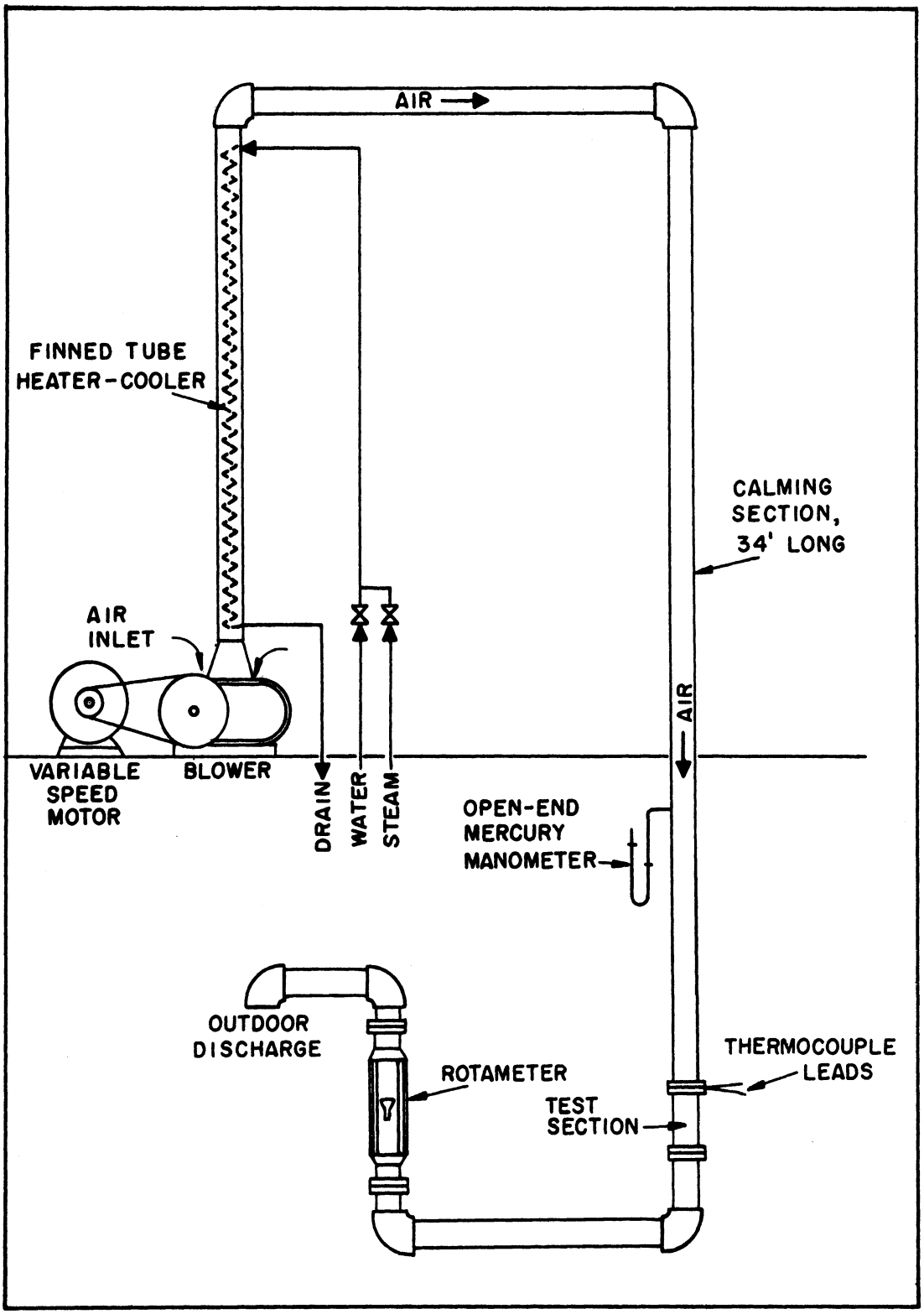

Fig. 1 Schematic Diagram of Apparatus

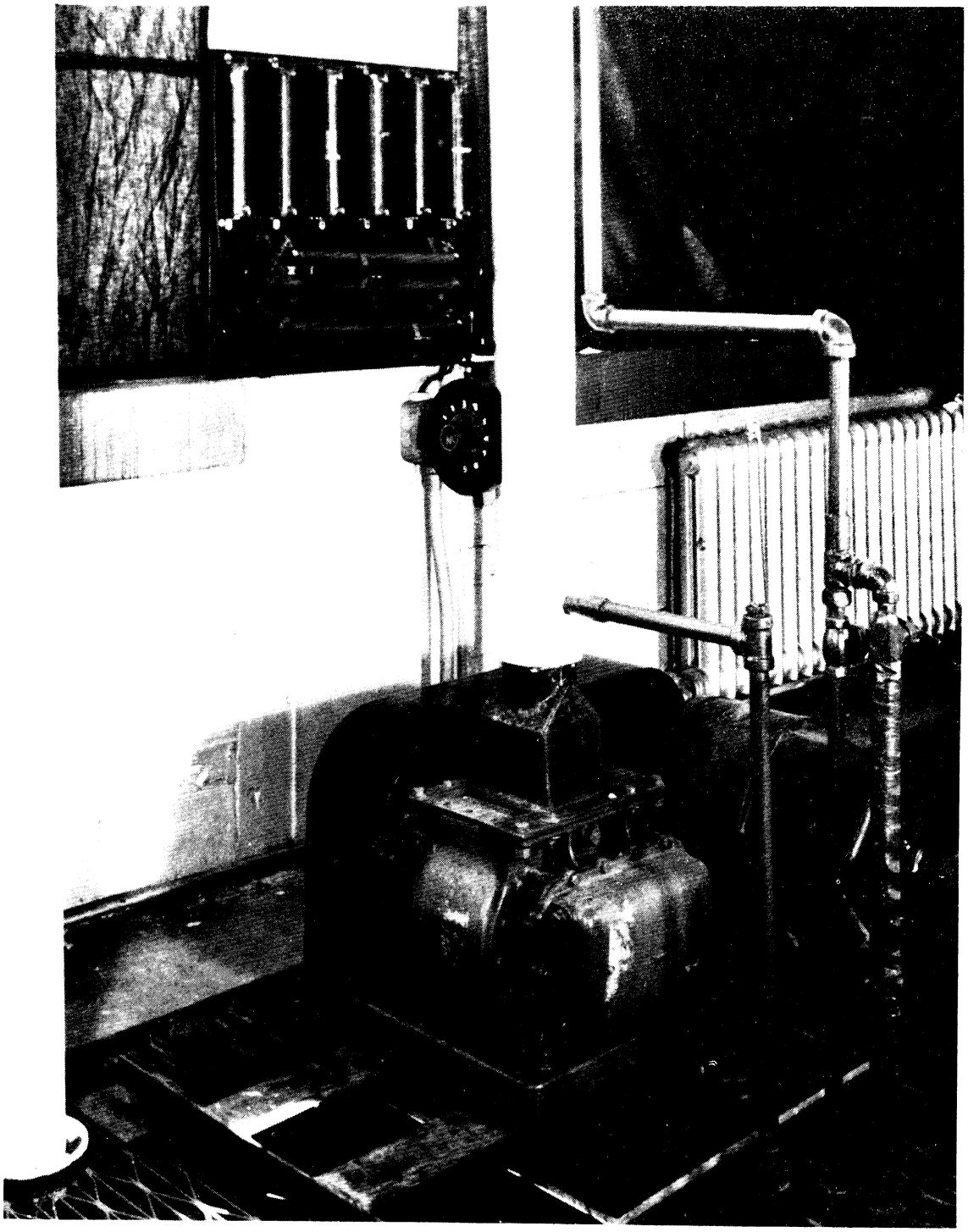

Fig. 2. Air Supply System - Motor and Blower, Resistor Board, and Heater-Cooler Inlet and Drain Lines.

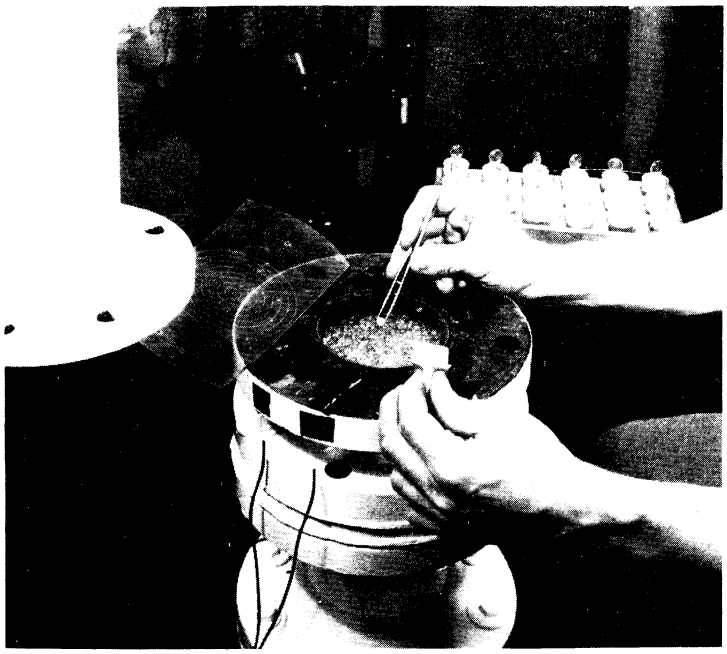

Fig. 3. Close-ups of Test Section. Above - Loading p-dibromobenzene pellets. Below - Assembling into air supply line.

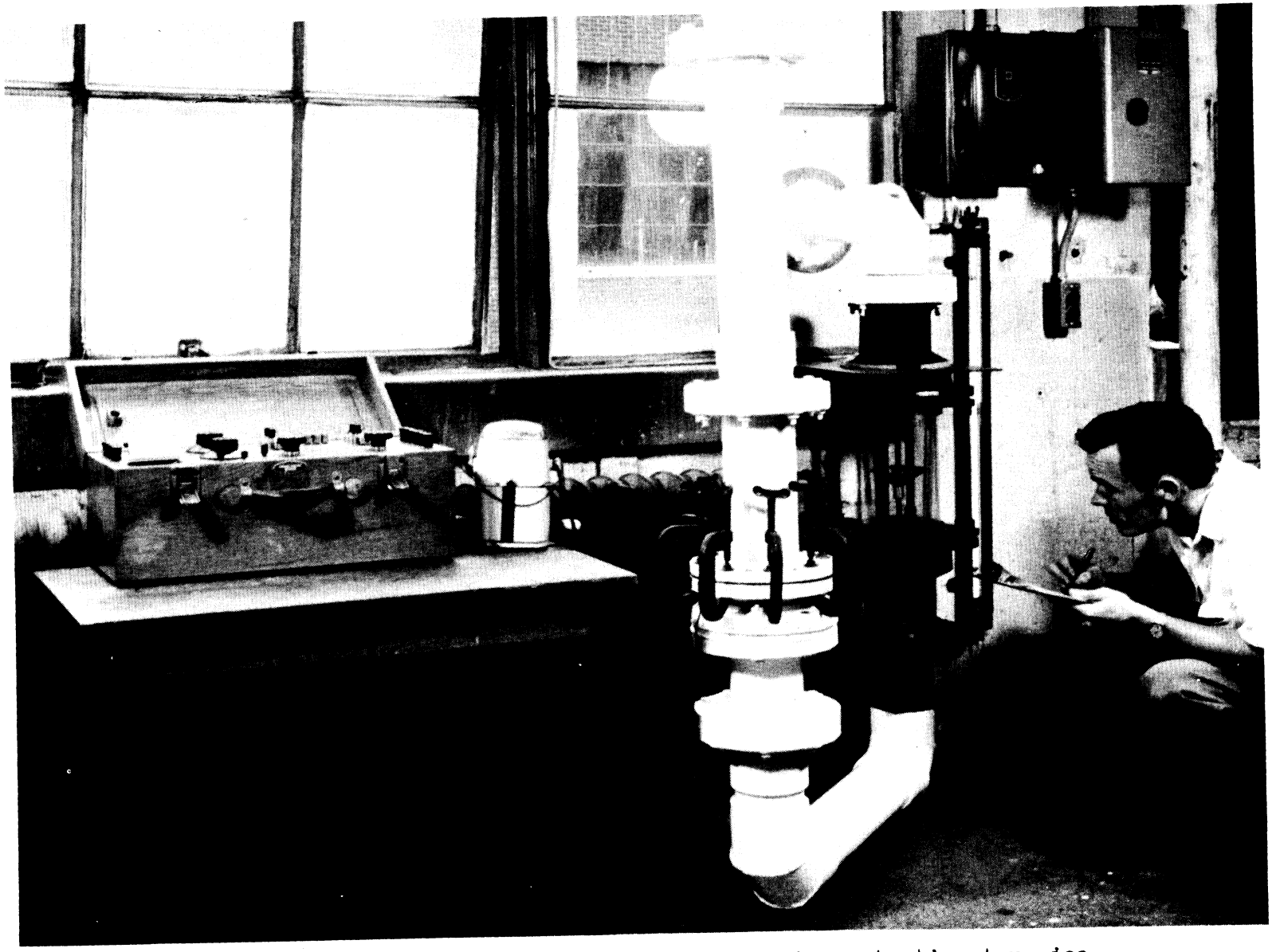

Fig. 4. Test Section in Operating Position, showing potentiometer, ice bath, rotameter, manometer, master switch, and motor starting box.

into the armature circuit. The resistor board for the latter circuit, visible in Figure 2, consisted of six fixed and two variable slide-wire resistors which could be wired in various parallel and series combinations to provide a wide range of resistance without overload.

Piping. Pipe having a nominal inside diameter of 4 inches was used throughout the air supply line, including the calming section and test section. Except for flanges, which were hard rubber, all piping and fittings were made of styrene co-polymer and were obtained from the Michigan Carlon Pipe Company. Fittings were of the "slip-sleeve" type and all permanent joints were cemented with solvent supplied by the same company. Naturally black, the pipe and fittings were painted with white enamel to minimize the effect of solar radiation on the air temperature.

Heater-cooler. During preliminary tests it was found that the blower heated up during its operation, and that the temperature of the outlet air gradually rose accordingly. In view of the sensitivity to temperature of the vapor pressure of p-dibromobenzene, steady-state operation was highly desirable and was achieved by installing a combination heater and cooler in the air supply line immediately over the blower outlet.

The heater-cooler consisted of three parallel lengths of 1-inch (fin diameter) helically-finned copper tubing obtained through the courtesy of the Wolverine Tube Division of the Calumet and Hecla Consolidated Copper Company. The

tubes were bent into a tight spiral approximately 9 feet long which could be inserted into the 4-inch air line, and were connected to a manifold at each end. Water was supplied to the upper manifold and passed down the tubes countercurrent to the direction of air flow.

Because the heater-cooler was designed to maintain an outlet air temperature closely approaching that of the inlet water, regardless of fluctuations over a reasonable range in the air temperature at the blower outlet, air temperatures could be controlled by regulating the inlet water temperature. This was accomplished by bleeding low-pressure steam into the water line, the steam rate being controlled by a needle valve. The steam and water inlet lines and the drain line can be seen in Figure 2.

Calming section. By locating the motor and blower on one floor of the laboratory and the test section on the floor below, it was possible to include in the air supply line a straight section of piping completely devoid of elbows or other fittings which might disturb the flow. This calming section, approximately 34 feet long, was connected directly to the top of the test section and thereby insured against abnormal velocity perturbations in the air entering the bed.

Manometer. An open-end mercury manometer was connected to the air supply line just above the test section. Since runs made with an empty test section showed a negligible pressure drop between the manometer tap and the exhaust

end of the air line, manometer readings taken when the test section was packed with pellets were a direct indication of the pressure drop across the bed and the inlet orifice (when one was used).

Rotameter. Because of the calming section upstream from the test section, the rotameter was located between the packed bed and the exhaust point. The meter itself was a size 12 Fischer and Porter Flowrator (Tube No. 12-LL25, Serial No. D8-1612), with a capacity of 0-200 standard cubic feet per minute of 0.877 specific gravity gas, at 14.7 psia and 60°F. The scale was graduated in increments of 2 SCFM.

In the absence of test equipment suitable for calibrating the meter at high rates of flow, calibration was accomplished by passing through the meter an air stream enriched with oxygen metered through a calibrated smaller meter, and determining the concentration of oxygen in the enriched air mixture. Calibration by this method was found to be reproducible within approximately ± 1.5 per cent.

Exhaust. To insure against the presence of p-dibromobenzene vapor in the air entering the blower, the air-vapor mixture leaving the test section and rotameter was discharged out-of-doors.

Test Section

The test section consisted of a 6-inch length of the same piping as was used in the air supply system, flanged at both ends for assembly into the line. The lower flange was

bolted to its mate on the downstream end of the air supply line, but C-clamps were used with the upper flange to facilitate assembly and disassembly between runs. With the clamps removed, the test section could be swung out from under the air supply line, as shown in Figure 3, exposing the top of the bed and facilitating the introduction and recovery of the active pellets. This lateral movement of the test section was made possible by mounting the rotameter section of the line in wall brackets within which it could turn and using an uncemented slip-sleeve fitting above the rotameter. Thus the test section could be rotated about an axis through the meter.

Inert pellets. Spherical glass beads of the type obtainable from any laboratory supply company were used as inert pellets for two of the diameters tested--1/8-inch or 3-mm, and 1/4-inch or 6-mm. For tests with a nominal pellet diameter of 1/2 inch, ordinary glass marbles were used. The precise dimensions of all three sizes of inert spheres together with indications of size uniformity are presented in Appendix B.

Pellet support screen. Since air flow was downward through the bed, and exit geometry was not significant, no special considerations were involved in designing a pellet support screen, and a heavy-duty screen mounted in a steel ring having the same diameter as the flanges was used.

Orifices. Preliminary tests showed that the packed bed always settled slightly during runs because of vibration.

When rigid orifice plates were used, the resulting separation, however slight, between the plate and the top layer of pellets was found to have a significant effect on the flow distribution in the bed. To overcome this difficulty, orifice rings of 1/32-inch cellulose acetate were cemented to annular rubber gaskets whose flexibility permitted the orifice to settle with the bed. As an added precaution, the bed was always loaded to a level about 1/16 of an inch above the surface of the upper flange, so that the orifice gasket was placed under slight tension when the bed was clamped to the line.

Temperature measurement. Two chromel-alumel thermocouple junctions were placed in the bed at the same depth and radius as the active pellets, except at locations close to the center of the bed where the junctions were placed immediately above and below the active pellets. No particular care was exercised in locating the couples at or away from pellet surfaces, since tests indicated a negligible difference between readings made at the pellet surface and those made in the interstitial space. This observation was in agreement with those of other investigators (3, 8).

From the test section, the thermocouple leads were run to a cold junction in a melting ice bath and to a rotary selector switch from which one couple at a time could be routed to a Leeds and Northrup Portable Precision Potentiometer (Model 8662, Serial No. 729427).

Position measurement. The depths at which active pellets were located were indicated by rings scribed at 1/2-inch intervals on the inside wall of the test section. Radial positions were measured with a circular Lucite plate, closely fitting the test section, upon which concentric circles were scored in 1/4-inch radial increments, or with a 1/32-inch sheet of cellulose acetate, similarly scored, which was aligned by means of two small studs projecting from the upper flange surface and was used at shallow bed depths. The studs also served to center the orifice gaskets.

Due to radial symmetry, angular measurements were not required. Since all active pellets used in a run were located at the same depth and radius, the identity of individual pellets was preserved by consistently loading and unloading in a clock-wise direction from a reference mark on the face of the upper flange.

P-dibromobenzene Pellets

Spherical pellets of p-dibromobenzene were pressed in a Stokes Model F Pelleting Machine (F. J. Stokes Company), using special 1/8-, 1/4-, and 1/2-inch spherical punches and dies obtained from the same company. Granulated p-dibromobenzene was obtained from the Eastman Kodak Company and was ground in a Stokes Oscillating Granulator, Model 2A, equipped with a No. 10 heavy wire screen, before feeding to the pelleting machine.

As formed by the press, the pellets were essentially spherical except for a narrow "waist" around the middle,

where the punches came together. The pellets were then "cured" before use by storing for a week or ten days in a covered jar at atmospheric temperature. Normal temperature fluctuations caused alternate vaporization and condensation on a limited scale, with the result that the waist was practically non-existent by the time the pellets were used. The actual dimensions and other physical characteristics of the active pellets are presented in Appendix B.

The pellets were weighed in glass-stoppered weighing bottles 25 millimeters in diameter and 40 millimeters high (Kimble No. 15145), using a notched-beam chain-o-matic analytical balance (Wm. Ainsworth & Sons, Inc., Type DLB; Serial No. 16644) equipped with a magnetic damper.

EXPERIMENTAL PROCEDURE

In the original planning of the research program, it was anticipated that the experimental operating procedure would consist of six basic steps: pre-weighing of the active p-dibromobenzene pellets, warming up the apparatus and establishing desired operating conditions, loading the active pellets into the bed, making the experimental run, recovering the pellets, and post-weighing. The active pellets to be used in any single run would be located at the same radius and depth, to avoid any possibility of the transfer from one pellet being affected by that from another, but full advantage would be taken of radial symmetry. Thus, more pellets would be used per run at positions near the wall than at positions near the center of the bed.

In general, experimental runs were to be grouped into two-man "shifts" of from 3 to 4 hours in duration, including weighing time, in order to minimize the time spent warming up and adjusting the apparatus. Preliminary work indicated that from 30 to 45 minutes would be required for pre-weighing, 20 to 30 minutes for warm-up, and another 30 to 45 minutes for post-weighing.

Although this basic plan was found to be suitable, experience dictated several modifications in the detailed procedure, and the actual method of operation is described in the paragraphs which follow, under appropriate sub-headings.

Pre-weighing

Preliminary runs indicated that little advantage was to be derived from the separate weighing of each of the active pellets to be used in a multi-pellet run, and all pellets to be used in a given run were therefore placed in the same weighing bottle and weighed together. Individual weighings were, of course, necessary when positions close to the center of the bed were being investigated and only one pellet could be run at a time. The data for these runs (Appendix A) provide an indication of the degree to which individual weight losses were found to deviate from the average.

Except for the determination of pellet density (Appendix B), no attempt was made to obtain the absolute weights of the pellets used. Although all weighings were made with an empty tare bottle on the opposite pan, the weights of the various weighing bottles were all different, and the balance reading was therefore somewhat different from the actual weight of the pellets. This difference obviously cancels out when the final weight is subtracted from the initial to obtain the weight loss.

The analytical balance used for the weighings had a sensitivity of $\pm$ 0.05 milligrams, and weighings made during any one weighing period were reproducible within that range. It was discovered, however, that reproducibility could not be carried over from one period to another. Attempts to identify the cause of this discrepancy were unsuccessful,

but its effects were circumvented by a technique which will be described in the section on run procedure.

Warm-up of Equipment

Before the blower was turned on for the warm-up period, the motor control resistances were wired to provide the approximate air flow rate desired and the temperature of the water entering the heater-cooler was set at an approximate value by adjusting the needle valve on the steam line. The two thermocouple junctions were placed in position at the bed location to be tested, and the bed was then packed with inert pellets, fitted with the desired orifice if one was to be used, and clamped in running position. Except for the absence of active pellets, the equipment was thus warmed up under actual test conditions.

During the warm-up period, the water and/or steam valves were adjusted until the potentiometer readings indicated a temperature closely approximating 80°F. in the test section. The desired air flow rate was established at the same time by making minor adjustments in the motor control resistance. When steady-state conditions with respect to both flow rate and temperature had been attained, the blower was stopped, the bed unclamped and swung aside, and the loading of active pellets was immediately started.

The warm-up procedure was also followed whenever any of the run conditions were changed in the middle of a shift.

Loading the Bed

Inert pellets were scooped out of the bed until the proper test depth was reached, as indicated by the lines on the inside wall of the test section, and the bed was then carefully leveled at this depth. Active pellets were then quickly removed from the weighing bottle with a pair of tweezers and pushed into the exposed inert layer at approximate radial and angular positions. Radial distances to the center of each pellet were checked with the radius gauge and corrected as necessary by gently pushing the pellets into place with the point of the tweezers. The distances were rechecked after each adjustment, until all active pellets were correctly located within approximately 1/32 of an inch.

Several inert pellets were then carefully placed around and on top of each active pellet, to minimize movement when the rest of the inert pellets were replaced. There was, of course, no assurance that the active pellets did not shift slightly during this process, although positions were usually found to be unchanged if the pellets were carefully re-exposed after running.

When all inert pellets had been replaced, a 1/4-inch steel plate was placed over the bed and the bed was rapped sharply several times to settle the pellets. Since the inert pellets returned to the bed were the same ones previously removed, and since the rapping procedure established a final bed level which was reproducible within approximately 1/32 of an inch, bed porosity could be assumed to be essentially

constant from run to run. Experimental measurement showed the fractional void space to be 0.36, 0.37, and 0.42 for pellet diameters of 1/8-inch, 1/4-inch, and 1/2-inch, respectively (Appendix B).

A procedure slightly different from that described above was followed when tests were to be made at bed depths of one or two pellet diameters. In this case, the active pellets were pushed into place without removing any inert pellets from the bed. For runs at the topmost layer, it would have been possible to avoid disturbing the inert bed completely by merely placing the active pellets in the holes left when pellets from the preceding run were removed. Because this practice would result in an exact reproduction of bed geometry which could not be achieved when inert pellets had to be removed and replaced, the bed was always deliberately scrambled between such runs by stirring with the point of the tweezers. The inert pellets were then leveled and settled as usual, and the active pellets emplaced by merely substituting them for inert pellets which were located at the desired positions.

The time required for the entire loading operation was usually between one and two minutes, depending on the test depth and the number of active pellets to be loaded. This variable time meant that the weight lost by the active pellets due to exposure to the atmosphere during loading was also variable, but this problem was surmounted by the "dry run" technique to be described in the following section.

Run Procedure

As soon as the test section was clamped in running position, the blower was turned on and came up to speed in about five seconds. The initial potentiometer readings were made as soon as steady-state temperature conditions were established in the bed, usually about 30 seconds after start-up. Additional readings were made throughout the run at one-minute intervals, and the rotameter and manometer were read at mid-run.

Running times were measured with a stop watch, and the stop button in the motor circuit was pushed at the end of the desired running time. The blower came to rest almost immediately, the second or two of extra operation compensating for the start-up time to some extent. The test section was then unclamped and the active pellets recovered as quickly as possible.

It was necessary that running times be long enough to produce a weight loss which could be determined within a few per cent by normal laboratory weighing techniques, and five-minute runs were found to be adequate in this regard. On the other hand, shorter runs obviously permitted the accumulation of more data in a shorter time. Preliminary tests made with running times varying from 1-1/2 to 5 minutes yielded consistent results and indicated that the start-up and shut-down times, as well as the time required to attain a steady-state temperature, were not critical factors. On the basis of these findings, actual running times were varied depending

on the test location, the air flow rate, and the number of active pellets in the bed. Because of the time required for a man to balance the potentiometer and to record the rotameter and manometer readings, running times of less than 1-1/2 minutes were not feasible.

Five runs were normally made with each given set of test conditions, and a shift normally comprised four of these five-run series, each made at a different air flow rate with the other run conditions constant. Nominal flow rates of 12.5, 25, 50, and 100 CFM were used, and a typical shift therefore provided all the necessary data for a given combination of pellet diameter, orifice diameter, and position within the bed, over the attainable range of air flow rates.

As noted, the active pellets lost some weight when they were exposed to the atmosphere during the loading and recovery operations, and a correction for this loss was necessary. One run in each five-run series, usually the middle run, was a "dry run" made without any air flowing through the bed but exactly duplicating the other runs in the series in every other respect, including running time. The loss in weight for this run could thus be attributed to the exposure during loading and recovery and to the slight amount of natural convection in the bed during the "run". Subtracting this loss from the measured weight losses for the other runs in the series yielded corrected weight losses which could be ascribed to the flow conditions alone. This operation is discussed further in the next section.

Although the weight losses obtained with the zero-velocity runs made during the same shift were generally in excellent agreement, considerable variations were observed from shift to shift, and the "losses" were even found to be negative, i.e., the final weight was greater than the initial, on some occasions. This can be seen from an inspection of the original data (Appendix A). These discrepancies were finally attributed to the actual weighing of the pellets, as was noted in detailing the weighing procedure, but attempts to identify the exact source of the trouble were unsuccessful. Since weighings made at any one time were reproducible, however, the measured dry-run weight loss also constituted a correction for changes in balance readings between weighing periods, and corrected weight losses were generally found to be consistent, even when compared with re-runs made several days or even weeks later.

In view of the obvious importance of the measured dry-run weight losses in obtaining the correct losses for the actual data runs, at least three dry runs were included in each group of weighings, and the losses for these runs were checked for consistency. Agreement within 0.10 or 0.20 milligrams was usually obtained among all three measurements.

In preliminary work, the true dry-run weight loss was measured by adding a sixth weighing bottle to each set of five and leaving it untouched during the experimental runs. The change in weight of this spare bottle was therefore a measure of the actual weighing correction, and could be

subtracted from the indicated dry-run weight loss to obtain the true loss attributable to exposure and natural convection. The true losses determined in this manner were found to lie between 0.05 and 0.15 milligrams, and shift-to-shift consistency was very good.

Pellet Recovery

As soon as the blower stopped at the end of a run, the test section was unclamped and swung aside, and inert pellets were quickly scooped out of the bed until the active pellets were located. No attempt was made to avoid moving the active pellets during this operation, except in preliminary runs made to determine the extent to which the pellets shifted from their original positions during the loading of the bed. As fast as the active pellets were uncovered, they were picked up with the tweezers and returned to the weighing bottle. The entire recovery operation usually took less than 30 seconds.

Post-weighing

All active pellets were post-weighed at the end of the same shift in which they were run, to avoid any possibility of loss in weight due to prolonged storage, and the actual weighing procedure was the same as that used in pre-weighing.

A sample data sheet for the experiments is shown in Figure 5. In addition to the experimental data, pertinent processed data were also included on each sheet, and the completed form thus constitutes an integrated record of the results for each run.

Date 14 Nov 53 Page 72

D_p 1/4 - in.	Bed Depth 6"	Rheo. Set. 5 - 0	Run Time 2 min.	Test Depth 3/8"
D_o 1 in.		Arm. Res. 0 - 4	No. Pellets 4	Test Rad. 1 1/2"

Arm. 4, Rheo. 0.

EC Temp				
1 - 1.021	1.023		Ave 1.022	
2 - 1.020	1.022		C_T 1.106	
Run 608	Manom. Rdg, "Hg	Bot 19	$-\Delta W_d$ 7.45	
Rot. 80.5	Rt 5.14	W_i 1071.40	$-\Delta W_t$ 8.24	
Re 1960	Lft 5.60	W_f 1062.30	k" 56.8	
G' 146.9	Tot 10.74	$-\Delta W$ 9.10	k'/G' 3.35	

EC Temp				
1 - 1.065	1.066		Ave 1.062	
2 - 1.059	1.060		C_T 0.982	
Run 613	Manom. Rdg, "Hg	Bot 24	$-\Delta W_d$ 6.85	
Rot. 46.5	Rt 1.60	W_i 1084.80	$-\Delta W_t$ 6.73	
Re 1067	Lft 1.85	W_f 1076.10	k" 46.2	
G' 80.0	Tot 3.45	$-\Delta W$ 8.70	k'/G' 5.01	

EC Temp				
1 - 1.030	1.028		Ave 1.027	
2 - 1.026	1.024		C_T 1.090	
Run 609	Manom. Rdg, "Hg	Bot 20	$-\Delta W_d$ 8.55	
Rot. 85.0	Rt 4.75	W_i 1040.50	$-\Delta W_t$ 9.32	
Re 2078	Lft 5.16	W_f 1030.30	k" 64.0	
G' 155.8	Tot 9.91	$-\Delta W$ 10.20	k'/G' 3.57	

EC Temp				
1 - 1.062	1.062		Ave 1.056	
2 - 1.050	1.050		C_T 1.000	
Run 614	Manom. Rdg, "Hg	Bot 25	$-\Delta W_d$ 6.55	
Rot. 43.5	Rt 1.60	W_i 1033.70	$-\Delta W_t$ 6.55	
Re 988	Lft 1.84	W_f 1025.30	k" 44.9	
G' 74.1	Tot 3.45	$-\Delta W$ 8.40	k'/G' 5.26	

EC Temp				
1 - 1.020	1.018		Ave —	
2 - 1.015	1.012		C_T —	
Run 610	Manom. Rdg, "Hg	Bot 21	$-\Delta W_d$ —	
Rot. 0	Rt —	W_i 1015.50	$-\Delta W_t$ —	
Re Dry	Lft —	W_f 1013.85	k" —	
G' —	Tot —	$-\Delta W_o$ 1.65	k'/G' —	

EC Temp				
1 - 1.050	1.047		Ave —	
2 - 1.038	1.036		C_T —	
Run 615	Manom. Rdg, "Hg	Bot 26	$-\Delta W_d$ —	
Rot. 0	Rt —	W_i 1013.45	$-\Delta W_t$ —	
Re Dry	Lft —	W_f 1011.60	k" —	
G' —	Tot —	$-\Delta W_o$ 1.85	k'/G' —	

EC Temp				
1 - 1.050	1.053		Ave 1.060	
2 - 1.066	1.069		C_T 0.988	
Run 611	Manom. Rdg, "Hg	Bot 22	$-\Delta W_d$ 7.85	
Rot. 84.5	Rt 4.71	W_i 1020.75	$-\Delta W_t$ 7.76	
Re 2065	Lft 5.11	W_f 1011.25	k" 53.2	
G' 154.8	Tot 9.82	$-\Delta W$ 9.50	k'/G' 2.99	

EC Temp				
1 - 1.048	1.049		Ave 1.046	
2 - 1.044	1.045		C_T 1.030	
Run 616	Manom. Rdg, "Hg	Bot 27	$-\Delta W_d$ 5.40	
Rot. 47.0	Rt 1.59	W_i 1019.30	$-\Delta W_t$ 5.56	
Re 1081	Lft 1.80	W_f 1012.05	k" 38.2	
G' 81.0	Tot 3.39	$-\Delta W$ 7.25	k'/G' 4.09	

EC Temp				
1 - 1.070	1.072		Ave 1.066	
2 - 1.060	1.062		C_T 0.971	
Run 612	Manom. Rdg, "Hg	Bot 23	$-\Delta W_d$ 8.30	
Rot. 84.0	Rt 4.68	W_i 1021.20	$-\Delta W_t$ 8.06	
Re 2052	Lft 5.10	W_f 1011.25	k" 55.3	
G' 153.8	Tot 9.78	$-\Delta W$ 9.95	k'/G' 3.13	

EC Temp				
1 - 1.057	1.058		Ave 1.056	
2 - 1.055	1.056		C_T 1.000	
Run 617	Manom. Rdg, "Hg	Bot 28	$-\Delta W_d$ 6.20	
Rot. 47.5	Rt 1.55	W_i 1072.60	$-\Delta W_t$ 6.20	
Re 1094	Lft 1.75	W_f 1064.55	k" 42.5	
G' 82.0	Tot 3.30	$-\Delta W$ 8.05	k'/G' 4.50	

G - lbs/ft^2-hr; G' - lb-mols/ft^2-hr; k" - mg/cm^2/hr; k' - lb-mols/cm^2/hr; all weights in milligrams. k'/G' is x 10^6.

Fig. 5. Sample Data Sheet.

DATA PROCESSING

Dry-Run Correction

The first step in processing the raw data was to compare the measured weight losses for the dry runs (three or more) made during each shift and to reject any inconsistent values. In general, the agreement among all these losses was good, and only rarely was more than one found to be inconsistent. The measured losses in weight for the actual data runs in each five-run series, obtained by merely subtracting final from initial weights, were then corrected to true losses by subtracting the dry-run weight loss for the same series. As noted in the preceding section, this procedure eliminated the effect of pellet exposure during the loading and recovery operations and also corrected for any fixed error in either the pre- or post-weighings, and therefore yielded a true weight loss which was directly attributable to the actual flow of air through the bed during the experimental run. If the dry run in a particular series had been rejected, the dry-run correction for that series was obtained by averaging the other dry runs in the shift.

The true weight loss for each data run, i.e., the loss in weight corrected for the dry run, is designated ΔW_d on the original data sheets (Figure 5).

Temperature Correction

The driving force for the transfer of mass from a solid surface into a gas stream is usually taken to be the difference between the partial pressure of the transferring component in the main gas stream and that at the gas-solid interface. Assuming equilibrium at the interface and ideal gases, the partial pressure at the interface will be equal to the vapor pressure of the solid, making the driving force for the transfer, and hence the actual rate of transfer itself, a function of the vapor pressure. The latter, in turn, is a function of the temperature, and it is therefore essential that the temperature at the interface be known if the mass-transfer data are to be correctly interpreted.

As has been noted, temperature measurement was accomplished in these studies by placing thermocouple junctions in the bed at positions equivalent to those occupied by the active pellets. Since junctions were actually located in the interstitial space between pellets rather than on a pellet surface, the true surface temperature was not determined. However, preliminary tests indicated that the measured temperature was within a fraction of a degree of the temperature at the surface. This observation is in agreement with the findings of other investigators (3,8) and is further confirmed by the analytical study presented in Appendix E.

Because it was not possible to make all runs at exactly the same temperature, the data had to be corrected to an arbitrary base temperature before they could be compared

and correlated. Experimental conditions made it desirable to take most of the data at temperatures around 80°F., and this temperature was therefore selected as the base to which the data were corrected.

Unfortunately, the agreement among the vapor pressure data reported in the literature is not particularly good, as can be seen from Figure 6, and experimental measurement of the vapor pressure was therefore considered. At the same time, it was recognized that the effect of temperature might not be confined to its influence on vapor pressure, and it was therefore decided to check the temperature effect directly under actual experimental conditions rather than to make a separate investigation of vapor pressure.

Accordingly, a series of experimental runs were made at various temperatures covering the range of interest, with all other run conditions held constant. The weight losses for these runs, corrected for the dry-run weight loss, were plotted against the reciprocal of the absolute temperature on semi-log paper, and a straight line was drawn through the data in keeping with its presumed relation to vapor pressure. As a check on the slope of the line thus obtained, a second series of runs was made under completely different test conditions, and these data were found to fit a line of the same slope. The original data for both series of runs are tabulated in Appendix C, and are plotted along with the correlating lines in Figure 7. The slope of the lines is also shown in Figure 6, for comparison with the slopes of the various vapor pressure curves, and is seen to be in general agreement.

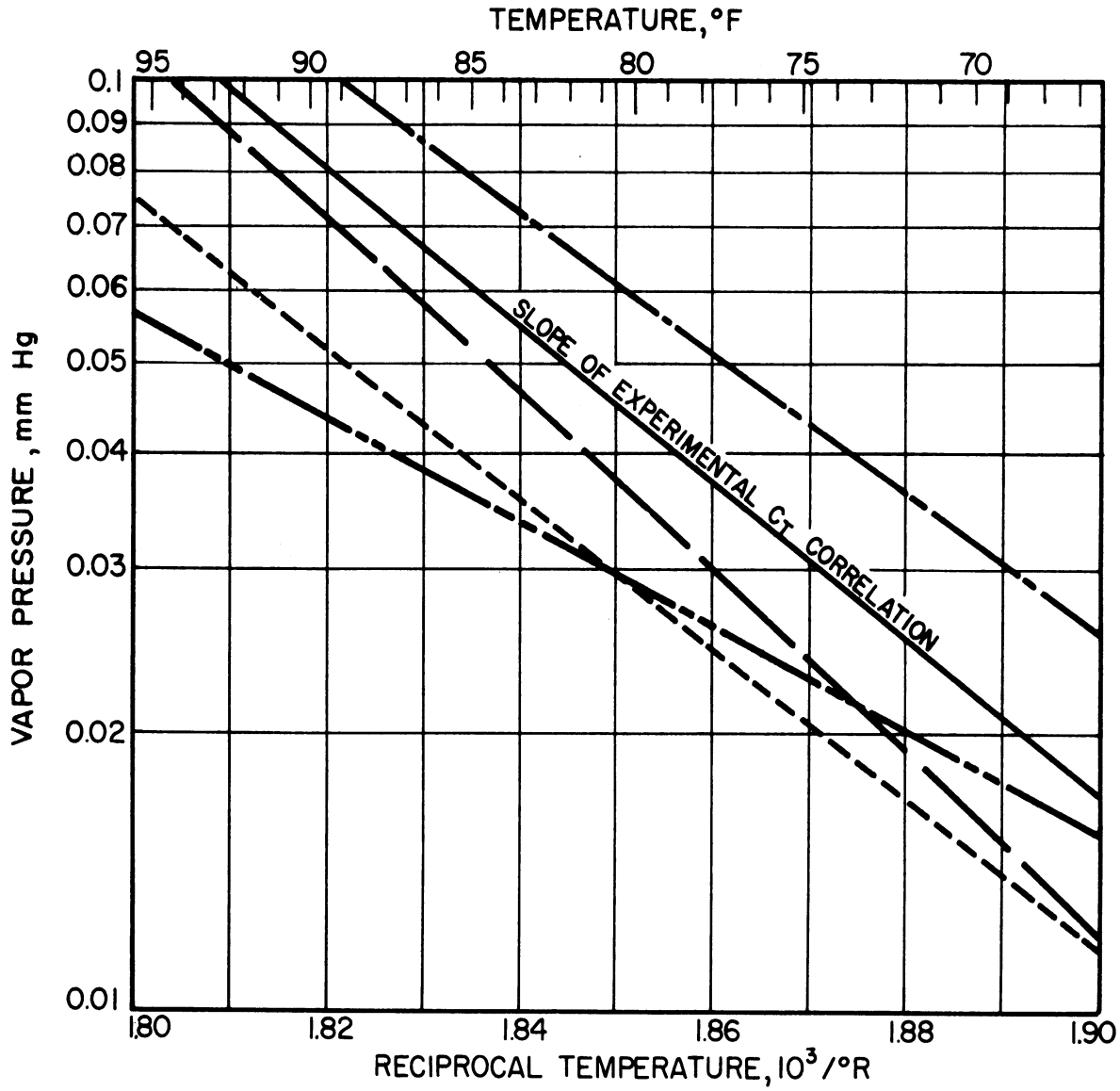

Fig. 6. Vapor Pressure of p-dibromobenzene

INTERNATIONAL CRITICAL TABLES (37)

CHEMICAL ENGINEERS' HANDBOOK (51)[1]

BEDINGFIELD AND DREW (5)[2]

ZIL'BERMAN (68)

EXPERIMENTAL C_T CORRELATION FOR COMPARISON OF SLOPE ONLY

[1] EXTRAPOLATED FROM 142°F

[2] EXTRAPOLATED FROM 114°F

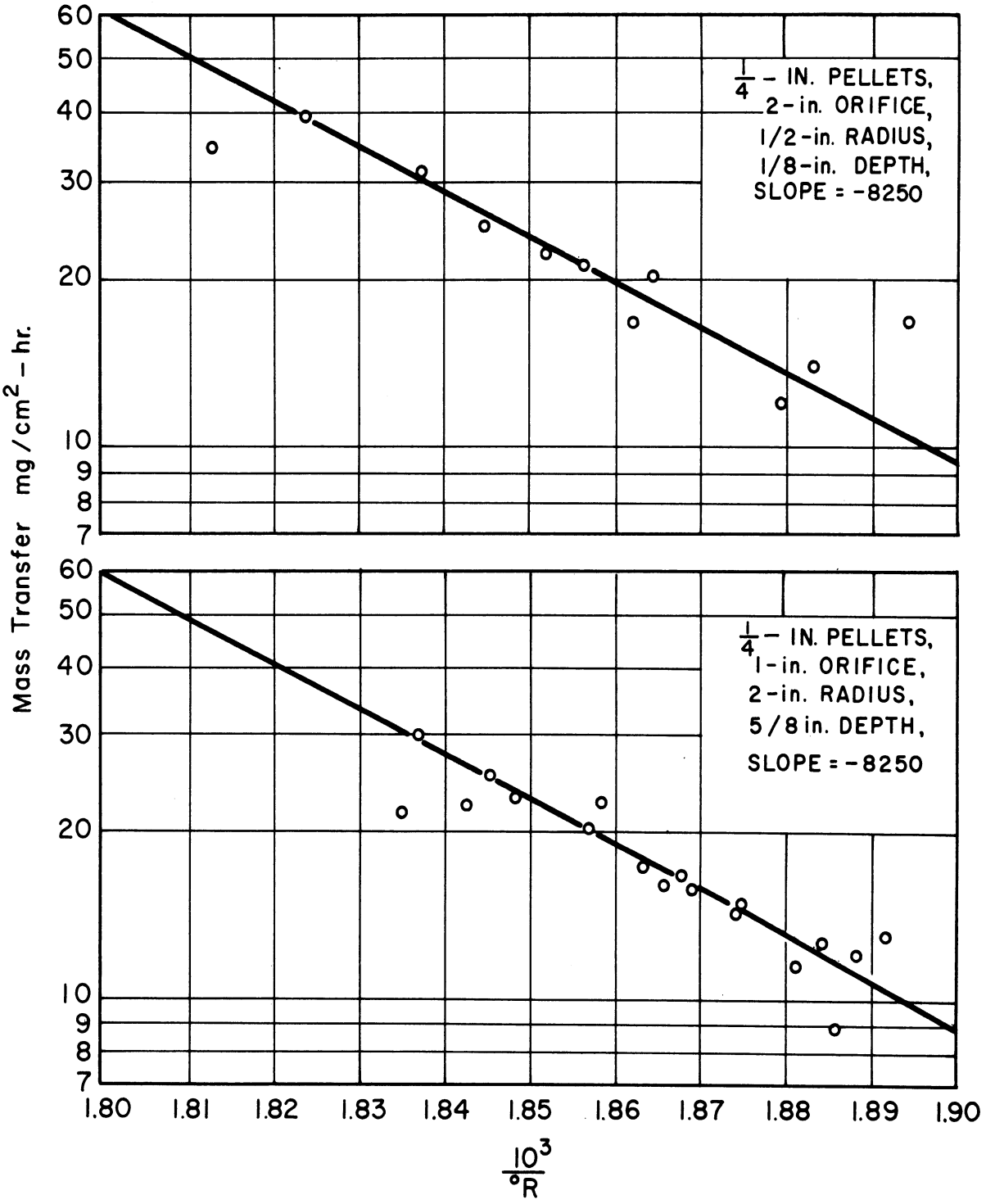

Fig. 7. Effect of Temperature on Mass Transfer.

The lines in Figure 7 can be represented by the equation

$$\log (-\Delta W_d) = B - \frac{8250}{T} \quad , \tag{28}$$

where B is a constant for any given combination of pellet diameter, orifice diameter, position in the bed, and air flow rate. At 80°F., then,

$$\log [-\Delta W_{d(80^\circ)}] = B - \frac{8250}{540} \quad , \tag{29}$$

and subtracting Equation 28 from Equation 29 yields

$$\log \frac{-\Delta W_{d(80^\circ)}}{-\Delta W_{d(T^\circ)}} = \frac{8250}{T} - \frac{8250}{540} = \log C_T \quad , \tag{30}$$

which defines the temperature correction factors, C_T. A plot of this factor versus temperature is presented in Appendix C.

The first step in correcting the measured weight losses for temperature was to average the potentiometer readings for each run. As indicated in the section on Experimental Apparatus and Equipment, two thermocouples were used with each run, and the readings from these two couples usually differed by less than 0.01 millivolts (0.45°F.), equivalent to a change of approximately 3 per cent in the temperature correction factor, C_T. Temperature changes during runs were equally small, and the average potentiometer reading was therefore considered an adequate basis for the temperature correction.

Both the average potentiometer reading and the corresponding temperature correction factor were entered on the data sheet, and the actual weight loss for the run (ΔW_d) was then multiplied by the temperature correction factor and the product (ΔW_t) recorded on the data sheet, as can be seen in Figure 5.

Conversion to Transfer Rate

The corrected weight loss, ΔW_t, was divided by the number of pellets in the weighing group and by the surface area per pellet (Appendix B) to obtain the weight loss per square centimeter of surface area, and then by the running time in hours to obtain the actual rate of mass transfer in milligrams per square centimeter per hour. This figure appears on the data sheet as k".

Reynolds Number

Rotameter readings were converted to standard cubic feet (60°F. and one atmosphere) per minute by means of the rotameter calibration curve, and the volumetric flow rate thus obtained was multiplied by the density of air at 60°F. and divided by the cross-sectional area of the bed to obtain the superficial mass flow rate, G, based on the empty bed.

The Reynolds number, D_pG/μ , was then calculated, using the diameter of the inert pellets as the characteristic length and a viscosity equal to 0.0436 pounds per foot per hour (at 80°F.) as given by McAdams (47). The Reynolds number for each run was entered on the original data sheet.

For reasons to be explained in the section on correlation, the dimensionless ratio of the transfer rate to the mass flow rate, both in molal units, was also calculated, and appears on the data sheet as k'/G' (times 10^4).

A summary of all original and processed data is presented in Appendix A. Sample processing calculations for Run No. 608, which is included on the sample data sheet in Figure 5, are summarized in Appendix D.

CORRELATION OF DATA

Preliminary Correlation

In the survey of the literature presented at the outset of this report, it was noted that almost all previous mass-transfer data were correlated in terms of the j-factor for mass transfer, defined as

$$j_d = \frac{k_g p_{gf}}{G/M_m} \left(\frac{\mu}{\rho D_G}\right)^{2/3} . \qquad (4)$$

Further, almost all previous investigators found j_d to be a straight-line function of the Reynolds number, $D_p G/\mu$, when plotted on log-log paper. Although these findings were based entirely on overall mass-transfer data, it appeared likely that local mass-transfer rates might be satisfactorily correlated in a similar manner, and this method of correlation was therefore given first consideration.

It is apparent, however, that the j-factor as defined by Equation 4 includes terms which were not directly investigated in these studies, and a basic correlation including these terms would therefore be one step removed from the actual experimental data. Insofar as these terms were constant throughout the present work, they could be eliminated without altering the form of the correlation. The Schmidt number obviously falls in this category, and the mean partial pressure of the inert gas in the film, p_{gf}, is also constant for practical purposes since it can be effectively replaced

by the total pressure in view of the very low vapor pressure of p-dibromobenzene. The group to be correlated is thus reduced to $k_g M_m/G$, which should be a straight-line function of the Reynolds number to the same extent that j_d is.

In one further reduction, the mass-transfer coefficient, k_g, was replaced by the mass-transfer rate, k', to which it is related by the equation

$$k' = k_g(p^o - p_v)_{lm} \quad . \tag{31}$$

This substitution would also leave the form of the correlation unaltered provided the mean driving force, $(p^o - p_v)_{lm}$, could be assumed to be constant. At first glance this seemed highly unlikely, but a more careful analysis in the light of actual experimental conditions provided considerable justification for the assumption.

As applied in correlating overall mass-transfer data, the logarithmic mean driving force is defined as

$$(p^o - p_v)_{lm} = \frac{(p^o - p_2) - (p^o - p_1)}{\ln \dfrac{p^o - p_2}{p^o - p_1}} \quad , \tag{32}$$

where p_1 and p_2 refer to the partial pressure of the diffusing component at the inlet and outlet of the bed, respectively. In the present studies, it is apparent that these subscripts correspondingly refer to the partial pressures immediately upstream and downstream from the individual active pellet being considered, each active pellet being completely surrounded by inert pellets. Under the experimental

conditions, no p-dibromobenzene vapor was present in the inlet air, making the upstream partial pressure always zero, and Equation 32 therefore reduces to

$$(p^o - p_v)_{lm} = \frac{-p_2}{\ln \frac{p^o - p_2}{p^o}} = \frac{-p_2}{\ln \left(1 - \frac{p_2}{p^o}\right)} \quad . \qquad (33)$$

If considerable turbulent mixing occurred in the interstitial space surrounding each active pellet, the p-dibromobenzene vapor transferred from the solid surface would be continuously swept away from the surface and replaced with vapor-free air, making p_2 quite small and the logarithm of $1 - p_2/p^o$ approximately equal to $-p_2/p^o$. From Equation 33, the logarithmic mean driving force is then seen to be equal to the vapor pressure. Since all weight losses were corrected to the same temperature, the driving force would accordingly be constant.

Because each active pellet was completely isolated from all other active pellets, it appeared likely that considerable mixing and dilution would in fact be encountered. It was hoped that previous studies of fluid mixing in packed beds (6,7) might provide some indication of the degree of interstitial mixing to be expected, but the data reported pertain only to overall mixing phenomena.

Subject only to the assumption that the ratio p_2/p^o would be small under actual experimental conditions, then, it was anticipated that the data could be correlated by a straight line on a log-log plot of $k'M_m/G$ versus the Reynolds number, D_pG/μ . It will be noted that the mass flow

rate, G, appears in both the ordinate and abscissa of such a plot, and that the data might be correlated equally well by plotting k' itself against the Reynolds number. The particle diameter, D_p, was found to be a parameter when the data were plotted in this manner, however, whereas the data for all particle diameters could be correlated by a single straight line when G was included in the ordinate.

In summary, then, the first step in correlating the data was to plot k'/G' ($G' = G/M_m$) versus D_pG/μ for each combination of pellet diameter, orifice diameter, and position within the bed, and to draw least-square lines through the plotted data, the general equation of the lines being

$$k'/G' \times 10^6 = B \left(\frac{D_pG}{\mu}\right)^m \quad . \tag{34}$$

Equation 34 correlated all the data with an average deviation of less than 8 per cent. However, the lines are not completely independent of each other and cross-correlation was also required. The two different procedures used for this purpose will be described separately in the sections which follow.

Cross-Correlation, No Orifice

In comparing the initial correlations for the data obtained with no orifice across the entrance to the bed, it was first noted that the correlating lines for a given depth were practically identical, i.e., that mass-transfer rates were independent of radius, and the data for each depth were therefore combined on a single plot. Plots for each of the depths investigated are presented in Figures 8-10. Slopes

and intercepts of the least-square lines (not shown in the figures) through the combined data were then plotted against depth as shown in Figure 11, and smooth curves drawn through the points. The lines shown in Figures 8-10 have been drawn using smoothed values of both slope and intercept, and therefore indicate the validity of the complete correlation.

Pellet diameter was not found to be a parameter in plotting either slope or intercept versus depth. Further support for this conclusion is presented in Figure 17, in which data for all three pellet diameters taken at the same position in the bed are consolidated.

It will be noted that the flat portions of both curves in Figure 11 lie below all the points which they presumably correlate, suggesting that the lines should be raised. Actually, the correlation presented is also influenced by data taken with the 1- and 2-inch orifices, since these data and those for no orifice should become identical at some bed depth sufficiently far from the entrance and should remain unchanged thereafter. Thus, the flat portions of the curves in Figure 11 have been pulled down slightly to bring the correlation into agreement with those for the 1- and 2-inch orifices.

Cross-Correlation, Orifice Entry

In cross-correlating the data taken when the air entered the bed through an orifice, it was not sufficient merely to draw smooth curves through the cross-plotted data in view of certain other requirements: (1) the transverse

and longitudinal profiles had to be in agreement at comparable points; (2) the correlations for both the 1- and 2-inch orifices and for no orifice had to become identical at some sufficient bed depth and remain unchanged thereafter; and (3) transverse profiles had to have zero slope at zero radius. The first requirement in particular was found to be exceedingly helpful in determining how the correlating lines should be drawn.

With these considerations in mind, then, the slopes and intercepts of all the least-square lines on the original data plots were plotted against both radius at constant depth and depth at constant radius, for each of the two orifices. It was immediately observed that the variation of slope with radius and with depth was completely random, but that distinct trends were present in the intercept plots. The first observation suggested that all the data should be correlated with lines of the same slope, and horizontal lines were therefore drawn through the points on each slope cross-plot and adjusted until all were in agreement. The average slope thus obtained was -0.35. The no-orifice data for bed depths greater than 1/2 inch were included in this step, as has been noted previously.

New lines, having a common slope of -0.35, were then drawn through each set of data on the original data plots, and the intercepts of these lines determined and plotted against radius and against depth. Smooth curves were drawn through the points in keeping with the qualitative requirements noted above, and the smoothed intercepts thus obtained

were then used to put the final correlating lines on the original data plots.

The decision to determine first the smoothed slope and then the smoothed intercepts was somewhat arbitrary, since the determinations might equally well have been made in the reverse order. As a check against the suitability of the order actually used, the reverse-order determination was carried out for the 1-inch orifice data. Smooth curves were drawn through the transverse and longitudinal profiles of intercepts taken from the original least-square lines through the data, and new "best" lines were then drawn through the original data using the smoothed intercept values. The variation in slope of these lines with radius and with depth was found to be as random as that of the original least-square lines, and again the use of an average slope seemed warranted. When the average was determined, it was found to agree closely with that previously established, -0.35, and the two methods of correlation therefore yield identical results.

The final correlating lines and their agreement with the original data can be seen in Figures 12-16. Figures 12a-e are for the 1-inch orifice with 1/8-inch pellets; Figures 13a-g, for the 1-inch orifice with 1/4-inch pellets; Figure 14, for the 1-inch orifice with 1/2-inch pellets; Figure 15a-c, for the 2-inch orifice with 1/8-inch pellets; and Figures 16a-f, for the 2-inch orifice with 1/4-inch pellets.

The smoothed transverse and longitudinal profiles fitted the data for all pellet diameters equally well, and it was therefore concluded that pellet diameter was not a parameter beyond its use as the characteristic length in the Reynolds number, as was the case with no orifice. This is also indicated in Figure 18, which shows the consolidated data for all three pellet diameters taken with the 1-inch orifice at a depth of 2 inches and a radius of 1 inch. A comparison of Figures 17 and 18 also shows that at this position the data for the 1-inch orifice are in agreement with those for no orifice, the same line having been used to correlate both.

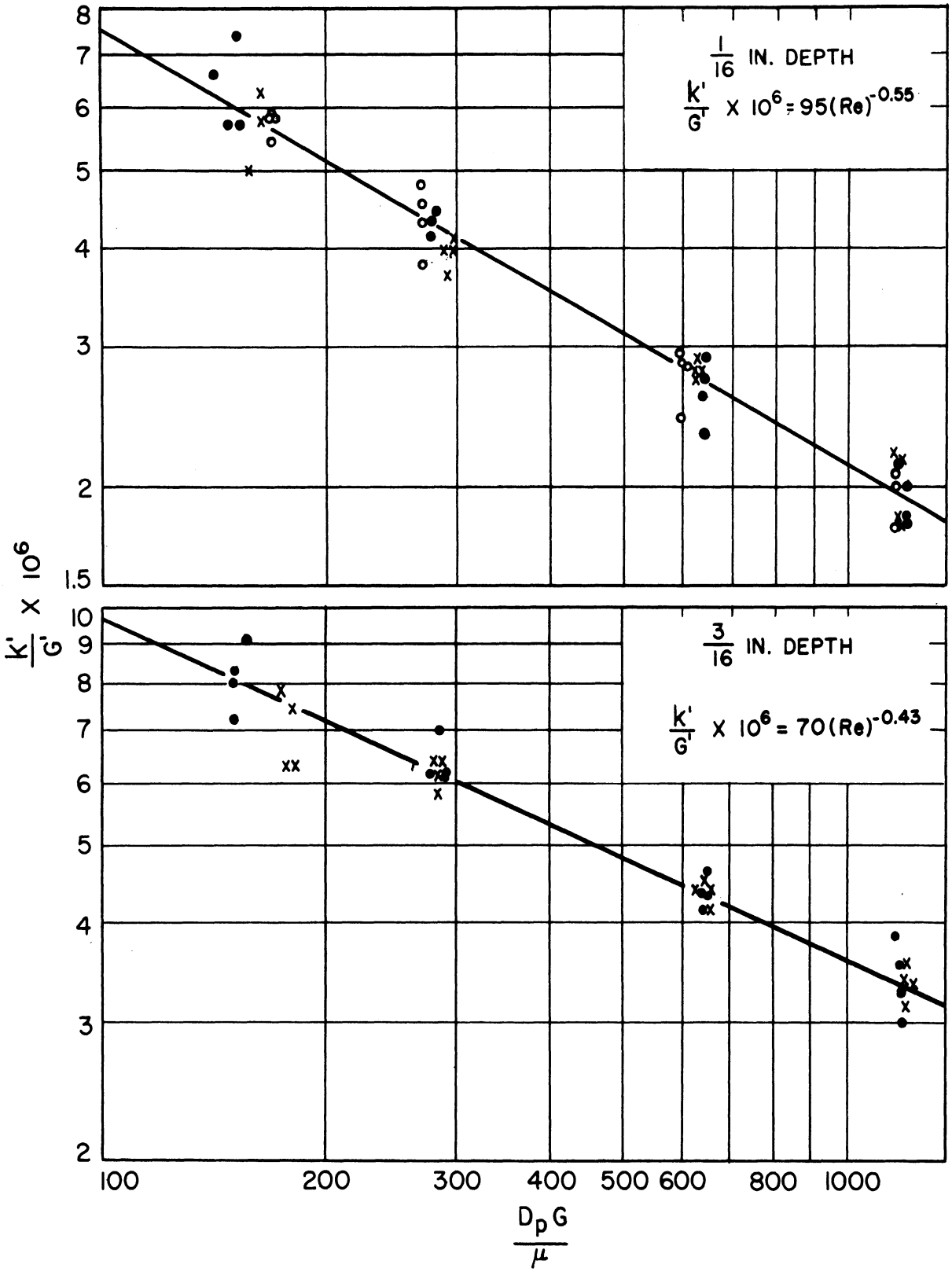

Fig. 8a. Original Data Plot, $\frac{k'}{G'}$ vs Re, for No Orifice, $\frac{1}{8}$ in. Pellets.
(x = 1 in. radius, o = $1\frac{1}{2}$ in. radius, ● = 2 in. radius)

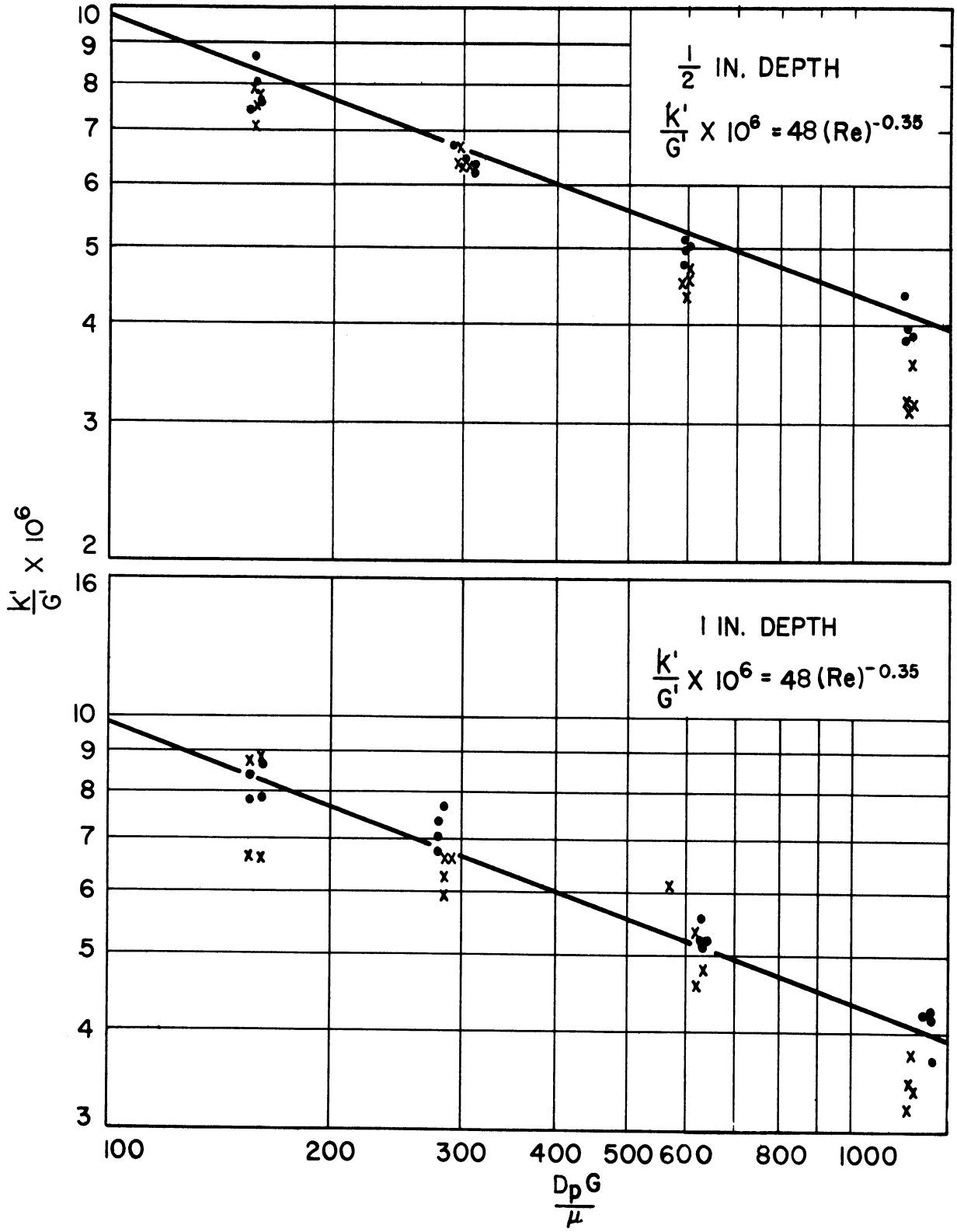

Fig. 8b. Original Data Plot $\frac{k'}{G'}$ vs Re, for No Orifice, $\frac{1}{8}$ in. Pellets.
(x = 1 in. radius, • = 2 in radius

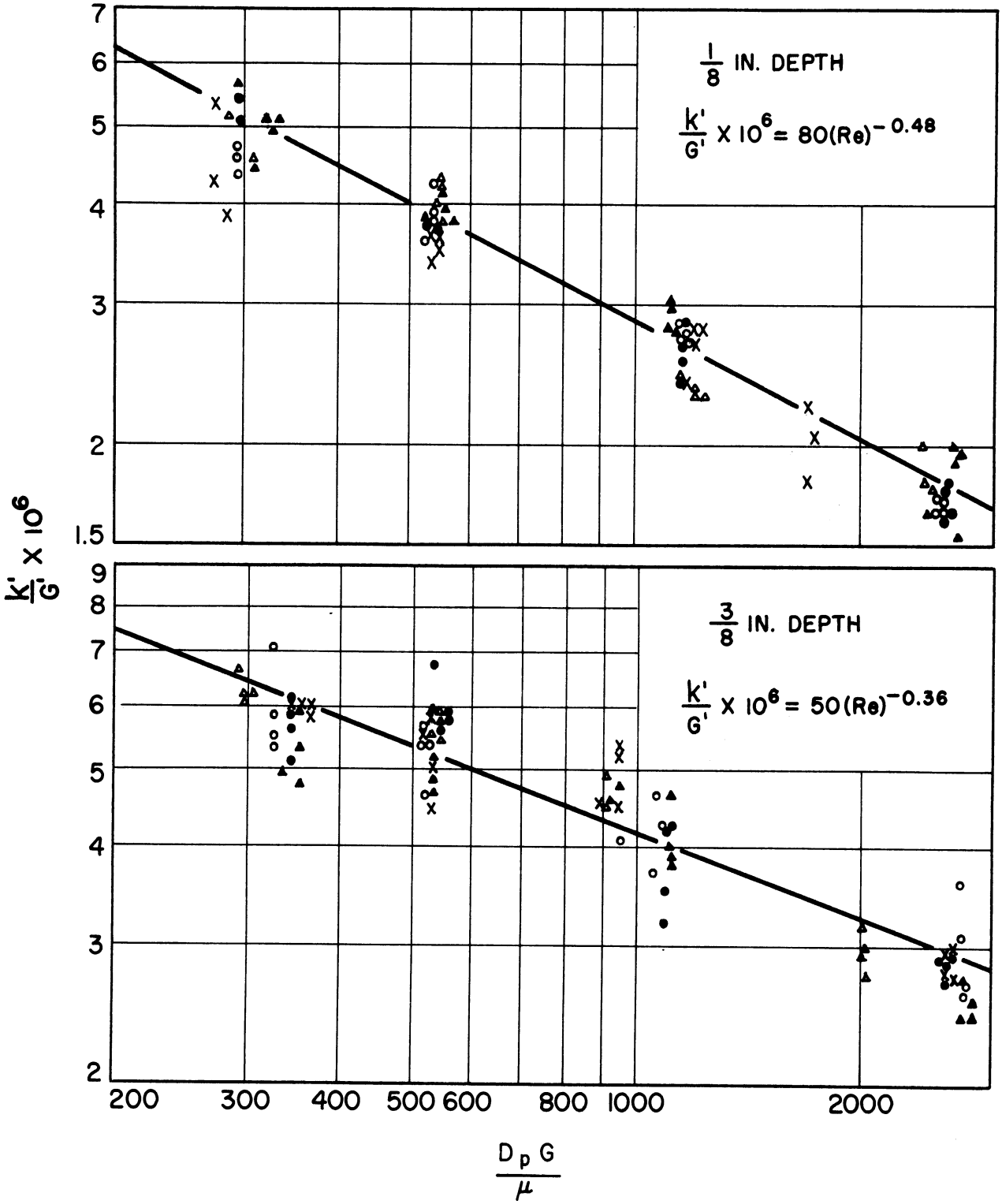

Fig. 9a. Original Data Plot, $\frac{k'}{G'}$ vs Re, for No Orifice, $\frac{1}{4}$ in. Pellets.
(Δ = 0 in. radius, $\blacktriangle$ = $\frac{1}{2}$ in. radius, x = 1 in. radius, o = $1\frac{1}{2}$ in. radius, $\bullet$ = 2 in. radius)

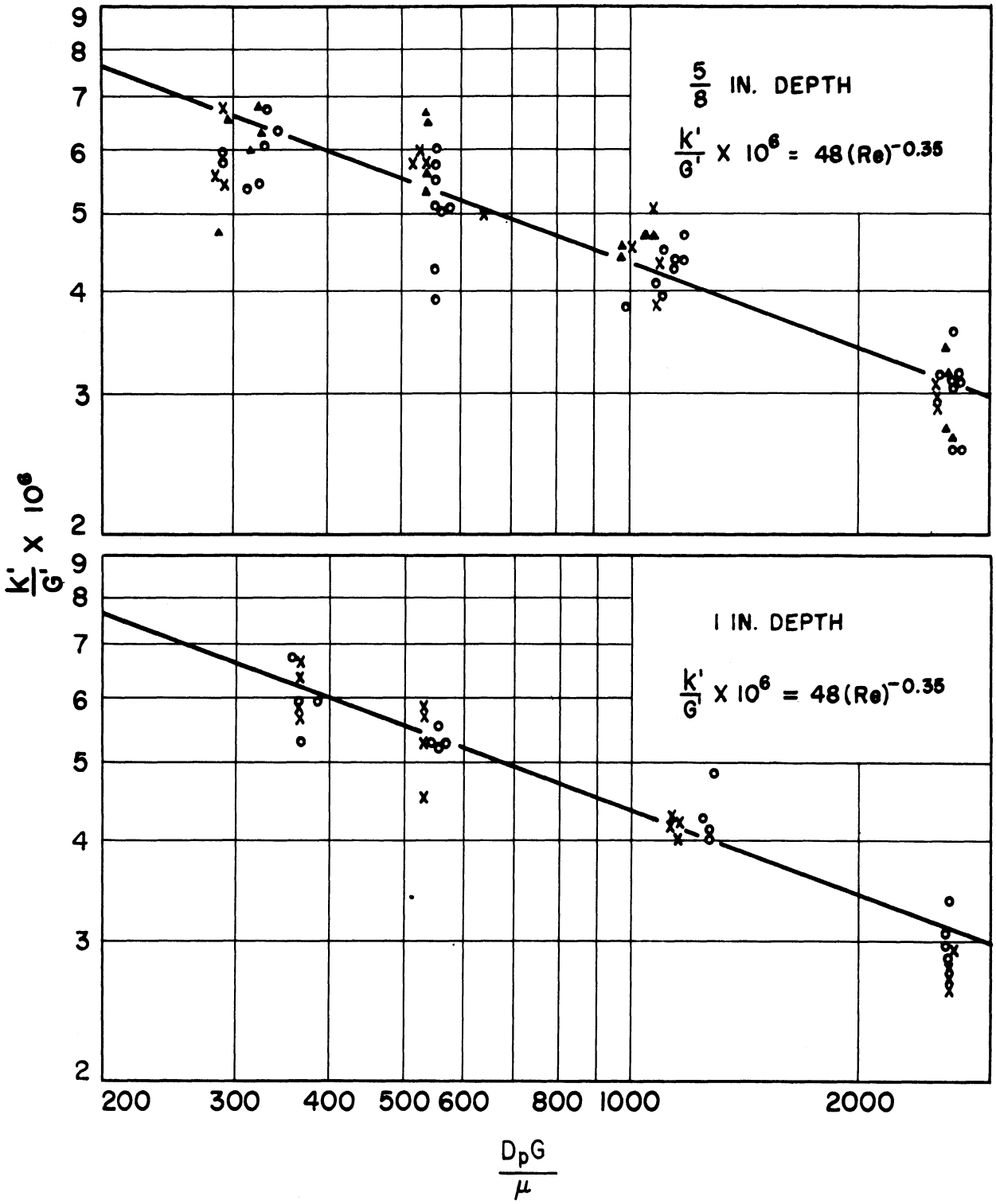

Fig. 9b. Original Data Plot, $\frac{k'}{G'}$ vs Re, for No Orifice, $\frac{1}{4}$ in. Pellets.

(▲ = $\frac{1}{2}$ in. radius, x = 1in. radius, o = $1\frac{1}{2}$ in. radius, ● = 2 in. radius)

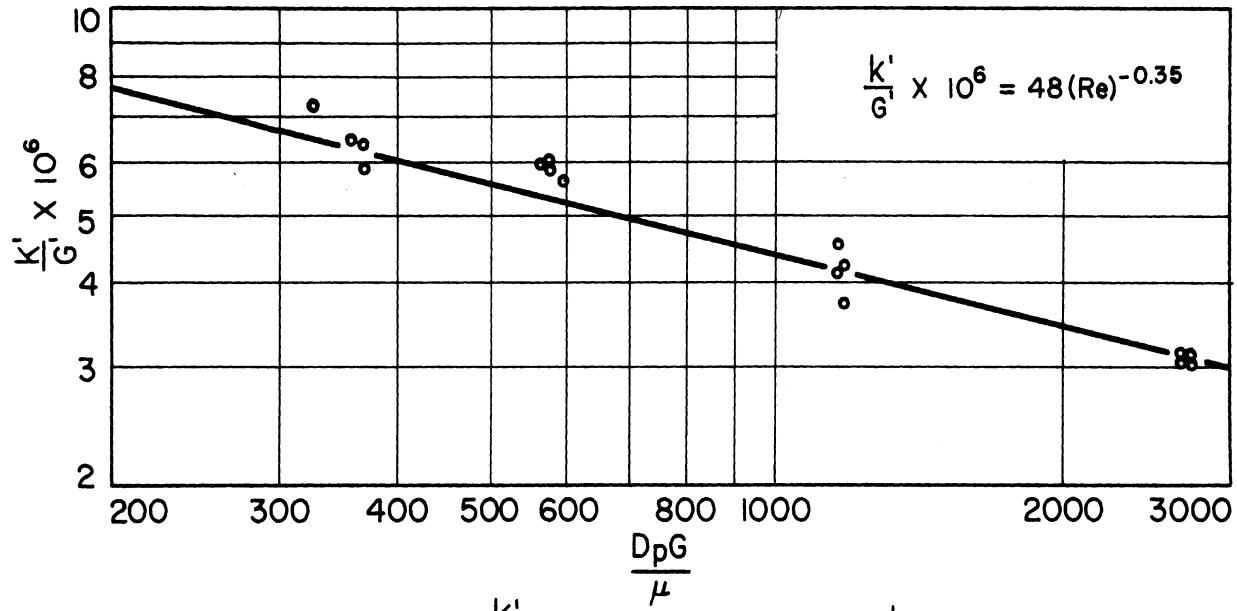

Fig. 9c. Original Data Plot, $\frac{k'}{G'}$ vs Re, for No Orifice, $\frac{1}{4}$ in. Pellets 2 in. Depth, 2 in. Radius.

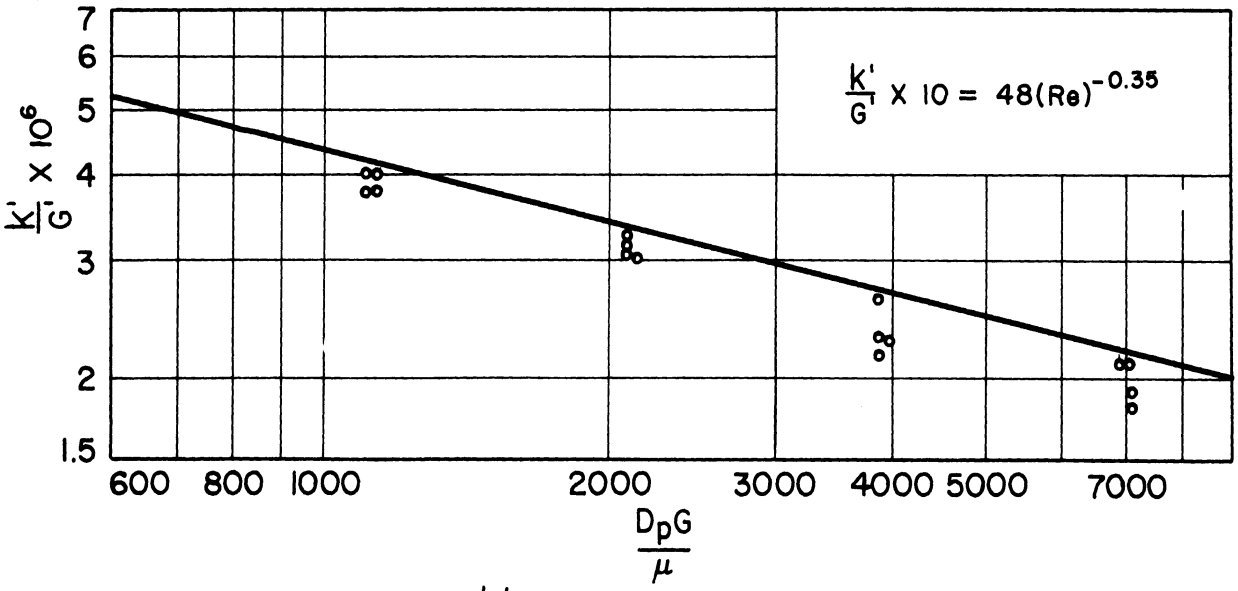

Fig. 10 Original Data Plot, $\frac{k'}{G'}$ vs Re, for No Orifice, $\frac{1}{2}$ in. Pellets 1 in. Depth, $1\frac{1}{2}$ in. Radius.

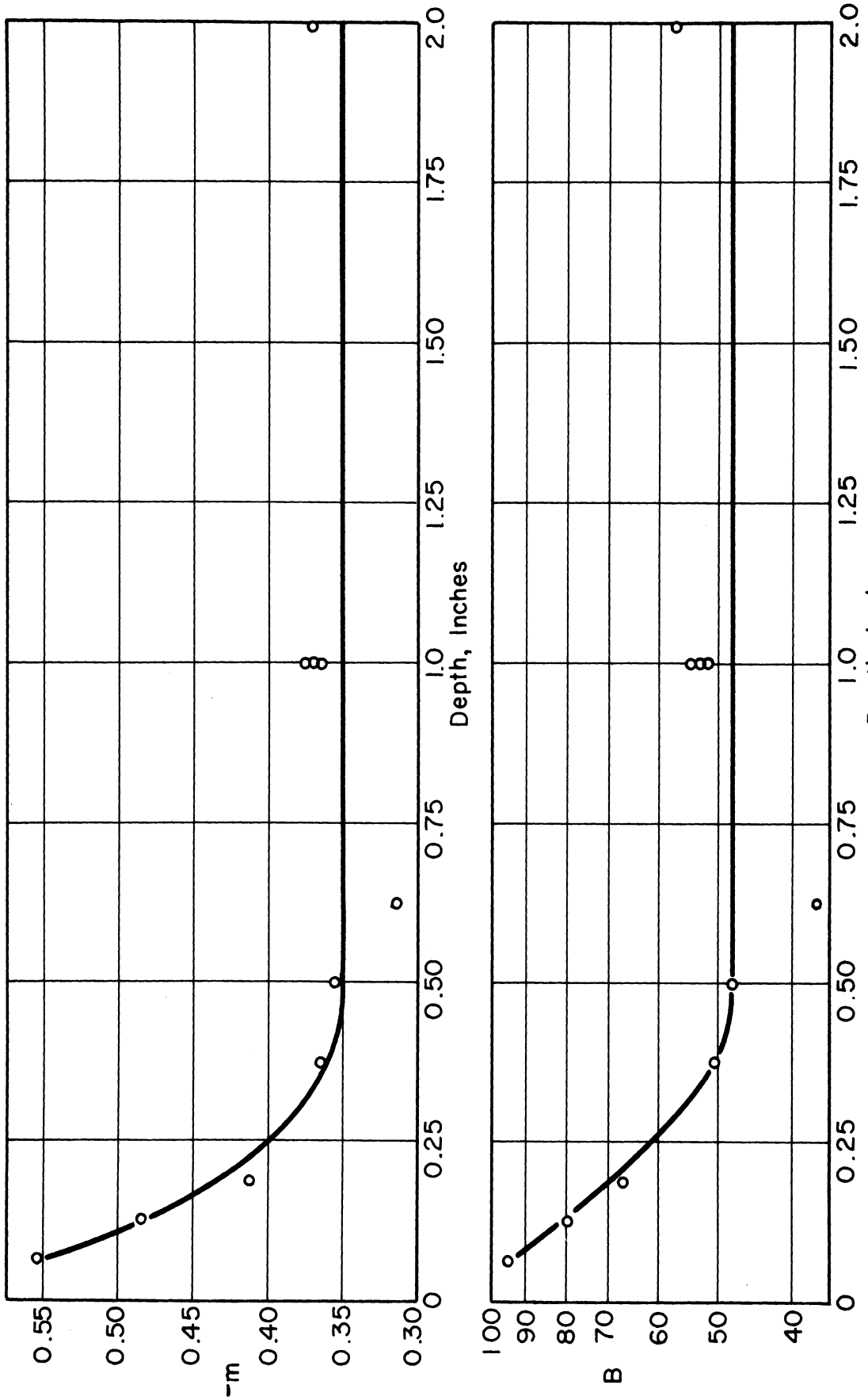

Fig. 11. Effect of Depth on Mass Transfer Rate – Variation of Constants B and m in the Equation $\frac{K'}{G'} \times 10^6 = B\left(\frac{D_p G}{\mu}\right)^m$

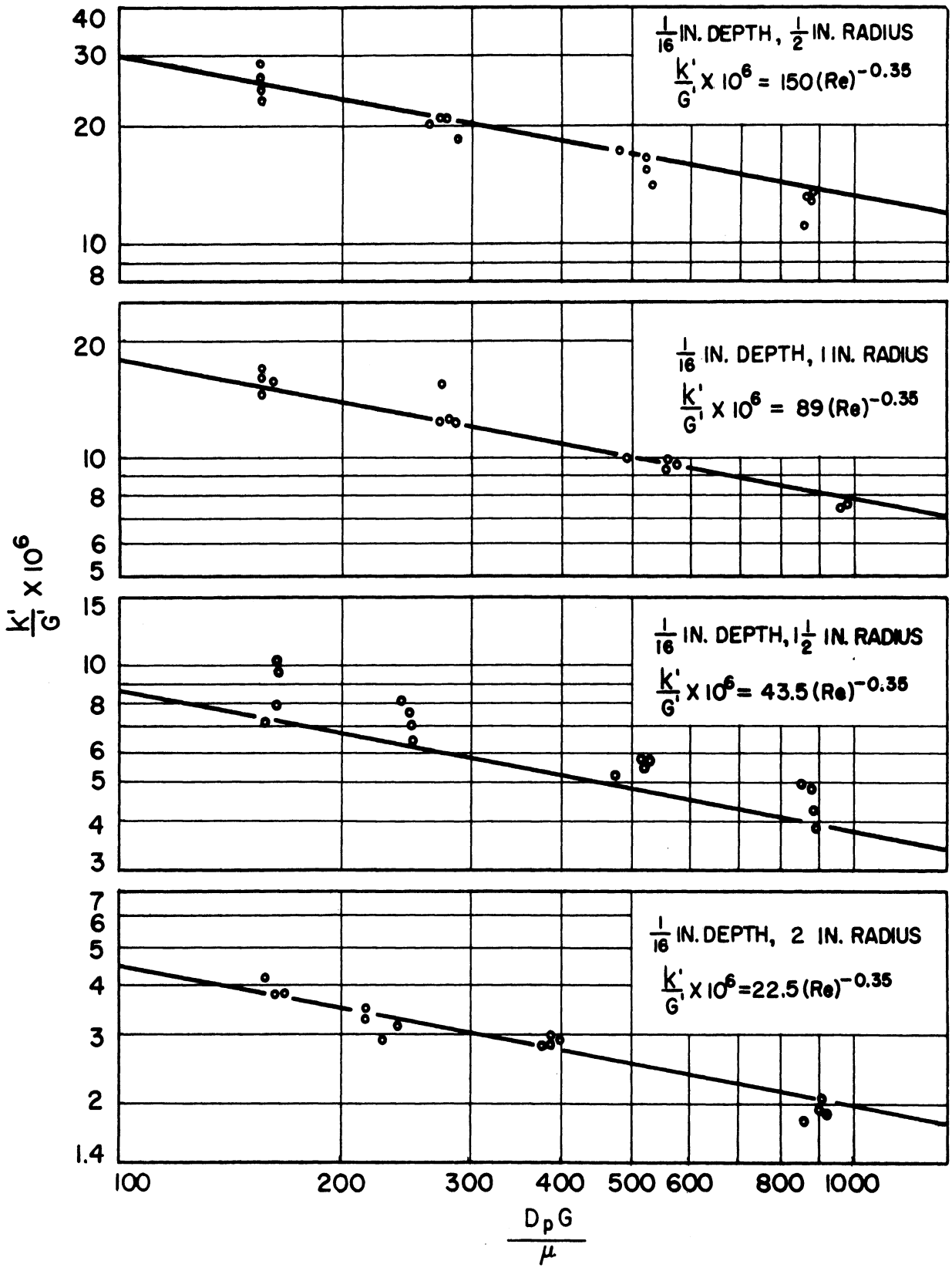

Fig.12a. Original Data Plots, $\frac{k'}{G'}$ vs Re, for 1 inch Orifice, $\frac{1}{8}$ in. Pellets

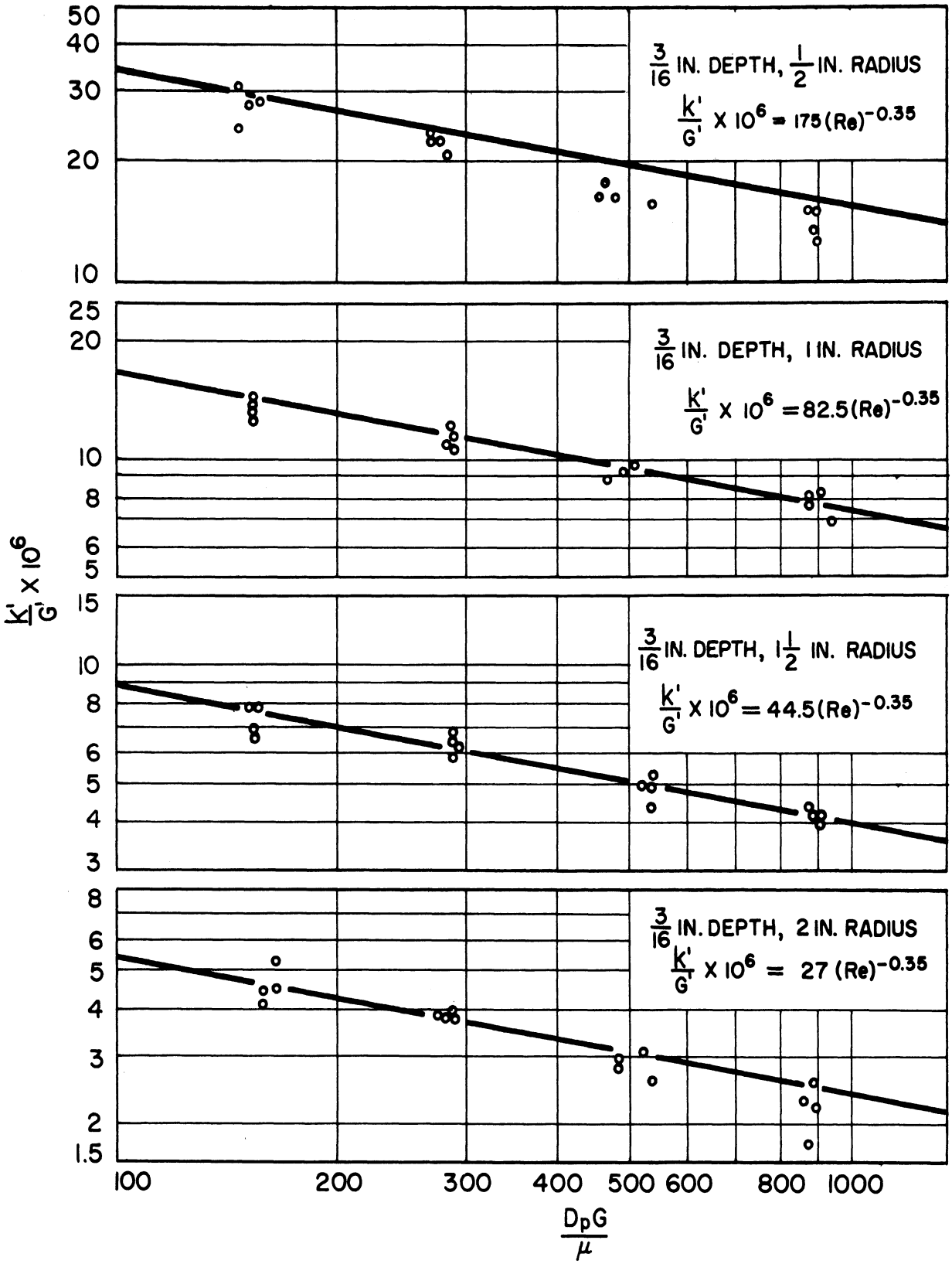

Fig. 12b. Original Data Plots, $\frac{K'}{G'}$ vs Re, for 1 inch Orifice; $\frac{1}{8}$ inch Pellets, (cont'd)

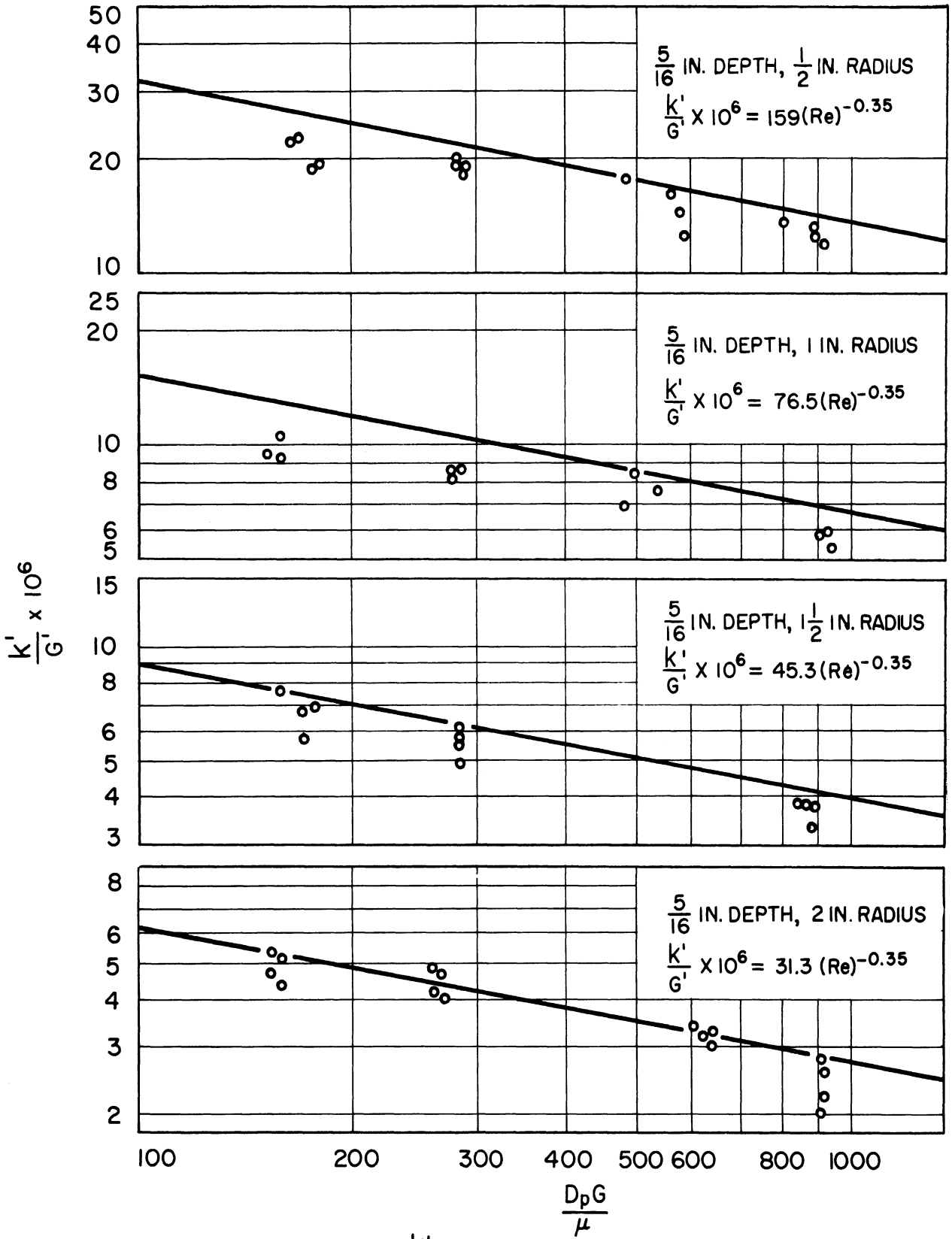

Fig. 12c. Original Data Plot, $\frac{k'}{G'}$ vs Re, for 1 inch Orifice, $\frac{1}{8}$ in. Pellets (cont'd)

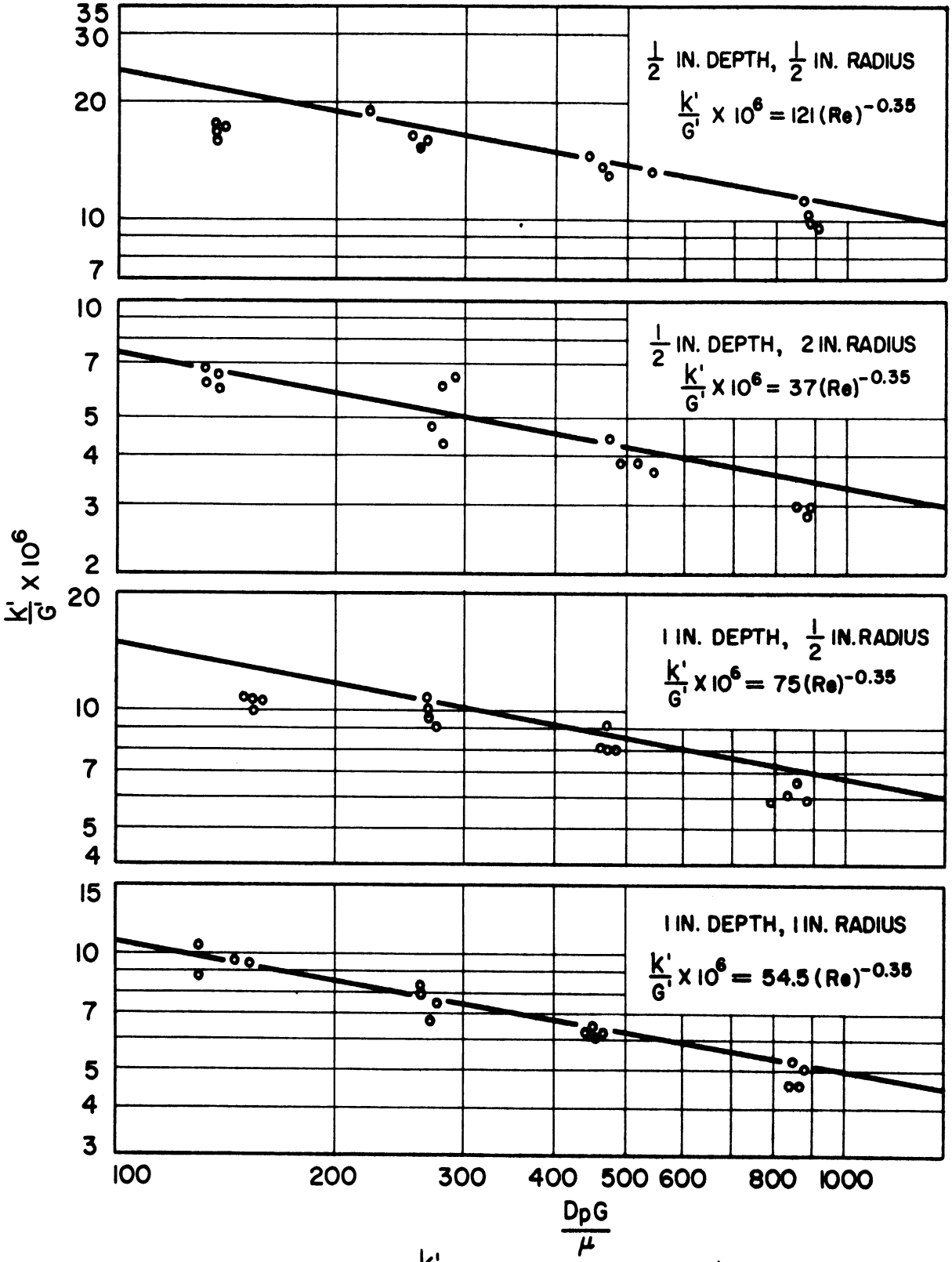

Fig.12d. Original Data Plots, $\frac{k'}{G'}$ vs Re, for 1 in. Orifice, $\frac{1}{8}$ in. Pellets (cont'd)

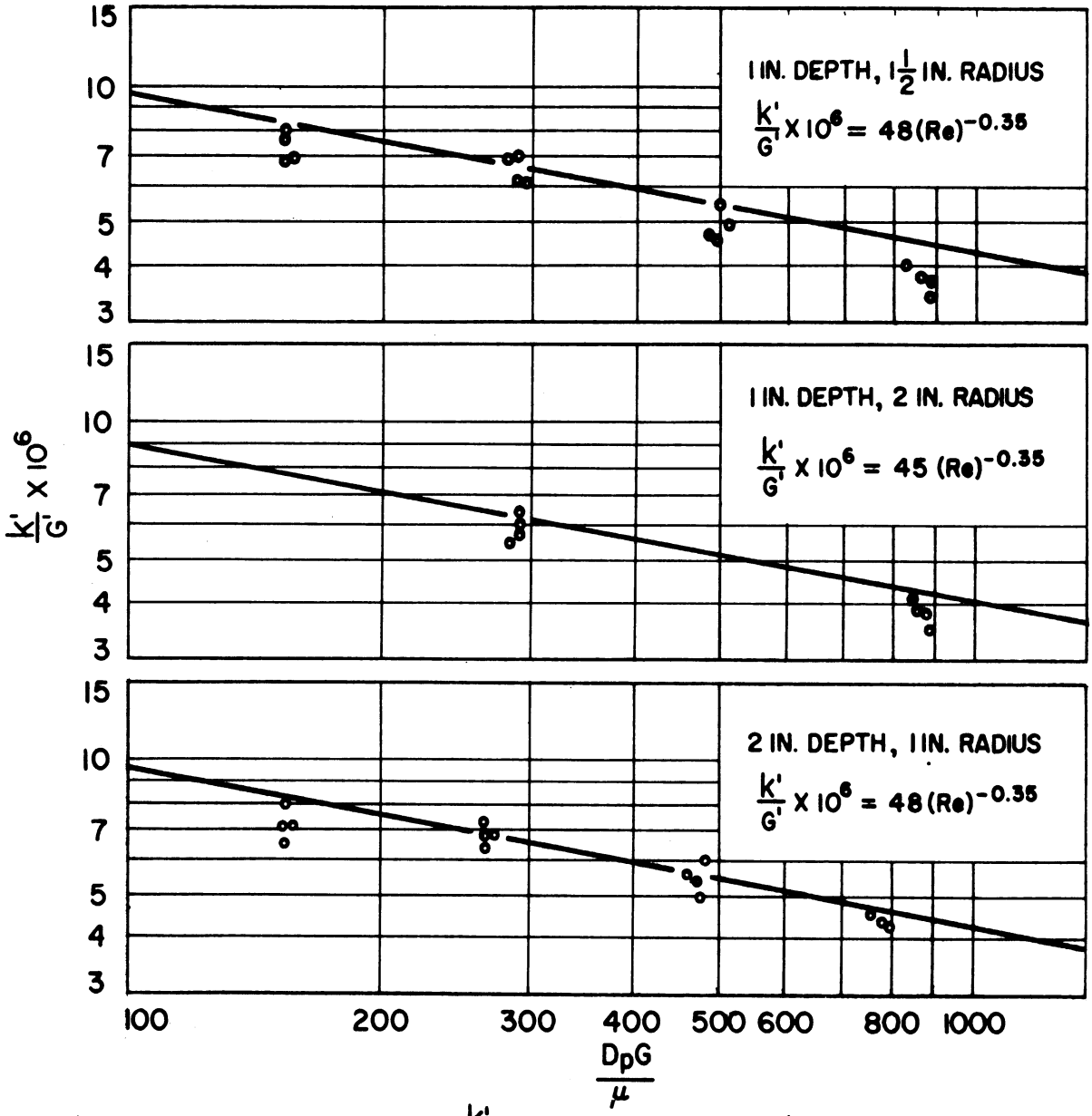

Fig.12e. Original Data Plots, $\frac{k'}{G'}$ vs Re, for 1 in. Orifice, $\frac{1}{8}$ in. Pellets (concluded)

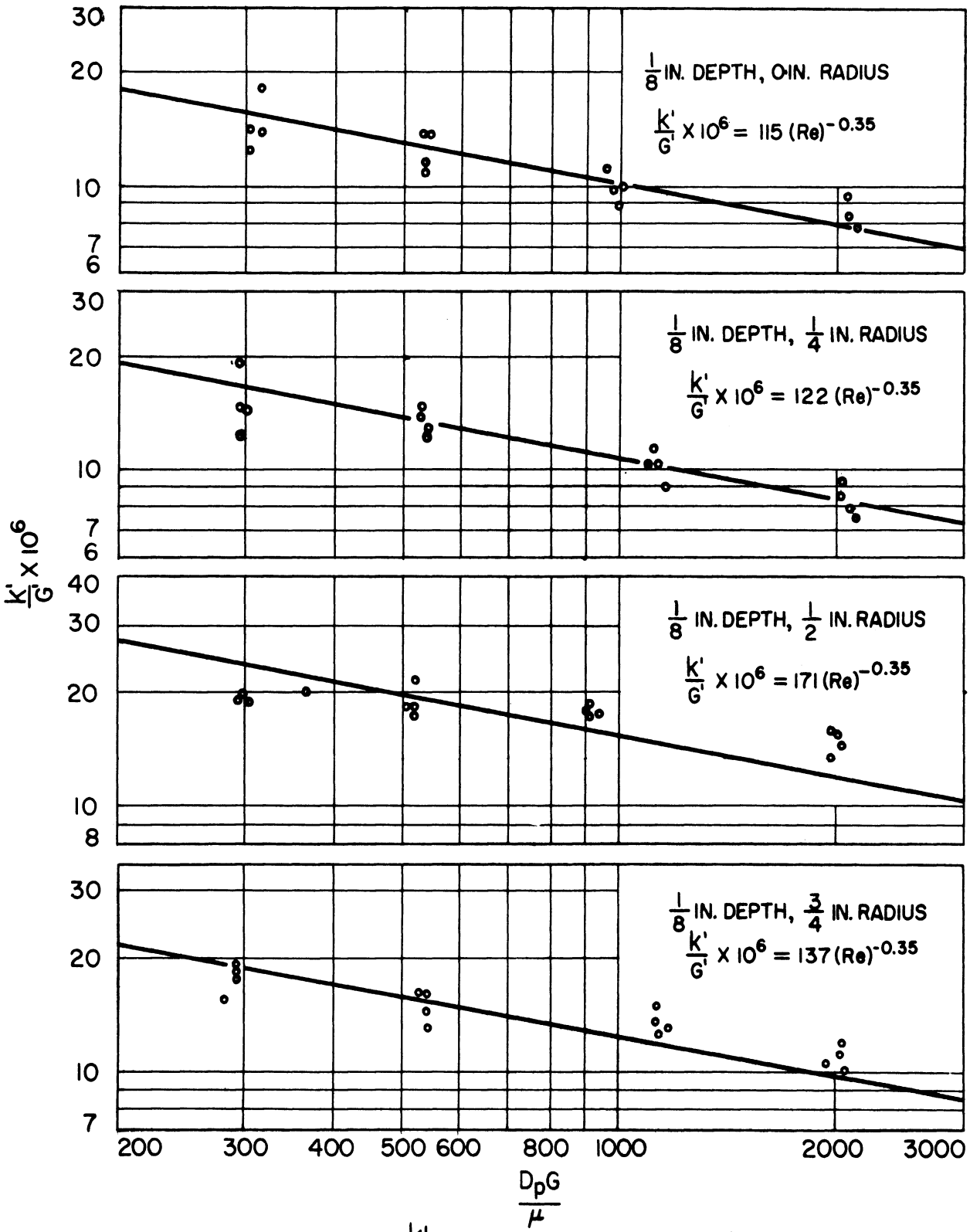

Fig.13a. Original Data Plots, $\frac{k'}{G'}$ vs Re, for 1 inch Orifice, $\frac{1}{4}$ inch Pellets.

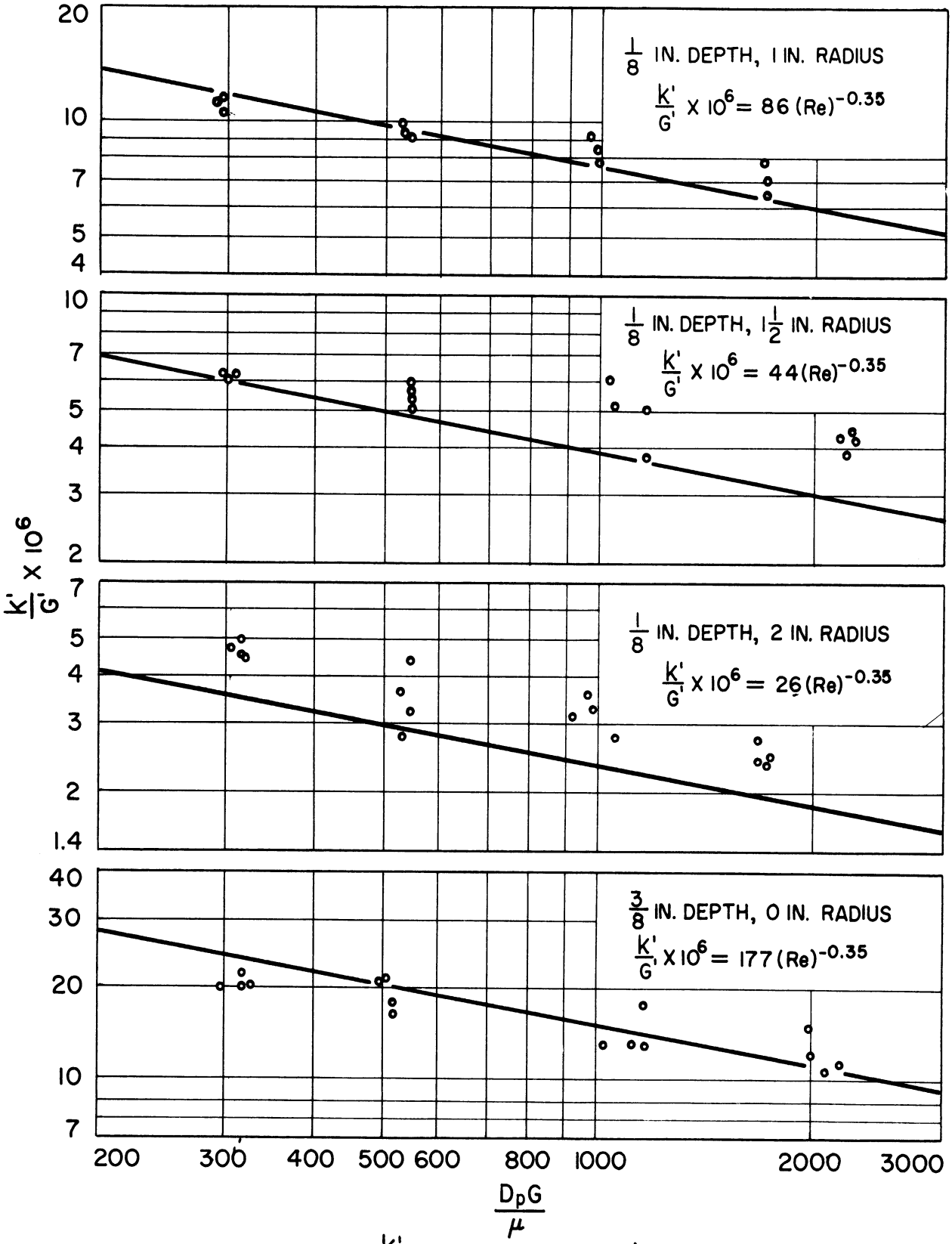

Fig.13b. Original Data Plots, $\frac{k'}{G'}$ vs Re, 1 in. Orifice, $\frac{1}{4}$ in. Pellets. (cont'd)

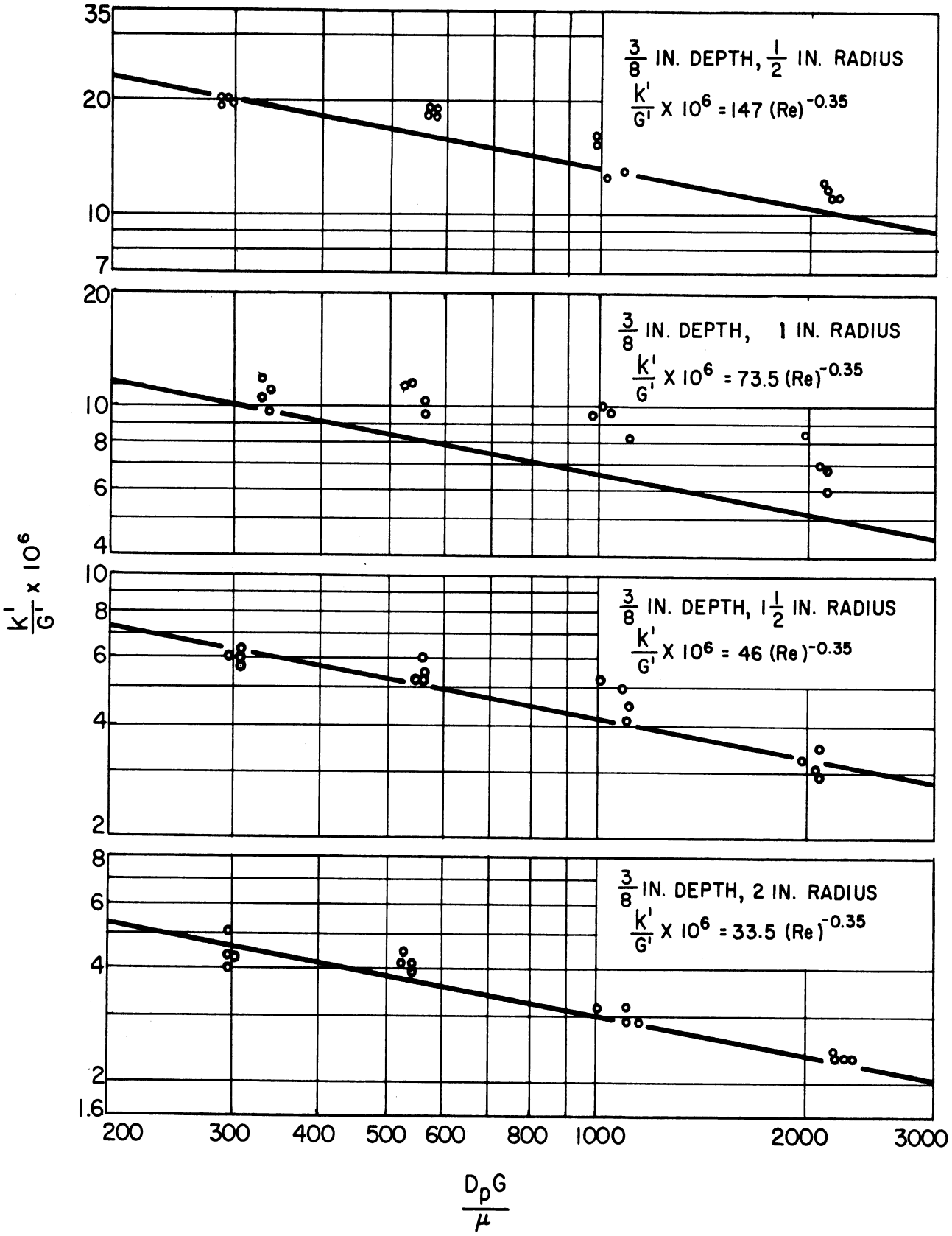

Fig.13c. Original Data Plot, $\frac{k'}{G'}$ vs Re, for 1 inch Orifice, $\frac{1}{4}$ in. Pellet (cont'd)

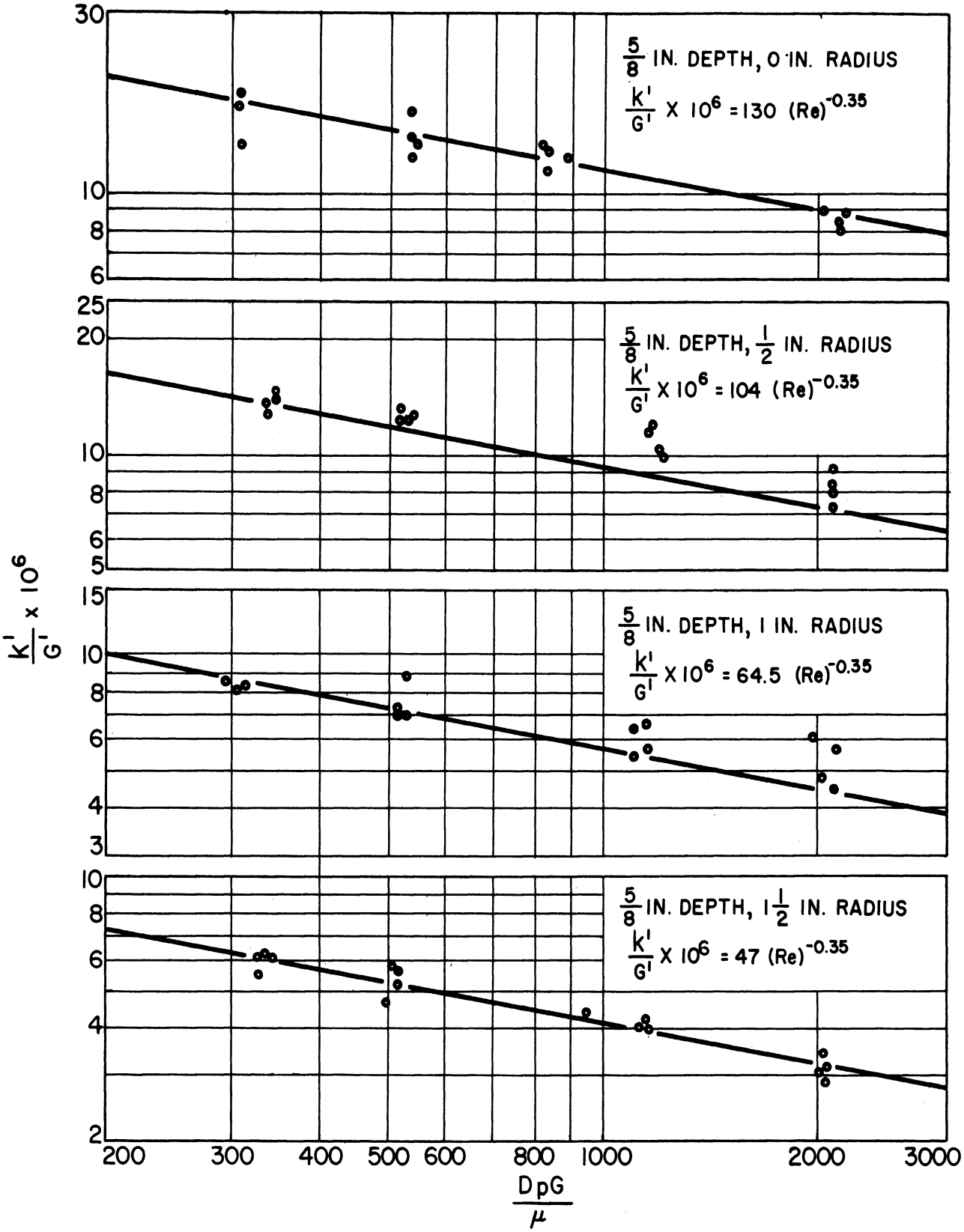

Fig.13d. Original Data Plot, $\frac{k'}{G'}$ vs Re, for 1 inch Orifice, $\frac{1}{4}$ in. Pellet (cont'd)

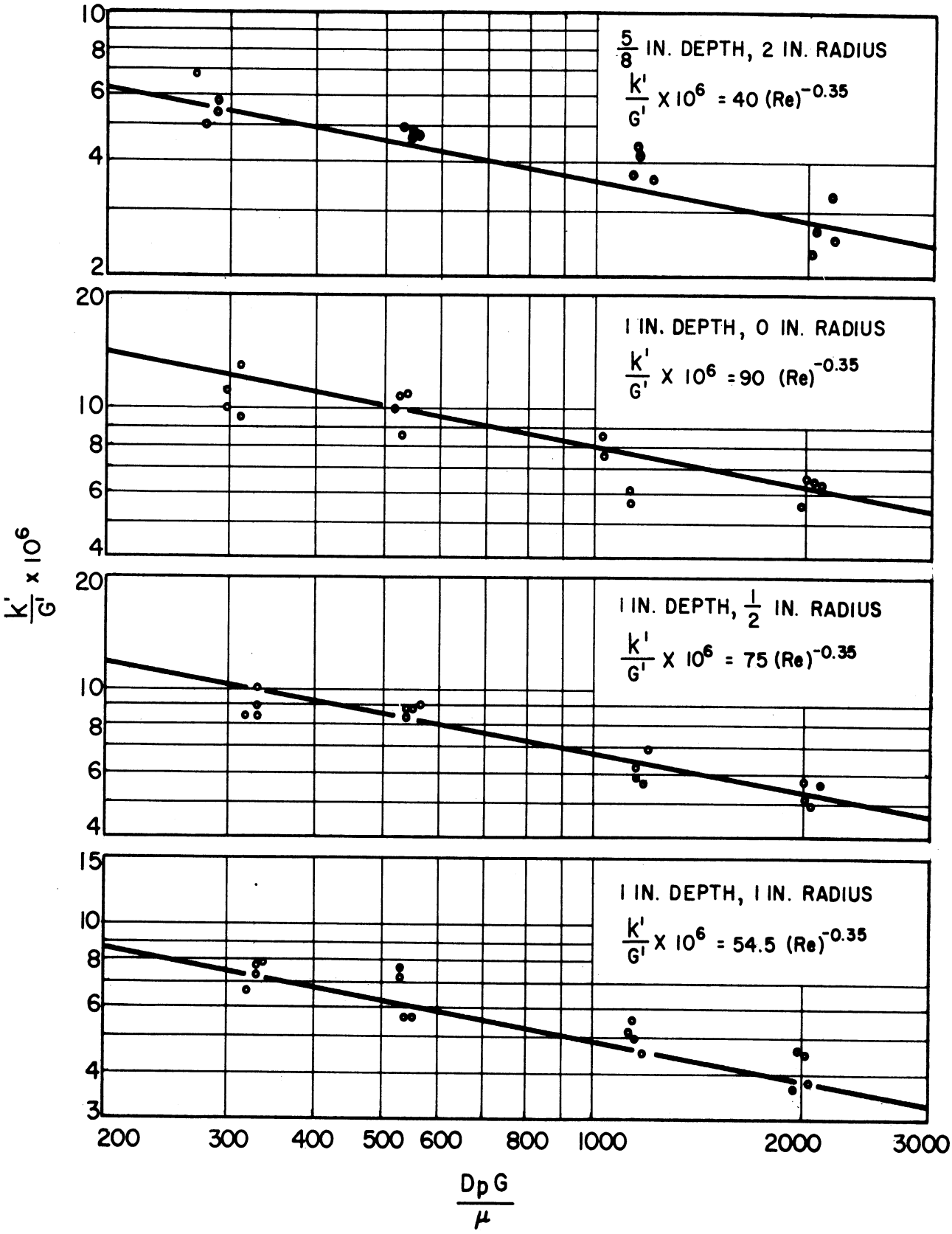

Fig.13e. Original Data Plot, $\frac{k'}{G'}$ vs Re, for 1 inch Orifice, $\frac{1}{4}$ in Pellet (cont'd)

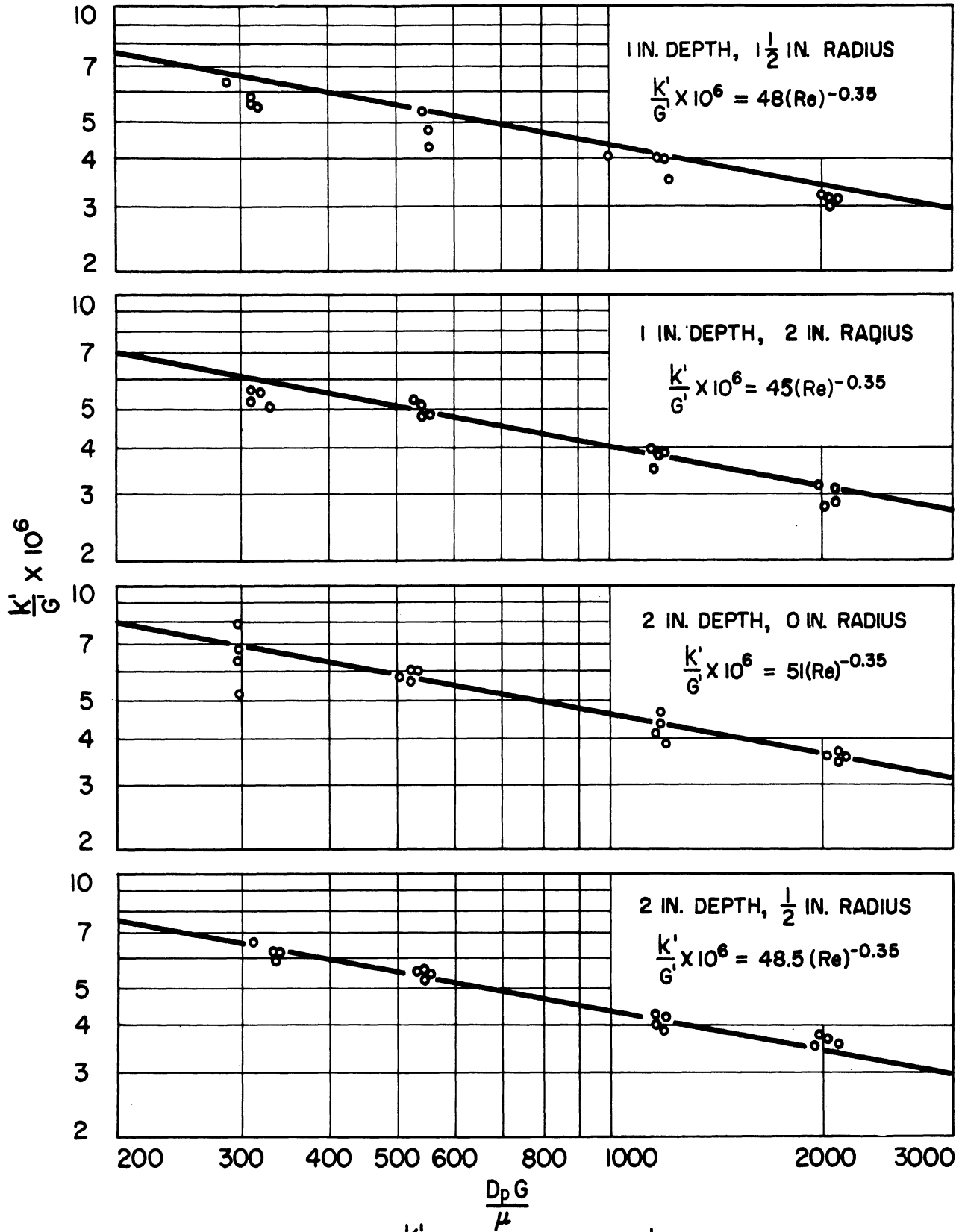

Fig.13f. Original Data Plot, $\frac{k'}{G'}$ vs Re, 1 in. Orifice, $\frac{1}{4}$ in. Pellets, (cont'd)

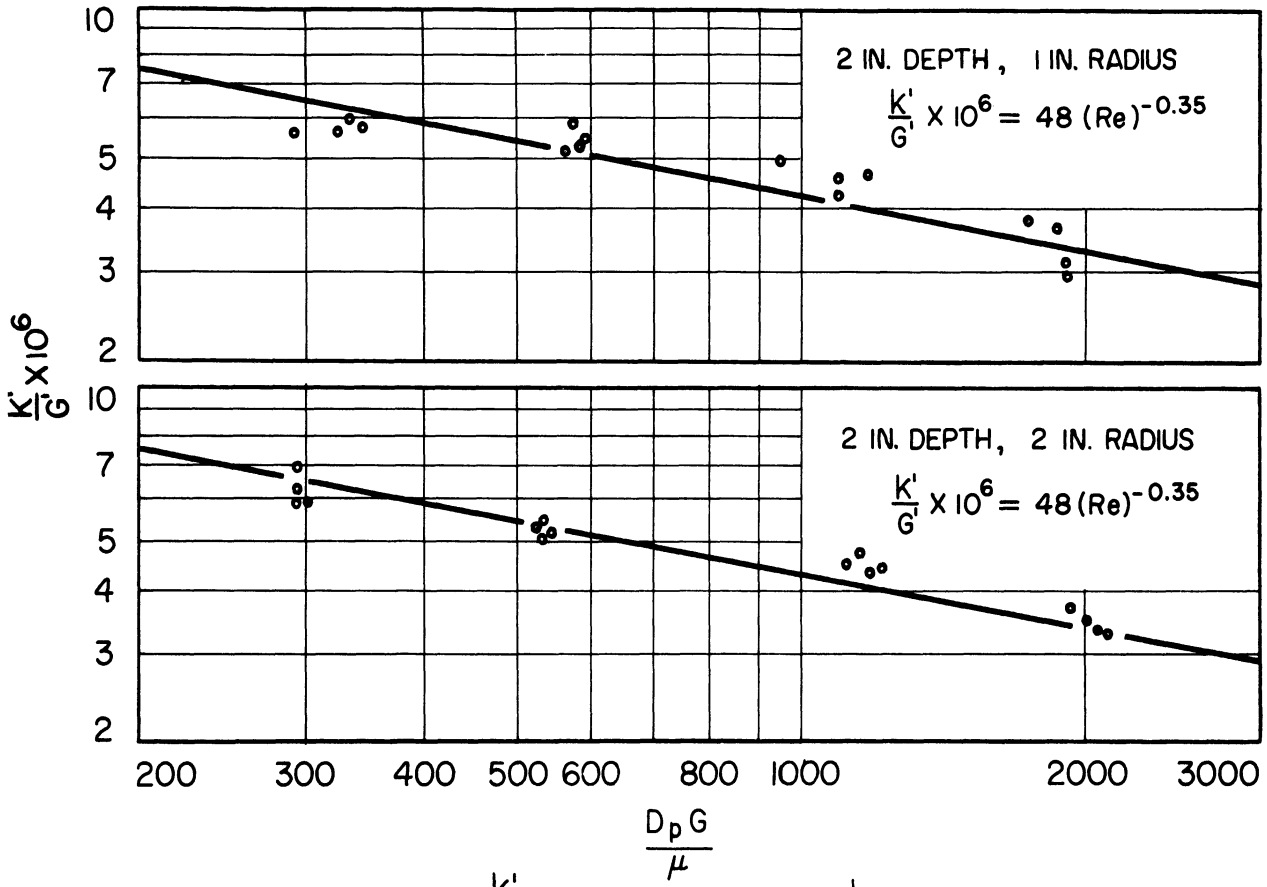

Fig.13g. Original Data Plots, $\frac{k'}{G'}$ vs. Re, 1 in. Orifice, $\frac{1}{4}$ in. Pellets. (concluded)

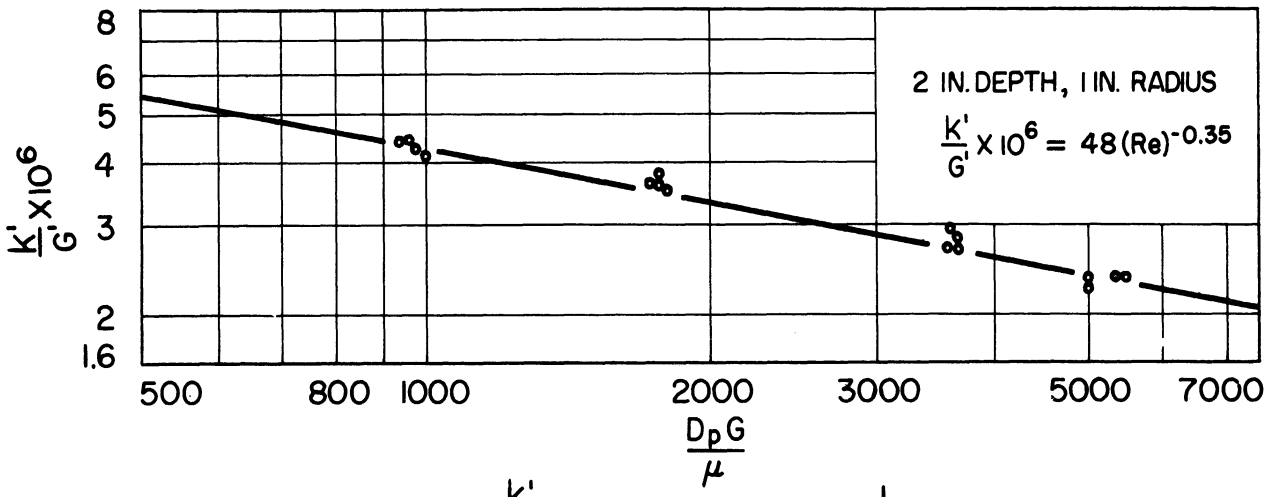

Fig.14. Original Data Plot, $\frac{k'}{G'}$ vs Re, 1 in. Orifice, $\frac{1}{2}$ in. Pellets.

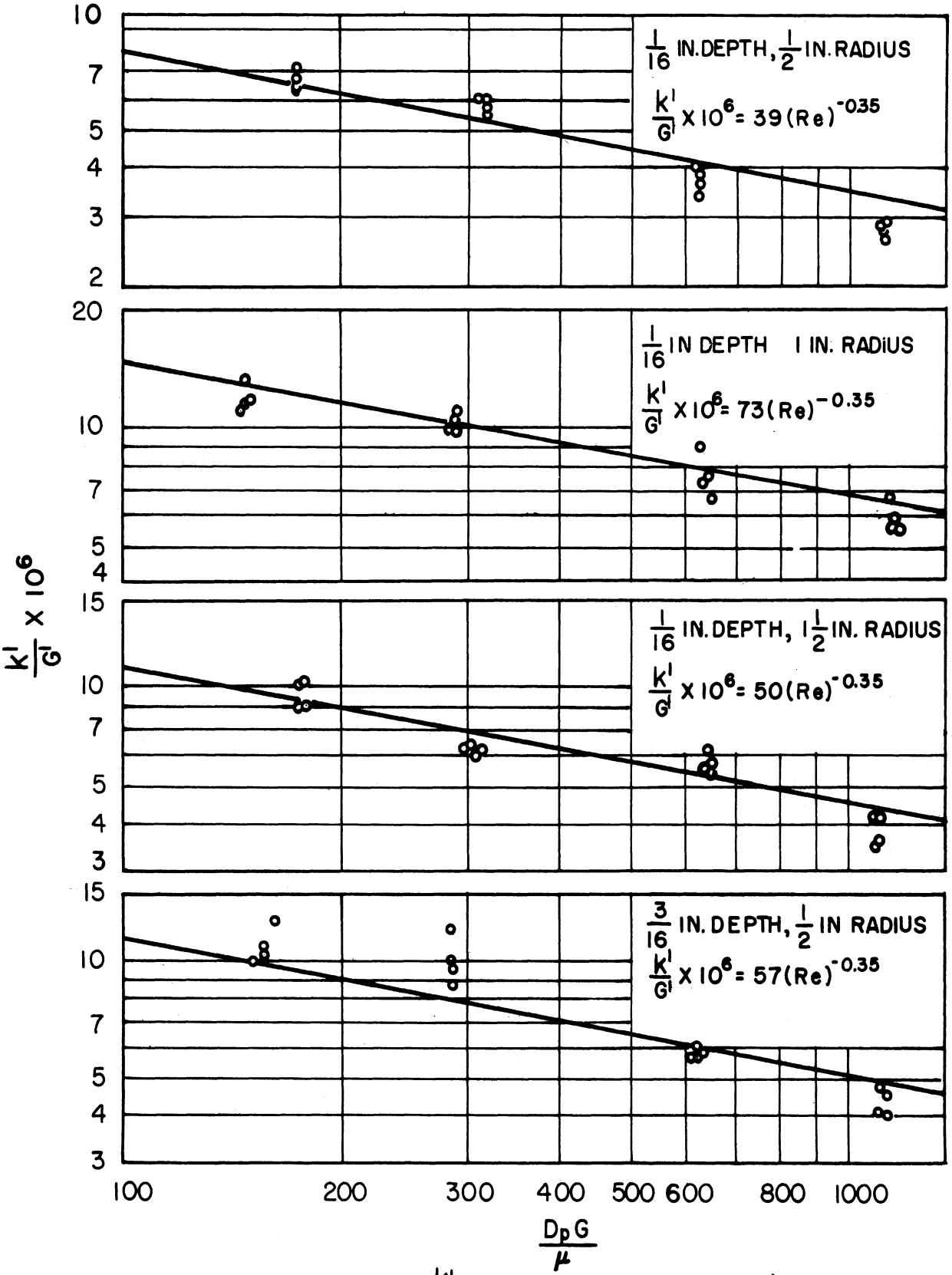

FIG.15a. Original Data Plot, $\frac{k'}{G'}$ vs Re, for 2 inch Orifice, $\frac{1}{8}$ in. Pellets

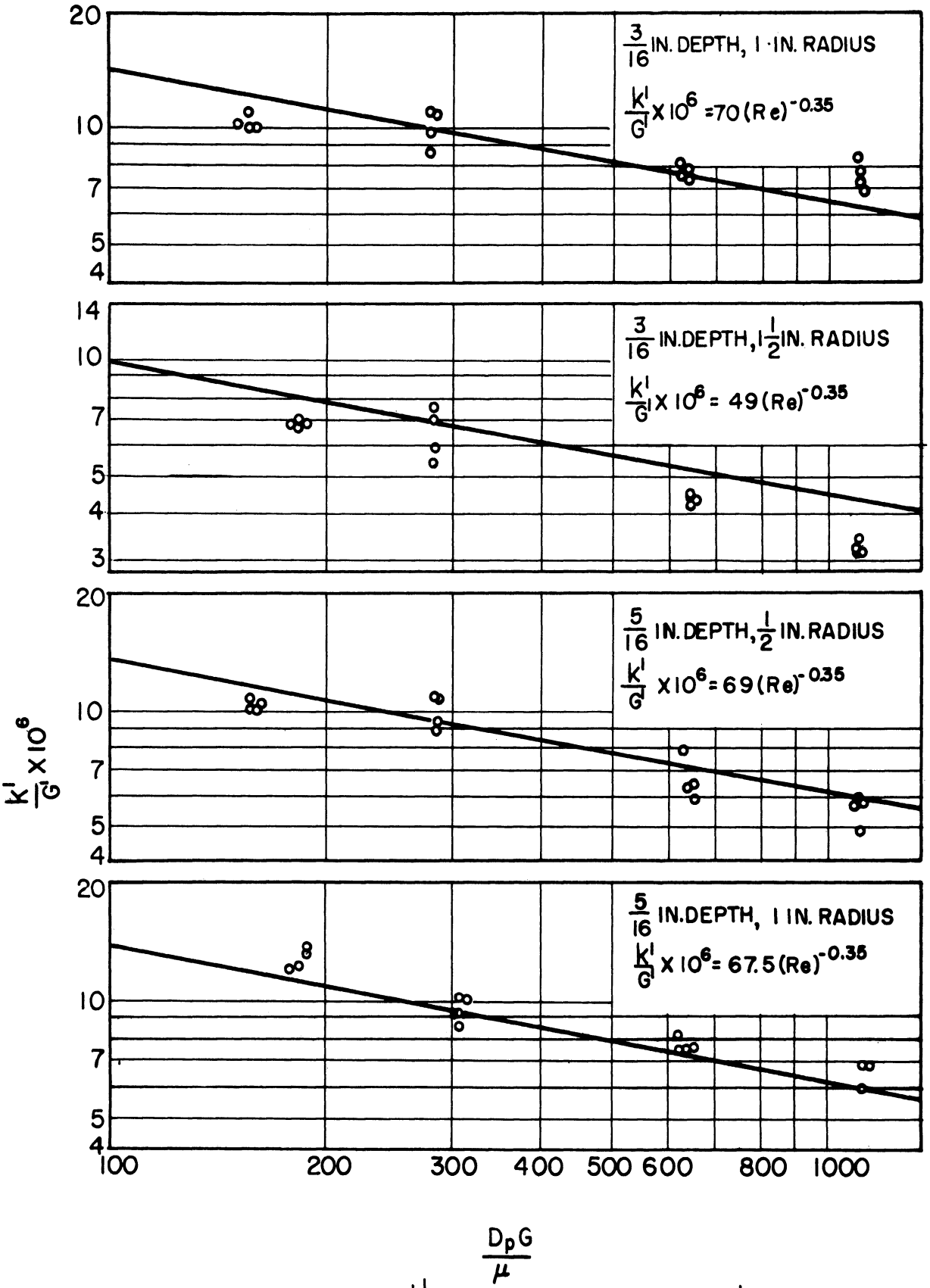

Fig. 15b. Original Data Plot, $\frac{k'}{G'}$ vs Re, for 2 Inch Orifice, $\frac{1}{8}$ Inch Pellet (cont'd)

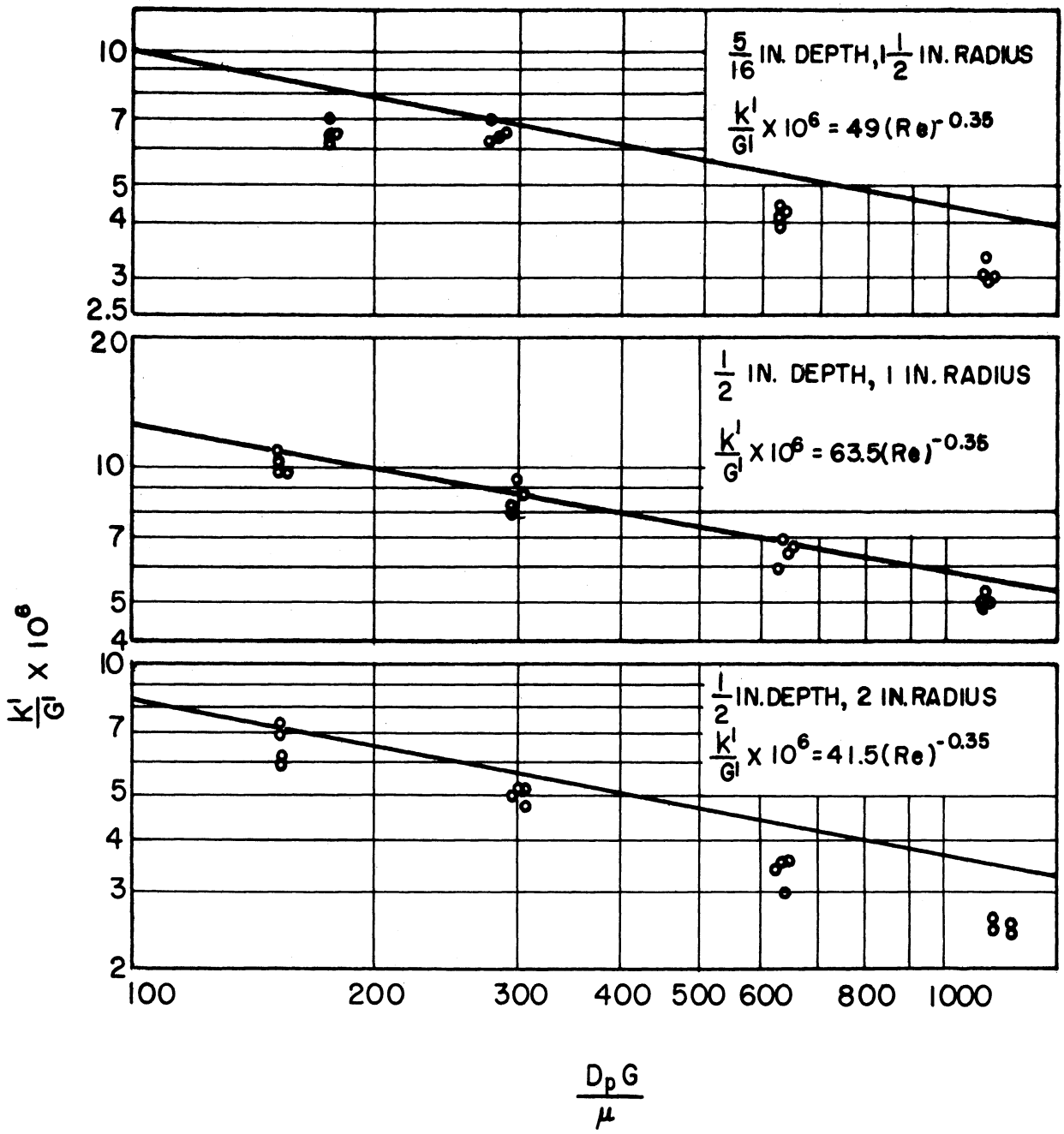

Fig. 15c. Original Data Plots, $\frac{k'}{G'}$ vs Re; 2 Inch Orifice, $\frac{1}{8}$ Inch Pellets (concluded)

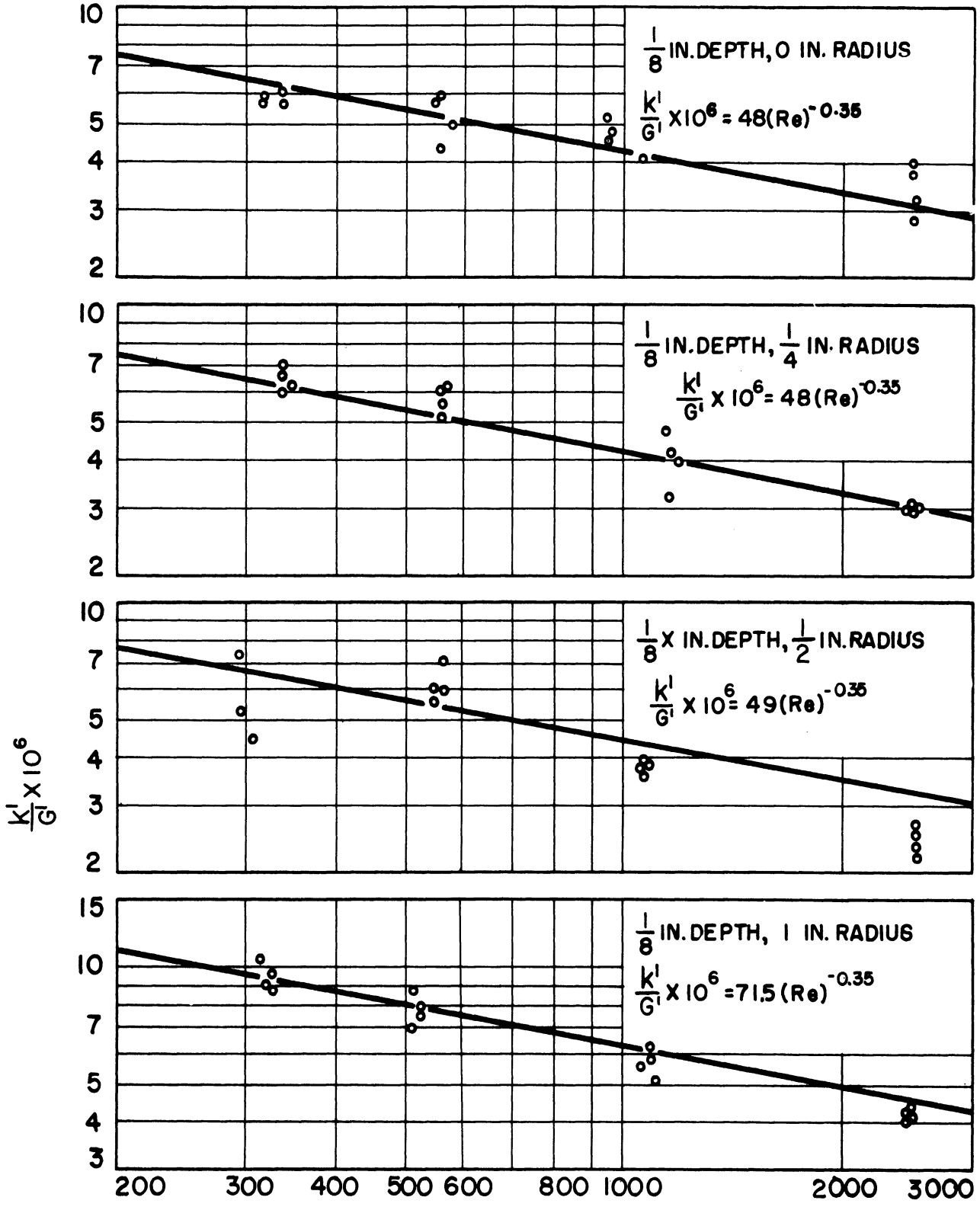

Fig.16a. Original Data Plots, $\frac{k'}{G'}$ vs Re; 2 Inch Orifice, $\frac{1}{4}$ Inch Pellets.

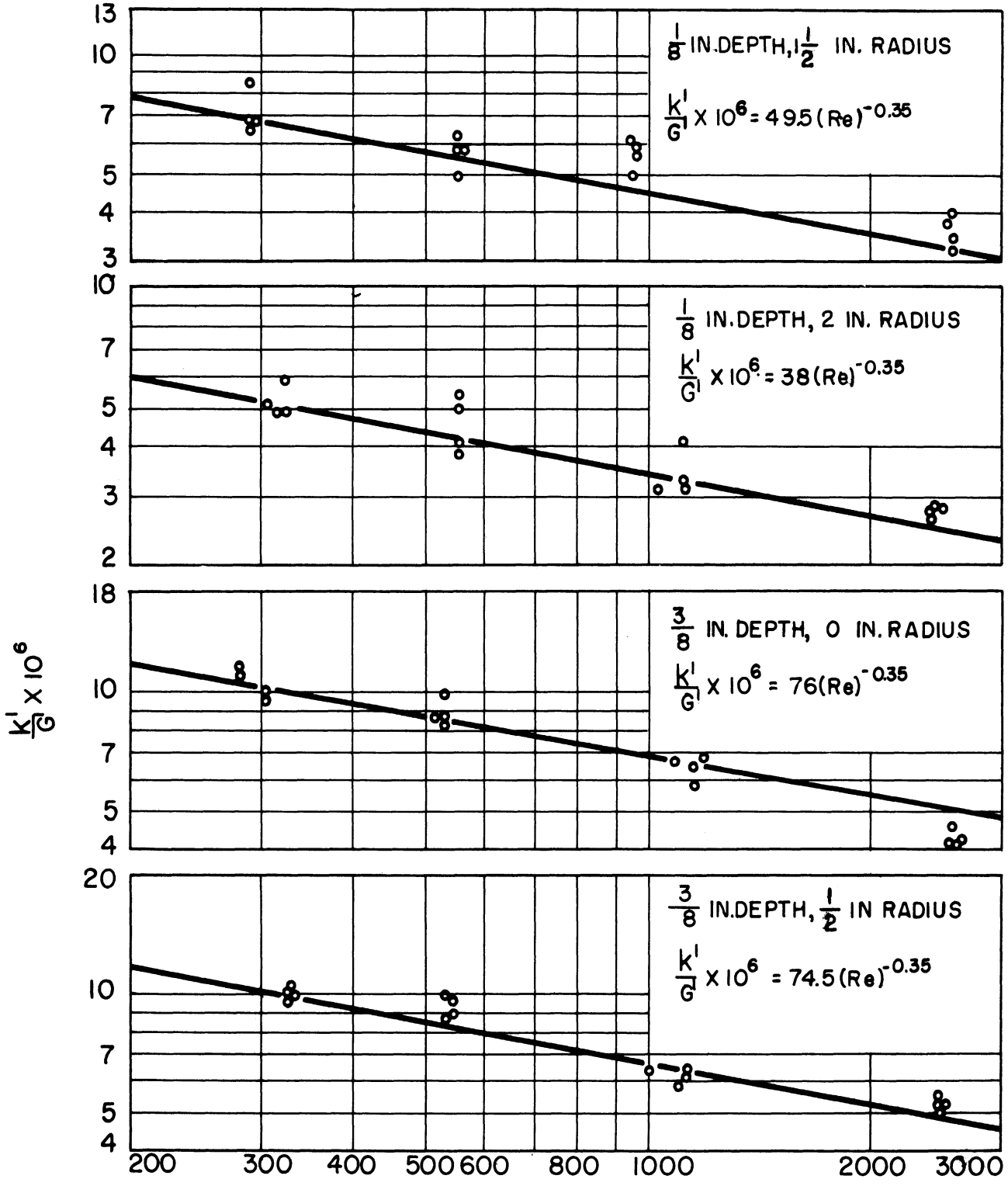

Fig.16b. Original Data Plots, $\frac{k'}{G'}$ vs Re; 2 Inch Orifice, $\frac{1}{4}$ Inch Pellets (Cont'd)

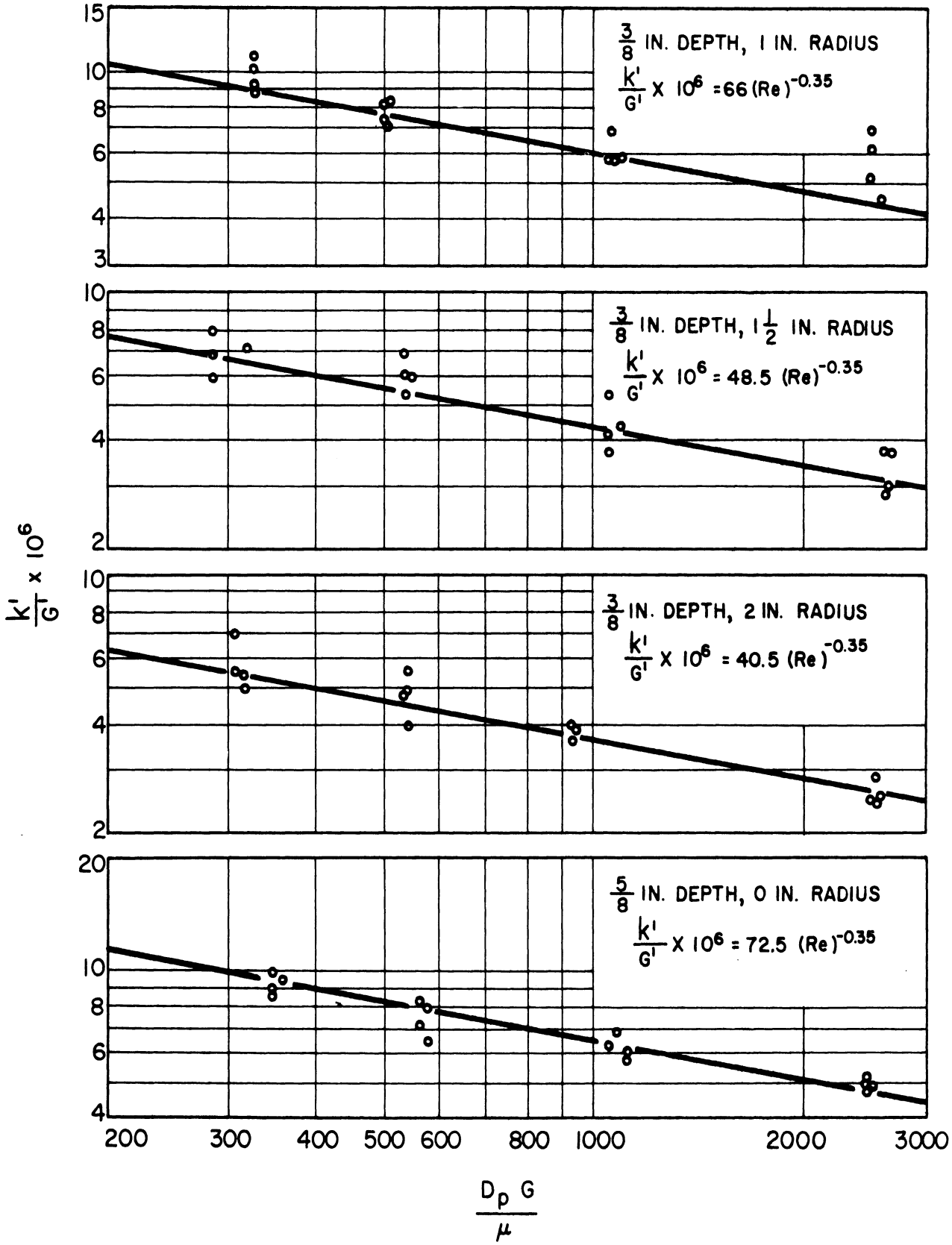

Fig.16c. Original Data Plots, $\frac{k'}{G'}$ vs Re, for 2 inch Orifice, $\frac{1}{4}$ inch Pellets (cont'd)

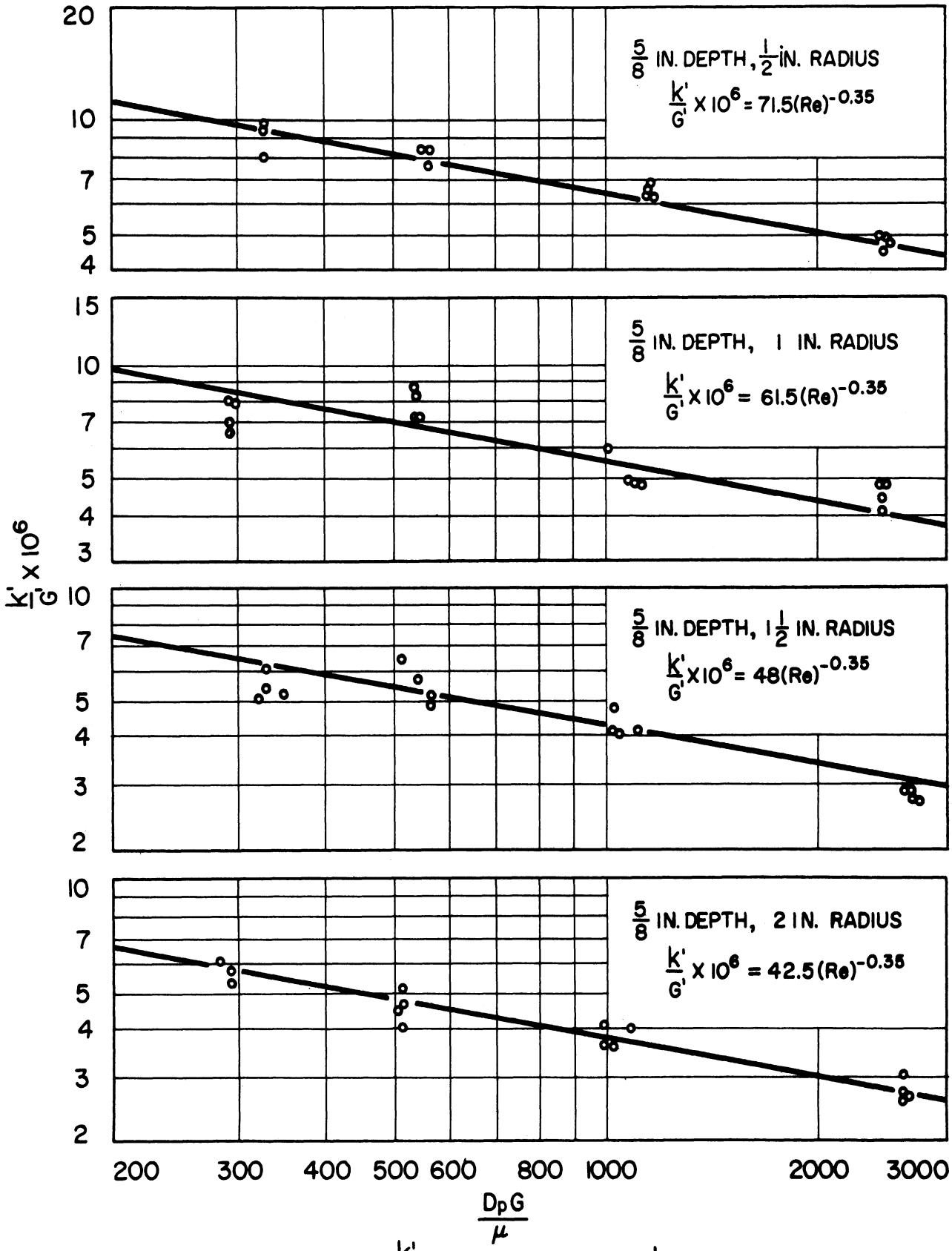

Fig.16d. Original Data Plot, $\frac{k'}{G'}$ vs Re, 2 in. Orifice, $\frac{1}{4}$ in. Pellets (cont'd)

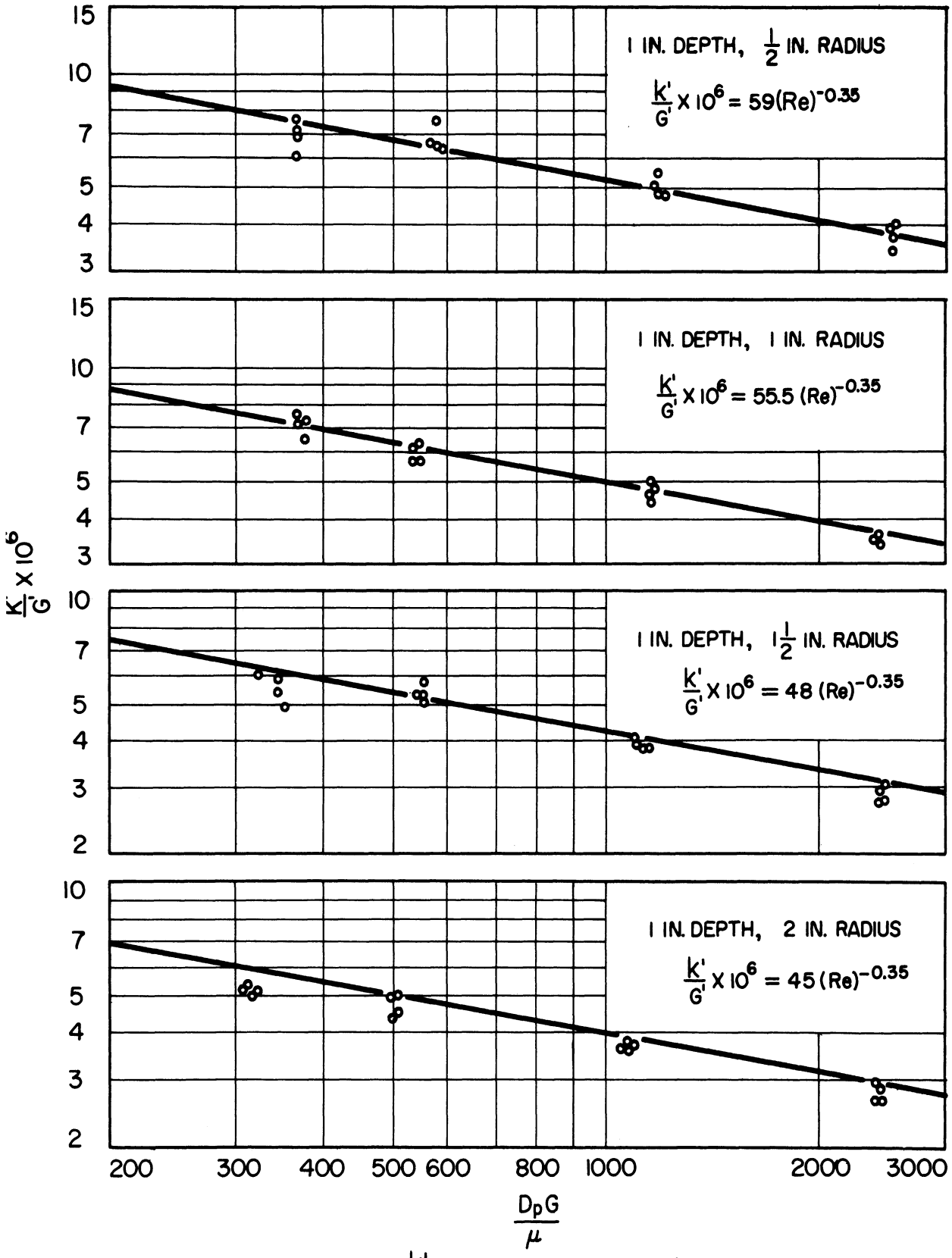

Fig.16e. Original Data Plots, $\frac{k'}{G'}$ vs Re, 2in. Orifice, $\frac{1}{4}$ in. Pellets, (cont'd)

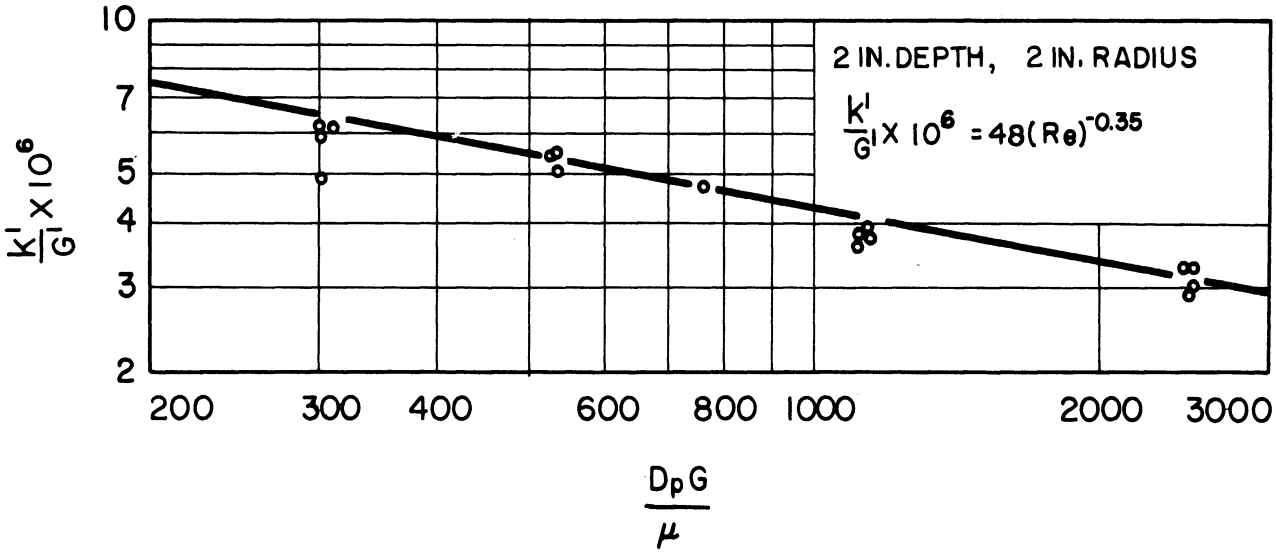

Fig.16f. Original Data Plot, $\frac{k'}{G'}$ vs Re; 2 Inch Orifice, $\frac{1}{4}$ in. Pellets

(Concluded)

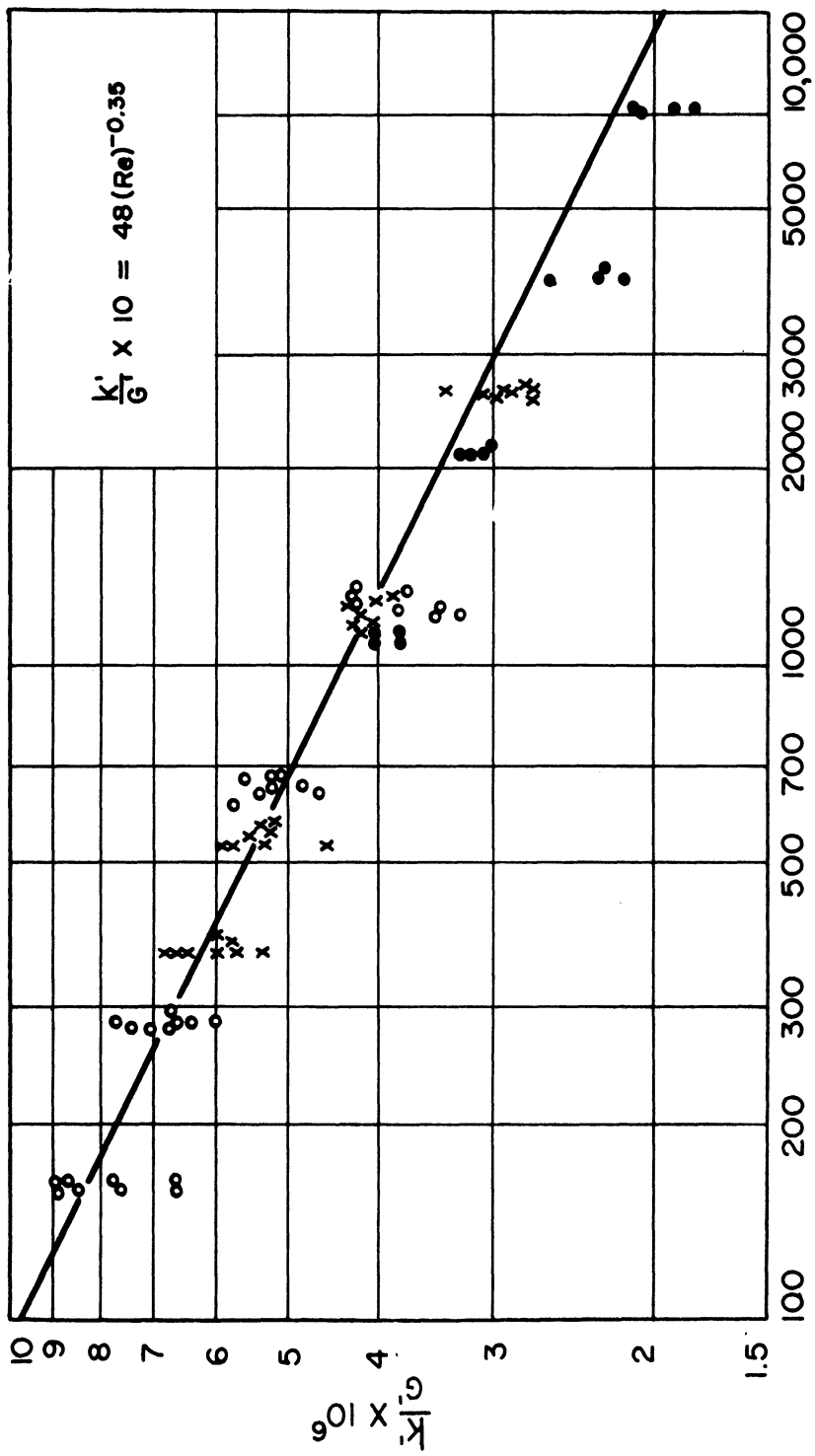

Fig.17. Original Data Plot, $\frac{k'}{G'}$ vs Re, for 4 inch Orifice, 1 in. Depth. (Consolidation)

KEY:
- o $\frac{1}{8}$ inch P
- x $\frac{1}{4}$ inch P
- ● $\frac{1}{2}$ inch P

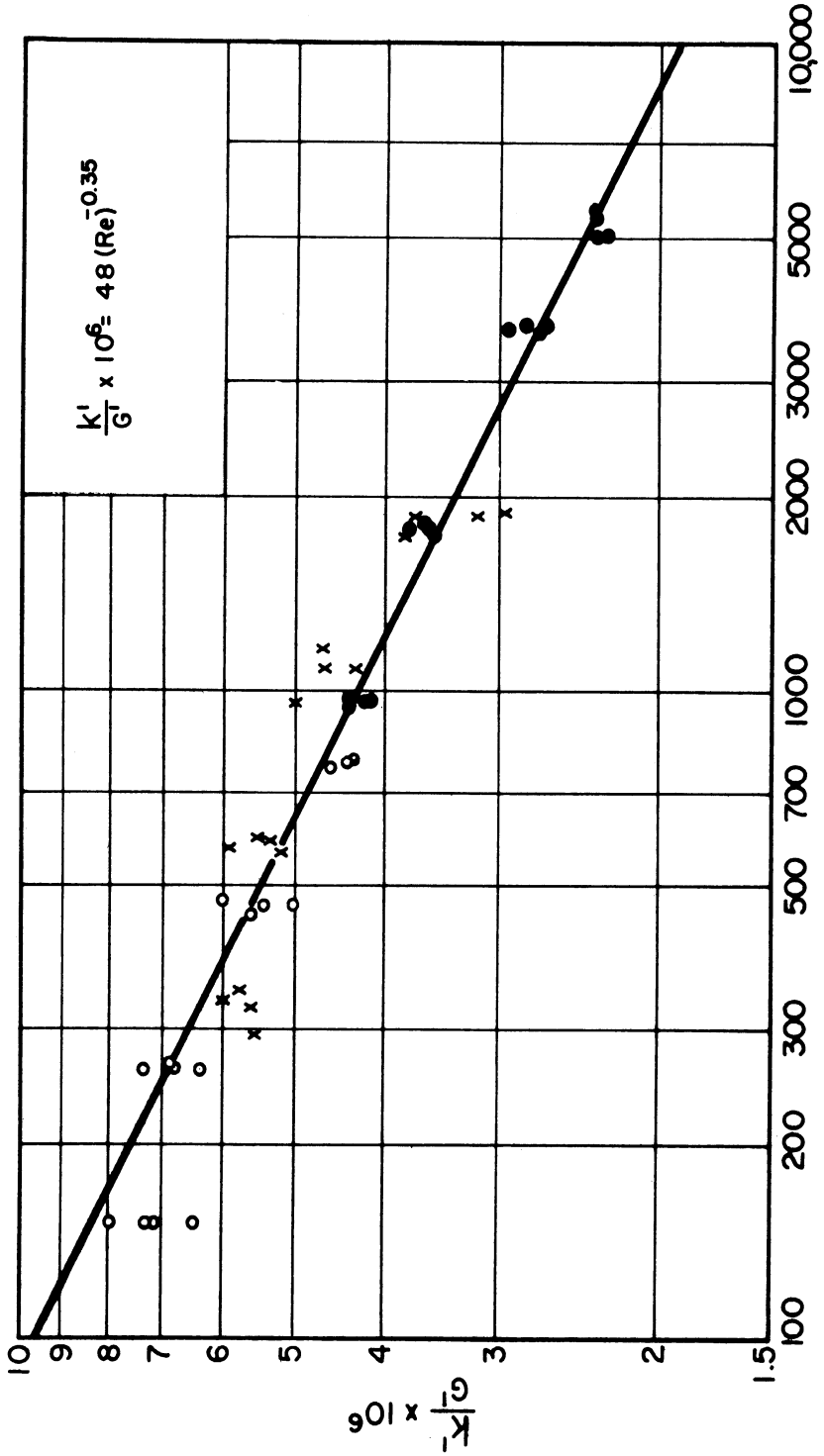

Fig. 18. Original Data Plot, $\frac{k'}{G'}$ vs Re, for 1 inch Orifice, 2 inch Depth, 1 inch Radius (Consolidation)

EXPERIMENTAL RESULTS

All experimental data were satisfactorily correlated by straight lines on log-log plots of k'/G' versus the Reynolds number, D_pG/μ , separate plots being made for each combination of pellet diameter, orifice diameter, and position in the bed. These original data plots are included in the preceding section, and the correlating lines can be represented by an equation of the form

$$k'/G' \times 10^6 = B \left(\frac{D_pG}{\mu}\right)^m \quad , \qquad (34)$$

where B and m are constant for any given combination of the experimental conditions.

With no orifice at the entrance to the bed, B and m were found to be independent of radial position and pellet diameter, but to vary with depth up to a depth of 1/2 inch, beyond which they were constant. The values used in correlating the data and to be used in applying the correlation are given in Table 1.

Table 1

Constants Used in Equation 34, for No Orifice

Depth, in.	B	-m
1/16	95	0.55
1/8	80	0.48
3/16	70	0.43
1/4	61	0.40
5/16	55	0.375
3/8	50	0.36
1/2	48	0.35
> 1/2	48	0.35

As was explained in the section on correlation, smoothing was accomplished by cross-plotting the intercepts and slopes of the individual straight lines through the data, the intercepts being equivalent to the value of $k'/G' \times 10^6$ at a Reynolds number of unity as is apparent from Equation 34. Since the original data were taken at various Reynolds numbers, it was not possible to show them on a plot of this type. Once the exponent m was found to be independent of radius, however, the original data could be shown on transverse profiles of the intercept, B. In essence, this was done by solving Equation 34 for B, giving

$$B = \left(\frac{k'}{G'}\right) \left(\frac{D_p G}{\mu}\right)^{-m} \times 10^6 \quad , \qquad (35)$$

and calculating the value of the right-hand group in this equation for each experimental datum point. Plots of this group versus radial position, with depth as a parameter, are shown in Figure 19. Longitudinal profiles might have been prepared in a similar manner, but would be less meaningful since the exponent m is not independent of depth.

The experimental results for the case of no orifice at the entrance to the bed, then, are described by Equation 34 with values of B and m as given in Table 1, and are shown graphically along with the original data in Figure 19. The conclusions to be drawn from these results will be listed and discussed at the end of this section, along with those obtained from the results of the orifice studies.

The experimental results obtained when the air stream entered the bed through an orifice were also correlated by the general Equation 34, but the exponent on the Reynolds number was found to vary randomly with orifice diameter, pellet diameter, and position within the bed, and was therefore assigned an average constant value of -0.35. Equation 34 thus becomes

$$k'/G' \times 10^6 = B \left(\frac{D_p G}{\mu}\right)^{-0.35} , \qquad (36)$$

where B depends only on orifice diameter and position within the bed. Values of B used in correlating the data and to be used in applying the correlation are given in Tables 2 and 3.

Since all these data were correlated with lines having the same slope, the original data could be shown on the transverse and longitudinal cross-plots by means of the same technique used with the no-orifice data. Equation 36 was solved for B, giving

$$B = \left(\frac{k'}{G'}\right) \left(\frac{D_p G}{\mu}\right)^{0.35} \times 10^6 , \qquad (37)$$

and the right-hand group in this equation was evaluated for each datum point and plotted against radius with depth as a parameter and also against depth with radius as a parameter. The resulting plots are shown in Figures 20-23, Figures 20 and 21 being the transverse and longitudinal profiles for the 1-inch orifice and Figures 22 and 23 the corresponding profiles for the 2-inch orifice. Where no experimental data

Table 2

Constants for Use in Equation 36

for 1-inch orifice[1]

Radius / Depth	0	1/4	1/2	3/4	1	1-1/4	1-1/2	1-3/4	2
1/16	102	111	150	130	89	62	43.5	31	22.5
1/8	115	122	171	137	86	61	44	32.5	24.5
3/16	142	150	175	125	82.5	59.5	44.5	34.5	27
1/4	162	165	170	117	79.5	59	45	35.5	29
5/16	175	174	159	110	76.5	58	45.5	37	31.5
3/8	177	172	147	103	73.5	57	46	38.5	33.5
1/2	154	143	121	92	68.5	55.5	46.5	41	37
5/8	130	120	104	81.5	64.5	54	47	43	40
3/4	113	106	92	75	60.5	52.5	47.5	44.5	42
1	90	86.5	75	62	54.5	50.5	48	46.5	45
1-1/2	64.5	62	56	50.5	48.5	48	48	48	48
2	51	50	48.5	48	48	48	48	48	48

[1] Radius and depth given in inches.

Table 3

Constants for Use in Equation 36

for 2-inch orifice[1]

Radius / Depth	0	1/4	1/2	3/4	1	1-1/4	1-1/2	1-3/4	2
1/16	38	38.5	39	44	73	61.5	50	42.5	37
1/8	48	48	49	54.5	71.5	62	49.5	43	38
3/16	58.5	58	57	60.5	70	60	49	43	38.5
1/4	67.5	66.5	63.5	63	68.5	58	49	43	39.5
5/16	73	72	69	67	67.5	57.5	49	43.5	40
3/8	76	76	74.5	71.5	66	56.5	48.5	44	40.5
1/2	77.5	77	76.5	73	63.5	54.5	48.5	44.5	41.5
5/8	72.5	73	71.5	67	61.5	54	48	45	42.5
3/4	68	68	67	64	59	52.5	48	45.5	43.5
1	60	60	59	57.5	55.5	52	48	46.5	45
1-1/2	50.5	50.5	50.5	50	50	49	48	47.5	47
2	48	48	48	48	48	48	48	48	48

[1] Radius and depth given in inches.

are shown, the profiles were obtained by interpolation and are included to show more clearly how the transverse profiles change with depth and the longitudinal profiles with radius.

When either the longitudinal or transverse profiles are viewed by themselves, it may seem that other curves would fit the data more closely, and that poor judgment was exercised in drawing the curves actually used. It must be remembered, however, that the two sets of profiles are interdependent and must give identical values at comparable points. and if a transverse profile seems low, for example, it is because the curve is pulled down by adjacent points on the corresponding longitudinal profile. Indeed, the required agreement between the two sets of profiles was a powerful factor in smoothing the data, and lends much to the acceptability of the final correlation.

Conclusions

Local rates of mass transfer in a packed bed of spheres have been measured and correlated with respect to position within the bed, pellet diameter, air flow rate, and velocity perturbations at the entrance to the bed. A cylindrical bed 4 inches in diameter was used, with measurements being taken to within 1/16 of an inch of the wall[1], and the investigation covered pellet diameters of 1/8, 1/4, and 1/2

[1] A nominal radial distance of two inches has been used in correlating data taken adjacent to the wall, although distances to the center of the pellets were really only 1-15/16 and 1-7/8 inches for the 1/8- and 1/4-inch pellets respectively.

inch and embraced a Reynolds number range of $150 < D_pG/\mu < 7{,}000$. The entrance conditions studied included completely unobstructed air entry and entry through 1- and 2-inch orifices.

Subject to the above limitations in scope, the conclusions to be drawn from the results of this investigation are as follows:

A. No Orifice at Bed Entrance

(1) Local mass-transfer rates are proportional to a power function of the Reynolds number, and may be correlated by the general equation

$$k'/G' \times 10^6 = B \left(\frac{D_pG}{\mu}\right)^m \qquad (34)$$

(2) Entrance effects are confined to the first 1/2 inch of bed depth, beyond which local mass-transfer rates are uniform, i.e., independent of both radial and longitudinal position, and are given by the equation

$$k'/G' \times 10^6 = 48 \left(\frac{D_pG}{\mu}\right)^{-0.35} \qquad (38)$$

(3) Within the entrance length, the absolute values of B and m in Equation 34 are highest at the exposed surface layer of packing and decrease with depth until Equation 38 applies, the actual values for these constants being given in Table 1. All experimental data fit the correlation with an average deviation of 7.7 per cent.

(4) Local rates of mass transfer within the entrance length are independent of radial position, i.e., the radial transfer-rate profiles are flat.

(5) The entrance length is independent of pellet diameter.

(6) Except for its use as the characteristic length in the Reynolds number, pellet diameter is not a parameter in correlating local mass-transfer rates in packed beds.

B. Orifice at Bed Entrance. Since only two orifice diameters were used in these studies, no attempt has been made to obtain a quantitative correlation of the effect of orifice diameter. However, the following additional conclusions are to be inferred:

(7) Local mass-transfer rate data may be correlated by Equation 34 with a constant value of -0.35 assigned to the exponent m.

(8) The values to be assigned to B in Equation 34 are functions of orifice diameter and position in the bed, and are given in Tables 2 and 3. The data fit the correlation with an average deviation of 10.7 per cent.

(9) The shape of all transverse and longitudinal transfer-rate profiles is independent of air flow rate, i.e., changes in total flow affect all positions within the bed equally.

(10) The local mass-transfer rate is significantly higher in the vicinity of the orifice than elsewhere, and reaches a maximum at a point on the axis of the bed approximately 3/8 of an inch in from the inlet.

(11) At depths of less than 3/8 of an inch, wall-to-wall profiles of local transfer rates are characteristically M-shaped, with maxima corresponding to the edges of the orifice.

(12) Perturbations in mass-transfer rate created by the orifice are completely dissipated at a bed depth of approximately 2 inches, beyond which the rates are the same as when no orifice is present and can be correlated by Equation 38.

(13) The depth required to dissipate entrance perturbations is slightly less for the 2-inch orifice than for the 1-inch, as would be expected.

(14) At bed depths between 3/8 of an inch and approximately 2 inches, the wall-to-wall transfer-rate profiles are dome-shaped, with a maximum at the center of the bed and minima at the walls. It is interesting to note that these profiles are quite similar to the velocity profiles produced by a free jet (23).

(15) Near the wall of the bed, local mass-transfer rates are lowest in the entrance layer of packing and increase with depth until they become constant as required by (12) above.

(16) As in the no-orifice case, pellet diameter is not a parameter in correlating local rates, beyond its use as the characteristic length in the Reynolds number. This statement correctly implies that the transfer rate at any point in the bed depends on the absolute coordinates of the

point rather than on coordinates expressed in terms of the pellet diameters.

(17) On the basis of preliminary tests, it can also be noted that if the orifice is separated from the top layer of packing by as little as 1/16 of an inch, the perturbations in mass-transfer rate created by the orifice are drastically reduced.

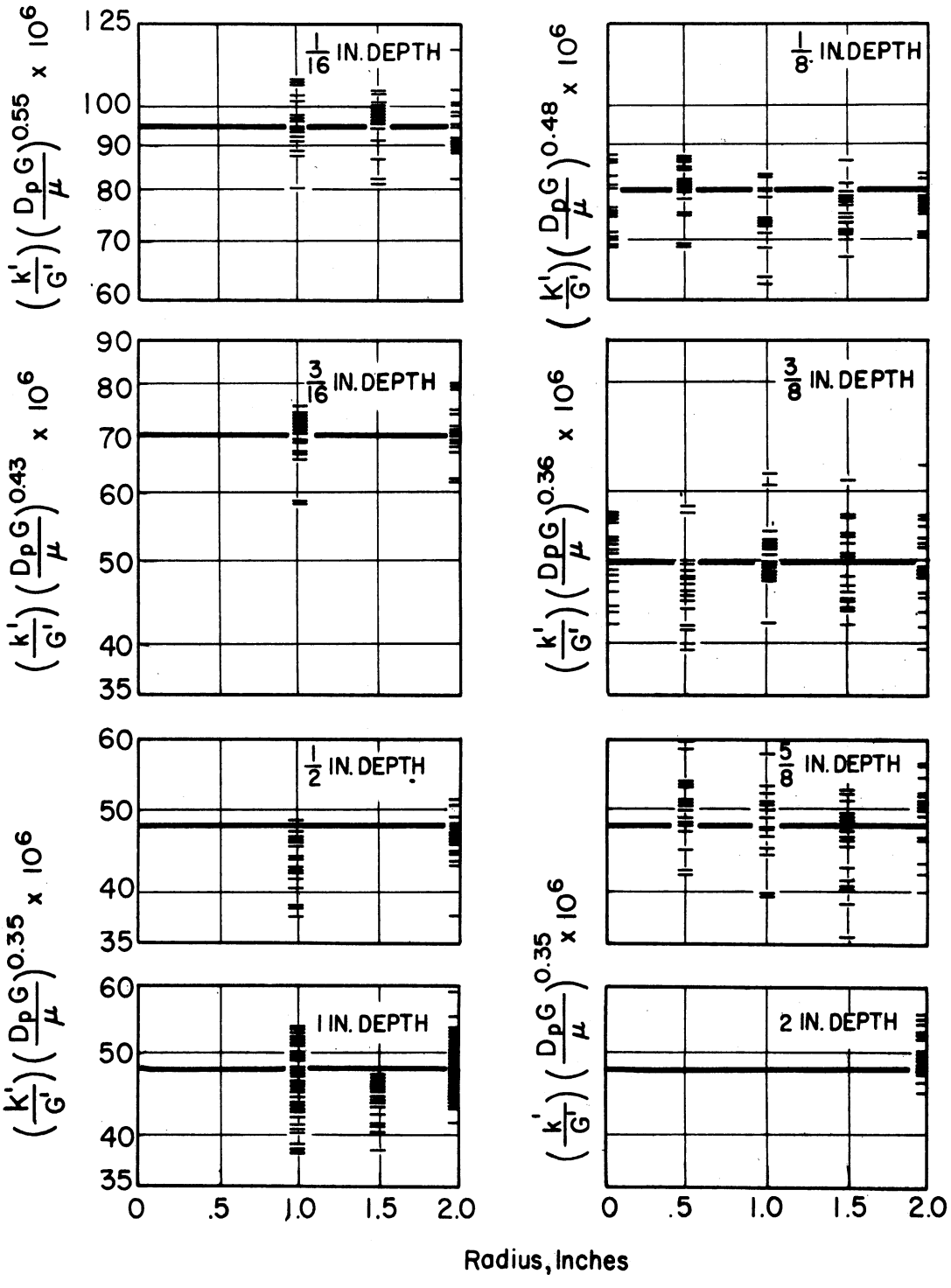

Fig. 19. Effect of Radius and Depth on Mass Transfer Rate — Transverse Profiles with No Orifice.

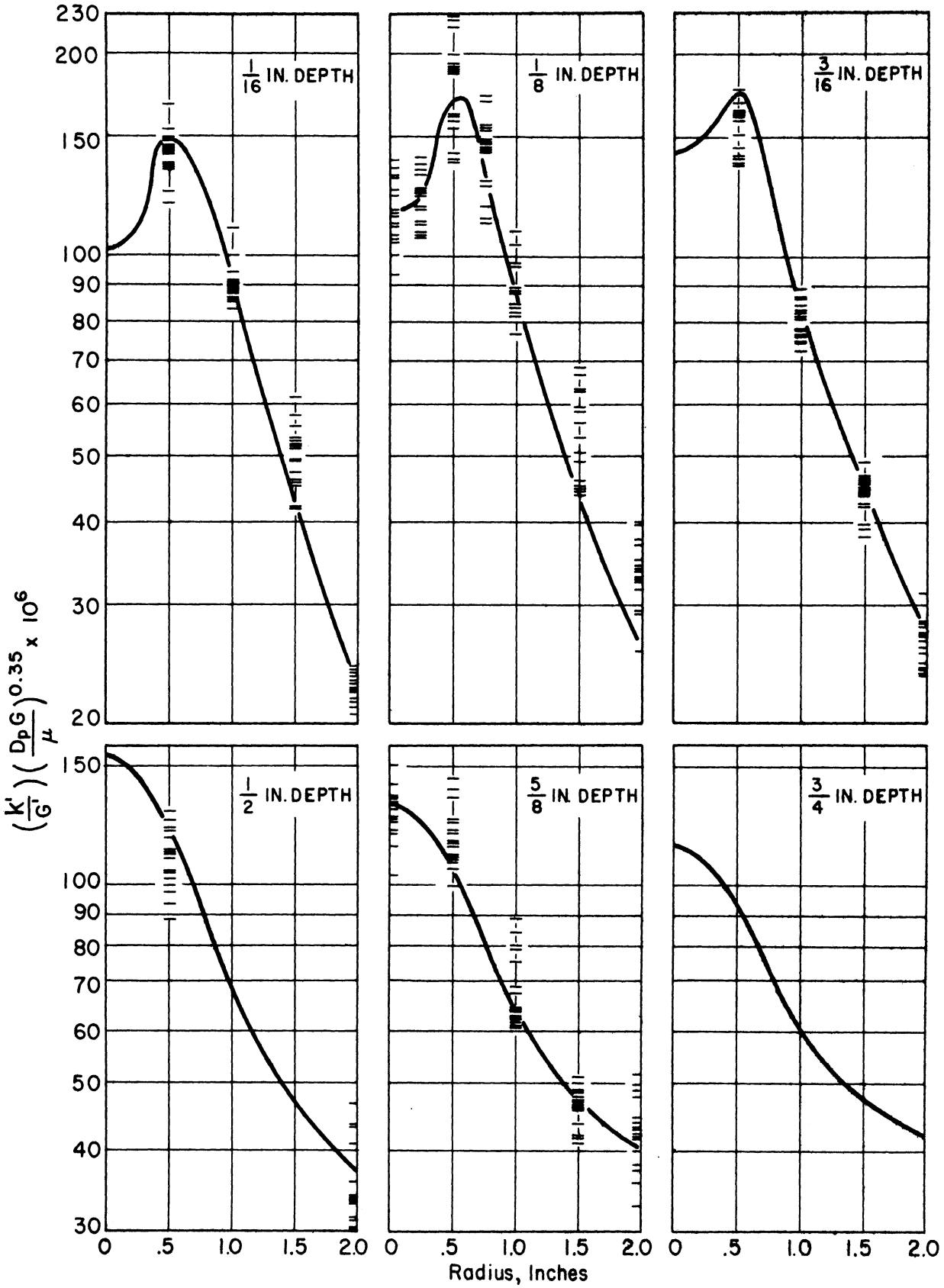
1/16 IN. DEPTH
1/8 IN. DEPTH
3/16 IN. DEPTH
1/2 IN. DEPTH
5/8 IN. DEPTH
3/4 IN. DEPTH
(k'/G') (DpG/μ)^0.35 x 10^6
Radius, Inches
230
200
150
100
90
80
70
60
50
40
30
20
0
.5
1.0
1.5
2.0

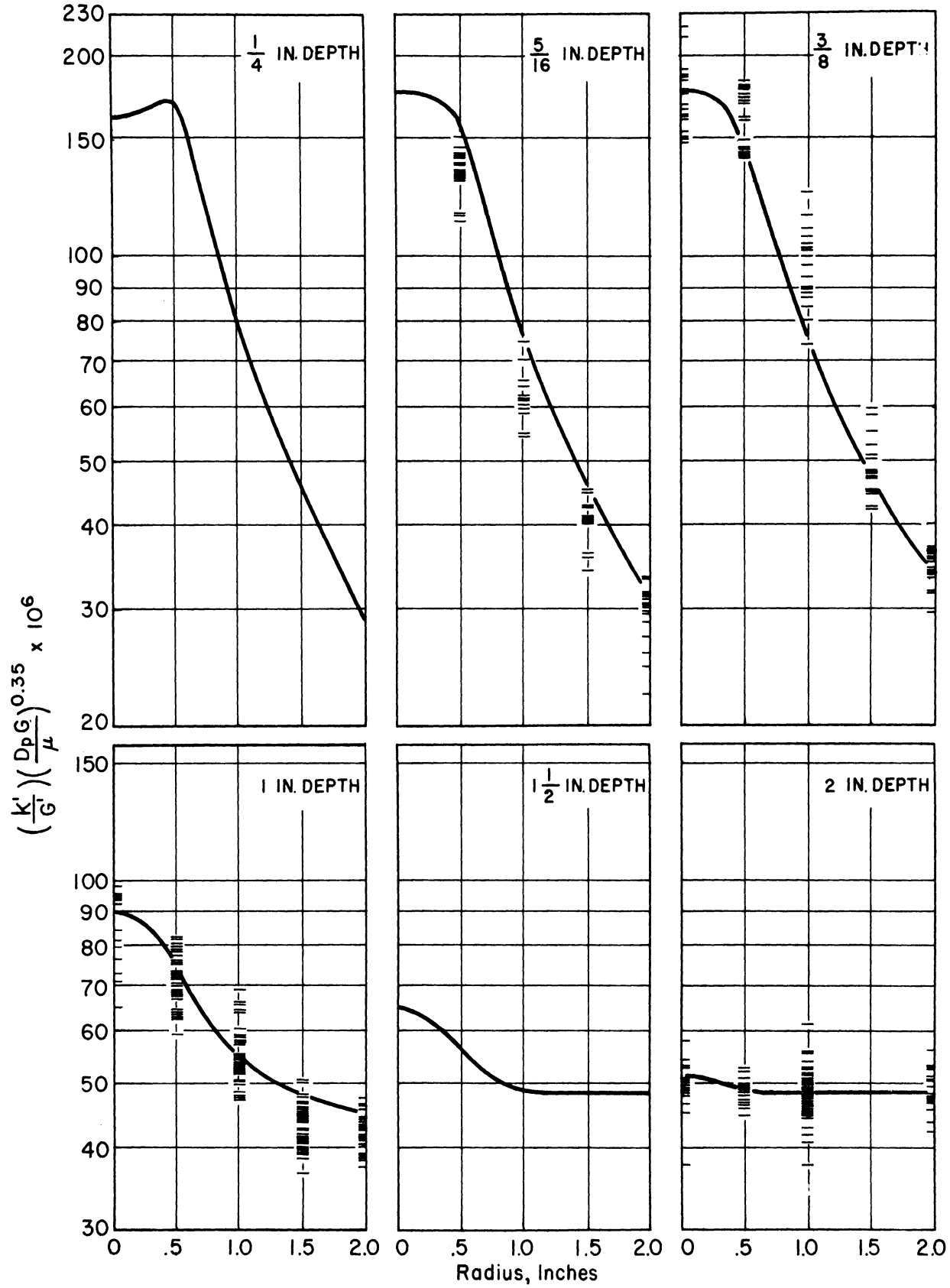

Fig.20. Effect of Radius and Depth on Mass Transfer Rate – Transverse Profiles for 1-Inch Orifice.

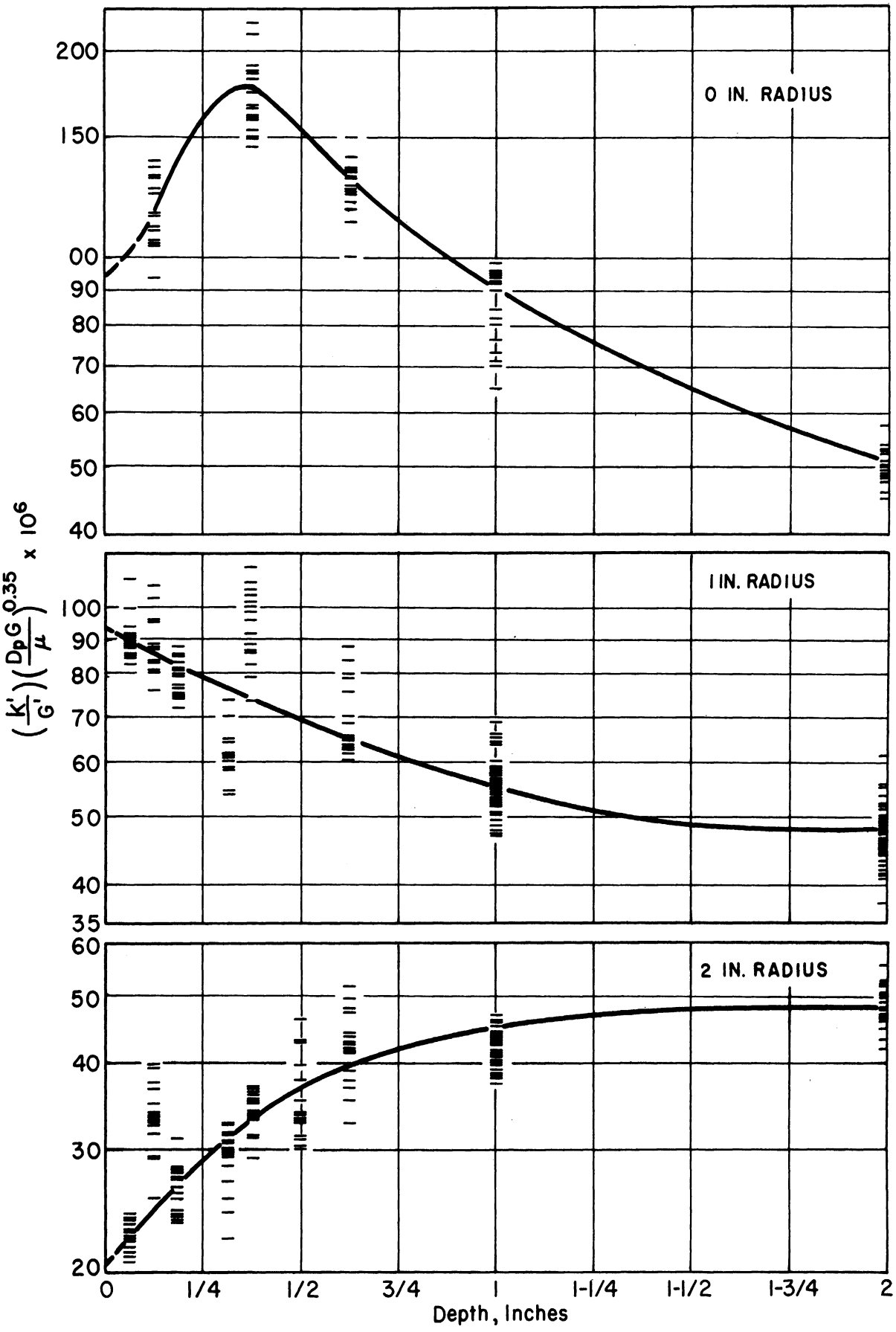
0 IN. RADIUS
1 IN. RADIUS
2 IN. RADIUS
$\left(\frac{K'}{G'}\right)\left(\frac{D_p G}{\mu}\right)^{0.35} \times 10^6$
200
150
00
90
80
70
60
50
40
100
90
80
70
60
50
40
35
60
50
40
30
20
0
1/4
1/2
3/4
1
1-1/4
1-1/2
1-3/4
2
Depth, Inches

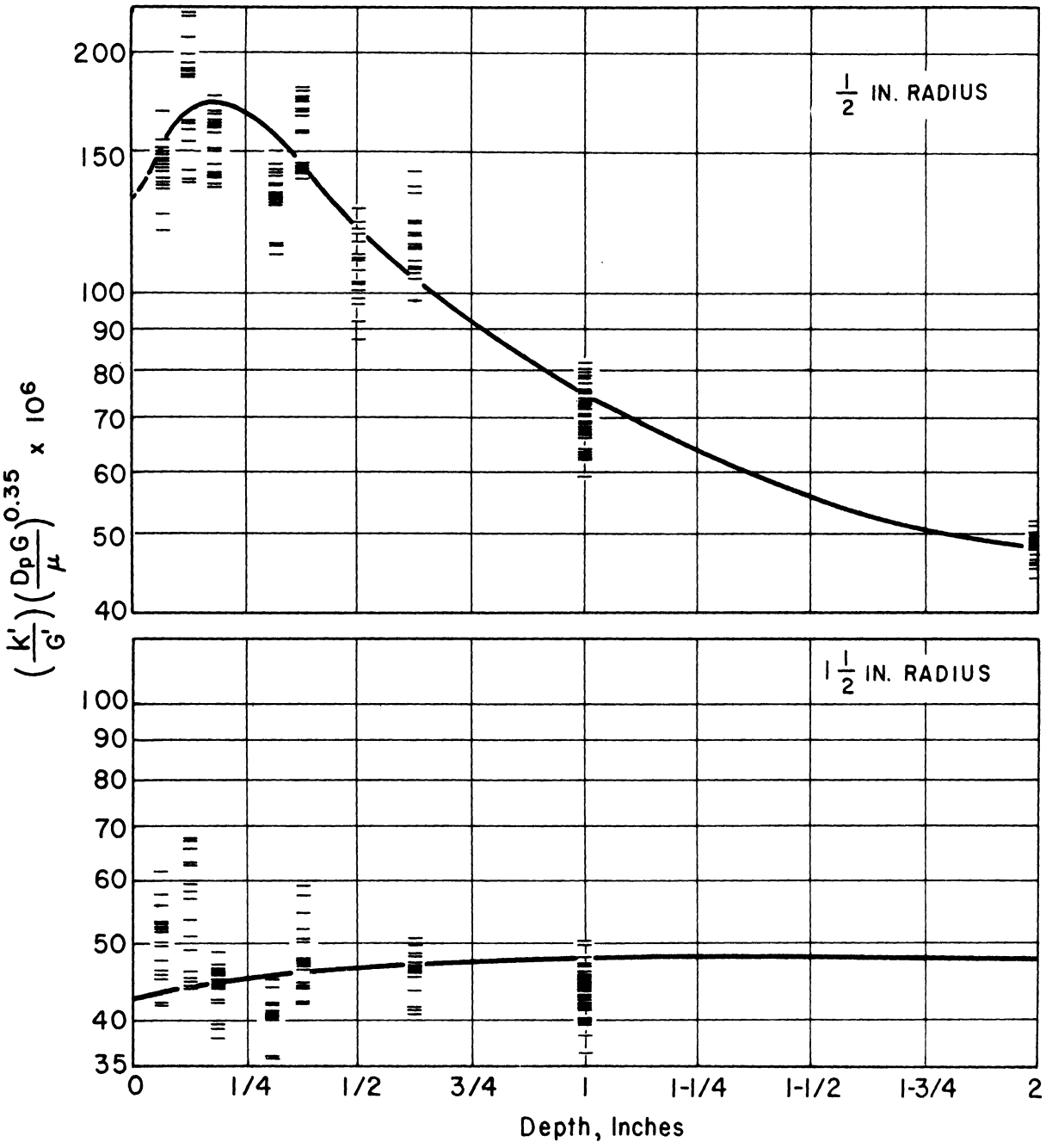

Fig. 21. Effect of Radius and Depth on Mass Transfer Rate – Longitudinal Profiles for 1-Inch Orifice.

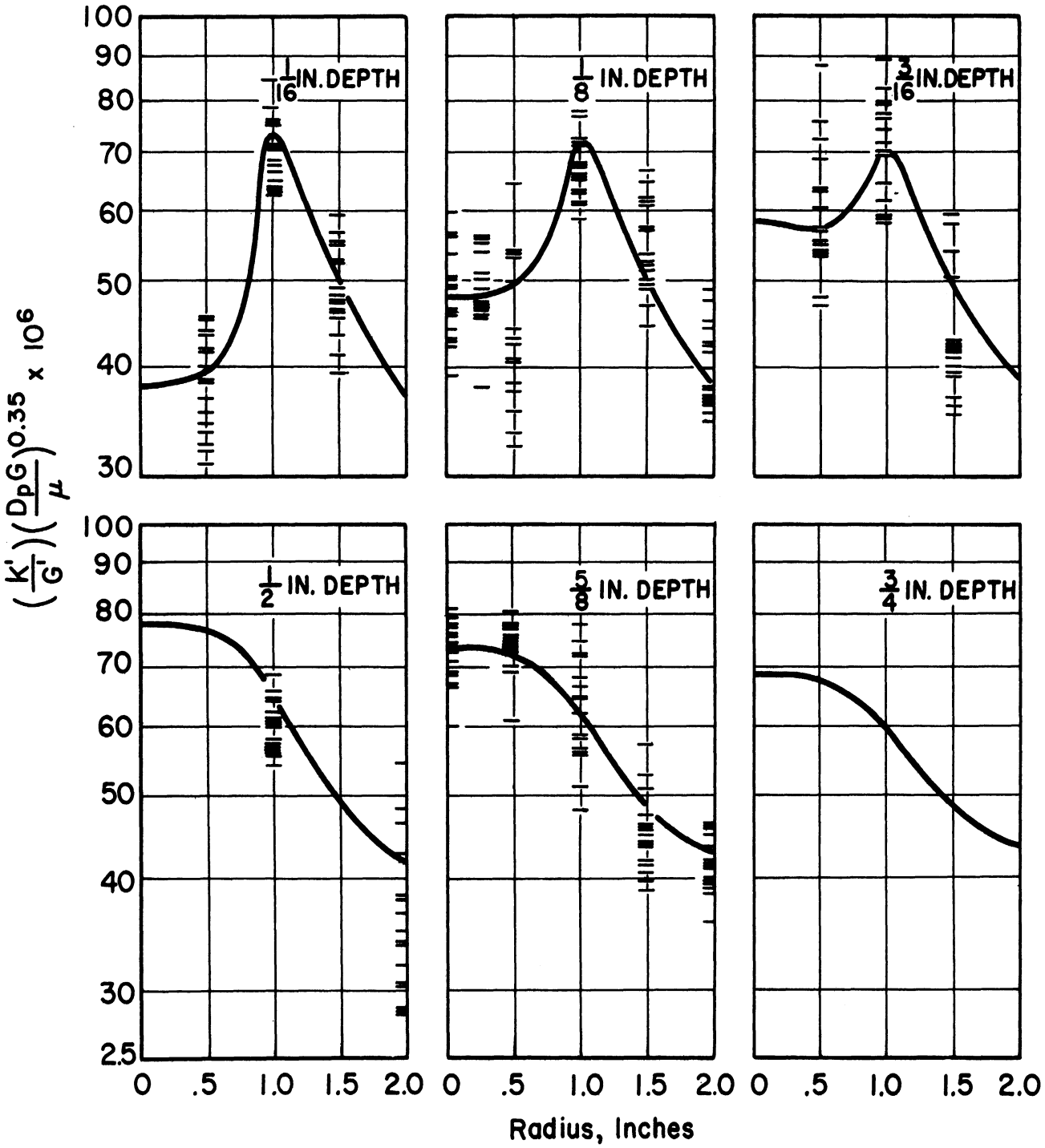
$\left(\frac{K'}{G'}\right)\left(\frac{D_p G}{\mu}\right)^{0.35} \times 10^6$
100
90
80
70
60
50
40
30
25
1/16 IN. DEPTH
1/8 IN. DEPTH
3/16 IN. DEPTH
1/2 IN. DEPTH
5/8 IN. DEPTH
3/4 IN. DEPTH
0
.5
1.0
1.5
2.0
Radius, Inches

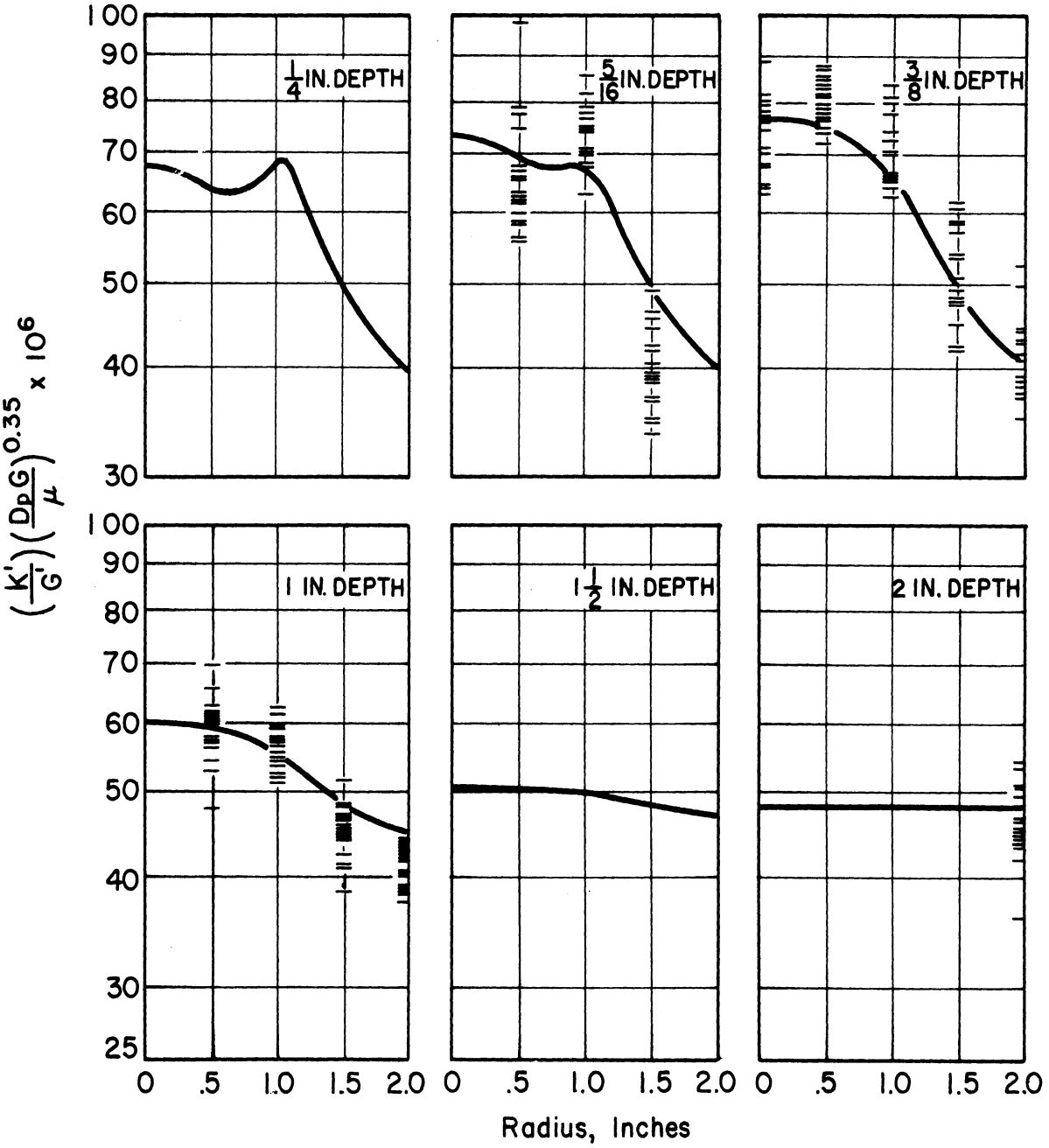

Fig. 22. Effect of Radius and Depth on Mass Transfer Rate - Transverse Profiles for 2-Inch Orifice.

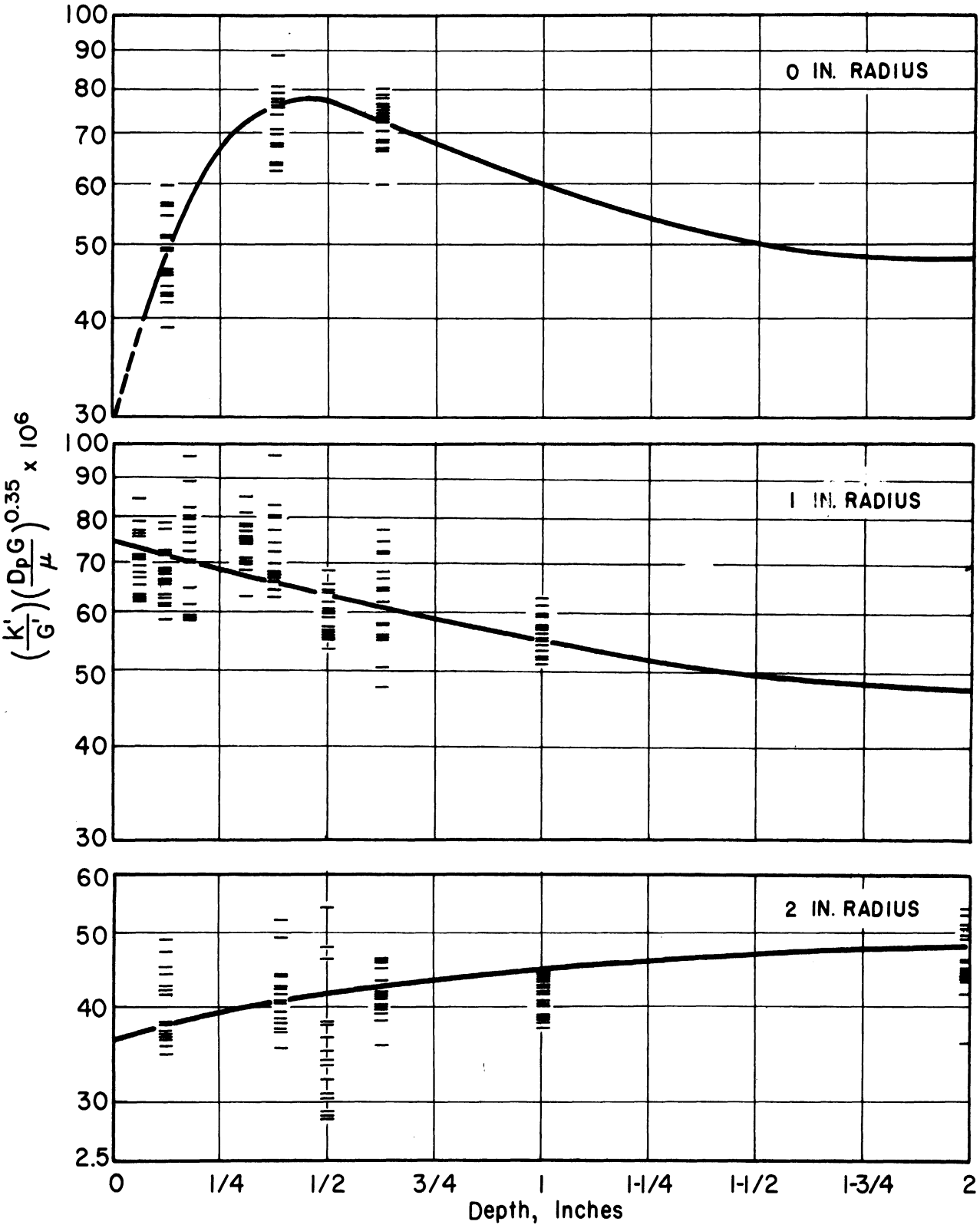
0 IN. RADIUS
1 IN. RADIUS
2 IN. RADIUS
$\left(\frac{K'}{G'}\right)\left(\frac{D_p G}{\mu}\right)^{0.35} \times 10^6$
100
90
80
70
60
50
40
30
60
50
40
30
2.5
0
1/4
1/2
3/4
1
1-1/4
1-1/2
1-3/4
2
Depth, Inches

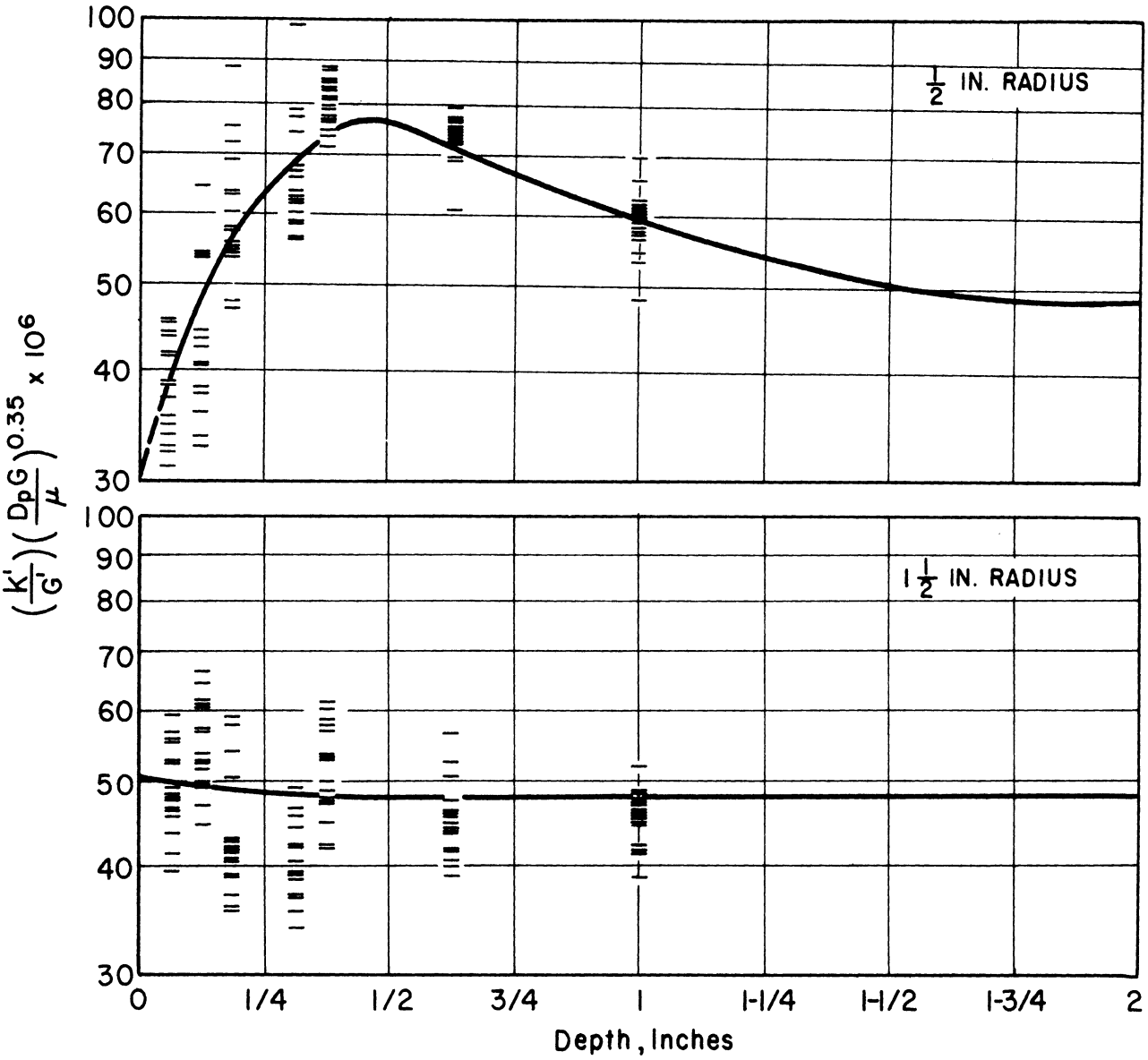

Fig. 23. Effect of Radius and Depth on Mass Transfer Rate - Longitudinal Profiles for 2-Inch Orifice.

RELIABILITY OF RESULTS

The reliability of the results obtained in any experimental investigation can be measured by the application of three general criteria: (1) the extent to which the experimental apparatus and technique can be criticized on either theoretical or practical grounds; (2) the degree of reproducibility of the experimental data and the extent to which they are internally consistent; and (3) the extent to which the results agree or conflict with the results of other investigations of a parallel nature. When interpretation of the data is required in order to arrive at the final results, this must also be considered.

From the standpoint of the first of these criteria, the various precautions taken to insure the validity of the data have been detailed in the sections on experimental apparatus and procedure, and are believed to have been adequate.

Internal consistency of the data was generally found to be good, while the reproducibility was excellent. Ample evidence of the consistency of the data is present in the original data plots, Figures 8-18, and in the transverse and longitudinal profile plots, Figures 19-23. The degree of reproducibility of the data, on the other hand, was established at the outset of the investigation and was checked periodically throughout its course by making duplicate runs several days or even weeks apart. Exact reproduction was

impossible, of course, because of the random packing of the bed, but duplicate sets of data almost always agreed to the extent that either set fit the general correlation equally well.

Check runs were also made whenever the data for any given series of runs were not consistent with the comparable data from other runs. These check runs usually showed the original data to be in error. However, in some cases the check runs confirmed the original data. For example, it can be seen from the bottom-center plot of Figure 14b that the data taken at a depth of 1/8 inch and a radius of 2 inches, with the 1-inch orifice across the entrance to the bed, lie well above the correlating line and might therefore be questioned. These data were reproduced not once but twice by two separate series of check runs.

Although this and similar results attest to the reproducibility of the data, they also suggest that the data are valid and hence that the correlation is poor. Fortunately, appreciable disagreement between the actual data and the correlating line is the exception rather than the rule, as can be seen from a study of the other original data plots, and the general correlation is therefore supported by the bulk of the experimental data. However, the significance of reproducible data disagreeing with the general correlation cannot be disregarded. The use of a constant slope in correlating all 1- and 2-inch orifice data and the smooth profiles shown in Figures 19-23 perhaps constitute an overly

simplified correlation. With the majority of the data supporting the correlation, however, the anomalies can only be left as points for conjecture.

As was noted in the survey of the literature presented at the beginning of this report, there are few quantitative data available which are comparable to the present findings, and any comparison with previous data must therefore be largely qualitative. The transfer-rate profiles obtained do not appear to be consistent with the velocity profiles of Smith, et al. (50,62), for example, but an explanation for this has already been advanced. The profiles <u>are</u> in agreement with the findings of Coberly and Marshall (13). As a minor point, it might also be noted that the present studies show the shape of all transverse and longitudinal transfer-rate profiles to be independent of total air flow rate, which is consistent with Smith's conclusion that <u>velocity</u> profiles are independent of the total flow rate.

As far as a comparison with other mass-transfer rate correlations is concerned, it is perhaps significant that mass-transfer rates were found to be proportional to a power function of the Reynolds number, as has also been observed by others. Further, the observation that pellet diameter is a factor in the correlation only through its presence in the Reynolds number is consistent with the conclusions drawn by the majority of previous investigators.

Perhaps the most informative analysis of the results of this investigation in the light of previous work is to be

made by comparing the correlation obtained at bed positions beyond the entrance length with previous correlations for the j-factor for mass transfer. If it is true that the entrance length in a packed bed is only 1/2 inch as has been indicated, the inclusion of entrance effects in the work done by others should be of little consequence provided their beds were sufficiently deep. Their overall correlations, therefore, might be expected to agree reasonably well with Equation 38,

$$k'/G' \times 10^6 = 48 \left(\frac{D_p G}{\mu}\right)^{-0.35} , \qquad (38)$$

which correlates all the present data taken beyond the entrance length.

The primary difficulty in effecting such a comparison lies in converting Equation 38 to its equivalent in terms of the j-factor for mass transfer. The first step in the conversion is to introduce the mass-transfer coefficient, k_g, by use of the equation

$$k' = k_g(p^o - p_v)_{lm} , \qquad (31)$$

and the difficulty in accurately defining the driving force, $(p^o - p_v)_{lm}$, has already been mentioned. It will be assumed that this term may be replaced by p^o, the vapor pressure of p-dibromobenzene, in accordance with the previous discussion.

In view of the disagreement among the data reported in the literature for the vapor pressure of p-dibromobenzene, a second difficulty now arises, namely, what value to assign to p^o. The decision must necessarily be somewhat arbitrary,

and a value of 0.038 millimeters of mercury, obtained by interpolation from the data given in the International Critical Tables (see Figure 6), is probably as good as any.

The relationship between the mass-transfer rate, k', and the j-factor for mass transfer can now be determined, recognizing that the partial pressure of the inert gas, p_{gf}, is for practical purposes equal to the total pressure, P:

$$j_d = \frac{k_g p_{gf}}{G/M_m} \left(\frac{\mu}{\rho D_G}\right)^{2/3} \qquad (4)$$

$$= \frac{k' P}{G' p^o} \left(\frac{\mu}{\rho D_G}\right)^{2/3}$$

$$= \frac{760}{0.038} \left(\frac{\mu}{\rho D_G}\right)^{2/3} \left(\frac{k'}{G'}\right)$$

$$= 0.02 \left(\frac{\mu}{\rho D_G}\right)^{2/3} \left(\frac{k'}{G'}\right) \times 10^6 \quad . \qquad (39)$$

The molecular diffusivity of air and p-dibromobenzene at 80°F, D_G, must be known in order to evaluate the Schmidt number, and in the absence of experimental data can be calculated by use of the Gilliland equation (28). The calculations are summarized in Appendix E, and yield a value of 0.245 square feet per hour. The Schmidt number is then found to be 2.41 (Appendix E), which is consistent with the value of 2.37 obtained by Bedingfield and Drew (5) at 0°C. Substituting this value in Equation 39 gives

$$j_d = 0.036 \left(\frac{k'}{G'}\right) \times 10^6 \quad , \qquad (40)$$

and combining Equation 38 with this equation produces the final relationship,

$$j_d = 1.73 \left(\frac{D_p G}{\mu}\right)^{-0.35} . \qquad (41)$$

Written in this form, the present correlation can be directly compared with those of Gamson et al. (27), McCune and Wilhelm (48), and Hobson and Thodos (33), and the comparison is presented graphically in Figure 24. By suitably modifying the Reynolds number, comparison may also be made with the correlations of Gaffney and Drew (25) and Gamson (26). Using a fractional void volume, ϵ, of 0.37 (Appendix B), Equation 41 becomes

$$\begin{aligned} j_d &= 1.73\ (\epsilon)^{-0.35} \left(\frac{D_p G}{\mu \epsilon}\right)^{-0.35} \\ &= 1.73\ (0.37)^{-0.35} \left(\frac{D_p G}{\mu \epsilon}\right)^{-0.35} \\ &= 2.45 \left(\frac{D_p G}{\mu \epsilon}\right)^{-0.35} \end{aligned} \qquad (42)$$

Since Gaffney and Drew used an exponent of 0.58 on the Schmidt number in defining their j-factor, Equation 42 must be further corrected by introducing the factor $(Sc)^{-0.087}$:

$$\begin{aligned} j_d' &= 2.45\ (2.41)^{-0.087} \left(\frac{D_p G}{\mu \epsilon}\right)^{-0.35} \\ &= 2.27 \left(\frac{D_p G}{\mu \epsilon}\right)^{-0.35} . \end{aligned} \qquad (43)$$

This equation is compared with the Gaffney-Drew correlation as approximated by Ergun (20) in Figure 25.

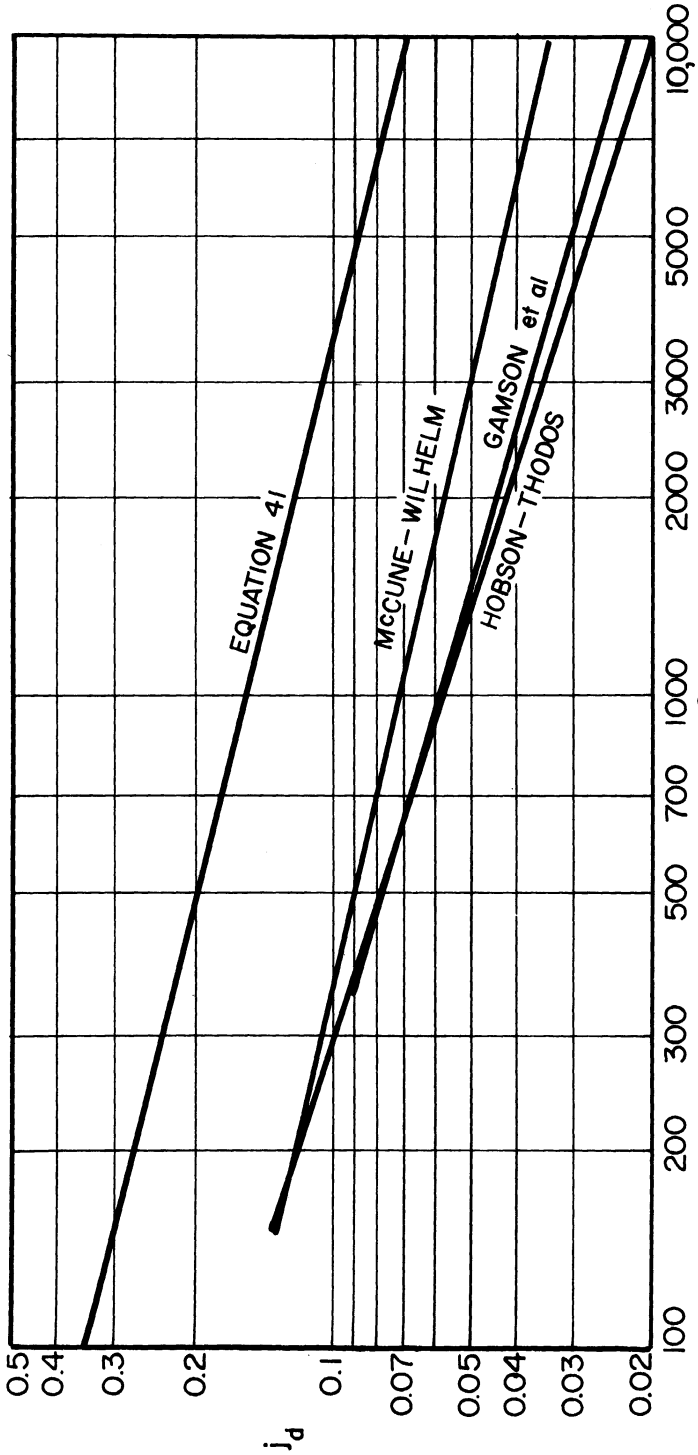

Fig. 24. Comparison of Equation 41 with Correlations of McCune and Wilhelm (48), Gamson et al (27), and Hobson and Thodos (33)

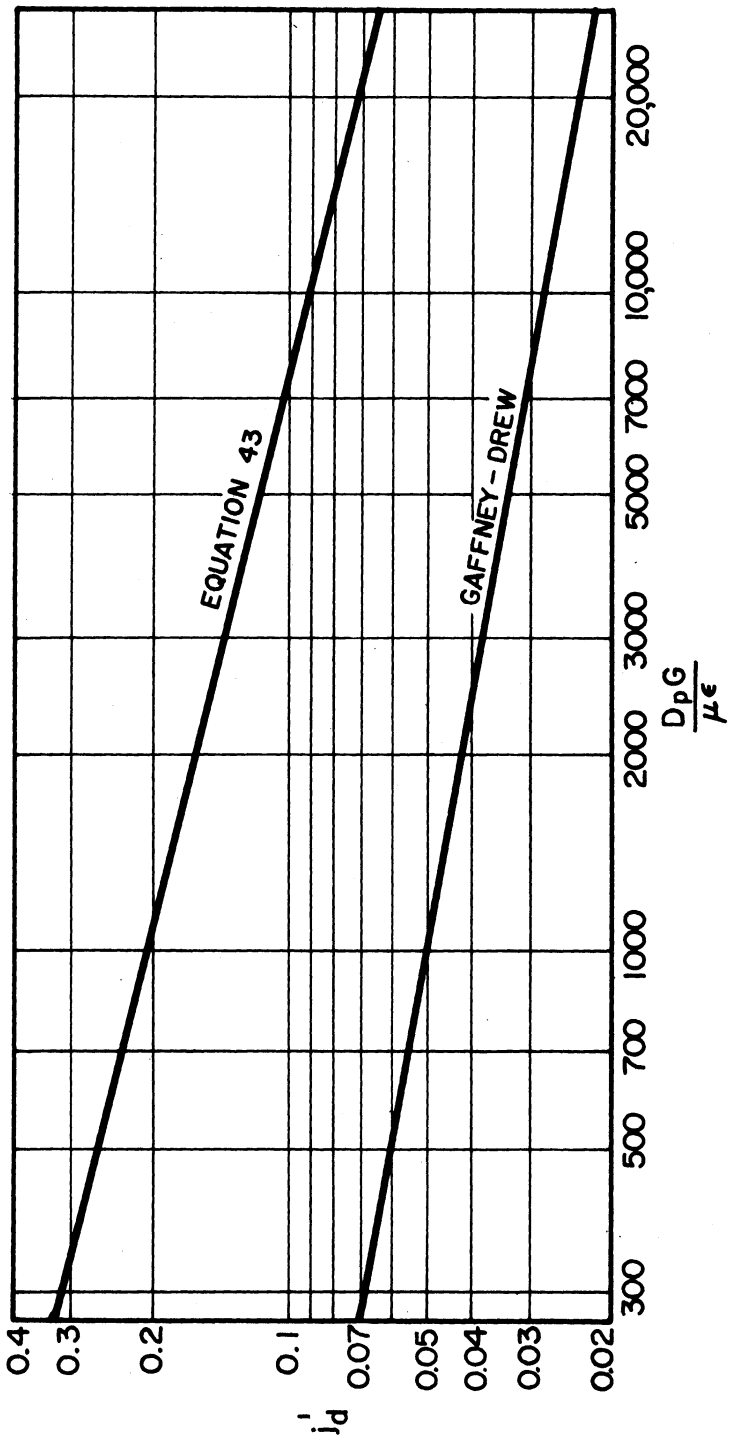

Fig. 25. Comparison of Equation 43 with Correlation of Gaffney and Drew (25)

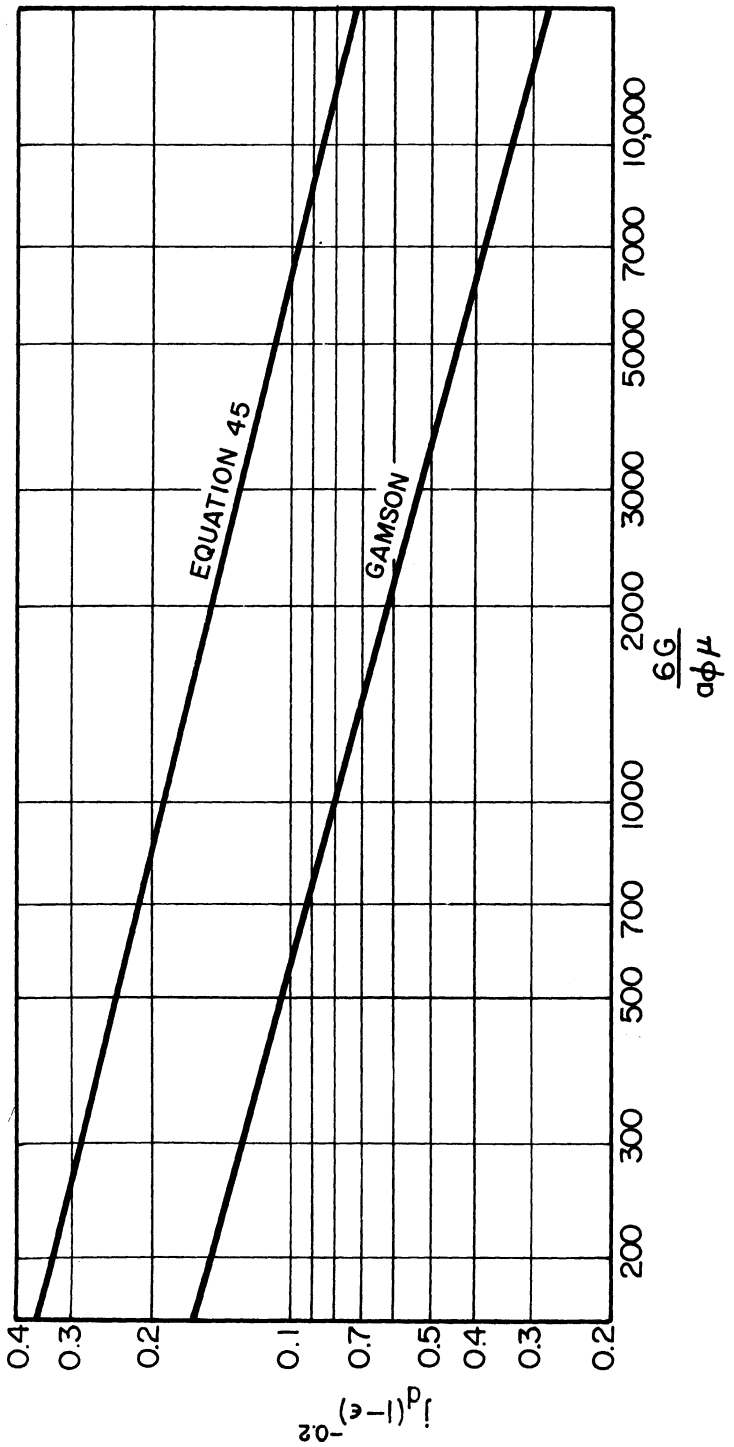

Fig. 26. Comparison of Equation 45 with the Correlation of Gamson (26)

Converted to correspond to the Gamson correlation, Equation 41 becomes

$$j_d = 1.73\ (1 - \epsilon)^{-0.35}\left[\frac{D_pG}{\mu(1 - \epsilon)}\right]^{-0.35},$$

and

$$\begin{aligned} j_d(1 - \epsilon)^{-0.2} &= 1.73\ (1 - \epsilon)^{-0.55}\left[\frac{D_pG}{\mu(1 - \epsilon)}\right]^{-0.35} \\ &= 1.73\ (0.63)^{-0.55}\left[\frac{D_pG}{\mu(1 - \epsilon)}\right]^{-0.35} \\ &= 2.155\left[\frac{D_pG}{\mu(1 - \epsilon)}\right]^{-0.35} \end{aligned} \qquad (44)$$

For the spherical shapes used in these studies, $D_pG/\mu(1 - \epsilon)$ is equal to the group $6G/a\varphi\mu$ used by Gamson, and Equation 44 thus becomes

$$j_d(1 - \epsilon)^{-0.2} = 2.155\left(\frac{6G}{a\varphi\mu}\right)^{-0.35}. \qquad (45)$$

The comparison with Gamson's correlation is shown in Figure 26.

Figures 24-26 show rather conclusively that the present correlation as represented by Equation 41, although of the same order of magnitude as the others, lies above all of them by a factor of approximately two. Even though some encouragement is to be drawn from the similarity in slope, the discrepancy is rather disturbing at first glance.

A careful review of the experimental technique failed to disclose any factors which might account for this discrepancy, and the original data are believed to be valid. This being the case, the difficulty must lie either in converting these data to transfer rates or in converting the rates, in turn, to actual coefficients. Both of these steps are somewhat vulnerable to the introduction of errors which could account for the vertical displacement of the j-factor correlation, and will therefore be discussed separately.

In converting the raw weight-loss data to transfer rates expressed as mass per unit time per unit surface area, the significant factors are obviously the actual weight loss, the time interval over with the loss occurred, and the effective surface area of the pellet. The first two may be dismissed in view of the reproducibility of the data, but the surface area cannot be affirmed quite so readily.

Areas were calculated from pellet diameters, which were in turn determined both by direct measurement and by calculation from the measured volumetric displacement, with the results from both methods being in good agreement (Appendix B). Calculation of the area from the measured diameter, however, presumes a completely smooth surface, and this condition was not entirely realized.

The p-dibromobenzene pellets appeared to have a smooth, shiny surface as they came from the pelleting press, but the alternate vaporization and condensation presumed to occur on a limited scale during storage eventually produced a much

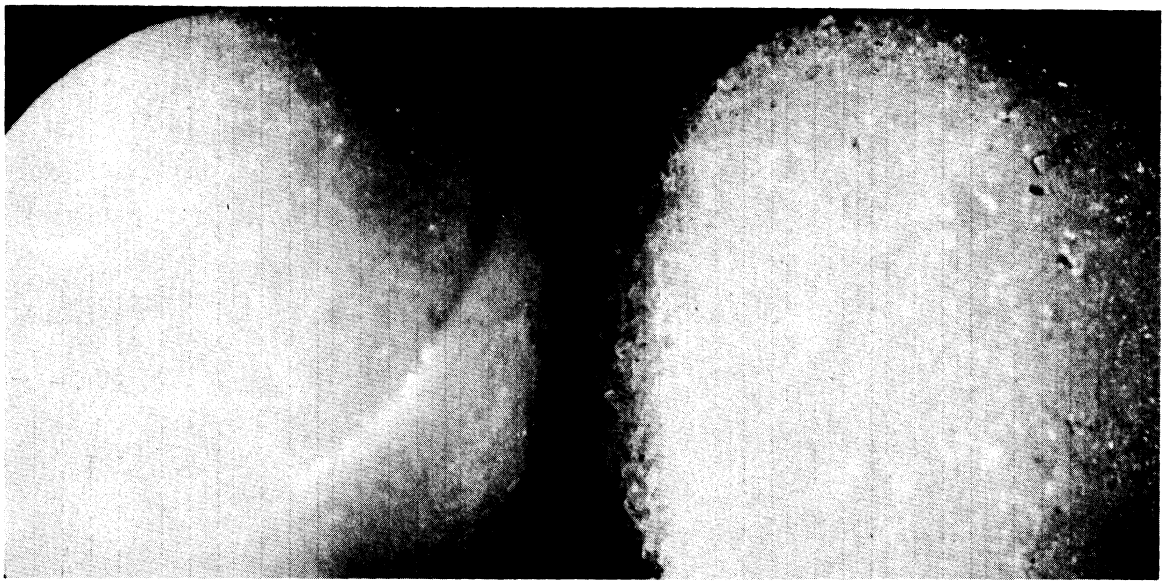

Fig. 27. Surface Condition of the P-dibromobenzene Pellets. Left as pressed; Right after storage.

rougher surface, crystalline in appearance, as can be seen in Figure 27. It was accordingly expected that fresh pellets would lose weight less rapidly under test conditions than would those which had been stored for some time, but no significant difference was noted in comparative tests.

The calculated specific gravity of the pressed pellets was found to be slightly less than the specific gravity of pure p-dibromobenzene (Appendix B), which suggests the presence of at least some pore space in the pellets. This might well mean an effective surface area significantly larger than the calculated spherical area because of exposed surface pores, particularly if the pressed pellets should happen to be more porous near the surface than at the center.

In any event, the spherical areas calculated from pellet diameters are conservative at best, and the actual surface roughness might well account for the displacement of the processed data.

As for the conversion of the transfer rates to actual coefficients, the use of a higher value for the vapor pressure of p-dibromobenzene would obviously lower the correlation somewhat, and might be justified in view of the disagreement among the reported data.

Also pertinent is the basic difference between the experimental conditions which prevailed during this study and those which pertained to the work of others, namely, the isolation of each individual active pellet from other active pellets. The partial pressure of p-dibromobenzene in the gas stream immediately adjacent to each active pellet is probably quite low under these conditions, because the transfer process is localized and considerable dilution of the air-vapor mixture is to be expected. With transfer occurring throughout the bed, however, there will be no vapor-free air available for dilution, and the partial pressure will therefore be higher.

No quantitative appraisal of the significance of this difference is possible in the absence of actual data, and it has presumably been taken into account in setting the driving force, $(p^{o} - p_{v})_{lm}$, equal to the vapor pressure. Indeed, if partial pressures <u>were</u> appreciable in these studies, the final correlation should be raised further, since for the same

value of k' a lower value of $(p^{o} - p_{v})_{lm}$ will yield a higher value of k_g, as can be seen from Equation 31. Even so, it is possible that the present results might have been altered somewhat, and in the right direction, if each active test pellet had been surrounded by other active pellets.

In summary, it is firmly believed that the original data presented in this report may be accepted as valid within rather close limits of experimental error, and hence that the relative effects of packing diameter, air flow rate, position in the bed, and orifice diameter on local rates of mass transfer are correctly delineated.

On the other hand, the absolute correlations obtained for both transfer rates and the j-factor are admittedly less definitive in view of their obvious displacement from the other correlations. Indeed, if these previous correlations are presumed to be correct, it might be entirely proper to compensate for the possible inaccuracies discussed in the foregoing paragraphs by introducing into the present correlation an empirical factor of 0.43, which would make it practically coincident with that of McCune and Wilhelm (48).

APPLICATION OF RESULTS

It is fully anticipated that the application of the results of this investigation will be largely qualitative rather than quantitative, not only because of the disagreement with other correlations noted in the preceding section, but also because the conclusions reached are themselves largely qualitative. In terms of their application, these conclusions may be restated as follows, using the same general order of listing as was used at the end of the section on Experimental Results.

No Orifice at Bed Entrance

(1) Insofar as it affects transfer phenomena, the assumption of a uniform velocity distribution in packed beds has long been useful, but was supported by only very limited experimental evidence. The present findings provide such evidence and thereby permit a freer use of the assumption.

(2) The fact that the entrance length was found to be surprisingly short provides a firmer basis for the general assumption that entrance effects are negligible in packed beds of reasonable depth.

(3) The quantitative correlations found to apply within the entrance length may be used to predict overall rates of mass transfer in shallow beds. This application is given further consideration below.

(4) The findings relative to the effect of pellet diameter are not new, but do provide additional confirmation for the conclusions reached by others.

Orifice at Bed Entrance

The conclusions pertaining to the effect of velocity perturbations at the entrance to a packed bed are probably even less likely to be applied quantitatively than are the foregoing, since extrapolation to other conditions is much more difficult. However, certain of the findings are apt to be useful in a qualitative sense and may be listed as follows:

(5) Conditions within a packed bed at any flow rate may be predicted from known conditions at a single flow rate, on the basis of the conclusion that changes in total flow affect all positions within the bed equally.

(6) Local transfer rates will be maximized in any regions subjected to perturbations in velocity. This implies, for example, that a fixed-bed catalytic reactor will be more susceptible to local hot spots in the region immediately adjacent to the catalyst support.

(7) Velocity perturbations such as those created by an orifice can result in local rates of transfer which are as much as 300 per cent higher than those obtainable when fully developed flow prevails.

(8) The fact that even abnormal velocity perturbations are dissipated within a relatively few inches of bed depth adds to the significance of conclusion (2), above.

(9) The observation that the velocity perturbations created by orifice entry into a packed bed (and hence by any similar stricture of the flow) are drastically reduced by a slight separation between the orifice plate and the bed may be of practical importance when it is desired to distribute the flow as evenly as possible. For example, the air entering a blast furnace would be dispersed throughout the charge more quickly if a lateral free space could be maintained around the inlet opening.

The complete analogy between heat and mass transfer in packed beds considered from the overall viewpoint has been questioned (2) because different transfer mechanisms may be involved. For example, heat may be transferred by intra-particle conduction, but there is no comparable mechanism in mass transfer. These objections are obviously not applicable to the present studies, which are concerned entirely with convective transfer between the gas stream and the surfaces of individual pellets. For this case, the analogy should hold, and the results summarized above should therefore be equally applicable in the field of heat transfer.

Sample Problem

It was noted in sub-paragraph (3) above that the quantitative correlations found in this investigation to be applicable within the entrance length in a packed bed may be used to predict overall rates of mass transfer in shallow beds. As an example of this application, and also as a means

of clarifying the interpretation of the present results, the solution to a sample problem will be outlined.

Problem: Calculate the concentration of naphthalene in the effluent stream when air at 20°C. and one atmosphere pressure is blown at a rate of 5000 pounds per square foot per hour through a 1-inch layer of uniform spherical naphthalene pellets having a diameter of 0.20 inches. The layer may be assumed to have a fractional void volume of 0.42.

Solution: The following physical constants and derived quantities will be needed:

For the bed, let $S = 1\ ft^2$; $H = 0.0833$ ft; $\epsilon = 0.42$;

$$D_p = 0.01667 \text{ ft}; \quad a = (1 - \epsilon)\frac{6\pi D_p^2}{\pi D_p^3} = 208.5\ ft^2/ft^3.$$

For air, $G = 5000\ lbs/ft^2/hr$; $\mu = 0.0428$ lbs/ft-hr (47);

$$\therefore Re = \frac{D_p G}{\mu} = \frac{(0.01667)(5000)}{0.0428} = 1950; \quad \text{and}$$

$$G' = \frac{5000}{29} = 172.5 \text{ lb-mols/ft}^2\text{-hr}.$$

For p-dibromobenzene at 80°F., $p^\circ = 0.038$ mm Hg (37);

$Sc = 2.41$; $\therefore (Sc)^{2/3} = 1.80$.

For naphthalene at 20°C., $p^\circ = 0.0527$ mm Hg (37);

$Sc = 2.57$ (28); $\therefore (Sc)^{2/3} = 1.887$.

Since the transfer rate is variable, the rate equation must be written in differential form:

$$dN_V' = k_g(p^\circ - p_V)\, dA = k_g(p^\circ - p_V)\, a\, S\, dH$$

$$\therefore dy = \frac{dN_V'}{G'S} = \frac{k_g(p^\circ - p_V)\, a\, S\, dH}{G'S} = \frac{k_g(p^\circ - p_V)\, a\, dH}{G'} \qquad (46)$$

But $y = p_v/P$, and hence $dy = dp_v/P$. Making this substitution in Equation 46 and separating variables yields

$$\frac{dp_v}{p^o - p_v} = \left(\frac{P\,a}{G'}\right) k_g\, dH$$

Integrating and substituting known numerical values,

$$-\ln \frac{0.0527 - p_2}{0.0527} = \frac{(760)(208.5)}{172.5} \int_0^{0.0833} k_g\, dH$$

$$= 920 \int_0^{0.0833} k_g\, dH \qquad (47)$$

The effluent partial pressure, p_2, may now be determined by evaluating the right-hand side of Equation 47 graphically. First, k_g for naphthalene can be related to k' for p-dibromobenzene as follows:

$$j_{nap} = j_{pdb} = \frac{k_g M_m P}{G} (Sc)^{2/3}$$

$$\therefore \left[\frac{k_g M_m P}{G} (Sc)^{2/3}\right]_{nap} = \left[\frac{k_g M_m P}{G} (Sc)^{2/3}\right]_{pdb}$$

Cancelling M_m, P, and G, and substituting for $(Sc)^{2/3}$,

$$1.887\ k_{g_{nap}} = 1.80\ k_{g_{pdb}} = 1.80 \left(\frac{k'}{p^o}\right)_{pdb} = \frac{1.80}{0.038} k'$$

$$\therefore k_{g_{nap}} = 25.1\ k' \qquad (48)$$

Substituting Equation 48 into Equation 38,

$$k'/G' \times 10^6 = B\,(Re)^m \quad , \qquad (38)$$

$$\therefore k_{g_{nap}} = (25.1)(G')(B)(Re)^m \times 10^{-6} \quad ,$$

$$= 4.33\ (B)(1950)^m \times 10^{-3} \ . \qquad (49)$$

Taking values of B and M from Table 1, numerical values of k_g may now be calculated and plotted as follows:

Table 4

$k_{g_{nap}}$ as a function of H

H, in.	B	-m	1950^{-m}	$k_g \times 10^{-3}$
1/16	95	0.55	64.0	6.42
1/8	80	0.48	37.9	9.14
3/16	70	0.43	26.0	11.66
1/4	61	0.40	20.7	12.77
5/16	55	0.375	17.1	13.92
3/8	50	0.36	15.3	14.27
1/2	48	0.35	14.2	14.63

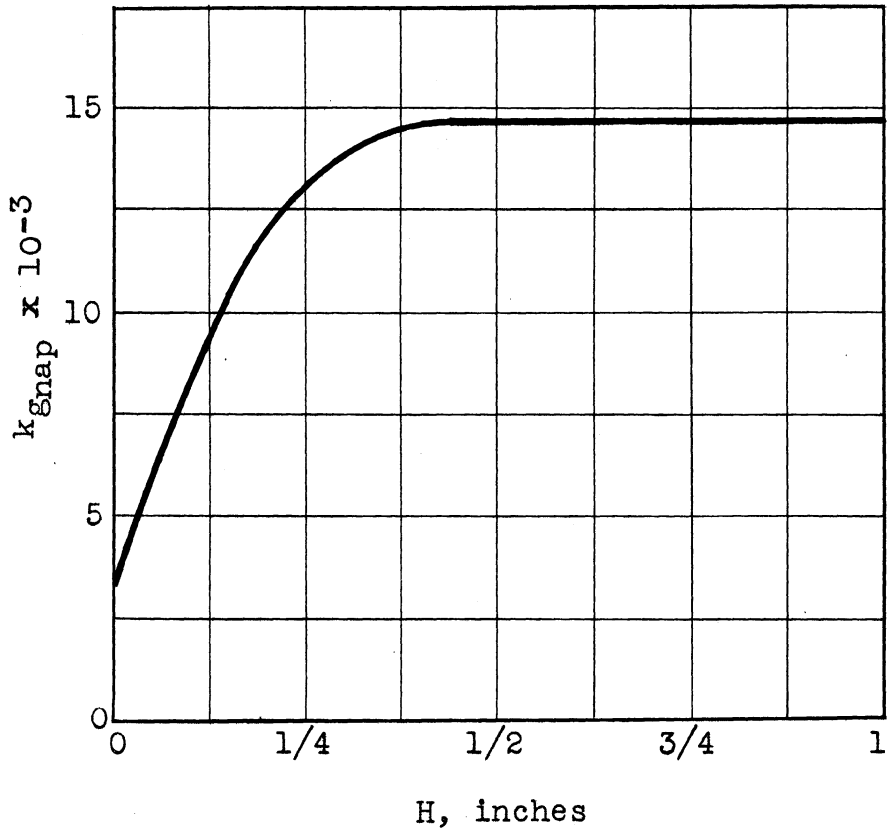

Fig. 28. $k_{g_{nap}}$ vs H (for graphical integration).

Graphical integration of Figure 28 yields an area under the curve of 13.0806×10^{-3} for H in inches, or 1.090×10^{-3} for H in feet. This figure may then be substituted for the integral in Equation 47:

$$- \ln \frac{0.0527 - p_2}{0.0527} = (920)(1.090 \times 10^{-3})$$

$$= 1.0028$$

$$\therefore \frac{0.0527 - p_2}{0.0527} = 0.367$$

$$p_2 = 0.0334 \text{ mm Hg}$$

(Neglecting entrance effects and using only Equation 38 yields an effluent partial pressure of 0.0356 mm Hg, which indicates that no appreciable error is introduced in neglecting entrance effects in even fairly shallow beds.)

SUMMARY

Local rates of mass transfer in a packed bed were determined by measuring the loss in weight of individual spherical pellets of p-dibromobenzene, carefully positioned in an otherwise inert bed of spheres through which a stream of air was passed. The test bed was 4 inches in diameter, sphere diameters were 1/8, 1/4, and 1/2 inch, and measurements were made to within 1/32 of an inch from the tube wall. The investigation covered a Reynolds number range of $150 < D_pG/\mu < 7{,}000$. The following conclusions were reached:

(1) Local rates of mass transfer may be correlated by the general equation

$$k'/G' \times 10^6 = B\left(\frac{D_pG}{\mu}\right)^m \quad , \qquad (34)$$

where B and m generally depend on axial distance but are independent of radial position, air flow rate, and pellet diameter.

(2) Entrance effects are confined to the first 1/2 inch of bed depth, beyond which transfer rates at all positions are given by

$$k'/G' \times 10^6 = 48\left(\frac{D_pG}{\mu}\right)^{-0.35} \quad . \qquad (38)$$

(3) Within the entrance length, B and m are highest at the inlet and decrease with depth, the actual values for these constants being given in Table 1.

(4) Except for its use as the characteristic length in the Reynolds number, pellet diameter is not a parameter.

Measurements were also made with the air entering the bed through 1- and 2-inch orifices, to determine the effect

of the resulting local velocity perturbations on transfer rates. Under these conditions, the following additional conclusions were drawn:

(5) The exponent m in Equation 34 is independent of pellet diameter, orifice diameter, position in the bed, and air flow rate, and is equal to -0.35.

(6) The values to be assigned to B in Equation 34 are functions of position in the bed and orifice diameter only, and are given in Tables 2 and 3.

(7) Perturbations created by the orifice are completely dissipated at a bed depth of approximately 2 inches.

(8) Transfer rates are as much as 300 per cent in the vicinity of the orifice than elsewhere, and are maximized at a point on the axis of the bed approximately 3/8 of an inch in from the surface. At lesser distances, the transverse transfer-rate profiles are characteristically M-shaped, with maxima corresponding to the edge of the orifice, while at greater distances the profiles are dome-shaped, with a maximum at the center of the bed and minima at the walls.

(9) As in the no-orifice case, pellet diameter is not a parameter, except for its use in the Reynolds number.

(10) Perturbations created by an orifice are drastically reduced if the orifice is separated from the packing surface by as little as 1/16 of an inch.

The relative effects of pellet diameter, air flow rate, position in the bed, and orifice diameter on local rates of mass transfer are believed to be correctly delineated by the proposed correlations, but the absolute correlations are less definitive in view of their displacement from the correlations based on previous investigations of overall transfer rates in packed beds.

APPENDICES

APPENDIX A

EXPERIMENTAL DATA

APPENDIX A

EXPERIMENTAL DATA

Table 5

SUMMARY OF ORIGINAL AND PROCESSED DATA FOR LOCAL MASS TRANSFER RATES

A. 4-inch orifice, 1/8-inch pellets

Run No.	Air, lb-mol/hr-ft^2	Temp °F	$\Delta\theta$, min	$-\Delta W$, mg	$-\Delta W_o$ mg	D_pG/μ	C_T	Rate x 10^4 lb-mols/hr-ft^2 Exper.	Rate x 10^4 lb-mols/hr-ft^2 Eqn 34	% Dev.
1/16-in. depth, 1-in. radius; 6 pellets per run										
2579	40.7	79.6	2.5	2.10	0.60	291	1.027	1.50	1.71	14.0
80	40.7	79.8	"	2.25	"	291	1.012	1.62	1.71	5.6
82	41.5	79.0	"	2.20	"	297	1.070	1.66	1.72	3.6
83	41.5	79.0	"	2.25	"	297	1.064	1.71	1.72	0.6
84	161.7	79.0	1.5	2.30	0.25	1156	1.070	3.55	3.17	10.7
85	162.7	79.3	"	2.35	"	1163	1.045	3.55	3.19	10.1
87	162.7	79.3	"	2.00	"	1163	1.049	2.98	3.19	7.0
88	163.7	79.7	"	2.05	"	1170	1.018	2.97	3.19	7.4
2716	87.9	79.7	2.0	2.10	0.15	628	1.018	2.42	2.42	0.0
17	87.9	80.2	"	2.20	"	628	0.985	2.46	2.42	1.6
19	87.9	80.2	"	2.20	"	628	0.985	2.46	2.42	1.6
20	88.9	81.1	"	2.45	"	636	0.929	2.60	2.42	6.9
42	22.8	82.0	3.0	2.30	0.45	163	0.875	1.31	1.32	0.8
43	22.0	82.5	"	2.05	"	157	0.851	1.10	1.30	18.2
45	23.5	79.5	"	2.00	"	168	1.033	1.30	1.33	2.3
46	22.8	78.5	"	2.05	"	163	1.106	1.43	1.32	7.7
									Ave.	6.1
1/16-in. depth, 1-1/2-in. radius; 6 pellets per run										
2615	37.5	80.8	2.5	2.30	0.75	268	0.950	1.43	1.65	15.4
16	37.5	82.0	"	2.75	"	268	0.878	1.71	1.65	3.5
18	37.5	81.5	"	2.80	"	268	0.904	1.80	1.65	8.3
19	37.5	81.7	"	2.60	"	268	0.895	1.61	1.65	2.5
21	163.7	80.3	1.5	2.35	0.50	1170	0.979	2.93	3.19	8.9
24	162.7	80.0	"	2.50	"	1163	1.003	3.26	3.19	2.1
25	162.7	79.7	"	2.55	"	1163	1.018	3.39	3.19	5.9
26	23.5	82.4	3.0	2.35	"	168	0.855	1.28	1.33	3.9
27	23.5	82.7	"	2.55	"	168	0.838	1.39	1.33	4.3
29	23.5	80.8	"	2.30	"	168	0.947	1.38	1.33	3.6
30	23.5	79.8	3.33	2.35	"	168	1.012	1.36	1.33	2.2

Table 5A (Continued)

Run No.	Air, lb-mol/hr-ft^2	Temp °F	$\Delta\Theta$, min	$-\Delta W$, mg	$-\Delta W_o$ mg	D_pG/μ	C_T	Rate x 10^4 lb-mols/hr-ft^2 Exper.	Eqn 34	% Dev.
1/16-in. depth, 1-1/2-in. radius; 6 pellets per run										
2631	83.0	79.3	2.5	2.90	0.50	593	1.049	2.45	2.35	4.1
32	83.0	79.4	"	2.85	"	593	1.039	2.37	2.35	0.8
34	83.0	79.4	"	2.50	"	593	1.042	2.02	2.35	16.3
35	83.0	79.6	"	2.85	"	593	1.027	2.34	2.35	0.4
									Ave.	5.5
1/16-in. depth, 2-in. radius; 6 pellets per run										
2604	165.6	80.8	1.5	2.80	0.65	1184	0.950	3.31	3.21	3.0
05	167.6	80.7	"	2.60	"	1198	0.953	3.01	3.23	7.3
07	163.7	80.9	"	2.95	"	1170	0.945	3.52	3.19	9.4
08	165.6	81.0	"	2.65	"	1184	0.937	3.03	3.21	5.9
09	39.1	79.5	2.5	2.50	0.80	280	1.036	1.74	1.67	4.0
12	38.3	79.5	3.0	2.70	"	274	1.036	1.59	1.66	4.4
13	38.3	79.5	2.5	2.50	"	274	1.009	1.67	1.66	0.6
2727	88.9	78.4	2.0	3.10	1.30	636	1.113	2.43	2.43	0.0
28	89.9	79.2	"	2.95	"	643	1.055	2.11	2.44	15.6
30	88.9	79.1	"	3.30	"	636	1.061	2.58	2.43	5.8
31	88.9	79.0	"	3.10	"	636	1.064	2.33	2.43	4.3
32	21.2	78.5	3.0	2.40	1.05	152	1.102	1.21	1.27	5.0
33	19.7	78.5	"	2.50	"	141	1.102	1.30	1.23	5.4
35	20.5	77.9	"	2.30	"	147	1.150	1.17	1.25	6.8
36	21.2	76.7	"	2.60	"	152	1.243	1.56	1.27	13.6
									Ave.	6.4
3/16-in. depth, 1-in. radius; 6 pellets per run										
2375	25.0	80.4	3.0	2.75	0.40	179	0.976	1.86	1.88	1.1
76	24.3	80.4	"	2.80	"	174	0.976	1.90	1.85	2.6
78	25.0	80.5	"	2.40	"	179	0.971	1.57	1.88	19.7
79	25.0	80.8	"	2.40	"	179	0.950	1.57	1.88	19.7
80	39.9	79.1	"	3.25	0.50	285	1.036	2.31	2.46	6.5
81	39.9	79.2	"	3.35	"	285	1.052	2.43	2.46	1.2
83	39.1	78.4	"	3.30	"	280	1.110	2.51	2.43	3.2
84	39.1	78.5	"	3.30	"	280	1.099	2.50	2.43	2.8
85	90.9	79.5	"	5.40	"	650	1.036	4.12	3.93	4.6
86	90.9	79.3	"	4.95	"	650	1.042	3.76	3.93	4.5
88	90.9	78.8	"	5.05	"	650	1.080	3.98	3.93	1.3
89	90.9	78.9	"	5.10	"	650	1.077	4.01	3.93	2.0
2451	169.6	79.6	1.5	4.10	0.65	1213	1.024	5.72	5.60	2.1
52	169.6	79.4	"	4.25	"	1213	1.039	6.06	5.60	7.6
54	169.6	81.7	"	4.35	"	1213	0.893	5.35	5.60	4.7
55	169.6	80.5	"	4.30	"	1213	0.965	5.70	5.60	5.1
									Ave.	5.5

Table 5A (Continued)

Run No.	Air, lb-mol/hr-ft^2	Temp °F	$\Delta\theta$, min	$-\Delta W$, mg	$-\Delta W_o$ mg	D_pG/μ	C_T	Rate x 10^4 lb-mols/hr-ft^2 Exper.	Eqn 34	% Dev.
3/16-in. depth, 2-in. radius; 6 pellets per run										
2487	90.9	79.6	2.0	3.40	0.25	650	1.027	3.94	3.93	0.3
88	89.9	80.1	"	3.35	"	643	0.991	3.73	3.90	4.6
90	90.9	78.8	"	3.25	"	650	1.080	3.94	3.93	0.3
91	90.9	79.0	"	3.50	"	650	1.064	4.21	3.93	6.7
93	162.7	79.6	"	4.85	-0.20	1163	1.024	6.28	5.47	9.7
94	165.6	80.6	"	4.40	"	1184	0.959	5.36	5.53	3.2
96	164.7	79.8	"	4.55	"	1178	1.015	5.86	5.50	6.1
97	166.6	79.7	"	3.80	"	1191	1.021	4.96	5.55	11.9
99	39.9	79.5	2.5	3.60	1.20	285	1.033	2.41	2.46	2.1
2500	39.9	79.7	"	3.65	"	285	1.018	2.42	2.46	1.7
02	39.9	80.7	"	4.20	"	285	0.953	2.78	2.46	11.5
03	39.9	80.5	"	3.80	"	285	0.971	2.45	2.46	0.4
2737	21.2	80.5	3.0	2.60	0.45	152	0.971	1.69	1.71	1.2
38	21.2	80.2	"	2.35	"	152	0.988	1.52	1.71	12.5
40	22.0	80.1	"	2.95	"	157	0.991	1.99	1.75	12.1
41	21.2	80.2	"	2.65	"	152	0.985	1.76	1.71	2.8
									Ave.	5.4
1/2-in. depth, 1-in. radius; 6 pellets per run										
2330	84.0	81.6	3.0	5.85	0.45	600	0.901	3.95	4.30	8.9
31	84.0	80.8	"	5.40	"	600	0.950	3.81	4.30	12.9
33	83.0	80.5	"	5.05	"	593	0.965	3.60	4.26	18.3
34	83.0	80.4	"	5.20	"	593	0.976	3.76	4.26	13.3
40	41.5	78.6	"	3.45	0.35	297	1.096	2.76	2.71	1.8
41	41.5	81.5	"	3.90	"	297	0.909	2.62	2.71	3.4
43	41.5	80.1	"	3.60	"	297	0.994	2.62	2.71	3.4
44	41.5	79.8	"	3.60	"	297	1.015	2.67	2.71	1.5
2440	168.6	81.3	1.5	3.80	0.15	1205	0.918	5.43	6.76	24.5
41	168.6	81.3	"	3.70	"	1205	0.920	5.30	6.76	27.5
43	166.6	80.3	"	3.90	"	1191	0.979	5.95	6.70	12.6
44	166.6	80.0	"	3.45	"	1191	1.003	5.36	6.70	25.0
2540	22.0	83.1	3.0	2.90	0.55	157	0.818	1.56	1.80	15.4
41	22.0	79.4	"	2.60	"	157	1.039	1.73	1.80	4.0
43	22.0	78.1	"	2.35	"	157	1.134	1.65	1.80	9.1
44	22.0	78.0	"	2.40	"	157	1.141	1.71	1.80	5.3
									Ave.	11.7
1/2-in. depth, 2-in. radius; 6 pellets per run										
2273	163.7	78.0	3.0	8.15	0.45	1170	1.141	7.12	6.63	6.9
74	165.6	79.1	"	8.05	"	1184	1.061	6.53	6.67	2.1
76	164.7	79.7	"	8.05	"	1178	1.021	6.29	6.65	5.7
77	166.6	79.9	"	8.30	"	1191	1.006	6.40	6.70	4.7

Table 5A (Continued)

Run No.	Air, lb-mol/hr-ft^2	Temp °F	$\Delta\Theta$, min	$-\Delta W$, mg	$-\Delta W_o$ mg	$\frac{D_p G}{\mu}$	C_T	Rate x 10^4 lb-mols/hr-ft^2 Exper.	Eqn 38	% Dev.
1/2-in. depth, 2-in. radius; 6 pellets per run										
2284	40.7	80.8	3.0	4.05	0.50	291	0.950	2.73	2.68	1.8
85	43.1	79.8	"	3.75	"	308	1.012	2.67	2.78	4.1
87	43.1	78.7	"	3.60	"	308	1.086	2.73	2.78	1.8
88	42.3	78.2	"	3.50	"	302	1.123	2.73	2.75	0.7
2425	84.0	79.7	"	5.25	0.40	601	1.018	4.00	4.30	7.5
26	83.0	79.9	"	5.60	"	593	1.006	4.24	4.26	0.5
27	83.0	80.1	"	5.50	"	593	0.994	4.11	4.26	3.6
29	83.0	79.4	"	5.30	"	593	1.039	4.13	4.26	3.1
2535	22.0	78.4	"	2.65	0.55	157	1.113	1.90	1.80	5.3
36	22.0	78.4	"	2.40	"	157	1.109	1.66	1.80	8.4
38	22.0	78.7	"	2.40	"	157	1.086	1.63	1.80	10.4
39	22.0	79.3	"	2.65	"	157	1.045	1.77	1.80	1.7
									Ave.	4.3
1-in. depth, 1-in. radius, 4* and 6 pellets per run										
2227	22.0	78.5	3.0	1.70	0.25	157	1.099	1.93	1.80	6.7
28	22.8	78.3	"	1.35	"	163	1.120	1.50	1.84	22.7
30	22.8	78.8	"	1.80	"	163	1.080	2.03	1.84	9.4
31	22.0	79.5	"	1.40	"	157	1.033	1.45	1.80	24.1
43	86.9	79.4	"	3.50	0.35	621	1.042	3.99	4.39	10.0
44	85.0	79.0	"	4.10	"	608	1.064	4.85	4.33	10.7
46	87.9	78.8	"	3.55	"	628	1.080	4.20	4.42	5.2
47	86.9	78.2	"	3.75	"	621	1.124	4.64	4.39	5.4
2415	39.9	79.5	"	3.30	0.15	285	1.033	2.63	2.65	0.8
16	39.9	79.3	"	3.10	"	285	1.045	2.50	2.65	6.0
18	39.9	79.2	"	3.25	"	285	1.052	2.64	2.65	0.4
19	39.9	79.0	"	2.90	"	285	1.067	2.37	2.65	11.8
2557	169.6	78.0	1.5	3.90	0.45	1213	1.141	6.39	6.78	6.1
58	167.6	79.3	"	3.65	"	1198	1.045	5.41	6.74	24.6
60	167.6	78.5	"	3.70	"	1198	1.099	5.79	6.74	16.4
61	167.6	78.5	"	3.65	"	1198	1.099	5.70	6.74	18.2
									Ave.	11.2
1-in. depth, 2-in. radius; 6 pellets per run										
2188	39.9	79.0	2.0	3.00	0.65	285	1.069	3.05	2.65	13.1
89	39.1	79.3	"	2.90	"	280	1.049	2.87	2.61	9.1
91	39.1	79.3	"	2.70	"	280	1.049	2.61	2.61	0.0
92	39.1	79.2	"	2.80	"	280	1.052	2.75	2.61	5.1
99	179.4	80.5	"	6.70	0.20	1283	0.968	7.65	7.03	8.1
2200	179.4	81.3	"	6.95	"	1283	0.917	7.52	7.03	6.5
02	179.4	80.5	"	6.65	"	1283	0.965	7.56	7.03	7.0

*Runs 2227-47

Table 5A (Continued)

Run No.	Air, lb-mol / hr-ft²	Temp °F	Δθ, min	-ΔW, mg	-ΔW₀ mg	D_pG/μ	C_T	Rate x 10^4 lb-mols/hr-ft² Exper.	Rate x 10^4 lb-mols/hr-ft² Eqn 38	% Dev.
1-in. depth, 2-in. radius; 6 pellets per run										
2203	183.4	81.0	2.0	6.15	0.20	1311	0.942	6.81	7.13	4.7
10	89.9	79.0	3.0	5.40	0.00	643	1.067	4.66	4.49	3.6
11	88.9	79.2	"	5.45	"	636	1.052	4.64	4.45	4.1
12	88.9	79.2	"	5.30	"	636	1.052	4.52	4.45	1.5
14	88.9	78.2	"	5.40	"	636	1.127	4.93	4.45	9.7
16	22.0	76.7	"	2.00	0.30	157	1.243	1.71	1.80	5.3
17	22.8	77.7	"	2.20	"	163	1.165	1.79	1.84	2.8
19	22.0	77.6	"	2.25	"	157	1.204	1.90	1.80	5.3
20	22.8	77.7	"	2.45	"	163	1.161	2.03	1.84	9.4
									Ave.	6.0

Table 5

B. 4-inch orifice, 1/4-inch pellets

Run No.	Air, lb-mol/hr-ft^2	Temp °F	$\Delta\theta$, min	$-\Delta W$, mg	$-\Delta W_o$ mg	$\frac{D_p G}{\mu}$	C_T	Rate x 10^4 lb-mols/hr-ft^2 Exper.	Eqn 34	% Dev.
1/8-in. depth, 0-in. radius; 1 pellet per run										
743	185.3	80.2	2.0	1.55	0.15	2472	0.988	3.28	3.48	6.1
44	183.4	80.2	"	1.45	"	2447	0.988	3.05	3.47	13.8
46	181.4	80.2	"	1.55	"	2420	0.985	3.28	3.45	5.2
47	179.4	80.0	"	1.65	"	2393	1.003	3.57	3.43	3.9
53	39.9	80.0	5.0	1.95	"	532	1.000	1.72	1.57	8.7
54	39.9	80.2	"	1.95	"	532	0.985	1.69	1.57	7.1
56	39.9	80.1	"	1.85	"	532	0.991	1.60	1.57	1.9
57	39.9	80.1	"	1.75	"	532	0.994	1.51	1.57	4.0
2125	85.9	79.8	3.0	1.35	0.05	1146	1.012	2.10	2.34	11.4
26	88.9	80.2	"	1.40	"	1186	0.988	2.11	2.38	12.8
28	88.9	80.0	"	1.35	"	1186	0.997	2.06	2.38	15.5
29	88.9	80.0	"	1.35	"	1186	1.000	2.06	2.38	15.5
3132	21.2	80.0	5.0	1.40	0.25	283	0.997	1.09	1.13	3.7
34	22.0	81.6	"	1.70	"	293	0.898	1.24	1.15	7.3
35	22.8	81.5	"	1.45	"	304	0.907	1.04	1.17	12.5
									Ave.	8.6
1/8-in. depth, 1/2-in. radius; 2 pellets per run										
2069	40.7	79.4	2.0	1.55	0.25	543	1.039	1.61	1.58	1.9
70	40.7	79.5	"	1.45	"	543	1.033	1.48	1.58	6.8
72	40.7	79.4	"	1.50	"	543	1.039	1.55	1.58	1.9
73	40.7	79.4	"	1.45	"	543	1.042	1.49	1.58	6.0
80	81.0	80.0	"	2.00	0.10	1081	1.003	2.27	2.27	0.0
81	83.0	80.1	"	2.15	"	1107	0.994	2.43	2.30	5.3
83	83.0	79.9	"	2.15	"	1107	1.006	2.51	2.30	8.4
84	83.0	80.0	"	2.05	"	1107	1.000	2.32	2.30	0.9
85	200.1	81.0	"	2.90	"	2669	0.937	3.12	3.62	16.0
86	200.1	80.3	"	3.45	"	2669	0.982	3.92	3.62	7.7
88	198.1	80.1	"	3.35	"	2643	0.991	3.84	3.61	6.0
89	197.1	80.2	"	3.45	"	2629	0.985	3.93	3.61	8.1
3136	22.8	82.5	2.5	1.55	0.30	304	0.853	1.02	1.17	14.7
37	24.3	80.4	"	1.60	"	324	0.976	1.21	1.21	0.0
38	24.3	78.9	"	1.50	"	324	1.074	1.23	1.21	1.6
39	24.3	77.6	"	1.40	"	324	1.171	1.23	1.21	1.6
									Ave.	5.4
1/8-in. depth, 1-in. radius; 4 pellets per run										
517	21.2	84.8	5.0	5.10	0.40	283	0.735	0.82	1.13	37.8
18	20.5	80.9	"	5.25	"	273	0.942	1.09	1.11	1.8
20	20.5	80.0	"	4.05	"	273	1.003	0.87	1.11	27.6

Table 5B (Continued)

Run No.	Air, lb-mol/hr-ft^2	Temp °F	$\Delta\Theta$, min	$-\Delta W$, mg	$-\Delta W_{\dot{\Theta}}$ mg	D_pG/μ	C_T	Rate x 10^4 lb-mols/hr-ft^2 Exper.	Rate x 10^4 lb-mols/hr-ft^2 Eqn 34	% Dev.
1/8-in. depth, 1-in. radius; 4 pellets per run										
540	127.3	80.3	5.0	13.05	0.80	1698	0.979	2.86	2.86	0.0
41	127.3	80.7	"	10.85	"	1698	0.953	2.28	2.86	25.4
43	130.2	79.2	"	11.40	"	1737	1.052	2.66	2.90	9.0
1847	88.9	79.8	2.0	4.30	0.35	1186	1.012	2.38	2.38	0.0
48	88.9	79.0	"	4.25	"	1186	1.067	2.48	2.38	4.0
50	88.9	79.3	"	4.35	"	1186	1.045	2.49	2.38	4.4
51	87.9	79.5	"	3.80	"	1173	1.030	2.11	2.36	11.8
3152	39.9	79.5	1.5	2.00	"	532	1.033	1.35	1.57	16.3
53	39.9	79.4	"	2.10	"	532	1.042	1.45	1.57	8.3
55	40.7	79.5	"	2.10	"	543	1.036	1.44	1.58	9.7
56	39.9	79.4	"	2.10	"	532	1.039	1.45	1.57	8.3
									Ave.	11.7
1/8-in. depth, 1-1/2-in. radius; 4 and 6* pellets per run										
648	39.9	79.3	2.0	4.70	2.20	532	1.049	1.56	1.57	0.6
49	39.9	80.3	"	4.80	"	532	0.982	1.52	1.57	3.3
51	39.9	80.5	"	5.15	"	532	0.968	1.70	1.57	7.6
52	39.9	80.5	"	4.70	"	532	0.968	1.44	1.57	9.0
54	22.0	80.8	"	3.90	"	293	0.947	0.96	1.15	19.8
56	22.0	80.9	"	4.00	"	293	0.944	1.01	1.15	13.9
57	22.0	80.5	"	4.00	"	293	0.965	1.04	1.15	10.6
3162	193.2	79.3	1.5	6.45	0.45	2577	1.049	3.33	3.55	6.6
63	192.2	79.4	"	6.25	"	2564	1.039	3.19	3.56	11.6
65	191.2	79.4	"	6.50	"	2551	1.039	3.33	3.54	6.3
66	192.2	79.6	"	6.30	"	2564	1.024	3.17	3.56	12.3
68	85.9	81.1	"	5.00	0.40	1146	0.932	2.27	2.34	3.1
69	86.9	81.1	"	5.00	"	1159	0.932	2.27	2.35	3.5
71	85.9	81.0	"	5.00	"	1146	0.937	2.28	2.34	2.6
72	85.0	81.0	"	5.15	"	1134	0.937	2.36	2.33	1.3
									Ave.	7.5
1/8-in. depth, 2-in. radius; 6 pellets per run										
496	39.1	81.2	5.0	10.45	0.30	522	0.926	1.49	1.55	4.0
98	39.9	80.4	"	9.95	"	532	0.973	1.49	1.57	5.4
514	22.0	77.6	"	13.95	7.55	293	1.168	1.19	1.15	3.4
16	22.0	78.0	"	13.95	"	293	1.141	1.12	1.15	2.7
3173	85.9	80.5	1.5	4.70	0.40	1146	0.965	2.20	2.34	6.4
74	85.9	80.9	"	4.55	"	1146	0.945	2.07	2.34	13.0
76	85.9	80.9	"	4.95	"	1146	0.942	2.27	2.34	3.1
77	85.0	80.8	"	5.25	"	1134	0.947	2.43	2.33	4.1
78	194.2	81.4	"	7.45	"	2591	0.915	3.41	3.57	4.7
79	193.2	81.4	"	6.95	"	2577	0.915	3.17	3.55	12.0
81	195.2	81.3	"	7.60	"	2604	0.920	3.50	3.57	2.0
82	193.2	81.2	"	6.90	"	2577	0.923	3.18	3.55	11.6
									Ave.	6.0

* Runs 3162-72

Table 5B (Continued)

Run No.	Air, lb-mol/hr-ft^2	Temp °F	$\Delta\theta$, min	$-\Delta W$, mg	$-\Delta W_o$ mg	D_pG/μ	C_T	Rate x 10^4 lb-mols/hr-ft^2 Exper.	Eqn 34	% Dev.
3/8-in. depth, 0-in. radius; 1 pellet per run										
793	71.2	79.6	5.0	3.70	0.20	950	1.027	3.42	3.02	11.7
94	69.2	79.6	"	3.45	"	923	1.024	3.17	2.96	6.6
96	68.2	79.0	"	3.50	"	910	1.067	3.35	2.93	12.5
97	68.2	79.3	"	3.25	"	910	1.049	3.05	2.93	3.9
98	149.9	81.0	"	5.50	0.15	2000	0.934	4.76	4.86	2.1
99	150.9	80.9	"	5.00	"	2013	0.942	4.35	4.87	12.0
801	151.9	79.2	"	4.65	"	2026	1.052	4.51	4.91	8.9
02	150.9	79.5	"	4.35	"	2013	1.036	4.14	4.87	17.6
09	40.7	81.1	"	4.45	1.95	543	0.932	2.22	2.11	5.0
10	40.7	78.6	"	4.25	"	543	1.093	2.39	2.11	11.7
13	40.7	77.9	"	4.10	"	543	1.150	2.35	2.11	10.2
14	39.9	79.1	"	4.15	"	532	1.061	2.22	2.08	6.3
60	22.0	79.0	"	1.65	0.30	293	1.067	1.37	1.42	3.6
61	22.0	79.2	"	1.65	"	293	1.055	1.35	1.42	5.2
63	22.8	79.1	"	1.70	"	304	1.061	1.42	1.46	2.8
64	22.0	79.2	"	1.65	"	293	1.055	1.46	1.42	2.7
									Ave.	7.7
3/8-in. depth, 1/2-in. radius; 2 pellets per run										
693	39.9	80.1	2.0	2.20	0.20	532	0.994	2.37	2.08	12.2
94	39.9	80.0	"	1.95	"	532	1.000	2.08	2.08	0.0
96	39.9	79.8	"	1.80	"	532	1.015	1.93	2.08	7.8
97	39.9	79.8	"	1.75	"	532	1.015	1.87	2.08	11.2
98	82.0	80.2	"	4.50	1.70	1094	0.988	3.30	3.30	0.0
99	83.0	80.0	"	4.35	"	1107	0.997	3.14	3.33	6.1
701	83.0	80.3	"	4.45	"	1107	0.979	3.20	3.33	4.1
02	83.0	80.3	"	5.10	"	1107	0.982	3.86	3.33	13.7
03	209.9	80.5	"	5.95	1.55	2800	0.971	5.09	6.02	18.3
04	208.9	80.5	"	6.35	"	2787	0.965	5.51	6.02	9.3
06	206.0	80.8	"	6.60	"	2748	0.947	5.69	5.95	4.6
07	205.0	81.0	"	6.00	"	2735	0.937	4.97	5.95	19.7
2107	25.0	82.8	"	1.35	0.10	334	0.835	1.24	1.54	24.2
08	26.6	80.9	"	1.50	"	355	0.942	1.57	1.61	2.5
10	26.6	79.7	"	1.15	"	355	1.018	1.27	1.61	26.8
11	26.6	79.6	"	1.25	"	355	1.024	1.41	1.61	14.2
									Ave.	10.9
3/8-in. depth, 1-in. radius; 2 and 4* pellets per run										
930	39.9	79.8	2.0	0.70	-0.95	532	1.015	1.99	2.08	4.5
31	39.9	80.1	"	0.55	"	532	0.994	1.77	2.08	17.5
33	39.9	79.9	"	0.95	"	532	1.006	2.27	2.08	8.4
34	39.9	80.1	"	0.90	"	532	0.994	2.19	2.08	5.0

* Runs 2102-06

Table 5B (Continued)

Run No.	Air, lb-mol/hr-ft^2	Temp °F	$\Delta\theta$, min	$-\Delta W$, mg	$-\Delta W_0$ mg	D_pG/μ	C_T	Rate x 10^4 lb-mols/hr-ft^2 Exper.	Rate x 10^4 lb-mols/hr-ft^2 Eqn 34	% Dev.
3/8-in. depth, 1-in. radius, 2 and 4* pellets per run										
935	198.1	75.8	2.0	3.70	0.15	2643	1.319	5.57	5.80	4.1
36	197.1	76.7	"	4.25	"	2629	1.240	6.05	5.79	4.3
38	197.1	78.1	"	4.30	"	2629	1.130	5.59	5.79	3.6
39	196.1	78.6	"	4.70	"	2616	1.093	5.92	5.77	2.5
40	71.2	78.6	"	3.00	"	950	1.093	3.72	3.02	18.8
41	70.2	78.2	"	3.10	"	950	1.083	3.80	3.02	20.5
43	70.2	78.2	"	2.50	"	936	1.127	3.16	2.99	5.4
44	67.2	78.6	"	2.50	"	896	1.093	3.06	2.91	4.9
2102	27.3	78.9	"	2.65	0.10	364	1.074	1.63	1.63	0.0
03	26.6	79.5	"	2.70	"	355	1.030	1.60	1.61	0.6
05	27.3	80.0	"	2.75	"	364	1.000	1.58	1.63	3.2
06	26.6	80.2	"	2.80	"	355	0.988	1.59	1.61	1.3
									Ave.	6.5
3/8-in. depth, 1-1/2-in. radius; 3 pellets per run										
975	24.3	78.0	2.0	2.40	0.50	324	1.137	1.72	1.52	11.6
76	24.3	79.2	"	2.20	"	324	1.052	1.42	1.52	7.0
78	24.3	79.7	"	2.10	"	324	1.018	1.29	1.52	17.8
79	24.3	80.0	"	2.20	"	324	0.997	1.34	1.52	13.4
80	39.1	79.4	"	2.70	"	522	1.042	1.82	2.05	12.6
81	39.1	79.3	"	3.15	"	522	1.049	2.21	2.05	7.2
83	39.1	79.1	"	3.00	"	522	1.061	2.10	2.05	2.4
84	39.1	78.9	"	2.95	"	522	1.074	2.09	2.05	1.9
85	205.0	80.2	"	9.20	2.20	2735	0.988	5.49	5.95	8.4
86	205.0	80.7	"	9.25	"	2735	0.956	5.35	5.95	11.2
88	204.0	81.1	"	10.75	"	2721	0.932	6.33	5.92	6.5
89	203.0	81.4	"	12.30	"	2708	0.915	7.34	5.91	19.5
90	80.0	79.3	"	6.30	"	1067	1.049	3.41	3.22	5.6
91	79.0	78.9	"	6.50	"	1054	1.074	3.67	3.22	12.3
93	79.0	78.5	"	5.55	"	1054	1.099	2.92	3.22	10.3
94	71.2	78.7	"	5.55	"	950	1.090	2.90	3.02	4.1
									Ave.	9.5
3/8-in. depth, 2-in. radius; 4 pellets per run										
1030	25.8	78.7	2.0	2.50	0.25	344	1.086	1.45	1.58	9.0
31	25.8	78.7	"	2.70	"	344	1.086	1.58	1.58	0.0
33	25.8	78.5	"	2.25	"	344	1.106	1.32	1.58	19.7
34	25.8	78.3	"	2.55	"	344	1.113	1.52	1.58	3.9
40	39.9	80.0	"	5.55	1.60	532	1.003	2.36	2.08	11.9
41	39.9	80.5	"	5.45	"	532	0.968	2.22	2.08	6.3
43	39.9	79.5	"	6.00	"	532	1.030	2.70	2.08	23.0
44	39.9	79.9	"	5.50	"	532	1.006	2.33	2.08	10.7

* Runs 2102-06.

Table 5B (Continued)

Run No.	Air, lb-mol/hr-ft^2	Temp °F	$\Delta\theta$, min	$-\Delta W$, mg	$-\Delta W_e$ mg	D_pG/μ	C_T	Rate x 10^4 lb-mols/hr-ft^2 Exper.	Eqn 36	% Dev.
3/8-in. depth, 2-in. radius; 4 pellets per run										
2091	81.0	79.8	2.0	4.55	0.25	1081	1.012	2.59	3.27	26.3
92	82.0	78.1	"	4.55	"	1094	1.130	2.89	3.30	14.2
94	81.0	77.4	"	5.05	"	1081	1.190	3.40	3.27	3.8
95	81.0	79.3	"	5.75	"	1081	1.049	3.44	3.27	4.9
96	195.2	79.5	"	9.55	0.35	2604	1.033	5.66	5.76	1.8
97	194.2	79.8	"	9.55	"	2591	1.015	5.56	5.73	3.1
99	193.2	79.6	"	9.45	"	2577	1.027	5.57	5.72	2.7
2100	193.2	80.4	"	9.25	"	2577	0.976	5.17	5.72	10.7
									Ave.	9.5
5/8-in. depth, 1/2-in. radius; 2 pellets per run										
1409	40.7	80.6	2.0	2.20	0.20	543	0.962	2.29	2.18	4.8
10	40.7	80.2	"	2.50	"	543	0.985	2.70	2.18	19.3
12	40.7	79.3	"	1.95	"	543	1.046	2.18	2.18	0.0
13	40.7	79.5	"	2.35	"	543	1.033	2.64	2.18	17.4
14	22.0	79.1	"	1.30	0.15	293	1.061	1.45	1.45	0.0
15	23.5	78.9	"	1.25	"	313	1.074	1.41	1.51	7.1
17	24.3	78.5	"	1.40	"	324	1.106	1.64	1.54	6.1
18	24.3	78.4	"	1.30	"	324	1.113	1.52	1.54	1.3
20	79.0	79.9	"	3.45	0.35	1054	1.006	3.72	3.32	10.8
21	74.1	80.1	"	3.20	"	988	0.994	3.37	3.18	5.6
23	73.1	79.6	"	3.00	"	975	1.024	3.23	3.16	2.2
24	80.0	79.8	"	3.45	"	1067	1.012	3.74	3.34	10.7
25	200.1	81.1	"	5.05	0.25	2669	0.932	5.32	6.06	13.9
26	199.1	79.9	"	5.50	"	2656	1.009	6.30	6.05	4.0
28	197.1	79.9	"	5.85	"	2629	1.009	6.73	6.01	10.7
29	197.1	79.8	"	4.65	"	2629	1.012	5.30	6.01	13.4
									Ave.	8.0
5/8-in. depth, 1-in. radius; 2* and 4 pellets per run										
1327	81.0	79.7	2.0	3.25	0.70	1080	1.021	3.10	3.37	8.7
28	75.1	79.6	"	3.50	"	1002	1.024	3.42	3.21	6.1
30	81.0	79.4	"	4.00	"	1080	1.039	4.09	3.37	17.6
31	84.0	79.5	"	3.65	"	1121	1.036	3.64	3.45	5.2
32	21.2	80.1	"	1.70	"	283	0.994	1.17	1.41	20.5
33	21.2	81.0	"	1.60	"	283	0.940	1.01	1.41	39.6
35	22.0	80.1	"	1.95	"	293	0.994	1.48	1.45	2.0
36	22.0	80.0	"	1.70	"	293	0.997	1.19	1.45	21.8
2004	193.2	80.3	"	10.00	-0.05	2577	0.982	5.88	5.93	0.9
07	193.2	80.4	"	9.85	"	2577	0.976	5.75	5.93	3.1
08	193.2	80.4	"	9.50	"	2577	0.976	5.55	5.93	6.8

* Runs 1327-36

Table 5B (Continued)

Run No.	Air, lb-mol/hr-ft^2	Temp, °F	$\Delta\theta$, min	$-\Delta W$, mg	$-\Delta W_d$, mg	$D_p G/\mu$	C_t	Rate x 10^4 lb-mols/hr-ft^2 Exper.	Rate x 10^4 lb-mols/hr-ft^2 Eqn 36	% Dev.
5/8-in. depth, 1-in. radius; 2* and 4 pellets per run										
2142	48.0	81.1	2.0	11.50	7.20	640	0.932	2.39	2.40	0.4
43	40.7	80.3	"	11.20	"	543	0.982	2.34	2.18	6.8
45	39.9	79.8	"	11.15	"	532	1.012	2.38	2.13	10.5
46	39.1	79.3	"	10.80	"	522	1.045	2.24	2.10	6.3
									Ave.	10.4
5/8-in. depth, 1-1/2-in. radius; 3 pellets per run										
1171	41.5	82.6	2.0	4.25	1.10	554	0.845	2.11	2.18	3.3
72	41.5	81.5	"	3.55	"	554	0.906	1.76	2.18	23.9
74	41.5	79.7	"	4.05	"	554	1.018	2.38	2.18	8.4
75	41.5	79.7	"	3.10	"	554	1.018	1.62	2.18	34.6
76	201.1	79.0	"	7.25	1.20	2683	1.067	5.13	6.09	18.7
77	205.0	79.9	"	7.70	"	2735	1.006	5.19	6.17	18.9
79	205.0	79.3	"	8.75	"	2735	1.049	6.29	6.17	1.9
80	205.0	79.7	"	8.95	"	2735	1.018	6.26	6.17	1.4
82	24.3	80.8	"	2.10	0.35	324	0.950	1.32	1.54	16.7
83	24.3	81.3	"	2.35	"	324	0.920	1.46	1.54	5.5
85	25.0	79.5	"	2.40	"	334	1.030	1.68	1.57	6.5
86	25.8	79.6	"	2.35	"	344	1.024	1.63	1.60	1.9
87	84.0	79.6	"	4.95	0.30	1121	1.024	3.78	3.45	8.7
88	83.0	79.3	"	4.25	"	1107	1.049	3.29	3.43	4.3
90	81.0	78.6	"	4.10	"	1081	1.093	3.30	3.37	2.1
91	74.1	78.6	"	3.55	"	988	1.096	2.83	3.18	12.4
									Ave.	10.6
5/8-in. depth, 2-in. radius; 4 pellets per run										
1060	205.0	79.5	2.0	11.85	1.35	2735	1.036	6.48	6.17	4.8
61	203.0	78.5	"	10.90	"	2708	1.099	6.25	6.13	1.9
63	201.1	78.0	"	10.70	"	2683	1.144	6.37	6.09	4.4
64	201.1	78.5	"	12.20	"	2683	1.106	7.15	6.09	14.8
70	42.3	78.1	"	3.70	0.55	564	1.130	2.12	2.21	4.2
71	42.3	78.3	"	3.75	"	564	1.120	2.13	2.21	3.8
72	41.5	78.2	"	4.25	"	554	1.127	2.48	2.18	12.1
74	41.5	77.6	"	3.80	"	554	1.171	2.27	2.18	4.0
75	22.0	80.1	"	4.55	2.40	293	0.994	1.27	1.45	14.2
76	22.0	79.8	"	4.55	"	293	1.015	1.30	1.45	11.5
78	23.5	79.5	"	4.45	"	314	1.030	1.26	1.51	19.8
2147	86.9	77.3	"	12.50	7.30	1159	1.193	3.69	3.53	4.3
48	88.9	77.6	"	13.30	"	1186	1.171	4.19	3.58	14.6
50	87.9	78.2	"	13.00	"	1173	1.123	3.82	3.56	6.8
51	87.9	78.7	"	13.20	"	1173	1.090	3.83	3.56	7.0
									Ave.	8.5

* Runs 1327-36

Table 5B (Continued)

Run No.	Air, lb-mol/hr-ft^2	Temp °F	Δθ, min	-ΔW, mg	-ΔW$_o$ mg	D_pG/μ	C_T	Rate x 10^4 lb-mols/hr-ft^2 Exper.	Eqn 38	% Dev.
1-in. depth, 1-in. radius; 3 pellets per run										
1654	86.9	79.6	2.0	4.85	0.35	1159	1.024	3.66	3.53	3.6
55	86.9	79.3	"	4.55	"	1159	1.049	3.50	3.53	0.9
57	86.9	79.0	"	4.60	"	1159	1.070	3.61	3.53	2.2
58	86.9	79.3	"	4.70	"	1159	1.049	3.62	3.53	2.5
59	200.1	79.7	"	7.65	0.50	2669	1.018	5.78	6.06	4.8
60	199.1	80.1	"	7.35	"	2656	0.994	5.41	6.05	11.8
62	198.1	80.1	"	7.45	"	2643	0.991	5.47	6.04	10.4
63	198.1	80.6	"	7.45	"	2643	0.962	5.31	6.04	13.7
65	27.3	79.1	"	2.30	0.25	364	1.061	1.73	1.66	4.0
66	27.3	78.8	"	2.35	"	364	1.083	1.80	1.66	7.8
68	27.3	78.0	"	1.95	"	364	1.141	1.54	1.66	7.8
69	27.3	78.6	"	2.05	"	364	1.096	1.56	1.66	6.4
70	39.9	79.7	"	3.15	"	532	1.018	2.34	2.13	9.0
71	39.9	79.8	"	3.10	"	532	1.015	2.29	2.13	7.0
73	39.9	78.8	"	2.35	"	532	1.080	1.80	2.13	18.3
74	39.9	79.2	"	2.75	"	532	1.055	2.10	2.13	1.4
									Ave.	7.0
1-in. depth, 2-in. radius; 4 pellets per run										
1536	27.3	78.3	2.0	3.30	0.55	364	1.120	1.83	1.66	9.3
37	27.3	78.9	"	2.80	"	364	1.074	1.44	1.66	15.3
39	27.3	79.1	"	3.10	"	364	1.061	1.61	1.66	3.1
40	28.9	78.8	"	3.20	"	386	1.080	1.70	1.73	1.8
41	198.1	79.2	"	10.90	0.35	2643	1.055	6.63	6.04	8.9
42	197.1	79.1	"	9.30	"	2629	1.058	5.64	6.01	6.6
44	195.2	78.4	"	9.00	"	2604	1.113	5.73	5.97	4.2
45	195.2	78.5	"	9.45	"	2604	1.099	5.96	5.97	0.2
46	95.8	79.2	"	8.00	0.60	1278	1.052	4.63	3.76	18.8
47	94.8	79.5	"	6.75	"	1265	1.036	3.79	3.74	1.3
49	94.8	78.0	"	6.35	"	1265	1.137	3.89	3.74	3.9
50	92.8	79.0	"	6.80	"	1238	1.070	3.95	3.68	6.8
51	41.5	79.3	"	3.85	0.40	554	1.049	2.16	2.18	0.9
52	41.5	78.6	"	3.90	"	554	1.093	2.28	2.18	4.4
54	41.5	79.3	"	3.90	"	554	1.045	2.18	2.18	0.0
55	41.5	79.5	"	3.95	"	554	1.030	2.18	2.18	0.0
									Ave.	5.3
2-in. depth, 2-in. radius; 4 pellets per run										
1715	43.1	77.6	2.0	4.35	0.75	575	1.171	2.51	2.24	10.8
16	43.1	79.1	"	4.85	"	575	1.061	2.59	2.24	13.5
18	44.7	78.8	"	4.65	"	596	1.080	2.51	2.29	8.8
19	43.1	79.1	"	4.80	"	575	1.061	2.56	2.24	12.5

Table 5B (Continued)

Run No.	Air, lb-mol / hr-ft^2	Temp °F	$\Delta\theta$, min	$-\Delta W$, mg	$-\Delta W_o$ mg	D_pG/μ	C_T	Rate x 10^4 lb-mols/hr-ft^2 Exper.	Rate x 10^4 lb-mols/hr-ft^2 Eqn 38	% Dev.
2-in. depth, 2-in. radius; 4 pellets per run										
1720	24.3	78.9	2.0	3.50	0.75	324	1.077	1.76	1.54	12.5
21	26.6	78.0	"	3.25	"	354	1.141	1.70	1.64	3.5
23	27.3	77.6	"	3.25	"	364	1.171	1.74	1.66	4.6
24	27.3	77.6	"	3.05	"	364	1.168	1.60	1.66	3.8
26	86.9	80.7	"	7.35	0.50	1159	0.956	3.90	3.53	9.5
27	86.9	80.4	"	6.60	"	1159	0.976	3.54	3.53	0.3
29	86.9	79.5	"	6.35	"	1159	1.036	3.61	3.53	2.2
30	87.9	79.2	"	5.80	"	1173	1.055	3.27	3.56	8.9
31	203.0	80.6	"	11.50	0.45	2708	0.959	6.31	6.13	2.9
32	203.0	80.5	"	11.00	"	2708	0.971	6.10	6.13	0.5
34	201.1	79.3	"	10.45	"	2683	1.049	6.25	6.09	2.6
35	201.1	79.1	"	10.15	"	2683	1.061	6.13	6.09	0.7
									Ave.	6.1

Table 5

C. 4-inch orifice, 1/2-inch pellets

Run No.	Air, lb-mol / hr-ft^2	Temp °F	Δθ, min	-ΔW, mg	-ΔW$_o$ mg	D_pG/μ	C_T	Rate x 10^4 lb-mols/hr-ft^2 Exper.	Eqn 38	% Dev.
1-in. depth, 1-1/2-in. radius; 1 pellet per run										
3183	35.9	79.0	5.0	8.75	0.45	1122	1.064	1.43	1.48	3.5
84	35.9	79.0	"	8.75	"	1122	1.064	1.43	1.48	3.5
86	35.9	79.2	"	8.30	"	1122	1.055	1.35	1.48	9.6
87	35.9	79.2	"	8.30	"	1122	1.055	1.35	1.48	9.6
88	67.2	79.4	3.0	7.50	0.25	2101	1.039	2.04	2.22	8.1
89	67.2	79.4	"	7.80	"	2101	1.039	2.12	2.22	4.7
91	67.2	79.6	"	8.05	"	2101	1.027	2.17	2.22	2.3
92	67.2	79.6	"	7.45	"	2101	1.027	2.00	2.22	11.0
94	124.3	80.0	2.0	7.00	0.00	3886	0.997	2.84	3.31	16.5
95	124.3	80.0	"	6.95	"	3886	0.997	2.81	3.31	17.8
97	124.3	80.0	"	6.55	"	3886	1.000	2.66	3.31	24.4
98	124.3	80.0	"	7.95	"	3886	1.000	3.23	3.31	2.5
3261	226.6	80.4	1.5	9.25	0.20	7084	0.974	4.77	4.89	2.5
62	226.6	80.4	"	8.40	"	7084	0.974	4.33	4.89	12.9
64	228.6	81.7	"	10.05	"	7146	0.895	4.78	4.91	2.7
65	228.6	81.7	"	8.80	"	7146	0.895	4.17	4.91	17.7
									Ave.	9.3

Table 5

D. 1-inch orifice, 1/8-inch pellets

Run No.	Air, lb-mol/hr-ft^2	Temp °F	$\Delta\theta$, min	$-\Delta W$, mg	$-\Delta W_0$ mg	$D_p G/\mu$	C_T	Rate x 10^4 lb-mols/hr-ft^2 Exper.	Eqn 37	% Dev.
1/16-in. depth, 1/2-in. radius; 4 pellets per run										
2772	73.1	79.5	2.0	6.55	0.20	523	1.033	11.96	12.26	2.5
73	67.2	79.5	"	6.35	"	480	1.036	11.61	11.62	0.1
75	73.1	79.5	"	6.15	"	523	1.033	11.21	12.26	9.4
76	75.1	79.0	"	5.55	"	537	1.067	10.41	12.48	19.9
77	123.3	78.5	1.5	6.50	0.30	882	1.102	16.60	17.23	3.8
78	122.3	77.0	"	5.80	"	874	1.221	16.34	17.15	5.0
80	120.4	80.3	"	5.95	"	861	0.982	13.49	16.95	25.6
81	122.3	80.4	"	6.90	"	874	0.976	15.66	17.15	9.5
82	37.5	80.4	2.5	5.90	0.55	268	0.974	7.60	7.95	4.6
83	40.7	80.7	"	5.95	"	291	0.953	7.51	8.38	11.6
85	39.1	81.1	"	6.55	"	280	0.929	8.12	8.16	0.5
86	38.3	80.8	"	6.35	"	274	0.947	8.01	8.06	0.6
87	22.0	81.3	3.0	5.40	"	157	0.920	5.42	5.62	3.7
88	22.0	80.9	"	5.00	"	157	0.945	5.11	5.62	10.0
90	22.0	77.8	"	5.05	"	157	1.154	6.31	5.62	10.9
91	22.0	78.8	"	4.95	"	157	1.083	5.80	5.62	3.1
									Ave.	7.6
1/16-in. depth, 1-in. radius; 6 pellets per run										
372	22.0	77.8	5.0	7.95	1.30	157	1.158	3.74	3.34	10.7
74	22.0	78.7	"	8.00	"	157	1.086	3.54	3.34	5.6
75	38.3	79.6	"	13.15	"	274	1.024	5.90	4.78	19.0
77	39.1	80.9	"	11.90	"	280	0.942	4.86	4.84	0.4
78	81.0	80.9	"	19.25	2.05	579	0.945	7.90	7.78	1.5
80	69.2	82.5	"	18.85	"	495	0.853	6.97	7.02	0.7
82	78.1	81.6	"	18.05	"	558	0.901	7.38	7.60	3.0
84	79.0	81.3	"	18.75	"	565	0.918	7.83	7.65	2.3
85	136.1	79.2	"	21.30	1.35	973	1.055	10.23	10.90	6.5
87	137.1	79.3	"	22.00	"	980	1.045	10.50	10.95	4.3
88	39.9	79.6	"	10.25	0.50	285	1.024	4.85	4.91	1.2
90	39.1	79.1	"	10.00	"	280	1.058	4.89	4.84	1.0
91	22.0	79.9	"	7.05	"	157	1.009	3.21	3.34	4.0
93	22.8	79.8	"	7.65	"	163	1.012	3.52	3.41	3.1
									Ave.	4.5
1/16-in. depth, 1-1/2-in. radius; 4* and 6 pellets per run										
2792	22.0	81.0	4.0	2.40	0.55	157	0.935	1.58	1.63	3.2
93	22.8	81.4	"	3.20	"	163	0.915	2.21	1.67	24.4
95	22.8	81.5	"	2.75	"	163	0.904	1.81	1.67	7.7
96	22.8	80.9	"	3.30	"	163	0.942	2.36	1.67	29.2

* Runs 2792-96

Table 5D (Continued)

Run No.	Air, lb-mol/hr-ft²	Temp °F	Δθ, min	-ΔW, mg	-ΔW₀ mg	D_pG/μ	C_T	Rate x 10^4 lb-mols/hr-ft² Exper.	Eqn 37	% Dev.
1/16-in. depth, 1-1/2-in. radius; 4* and 6 pellets per run										
2797	66.2	79.9	2.0	3.15	0.30	473	1.006	3.49	3.34	4.3
98	74.1	77.9	"	3.35	"	530	1.150	4.27	3.59	15.9
2800	74.1	80.9	"	4.10	"	530	0.945	4.36	3.59	17.7
01	74.1	80.5	"	3.80	"	530	0.965	4.11	3.59	12.7
02	35.1	81.3	"	2.60	0.55	251	0.918	2.29	2.21	3.5
03	35.1	80.1	2.5	3.15	"	251	0.991	2.51	2.21	12.0
05	34.3	79.5	"	3.15	"	245	1.033	2.62	2.17	17.2
06	33.5	78.5	"	3.10	"	240	1.106	2.74	2.14	21.9
07	118.4	79.9	1.5	3.95	0.30	847	1.006	5.95	4.86	18.3
08	121.4	79.4	"	3.80	"	868	1.042	5.92	4.94	16.6
10	123.3	80.5	"	3.65	"	882	0.971	5.27	4.99	5.3
11	124.3	80.1	"	3.30	"	889	0.994	4.83	5.02	3.9
									Ave.	13.6
1/16-in. depth, 2-in. radius; 8 pellets per run										
251	31.9	91.0	5.0	6.80	1.70	228	0.494	0.92	1.07	16.3
52	30.4	91.1	"	7.35	"	217	0.492	1.01	1.04	3.0
70	55.5	86.0	"	9.25	2.80	397	0.679	1.60	1.54	3.8
71	54.6	86.2	"	9.40	"	390	0.671	1.62	1.52	6.2
329	23.5	81.0	"	5.00	2.40	168	0.935	0.89	0.88	1.1
41	22.0	79.4	"	3.30	0.90	157	1.039	0.91	0.84	7.7
43	22.8	82.9	"	3.75	"	163	0.830	0.86	0.86	0.0
50	130.2	80.9	"	8.00	0.85	931	0.945	2.46	2.68	8.9
52	120.4	80.9	"	7.15	"	861	0.945	2.17	2.54	17.1
53	127.3	81.8	"	8.60	0.55	910	0.890	2.61	2.64	1.1
55	126.3	80.9	"	7.70	"	903	0.945	2.46	2.62	6.5
63	54.6	81.6	"	6.00	1.10	390	0.901	1.61	1.52	5.6
65	53.8	81.6	"	5.65	"	385	0.901	1.50	1.51	0.7
69	33.5	79.5	"	3.75	0.95	240	1.036	1.06	1.11	4.7
71	30.4	79.3	"	3.75	"	217	1.049	1.07	1.04	2.8
									Ave.	5.7
3/16-in. depth, 1/2-in. radius; 4 pellets per run										
2752	20.5	80.3	3.0	4.60	0.40	147	0.982	5.01	6.25	24.8
53	20.5	79.5	"	5.45	"	147	1.033	6.34	6.25	1.4
55	22.0	78.9	"	5.20	"	157	1.074	6.27	6.56	4.6
56	21.2	78.6	"	4.90	"	152	1.093	5.98	6.40	7.0
57	37.5	79.0	2.5	6.10	"	268	1.067	8.87	9.27	4.5
58	38.3	79.0	"	5.95	"	274	1.070	8.66	9.40	8.5
60	39.1	79.1	"	5.65	"	280	1.061	8.12	9.52	17.2
61	38.3	78.7	"	5.90	"	274	1.086	8.71	9.40	7.9

* Runs 2792-96

Table 5D (Continued)

Run No.	Air, lb-mol/hr-ft^2	Temp °F	Δθ, min	-ΔW, mg	-ΔW$_d$ mg	D_pG/μ	C_T	Rate x 10^4 lb-mols/hr-ft^2 Exper.	Eqn 36	% Dev.
3/16-in. depth, 1/2-in. radius; 4 pellets per run										
2762	124.3	78.5	1.5	7.00	0.20	889	1.102	18.21	20.20	10.9
63	123.3	80.9	"	7.40	"	882	0.942	16.48	20.09	21.9
65	122.3	81.3	"	8.45	"	874	0.920	18.45	20.01	8.5
66	125.3	81.9	"	7.55	"	896	0.885	15.80	20.30	28.5
67	66.2	79.8	2.0	6.10	0.30	473	1.015	10.74	13.43	25.0
68	75.1	79.3	"	6.35	"	537	1.049	11.58	14.55	25.6
70	62.6	80.0	"	5.85	"	448	1.000	10.12	12.93	27.8
71	64.4	78.3	"	5.90	"	460	1.120	11.43	13.18	15.3
									Ave.	15.0
3/16-in. depth, 1-in. radius; 6 pellets per run										
419	68.2	80.2	5.0	12.90	-0.15	488	0.985	6.25	6.44	3.0
21	65.3	81.0	"	12.50	"	467	0.935	5.75	6.26	8.9
23	70.2	80.6	"	14.10	"	502	0.959	6.69	6.57	1.8
2395	21.2	79.9	3.0	3.75	0.40	152	1.006	2.73	3.01	10.3
96	21.2	79.7	"	3.85	"	152	1.021	2.85	3.01	5.6
98	21.2	79.5	"	4.00	"	152	1.033	3.01	3.01	0.0
99	21.2	79.9	"	3.60	"	152	1.009	2.62	3.01	14.9
2400	39.9	80.0	"	6.50	0.65	285	1.003	4.76	4.55	4.4
01	39.1	80.1	"	5.85	"	280	0.994	4.19	4.48	6.9
03	39.1	80.2	"	5.75	"	280	0.988	4.08	4.48	9.8
04	39.9	80.3	"	6.30	"	285	0.982	4.50	4.55	1.1
56	122.3	80.8	1.5	6.30	0.30	874	0.950	9.24	9.43	2.1
57	126.3	78.3	"	6.00	"	903	1.117	10.32	9.62	6.8
59	122.3	79.5	"	6.15	"	874	1.036	9.82	9.43	4.0
60	131.2	80.8	"	6.20	"	938	0.947	9.06	9.87	8.9
									Ave.	5.9
3/16-in. depth, 1-1/2-in. radius; 6 pellets per run										
2658	122.3	79.4	1.5	4.15	1.00	874	1.039	5.30	5.09	4.0
59	126.3	80.7	"	4.20	"	903	0.953	4.94	5.19	5.1
61	126.3	80.8	"	4.35	"	903	0.947	5.14	5.19	1.0
62	125.3	81.0	"	4.40	"	896	0.935	5.15	5.16	0.2
64	39.9	79.2	3.0	3.75	0.60	285	1.055	2.69	2.46	8.6
65	39.9	80.2	"	3.80	"	285	0.988	2.54	2.46	3.1
67	39.9	81.0	"	3.65	"	285	0.937	2.32	2.46	6.0
68	39.9	80.1	"	3.65	"	285	0.994	2.46	2.46	0.0
74	75.1	78.2	2.0	3.45	"	537	1.127	3.90	3.70	5.1
75	74.1	77.8	"	3.20	"	530	1.154	3.65	3.67	0.5
77	73.1	79.1	"	3.40	"	523	1.061	3.61	3.64	0.8
78	75.1	79.4	"	3.15	"	537	1.042	3.23	3.70	14.6
2879	21.2	78.5	3.0	1.90	0.05	152	1.106	1.66	1.63	1.8
80	21.2	78.8	"	1.95	"	152	1.083	1.67	1.63	2.4
82	21.2	78.4	"	1.65	"	152	1.109	1.44	1.63	13.2
83	21.2	78.9	"	1.65	"	152	1.077	1.39	1.63	17.3
									Ave.	5.2

Table 5D (Continued)

Run No.	Air, lb-mol/hr-ft^2	Temp °F	Δθ, min	-ΔW, mg	-ΔW$_o$ mg	D_pG/μ	C_T	Rate x 10^4 lb-mols/hr-ft^2 Exper.	Eqn 36	% Dev.
3/16-in. depth, 2-in. radius; 6 pellets per run										
2636	73.1	79.1	2.5	2.40	0.20	523	1.058	2.27	2.21	2.6
37	67.2	79.1	"	2.00	"	480	1.061	1.86	2.09	12.4
39	67.2	78.9	"	2.10	"	480	1.074	1.98	2.09	5.6
40	75.1	79.0	"	2.10	"	537	1.067	1.97	2.25	14.2
42	22.0	80.0	3.0	1.60	0.40	157	1.003	0.97	1.01	4.1
43	22.0	80.5	"	1.55	"	157	0.965	0.90	1.01	12.2
45	22.8	77.5	"	1.65	"	163	1.182	1.20	1.03	14.2
46	22.8	79.8	"	1.65	"	163	1.012	1.02	1.03	1.0
47	39.1	80.7	2.5	2.20	0.60	280	0.953	1.48	1.47	0.7
48	39.1	81.3	"	2.25	"	280	0.920	1.48	1.47	0.7
50	39.1	81.2	"	2.30	"	280	0.926	1.53	1.47	3.9
51	39.9	81.1	"	2.25	"	285	0.932	1.50	1.49	0.7
53	121.4	80.0	1.5	2.00	0.65	868	1.000	2.19	3.07	40.2
54	120.4	79.4	"	2.30	"	861	1.039	2.77	3.05	10.1
56	124.3	79.2	"	2.25	"	889	1.055	2.74	3.12	13.9
57	125.3	78.7	"	2.85	1.00	896	1.086	3.26	3.13	4.0
									Ave.	8.8
5/16-in. depth, 1/2-in. radius; 4 pellets per run										
2524	22.8	81.3	4.0	6.60	0.50	163	0.920	5.11	6.09	19.2
25	22.8	80.8	"	6.30	"	163	0.947	5.00	6.09	21.8
27	24.3	80.4	"	5.55	"	174	0.974	4.48	6.35	41.7
28	24.3	80.0	"	5.55	"	174	1.000	4.60	6.35	38.0
2679	77.1	79.2	1.5	4.95	0.20	551	1.055	12.18	13.45	10.4
80	81.0	80.0	"	4.45	"	579	1.000	10.03	13.89	38.5
82	79.0	79.1	"	4.60	"	565	1.058	11.33	13.67	20.7
83	66.2	79.4	"	4.75	"	473	1.039	11.50	12.19	6.0
84	110.5	78.8	"	5.80	0.10	790	1.080	14.97	17.01	13.6
85	123.3	79.6	"	6.65	"	882	1.024	16.31	18.25	11.9
87	123.3	79.7	"	6.30	"	882	1.018	15.34	18.25	19.0
88	126.3	79.3	"	6.05	"	903	1.049	15.17	18.54	22.2
95	38.3	79.5	2.0	4.20	0.15	274	1.030	7.60	8.54	12.4
96	39.1	79.6	"	4.00	"	280	1.024	7.18	8.65	20.5
98	39.9	78.8	"	4.00	"	285	1.080	7.58	8.77	15.7
99	39.1	79.5	"	4.10	"	280	1.030	7.42	8.65	16.6
									Ave.	20.5
5/16-in. depth, 1-in. radius; 6 pellets per run										
394	22.0	83.5	5.0	6.35	1.15	157	0.799	2.02	2.87	42.1
96	22.0	84.5	"	6.80	1.45	157	0.749	2.31	2.87	24.2
98	21.2	80.7	"	5.75	"	152	0.953	1.99	2.80	40.7

Table 5D (Continued)

Run No.	Air, lb-mol/hr-ft^2	Temp °F	$\Delta\theta$, min	$-\Delta W$, mg	$-\Delta W_o$ mg	D_pG/μ	C_T	Rate x 10^4 lb-mols/hr-ft^2 Exper.	Eqn 36	% Dev.
5/16-in. depth, 1-in. radius; 6 pellets per run										
399	38.3	79.2	5.0	7.85	1.45	274	1.055	3.28	4.11	25.3
401	38.3	80.6	"	8.15	"	274	0.959	3.13	4.11	31.3
03	39.1	80.4	"	8.30	1.20	280	0.976	3.37	4.16	23.4
04	67.2	85.6	"	15.65	1.90	480	0.697	4.66	5.92	27.0
06	69.2	80.6	"	14.55	2.00	495	0.959	5.85	6.04	3.2
08	75.1	79.1	"	13.30	"	537	1.058	5.81	6.36	9.5
09	129.2	81.0	"	17.65	0.70	924	0.935	7.71	9.05	17.4
11	130.2	81.5	"	17.60	"	931	0.909	7.03	9.10	29.5
13	126.3	80.8	"	16.80	"	903	0.950	7.44	8.92	19.9
									Ave.	24.5
5/16-in. depth, 1-1/2-in. radius; 6 pellets per run										
2462	22.0	77.9	3.0	2.75	0.95	157	1.150	1.68	1.70	1.2
63	23.5	78.1	"	2.40	"	168	1.130	1.33	1.77	33.1
65	23.5	78.8	"	2.75	"	168	1.083	1.58	1.77	12.0
66	24.3	79.0	"	2.90	"	174	1.070	1.69	1.81	7.1
67	116.4	80.8	1.5	3.85	"	832	0.950	4.47	5.01	12.1
68	119.4	80.1	"	3.80	"	854	0.991	4.57	5.09	11.4
70	122.3	80.4	"	3.55	"	874	0.976	4.12	5.18	25.7
71	120.4	80.2	"	3.80	"	861	0.988	4.57	5.14	12.5
72	39.1	79.2	2.5	2.30	0.15	280	1.052	2.20	2.46	11.8
73	39.1	79.0	"	2.35	"	280	1.067	2.29	2.46	7.4
75	39.1	78.5	"	2.40	"	280	1.102	2.41	2.46	2.1
76	39.1	78.4	"	1.95	"	280	1.113	1.94	2.46	26.8
									Ave.	13.6
5/16-in. depth, 2-in. radius; 6 pellets per run										
2504	36.7	79.8	3.0	3.20	1.10	262	1.012	1.73	1.64	5.2
05	36.7	79.4	"	3.15	"	262	1.039	1.73	1.64	5.2
07	36.7	80.0	"	3.00	"	262	0.997	1.53	1.64	7.2
08	39.1	80.7	"	3.20	"	280	0.953	1.62	1.70	4.9
09	21.2	81.0	"	2.55	"	152	0.937	1.13	1.14	0.8
10	21.2	81.6	"	2.45	"	152	0.901	0.99	1.14	15.2
12	22.0	81.1	"	2.60	"	157	0.929	1.13	1.17	3.5
13	22.0	83.1	"	2.55	"	157	0.818	0.96	1.17	21.9
14	125.3	79.1	2.0	2.50	0.50	896	1.061	2.58	3.63	40.7
15	126.3	78.0	"	2.55	"	903	1.137	2.83	3.65	29.0
17	126.3	79.3	"	3.10	"	903	1.045	3.31	3.65	10.3
18	125.3	78.5	"	3.10	"	896	1.106	3.50	3.63	3.7
19	83.0	80.0	2.5	3.40	"	593	0.997	2.81	2.78	1.1
20	87.9	79.5	"	3.40	"	628	1.030	2.91	2.88	1.0
22	86.9	80.8	"	3.55	"	621	0.950	2.82	2.86	1.4
23	87.9	80.3	"	3.35	"	628	0.982	2.72	2.88	2.2
									Ave.	9.6

Table 5D (Continued)

Run No.	Air, lb-mol/hr-ft²	Temp °F	Δθ, min	-ΔW, mg	-ΔW₀ mg	D_pG/μ	C_T	Rate x 10^4 lb-mols/hr-ft² Exper.	Rate x 10^4 lb-mols/hr-ft² Eqn 36	% Dev.
1/2-in. depth, 1/2-in. radius; 4 pellets per run										
2812	31.1	78.7	2.5	4.00	0.25	222	1.086	5.94	5.68	4.4
13	35.9	80.1	"	4.05	"	257	0.994	5.51	6.23	13.1
15	36.7	80.4	"	4.30	"	262	0.974	5.75	6.33	10.1
16	35.1	80.6	"	4.30	"	251	0.962	5.69	6.14	7.9
17	19.0	80.9	3.0	2.80	0.20	136	0.944	2.98	4.12	38.3
18	19.0	80.2	"	3.00	"	136	0.985	3.35	4.12	23.0
20	19.0	80.0	"	2.80	"	136	1.000	3.16	4.12	30.4
21	19.0	79.7	"	2.85	"	136	1.018	3.28	4.12	25.6
23	61.7	79.1	2.0	4.65	0.00	441	1.061	8.99	8.86	1.4
24	63.5	79.9	"	4.70	"	454	1.006	8.62	9.03	4.8
26	65.3	80.1	"	4.60	"	467	0.994	8.33	9.19	10.3
27	75.1	80.2	"	5.55	"	537	0.988	9.99	10.06	0.7
28	120.4	80.0	1.5	5.30	-0.20	861	1.000	13.37	13.68	2.3
29	125.3	79.9	"	4.60	"	896	1.006	11.74	14.04	19.6
31	124.3	80.0	"	4.70	"	889	1.000	11.91	13.97	17.3
32	122.3	80.0	"	4.90	"	874	1.003	12.45	13.83	11.1
									Ave.	13.8
1/2-in. depth, 2-in. radius; 6 pellets per run										
2289	39.9	79.2	3.0	3.30	0.30	285	1.052	2.56	2.04	20.3
90	38.3	78.7	"	2.15	"	274	1.090	1.64	1.99	21.3
92	38.3	78.0	"	2.80	"	274	1.144	2.32	1.99	14.2
93	37.5	78.5	"	2.30	"	268	1.099	1.78	1.96	10.1
2431	18.2	78.9	"	1.70	0.40	130	1.077	1.13	1.23	8.8
32	18.2	79.1	"	1.80	"	130	1.061	1.21	1.23	1.7
34	19.0	78.9	"	1.70	"	136	1.077	1.13	1.26	11.5
35	19.0	79.0	"	1.80	"	136	1.067	1.21	1.26	4.1
2870	65.3	80.0	2.0	2.75	"	467	1.003	2.87	2.81	2.1
71	71.2	80.4	"	2.70	"	509	0.974	2.72	2.97	9.9
73	67.2	80.5	"	2.60	"	480	0.965	2.58	2.86	10.9
74	75.1	80.9	"	2.80	"	537	0.942	2.75	3.08	12.0
75	116.4	80.9	1.5	2.65	"	832	0.944	3.45	4.09	18.6
76	121.4	80.5	"	2.60	"	868	0.965	3.44	4.21	22.4
78	122.3	80.3	"	2.65	"	874	0.982	3.58	4.23	18.2
									Ave.	12.4
1-in. depth, 1/2-in. radius; 4 pellets per run										
2834	63.5	79.5	2.0	3.75	1.10	454	1.036	5.01	5.60	11.8
35	63.5	79.9	"	3.85	"	454	1.006	5.05	5.60	10.9
37	64.4	80.0	"	3.90	"	460	1.003	5.12	5.65	10.4
38	64.4	80.2	"	4.35	"	460	0.985	5.83	5.65	3.1
39	21.2	80.5	3.0	3.00	"	152	0.971	2.24	2.74	22.3
40	21.2	80.5	"	3.00	"	152	0.965	2.23	2.74	22.9
42	21.2	80.2	"	3.00	"	152	0.985	2.27	2.74	20.7
43	21.2	81.0	"	2.95	"	152	0.937	2.10	2.74	30.5

Table 5D (Continued)

Run No.	Air, lb-mol/hr-ft^2	Temp °F	$\Delta\theta$, min	$-\Delta W$, mg	$-\Delta W_o$ mg	D_pG/μ	C_T	Rate x 10^4 lb-mols/hr-ft^2 Exper.	Eqn 36	% Dev.
1-in. depth, 1/2-in. radius; 4 pellets per run										
2844	36.7	79.3	2.5	3.40	1.10	262	1.049	3.52	3.92	11.4
45	36.7	79.0	"	3.60	"	262	1.070	3.91	3.92	0.3
47	37.5	79.2	"	3.30	"	268	1.055	3.38	3.97	17.5
48	36.7	79.2	"	3.50	"	262	1.055	3.69	3.92	6.2
49	121.4	79.0	1.5	2.95	0.20	868	1.064	7.12	8.53	19.8
50	108.6	79.4	"	2.60	"	776	1.042	6.22	7.93	27.5
62	114.5	79.0	"	2.85	"	819	1.070	6.90	8.20	18.8
63	117.4	79.0	"	3.15	"	839	1.064	7.63	8.35	9.4
									Ave.	15.2
1-in. depth, 1-in. radius; 4 and 6* pellets per run										
2253	19.0	82.1	3.0	1.45	-0.10	130	0.870	1.64	1.89	15.2
54	19.0	77.7	"	1.30	"	130	1.165	1.98	1.89	4.5
56	20.5	77.4	"	1.25	"	147	1.190	1.96	1.95	0.5
57	21.2	77.8	"	1.30	"	152	1.154	1.97	1.99	1.0
58	36.7	80.3	"	2.40	"	262	0.982	2.99	2.85	4.7
59	37.5	81.0	"	2.10	"	268	0.934	2.49	2.89	20.1
61	36.7	79.5	"	2.20	"	262	1.030	2.88	2.85	1.0
62	38.3	80.2	"	2.25	"	274	0.988	2.82	2.93	3.9
63	117.4	80.8	"	4.45	"	839	0.950	5.25	6.06	15.4
64	118.4	80.7	"	5.15	"	847	0.953	6.08	6.09	0.2
66	120.4	79.7	"	4.30	"	861	1.018	5.45	6.16	13.0
67	122.3	80.0	"	4.90	"	874	1.000	6.08	6.23	2.5
2420	61.7	79.5	"	4.75	0.20	441	1.030	3.80	3.99	5.0
21	63.5	79.7	"	4.90	"	454	1.018	3.87	4.07	5.2
23	63.5	79.5	"	4.90	"	454	1.030	3.92	4.07	3.8
24	63.5	79.9	"	5.00	"	454	1.009	3.92	4.07	3.8
									Ave.	6.2
1-in. depth, 1-1/2-in. radius; 6 pellets per run										
2884	21.2	78.9	3.0	1.90	0.05	152	1.077	1.61	1.75	8.7
85	21.2	79.5	"	2.05	"	152	1.030	1.67	1.75	4.8
87	21.2	79.5	3.5	2.05	"	152	1.036	1.44	1.75	21.5
88	21.2	79.6	3.0	1.80	"	152	1.027	1.46	1.75	19.9
89	119.4	80.3	1.5	2.85	"	854	0.982	4.46	5.40	21.1
90	114.5	80.0	"	2.85	"	819	1.000	4.54	5.25	15.6
92	122.3	81.5	"	2.90	"	874	0.907	4.18	5.49	31.3
93	122.3	81.1	"	3.05	"	874	0.932	4.54	5.49	20.9
94	68.2	82.0	2.0	3.45	0.50	488	0.878	3.15	3.75	19.0
95	67.2	81.1	"	3.30	"	480	0.932	3.17	3.72	17.4
97	71.2	81.3	"	3.65	"	509	0.920	3.52	3.86	9.7
98	69.2	80.7	"	3.75	"	495	0.953	3.77	3.79	0.5

* Runs 2420-24

Table 5D (Continued)

Run No.	Air, lb-mol / hr-ft^2	Temp °F	$\Delta\theta$, min	$-\Delta W$, mg	$-\Delta W_o$ mg	D_pG/μ	C_T	Rate x 10^4 lb-mols/hr-ft^2 Exper.	Eqn 36	% Dev.
1-in. depth, 1-1/2-in. radius; 6 pellets per run										
2899	39.9	80.7	2.5	3.65	0.65	285	0.956	2.79	2.65	5.0
2900	39.1	79.8	"	3.40	"	280	1.012	2.70	2.61	3.3
02	39.9	80.2	"	3.20	"	285	0.988	2.45	2.65	8.2
03	39.9	80.0	"	3.15	"	285	0.997	2.42	2.65	9.5
									Ave.	13.5
1-in. depth, 2-in. radius; 4 and 6* pellets per run										
2904	39.9	80.3	2.5	3.20	0.55	285	0.982	2.53	2.48	2.0
05	39.9	80.0	"	3.05	"	285	0.997	2.42	2.48	2.5
07	39.9	79.7	"	2.85	"	285	1.021	2.29	2.48	8.3
08	39.1	79.7	"	2.70	"	280	1.018	2.13	2.45	15.0
09	115.5	79.8	2.0	2.40	-0.15	826	1.012	4.70	4.95	5.3
11	121.4	79.5	"	2.10	"	868	1.036	4.25	5.12	20.5
12	118.4	79.6	"	2.30	"	847	1.024	4.58	5.03	9.8
14	120.4	79.6	"	2.30	"	861	1.027	4.59	5.09	10.9
									Ave.	7.6
2-in. depth, 1-in. radius; 4 pellets per run										
3502	65.3	81.9	2.0	2.35	0.15	467	0.883	3.54	3.64	2.8
03	63.5	80.2	"	2.10	"	454	0.988	3.52	3.58	1.7
05	67.2	79.9	"	2.35	"	480	1.006	4.03	3.72	8.2
06	66.2	79.5	"	1.90	"	473	1.033	3.30	3.68	11.5
07	21.2	80.2	3.0	1.30	0.05	152	0.985	1.50	1.75	16.7
08	21.2	80.3	"	1.45	"	152	0.982	1.67	1.75	4.8
10	21.2	80.3	"	1.20	"	152	0.979	1.37	1.75	27.7
11	21.2	80.2	"	1.30	"	152	0.985	1.50	1.75	16.7
13	37.5	80.5	2.5	1.95	0.15	268	0.971	2.55	2.54	0.4
14	36.7	80.1	"	1.85	"	262	0.994	2.47	2.51	1.6
16	36.7	80.1	"	2.00	"	262	0.994	2.68	2.51	6.3
17	36.7	80.1	"	1.75	"	262	0.994	2.32	2.51	8.2
20	111.5	80.2	1.5	2.15	"	797	0.988	4.81	5.16	7.3
22	109.6	80.3	"	2.15	"	784	0.982	4.76	5.10	7.1
23	106.6	80.5	"	2.20	"	762	0.971	4.84	5.02	3.7
									Ave.	8.3

* Runs 2904-08

Table 5

E., 1-inch orifice, 1/4-inch pellets

Run No.	Air, lb-mol/hr-ft^2	Temp °F	$\Delta\theta$, min	$-\Delta W$, mg	$-\Delta W_o$ mg	D_pG/μ	C_t	Rate x 10^4 lb-mols/hr-ft^2 Exper.	Eqn 36	% Dev.
1/8-in. depth, 0-in. radius; 1 pellet per run										
709	157.8	79.5	2.0	5.15	0.05	2105	1.033	12.55	12.46	0.7
11	153.8	79.0	"	5.85	"	2052	1.067	14.74	12.26	16.8
12	154.8	79.7	"	5.50	"	2065	1.018	13.22	12.31	6.9
13	75.1	79.7	"	3.20	"	1002	1.018	7.65	7.69	0.5
14	74.1	79.8	"	2.80	"	988	1.015	6.65	7.62	14.6
16	73.1	79.5	"	3.00	"	975	1.030	7.24	7.56	4.4
17	71.2	79.4	"	3.30	"	950	1.039	8.05	7.43	7.7
2970	39.9	80.9	"	2.35	-0.10	532	0.942	5.50	5.10	7.3
71	39.9	81.0	"	2.35	"	532	0.937	5.48	5.10	6.9
73	39.9	80.9	"	1.85	"	532	0.942	4.38	5.10	16.4
74	39.9	81.0	"	1.95	"	532	0.935	4.57	5.10	11.6
75	22.8	81.1	2.0	0.95	-0.35	304	0.929	2.88	3.54	22.9
76	22.8	80.6	2.25	1.25	"	304	0.959	3.24	3.54	9.3
78	23.5	78.8	"	1.30	"	314	1.080	4.24	3.61	12.5
79	23.5	79.0	"	0.95	"	314	1.067	3.31	3.61	9.1
									Ave.	9.8
1/8-in. depth, 1/4-in. radius; 1 pellet per run										
1880	39.1	80.4	2.0	2.60	0.25	522	0.974	5.45	5.34	2.0
81	39.9	80.6	"	2.50	"	532	0.962	5.15	5.41	5.0
83	39.9	80.5	"	2.40	"	532	0.965	4.93	5.41	9.7
84	39.1	80.6	"	2.75	"	522	0.962	5.74	5.34	7.0
85	22.0	80.0	"	1.40	0.05	293	1.003	3.22	3.68	14.3
86	22.0	79.8	"	1.80	"	293	1.012	4.22	3.68	12.8
88	22.0	79.5	"	1.35	"	293	1.033	3.19	3.68	15.4
89	22.0	79.5	"	1.15	"	293	1.033	2.72	3.68	31.6
90	82.0	80.0	"	3.70	"	1094	1.000	8.69	8.64	0.6
91	83.0	80.3	"	4.15	"	1107	0.982	9.60	8.71	9.3
93	83.0	80.1	"	3.80	"	1107	0.994	8.88	8.71	1.9
94	85.9	79.9	"	3.30	"	1146	1.006	7.79	8.90	14.2
95	157.8	81.3	"	4.45	-0.5	2105	0.917	12.01	13.22	10.1
96	151.9	79.5	"	5.80	"	2026	1.030	14.36	12.90	10.2
98	150.9	78.9	"	5.10	"	2013	1.074	13.17	12.85	2.4
99	154.8	78.9	"	4.85	"	2065	1.074	12.53	13.06	4.2
									Ave.	9.4
1/8-in. depth, 1/2-in. radius; 2 pellets per run										
850	38.3	76.7	2.0	5.10	0.35	511	1.240	7.01	7.38	5.3
51	38.3	77.5	"	5.35	"	511	1.182	7.04	7.38	4.8
53	38.3	78.2	"	6.45	"	511	1.127	8.18	7.38	9.8
54	38.3	78.5	"	5.45	"	511	1.106	6.72	7.38	9.8

Table 5 E (Continued)

Run No.	Air, lb-mol/hr-ft^2	Temp °F	$-\Delta\theta$, min	$-\Delta W$, mg	$-\Delta W_c$ mg	D_pG/μ	C_T	Rate x 10^4 lb-mols/hr-ft^2 Exper.	Eqn 36	% Dev.
1/8-in. depth, 1/2-in. radius; 2 pellets per run										
2948	149.9	75.3	2.0	13.65	0.20	2000	1.363	21.83	17.93	17.9
49	145.9	78.4	"	14.95	"	1946	1.113	19.56	17.63	9.9
51	146.9	77.0	"	16.15	"	1960	1.218	23.14	17.69	23.6
52	147.9	77.0	"	16.15	"	1973	1.218	23.14	17.77	23.2
53	69.2	79.7	"	10.20	0.25	923	1.018	12.06	10.85	10.0
54	67.2	79.9	"	10.55	"	896	1.006	12.34	10.64	13.8
56	67.2	79.8	"	10.25	"	896	1.012	12.05	10.64	11.7
57	67.2	79.7	"	9.95	"	896	1.018	11.76	10.64	9.6
2991	27.3	79.2	1.5	3.65	0.35	364	1.052	5.51	5.92	7.4
92	22.8	79.3	"	2.90	"	304	1.049	4.26	5.27	23.7
94	22.0	79.9	"	2.95	"	293	1.006	4.17	5.15	23.5
95	22.0	79.3	"	2.90	"	293	1.049	4.26	5.15	20.9
									Ave.	14.1
1/8-in. depth, 3/4-in. radius; 2 pellets per run										
1864	84.0	78.9	2.0	9.95	0.25	1121	1.074	12.41	9.85	20.6
65	85.9	79.9	"	9.65	"	1146	1.006	11.27	10.00	12.7
67	84.0	79.6	"	8.95	"	1121	1.024	10.61	9.85	7.2
68	83.0	79.4	"	9.20	"	1107	1.042	11.11	9.79	11.9
69	22.0	79.7	"	3.55	0.10	293	1.021	4.19	4.13	1.4
70	22.0	79.8	"	3.45	"	293	1.015	4.05	4.13	2.0
72	22.0	79.7	"	3.25	"	293	1.018	3.82	4.13	8.1
73	21.2	80.5	"	2.90	"	283	0.971	3.24	4.03	24.4
75	39.9	80.0	"	5.05	0.25	532	1.000	5.72	6.07	6.1
76	39.9	80.2	"	5.70	"	532	0.988	6.41	6.07	5.3
78	39.1	80.0	"	5.55	"	522	1.003	6.34	5.99	5.5
79	39.9	79.9	"	4.60	"	532	1.006	5.22	6.07	16.3
20	151.9	78.7	1.5	10.80	0.40	2026	1.086	17.93	14.48	19.2
21	153.8	80.8	"	10.75	"	2052	0.947	15.56	14.60	6.2
23	149.9	80.9	"	11.40	"	2000	0.942	16.45	14.36	12.7
24	142.0	80.3	"	10.10	"	1894	0.979	15.09	13.87	8.1
									Ave.	10.5
1/8-in. depth, 1-in. radius; 4 pellets per run										
458	22.0	78.9	5.0	10.75	0.90	293	1.077	2.53	2.59	2.4
59	22.0	79.2	"	10.05	"	293	1.055	2.30	2.59	12.6
61	21.2	82.0	"	9.90	"	283	1.110	2.38	2.53	6.3
62	39.1	79.5	"	16.75	1.05	522	1.030	3.85	3.76	2.3
63	39.9	80.6	"	16.85	"	532	0.962	3.62	3.81	5.2
65	39.1	79.6	"	16.05	"	522	1.027	3.67	3.76	2.5
78	126.3	80.9	"	40.75	0.40	1685	0.942	9.05	8.06	10.9
79	126.3	81.5	"	38.85	"	1685	0.906	8.30	8.06	2.9
81	125.3	79.1	"	40.00	"	1672	1.061	10.01	8.02	19.9
86	73.1	79.1	"	24.95	0.05	975	1.061	6.29	5.65	10.2
87	73.1	79.7	"	24.15	"	975	1.021	5.86	5.65	3.6
89	72.2	79.0	"	26.50	"	963	1.067	6.72	5.60	16.7
									Ave.	8.0

Table 5E (Continued)

Run No.	Air, lb-mol/hr-ft^2	Temp °F	$\Delta\theta$, min	$-\Delta W$, mg	$-\Delta W_o$ mg	D_pG/μ	C_T	Rate x 10^4 lb-mols/hr-ft^2 Exper.	Eqn 36	% Dev.
1/8-in. depth, 1-1/2-in. radius; 4 pellets per run										
628	75.1	79.9	2.0	7.95	0.40	1002	1.006	4.53	2.94	35.1
29	76.1	79.5	"	6.75	"	1015	1.036	3.92	2.97	49.7
31	85.0	78.8	"	7.05	"	1134	1.080	4.28	3.19	25.5
32	85.0	78.9	"	5.45	"	1134	1.077	3.24	3.19	1.5
33	160.7	79.8	"	10.70	"	2144	1.015	6.22	4.83	22.3
34	165.6	79.8	"	12.10	"	2209	1.012	7.05	4.92	30.2
36	163.7	79.5	"	12.20	"	2184	1.036	7.28	4.88	33.0
37	157.8	79.9	"	11.70	"	2105	1.006	6.77	4.77	29.5
39	22.0	80.9	"	3.45	1.10	293	0.942	1.32	1.33	0.8
41	22.0	80.4	"	3.40	"	293	0.976	1.33	1.33	0.0
42	22.0	80.1	"	3.40	"	293	0.991	1.36	1.33	2.2
43	39.9	78.1	"	4.60	"	532	1.134	2.36	1.95	17.4
44	39.9	79.3	"	4.70	"	532	1.049	2.25	1.95	13.3
46	39.9	80.0	"	4.75	"	532	1.000	2.17	1.95	10.1
47	39.9	79.6	"	4.45	"	532	1.024	2.04	1.95	4.4
									Ave.	18.3
1/8-in. depth, 2-in. radius; 6 pellets per run										
434	71.2	80.3	5.0	18.50	1.90	950	0.979	2.58	2.05	20.5
36	68.2	81.1	"	16.45	"	910	0.932	2.15	1.63	24.2
37	126.3	78.8	"	19.20	1.10	1685	1.080	3.10	2.44	21.3
39	126.3	80.8	"	21.35	"	1685	0.950	3.06	2.44	20.3
40	22.8	83.4	"	12.95	4.45	304	0.799	1.08	0.80	25.9
42	23.5	86.1	"	14.35	"	314	0.675	1.06	0.82	22.6
43	39.9	84.5	"	13.70	4.20	532	0.745	1.12	1.15	2.7
45	40.7	82.1	"	13.75	"	543	0.870	1.32	1.17	11.4
46	129.2	81.3	"	19.05	-3.00	1724	0.920	3.22	2.47	23.3
48	126.3	80.5	"	14.85	"	1685	0.968	2.74	2.44	10.9
49	73.1	79.7	"	15.25	0.35	975	1.021	2.42	1.71	29.3
51	79.0	79.5	"	13.70	"	1054	1.033	2.19	1.80	17.8
52	23.5	77.7	"	9.05	3.30	314	1.161	1.06	0.82	22.6
54	23.5	80.2	"	10.85	"	314	0.985	1.18	1.17	30.5
55	40.7	80.2	"	12.90	1.55	543	0.988	1.78	1.17	34.3
57	39.9	80.4	"	10.95	"	532	0.976	1.46	1.15	21.2
									Ave.	21.2
3/8-in. depth, 0-in. radius; 1 pellet per run										
778	37.5	80.4	5.0	9.05	0.60	500	0.973	7.83	7.54	3.7
79	38.3	81.2	"	8.50	"	511	0.923	6.95	7.64	9.9
81	37.5	79.5	"	8.50	"	500	1.033	7.77	7.54	3.0
82	38.3	79.8	"	7.40	"	511	1.015	6.57	7.64	16.3

Table 5E (Continued)

Run No.	Air, lb-mol / hr-ft^2	Temp °F	$\Delta\theta$, min	$-\Delta W$, mg	$-\Delta W_o$ mg	D_pG/μ	C_T	Rate x 10^4 lb-mols/hr-ft^2 Exper.	Eqn 36	% Dev.
3/8-in. depth, 0-in. radius; 1 pellet per run										
783	76.1	80.2	5.0	12.00	0.60	1015	0.988	10.73	11.94	11.3
84	86.9	80.9	"	14.25	"	1159	0.944	12.28	13.02	6.0
86	82.0	80.9	"	13.50	"	1094	0.944	11.61	12.53	7.9
87	86.9	80.3	"	17.10	"	1159	0.982	15.44	13.02	15.7
3023	22.0	79.7	1.5	1.35	0.00	293	1.021	4.38	5.33	21.7
24	23.5	79.6	"	1.55	"	314	1.024	5.05	5.56	10.1
26	23.5	79.6	"	1.30	-0.15	314	1.024	4.70	5.56	18.3
27	23.5	79.7	"	1.30	"	314	1.018	4.70	5.56	18.3
34	145.9	79.9	"	7.30	0.25	1946	1.006	22.52	18.25	19.0
35	147.9	80.5	"	6.65	"	1973	0.965	19.63	18.40	6.3
37	161.7	79.8	"	6.60	"	2157	1.012	20.42	19.50	4.5
38	153.8	81.0	"	6.45	"	2052	0.935	18.42	18.87	2.4
									Ave.	10.9
3/8-in. depth, 1/2-in. radius; 2 pellets per run										
678	43.1	80.5	2.0	7.10	0.30	575	0.971	7.86	6.85	12.8
79	42.3	80.8	"	7.50	"	564	0.947	8.12	6.77	16.6
81	42.3	80.6	"	7.05	"	564	0.959	7.71	6.77	12.2
82	43.1	81.0	"	7.70	"	575	0.940	8.29	6.85	17.4
83	21.2	80.7	"	4.05	"	283	0.953	4.25	4.32	1.6
84	21.2	80.7	"	4.05	"	283	0.953	4.25	4.32	1.6
86	21.2	81.0	"	3.95	"	283	0.940	4.09	4.32	5.6
87	21.2	81.0	"	4.05	"	283	0.940	4.20	4.32	2.9
3006	153.8	79.3	1.5	11.85	0.60	2052	1.049	18.74	15.67	16.4
07	153.8	80.0	"	12.05	"	2052	1.000	18.18	15.67	13.8
09	157.8	78.8	"	10.60	"	2105	1.080	17.15	15.93	7.1
10	161.7	78.9	"	10.90	"	2157	1.077	17.61	16.19	8.1
12	75.1	79.4	"	5.80	0.10	1002	1.042	9.43	9.83	4.2
13	73.1	79.0	"	7.10	"	975	1.067	11.86	9.66	18.5
15	80.0	79.4	"	6.25	"	1067	1.042	10.18	10.24	0.6
16	73.1	79.2	"	6.90	"	975	1.055	11.39	9.66	15.3
									Ave.	
3/8-in. depth, 1-in. radius; 4 pellets per run										
3067	77.1	80.2	1.5	9.70	0.30	1029	0.988	7.38	5.00	32.2
68	82.0	79.4	"	8.50	"	1094	1.042	6.78	5.20	23.3
70	73.1	79.1	"	8.55	"	975	1.061	6.95	4.83	30.5
71	76.1	78.7	"	9.25	"	1015	1.086	7.72	4.96	35.8
72	24.3	80.0	"	3.50	"	324	1.003	2.55	2.36	7.5
73	25.0	80.7	"	3.90	"	334	0.953	2.72	2.41	11.4
75	25.0	81.1	"	3.55	"	334	0.932	2.41	2.41	0.0
76	24.3	81.5	"	4.25	"	324	0.909	2.85	2.36	17.2

Table 5 E (Continued)

Run No.	Air, lb-mol / hr-ft^2	Temp °F	$\Delta\theta$, min	$-\Delta W$, mg	$-\Delta W_o$ mg	D_pG/μ	C_T	Rate x 10^4 lb-mols/hr-ft^2 Exper.	Rate x 10^4 lb-mols/hr-ft^2 Eqn 36	% Dev.
3/8-in. depth, 1-in. radius; 4 pellets per run										
3078	39.9	80.0	1.5	6.20	0.45	532	1.000	4.57	3.26	28.7
79	39.9	80.2	"	6.15	"	532	0.988	4.47	3.26	27.1
81	41.5	79.3	"	5.15	"	554	1.049	3.91	3.34	14.6
82	41.5	79.3	"	5.50	"	554	1.049	4.21	3.34	20.7
83	156.8	79.2	"	11.60	"	2092	1.055	9.34	7.93	15.1
84	146.9	79.0	"	15.30	"	1960	1.067	12.58	7.60	39.6
86	153.8	79.9	"	13.95	"	2052	1.006	10.78	7.83	27.4
87	156.8	79.0	"	12.95	"	2092	1.067	10.59	7.93	25.1
									Ave.	22.3
3/8-in. depth, 1-1/2-in. radius; 4 pellets per run										
608	146.9	78.5	2.0	9.10	1.65	1960	1.106	4.93	4.76	3.4
09	155.8	78.7	"	10.20	"	2078	1.090	5.56	4.95	10.6
11	154.8	80.2	"	9.50	"	2065	0.988	4.63	4.92	6.3
12	153.8	80.5	"	9.95	"	2052	0.971	4.81	4.90	1.9
13	80.0	80.3	"	8.70	1.85	1067	0.982	4.01	3.21	20.0
14	74.1	80.0	"	8.40	"	988	1.000	3.90	3.05	21.8
16	81.0	79.5	"	7.25	"	1081	1.030	3.31	3.23	2.4
17	82.0	80.0	"	8.05	"	1094	1.000	3.69	3.26	11.7
18	41.5	79.8	"	4.40	0.80	554	1.012	2.17	2.09	3.7
19	41.5	80.1	"	5.00	"	554	0.994	2.48	2.09	15.7
21	40.7	80.5	"	4.50	"	543	0.971	2.14	2.07	3.3
22	41.5	80.7	"	4.80	"	554	0.956	2.27	2.09	7.9
23	22.0	80.5	"	3.10	"	293	0.971	1.33	1.39	4.5
24	22.8	80.6	"	3.05	"	304	0.959	1.29	1.42	10.1
26	22.8	80.8	"	3.35	"	304	0.947	1.44	1.42	1.4
27	22.8	81.0	"	3.25	"	304	0.937	1.37	1.42	3.6
									Ave.	8.1
3/8-in. depth, 2-in. radius; 4 pellets per run										
588	22.0	79.7	2.0	2.25	0.80	293	1.018	0.88	1.01	14.8
89	22.0	79.6	"	2.35	"	293	1.024	0.95	1.01	6.3
91	22.0	80.2	"	2.40	"	293	0.985	0.94	1.01	7.4
92	22.0	80.5	"	2.70	"	293	0.965	1.09	1.01	7.3
93	39.9	80.4	"	3.55	0.85	532	0.976	1.57	1.49	5.1
94	39.1	80.4	"	3.85	"	522	0.976	1.74	1.47	15.5
96	39.1	80.3	"	3.60	"	522	0.982	1.61	1.47	8.7
97	39.1	80.3	"	3.60	"	522	0.982	1.61	1.47	8.7
98	81.0	79.7	5.0	12.85	2.30	1081	1.018	2.56	2.35	8.2
99	74.1	79.6	"	11.85	"	988	1.027	2.34	2.22	5.1
601	82.0	79.5	"	12.05	"	1094	1.030	2.39	2.37	0.8
02	85.0	79.2	"	12.10	"	1134	1.052	2.46	2.43	1.2
03	160.7	79.5	2.0	8.00	1.75	2144	1.030	3.84	3.67	4.4
04	160.7	79.3	"	7.75	"	2144	1.049	3.75	3.67	2.1
06	157.8	79.2	"	7.55	"	2105	1.055	3.64	3.63	0.3
07	159.7	79.4	"	7.65	"	2131	1.039	3.65	3.66	0.3
									Ave.	6.0

Table 5 E (Continued)

Run No.	Air, lb-mol/hr-ft	Temp °F	$\Delta\theta$, min	$-\Delta W$, mg	$-\Delta W_o$ mg	$\frac{D_p G}{\mu}$	C_T	Rate x 10^4 lb-mols/hr-ft^2 Exper.	Rate x 10^4 lb-mols/hr-ft^2 Eqn 36	% Dev.
5/8-in. depth, 0-in. radius; 1 pellet per run										
3089	157.8	77.9	2.0	5.05	0.15	2105	1.147	13.39	14.09	5.2
90	150.9	78.7	"	5.45	"	2103	1.090	13.77	13.69	0.6
92	159.7	79.2	"	5.85	"	2131	1.055	14.32	14.20	0.8
93	157.8	79.6	"	5.35	"	2105	1.024	12.67	14.09	11.2
94	39.9	80.5	"	2.55	"	532	0.965	5.53	5.76	4.2
95	39.9	81.2	"	2.40	"	532	0.923	4.95	5.76	16.4
97	39.9	80.3	"	2.50	"	532	0.979	5.48	5.76	5.1
98	39.9	79.4	"	2.80	"	532	1.042	6.57	5.76	12.3
99	61.7	80.0	"	3.25	0.30	823	1.003	7.05	7.65	8.5
3100	66.2	80.1	"	3.80	"	883	0.994	8.27	8.01	3.1
02	60.8	80.0	"	3.70	"	811	1.003	8.12	7.58	6.7
03	61.7	78.7	"	3.35	"	823	1.086	7.88	7.65	2.9
04	22.8	81.1	"	1.60	0.20	304	0.932	3.10	4.01	29.4
05	22.8	81.5	"	2.00	"	304	0.909	3.91	4.01	2.6
08	22.8	80.0	"	1.95	"	304	1.000	4.17	4.01	3.8
									Ave.	7.5
5/8-in. depth, 1/2-in. radius; 2 pellets per run										
1949	85.0	79.4	2.0	8.00	0.05	1134	1.042	9.86	7.54	23.5
50	86.9	80.2	"	8.95	"	1159	0.988	10.47	7.65	26.9
52	88.9	80.1	"	7.45	"	1186	0.994	8.77	7.76	11.5
53	87.9	80.5	"	7.85	"	1173	0.971	9.02	7.71	14.5
54	25.0	80.0	"	2.45	-0.15	334	0.977	3.19	3.40	6.6
55	25.8	80.2	"	2.85	"	344	0.988	3.53	3.48	1.4
57	25.8	80.3	"	3.05	"	344	0.988	3.76	3.48	7.4
58	25.0	80.3	"	2.75	"	334	0.982	3.39	3.40	0.3
60	39.9	80.5	"	4.60	0.20	532	0.971	5.09	4.61	9.4
61	38.3	80.5	"	4.60	"	511	0.965	5.06	4.49	11.3
63	38.3	80.1	"	4.10	"	511	0.994	4.62	4.49	2.8
64	39.1	80.0	"	4.35	"	522	1.000	4.94	4.55	7.9
65	153.8	78.8	"	10.30	0.15	2052	1.080	13.05	11.08	15.1
66	153.8	79.4	"	11.60	"	2052	1.042	14.21	11.08	22.0
68	153.8	79.2	"	9.20	"	2052	1.055	11.37	11.08	2.6
69	153.8	79.1	"	9.80	"	2052	1.061	12.20	11.08	9.2
									Ave.	10.8
5/8-in. depth, 1-in. radius; 2 pellets per run										
1387	86.9	76.3	2.0	3.90	0.60	1159	1.272	4.99	4.75	4.8
88	83.0	78.7	"	4.15	"	1107	1.086	4.60	4.61	0.2
90	83.0	79.7	"	5.05	"	1107	1.018	5.40	4.61	14.6
91	86.9	80.0	"	5.50	"	1159	0.997	5.82	4.75	18.3
92	22.0	80.1	"	2.20	"	293	0.991	1.89	1.94	2.6
93	22.8	80.3	"	2.60	1.00	304	0.979	1.87	1.99	6.4
96	23.5	80.4	"	2.70	"	314	0.976	1.98	2.03	2.5

Table 5E (Continued)

Run No.	Air, lb-mol/hr-ft^2	Temp °F	Δθ, min	$-\Delta W$, mg	$-\Delta W_o$ mg	D_pG/μ	C_T	Rate x 10^4 lb-mols/hr-ft^2 Exper.	Eqn 36	% Dev.
5/8-in. depth, 1-in. radius; 2 pellets per run										
1398	39.1	80.4	2.0	3.45	0.45	522	0.973	3.48	2.82	19.0
99	38.3	80.0	"	2.70	"	511	0.997	2.67	2.79	4.5
1401	39.1	80.0	"	2.75	"	522	1.000	2.74	2.82	2.9
02	38.3	80.0	"	2.80	"	511	1.000	2.80	2.79	0.4
03	146.9	79.2	"	7.70	"	1960	1.052	9.09	6.67	26.6
04	149.9	80.2	"	6.65	"	2000	0.988	7.29	6.76	7.3
06	157.8	80.3	"	8.20	"	2105	0.982	9.06	6.99	33.9
07	155.8	80.1	"	6.35	"	2078	0.994	6.98	6.94	0.6
									Ave.	9.6
5/8-in. depth, 1-1/2-in. radius; 4 pellets per run										
3045	36.7	78.9	1.5	2.65	0.65	490	1.074	1.71	1.97	15.2
46	38.3	78.6	"	2.95	"	511	1.096	2.00	2.03	1.5
48	38.3	80.3	"	3.40	"	511	0.982	2.14	2.03	4.2
49	37.5	80.1	"	3.40	"	500	0.994	2.17	2.00	7.8
50	24.3	80.1	"	2.65	0.95	324	0.991	1.33	1.51	13.5
51	24.3	79.8	"	2.80	"	324	1.012	1.48	1.51	2.0
53	24.3	79.6	"	2.80	"	324	1.027	1.51	1.51	0.0
54	25.0	79.5	"	2.80	"	334	1.036	1.52	1.54	1.3
56	70.2	78.9	"	4.30	0.65	936	1.074	3.11	3.01	3.2
57	83.0	78.1	"	4.35	"	1107	1.130	3.32	3.36	1.2
59	83.0	79.4	"	4.65	"	1107	1.042	3.31	3.36	1.5
60	83.0	79.3	"	4.75	"	1107	1.049	3.41	3.36	1.5
61	148.9	78.2	"	5.55	0.50	1986	1.127	4.52	4.90	10.6
62	151.9	79.7	"	6.40	"	2026	1.021	4.78	4.97	4.0
64	149.9	79.5	"	5.75	"	2000	1.036	4.32	4.93	14.1
65	149.9	79.6	"	6.80	"	2000	1.024	5.12	4.93	3.7
									Ave.	5.3
5/8-in. depth, 2-in. radius; 4 pellets per run										
1101	159.7	79.7	2.0	9.20	0.60	2131	1.018	5.21	4.37	16.1
02	161.7	80.0	"	7.45	"	2157	1.000	4.08	4.41	8.1
04	151.9	80.3	"	7.45	"	2026	0.979	4.00	4.23	5.8
05	149.9	79.7	"	6.30	"	2000	1.018	3.45	4.19	21.4
06	20.5	80.0	"	2.35	0.65	273	1.003	1.02	1.15	12.7
07	21.2	80.6	"	2.80	"	283	0.962	1.23	1.18	4.1
09	21.2	80.9	"	2.70	"	283	0.945	1.15	1.18	2.6
10	19.7	81.2	"	3.10	"	263	0.926	1.35	1.12	17.0
12	85.0	80.2	"	7.80	1.40	1134	0.988	3.76	2.90	22.9
13	85.0	80.1	"	7.50	"	1134	0.994	3.61	2.90	19.7
15	83.0	79.5	"	6.40	"	1107	1.030	3.07	2.86	6.8
16	88.9	79.8	"	6.70	"	1186	1.015	3.20	2.99	6.6

Table 5 E (Continued)

Run No.	Air, lb-mol / hr-ft^2	Temp °F	$\Delta\theta$, min	$-\Delta W$, mg	$-\Delta W_o$ mg	$D_p G / \mu$	C_T	Rate x 10^4 lb-mols/hr-ft^2 Exper.	Eqn 36	% Dev.
5/8-in. depth, 2-in. radius; 4 pellets per run										
1122	39.9	73.5	2.0	3.45	1.40	532	1.529	1.86	1.77	4.8
23	39.1	75.4	"	3.80	"	522	1.351	1.93	1.75	9.3
25	39.9	76.7	"	3.90	"	532	1.244	1.85	1.77	4.3
26	39.9	78.5	"	4.35	"	532	1.103	1.94	1.77	8.8
									Ave.	10.7
1-in. depth, 0-in. radius; 1 pellet per run										
1825	76.1	80.4	3.0	4.30	0.15	1015	0.973	6.42	6.07	5.5
26	76.1	80.9	"	3.95	"	1015	0.945	5.70	6.07	6.5
28	83.0	80.5	"	3.45	"	1107	0.971	5.08	6.43	26.6
29	83.0	81.2	"	3.30	"	1107	0.926	4.64	6.43	38.6
30	146.9	82.7	"	6.35	"	1960	0.840	8.27	9.31	12.6
31	150.9	80.0	"	6.30	"	2013	1.000	9.77	9.48	3.0
33	150.9	79.1	"	6.05	"	2013	1.061	9.94	9.48	4.6
34	151.9	80.4	"	6.50	"	2026	0.973	9.81	9.51	3.1
36	39.9	80.5	5.0	5.30	0.60	532	0.971	4.34	3.99	8.1
37	38.3	80.8	"	4.90	"	511	0.947	3.88	3.89	0.3
39	39.1	80.7	"	5.20	"	522	0.956	4.19	3.94	6.0
40	39.1	81.4	"	4.45	"	522	0.912	3.34	3.94	18.0
41	22.0	80.9	"	2.70	0.25	293	0.945	2.21	2.71	22.6
42	22.0	80.1	"	2.85	"	293	0.991	2.46	2.71	10.2
44	22.8	79.6	"	3.25	"	304	1.024	2.93	2.77	5.5
45	22.8	79.3	"	2.40	"	304	1.049	2.15	2.77	28.8
									Ave.	12.5
1-in. depth, 1/2-in. radius; 2 pellets per run										
1781	145.9	78.9	2.0	7.05	0.60	1946	1.074	8.25	7.73	6.3
82	149.9	79.4	"	6.50	"	2000	1.039	7.30	7.86	7.7
84	147.9	79.8	"	6.90	"	1973	1.012	7.60	7.80	2.6
85	153.8	80.1	"	7.90	"	2052	0.991	8.61	7.99	7.2
86	85.0	83.7	"	5.95	0.30	1134	0.785	5.29	5.44	2.8
87	86.9	82.1	"	5.00	"	1159	0.873	4.88	5.52	13.1
89	85.0	80.0	"	4.45	"	1134	0.997	4.93	5.44	10.3
90	87.9	79.9	"	5.35	"	1173	1.009	6.07	5.56	8.4
92	39.9	79.6	"	2.55	-0.20	532	1.027	3.36	3.32	1.2
93	40.7	79.7	"	2.75	"	543	1.018	3.57	3.37	5.6
95	41.5	79.3	"	2.80	"	554	1.049	3.75	3.41	9.1
96	39.9	79.4	"	2.60	"	532	1.042	3.48	3.32	4.6
97	23.5	79.5	"	1.40	"	314	1.030	1.97	2.36	19.8
98	24.3	79.4	"	1.75	"	324	1.039	2.42	2.41	0.4
1800	24.3	79.5	"	1.45	"	324	1.036	2.04	2.41	18.1
01	24.3	79.4	"	1.55	"	324	1.042	2.17	2.41	11.1
									Ave.	8.0

Table 5 E (Continued)

Run No.	Air, lb-mol/hr-ft^2	Temp °F	$\Delta\theta$, min	$-\Delta W$, mg	$-\Delta W_o$ mg	D_pG/μ	C_T	Rate x 10^4 lb-mols/hr-ft^2 Exper.	Rate x 10^4 lb-mols/hr-ft^2 Eqn 36	% Dev.
1-in. depth, 1-in. radius; 3 pellets per run										
1632	39.9	79.6	2.0	3.10	0.35	532	1.024	2.24	2.42	8.0
33	39.9	79.6	"	3.10	"	532	1.027	2.24	2.42	8.0
35	39.1	79.8	"	4.05	"	522	1.015	2.99	2.38	20.4
36	39.1	79.5	"	3.75	"	522	1.030	2.78	2.38	14.4
37	145.0	78.8	"	8.35	0.55	1934	1.080	6.69	5.59	16.4
38	149.9	78.9	"	7.25	"	2000	1.077	5.73	5.71	0.3
40	143.0	79.2	"	6.90	"	1908	1.052	5.30	5.54	4.5
41	145.9	79.2	"	8.45	"	1946	1.055	6.61	5.62	15.0
43	23.5	80.0	"	2.35	0.40	314	1.000	1.55	1.71	10.3
44	24.3	80.2	"	2.65	"	324	0.988	1.76	1.75	0.6
46	24.3	80.1	"	2.75	"	324	0.994	1.86	1.75	5.9
47	24.3	80.2	"	2.80	"	324	0.988	1.88	1.75	6.9
48	86.9	80.0	"	5.55	0.60	1159	0.997	3.92	4.01	2.3
49	85.0	79.9	"	5.90	"	1134	1.006	4.23	3.95	6.6
51	85.0	79.8	"	6.55	"	1134	1.012	4.78	3.95	17.4
52	84.0	79.9	"	6.00	"	1121	1.009	4.33	3.92	9.5
									Ave.	9.2
1-in. depth, 1-1/2-in. radius; 4 pellets per run										
1676	39.9	79.1	2.0	3.75	0.40	532	1.061	2.11	2.13	1.0
77	40.7	79.4	"	3.50	"	543	1.042	1.92	2.16	12.5
79	40.7	79.0	"	3.10	"	543	1.034	1.72	2.16	25.6
82	86.9	75.8	"	4.65	0.25	1159	1.315	3.45	3.53	2.3
83	73.1	78.1	"	4.65	"	975	1.130	2.96	3.16	6.8
85	86.9	77.8	"	5.25	"	1159	1.154	3.44	3.53	2.6
86	88.9	78.7	"	5.05	"	1186	1.086	3.10	3.58	15.5
87	145.9	79.1	"	7.60	"	1946	1.061	4.64	4.95	6.7
88	150.9	80.3	"	7.95	"	2013	0.982	4.50	5.05	12.2
90	153.8	78.1	"	7.40	"	2052	1.134	4.83	5.12	6.0
91	149.9	78.6	"	7.45	"	2000	1.093	4.69	5.03	7.2
2178	21.2	78.3	"	2.20	0.20	283	1.116	1.33	1.41	6.0
79	22.8	79.2	"	2.20	"	304	1.055	1.26	1.48	17.5
81	22.8	79.5	"	2.20	"	304	1.030	1.23	1.48	20.3
82	22.8	79.6	"	2.30	"	304	1.027	1.29	1.48	14.7
									Ave.	10.4
1-in. depth, 2-in. radius; 4 pellets per run										
1580	85.0	80.0	2.0	5.85	0.35	1134	1.003	3.29	3.26	0.9
81	86.9	79.7	"	5.70	"	1159	1.021	3.25	3.31	1.8
83	86.9	79.9	"	5.90	"	1159	1.009	3.33	3.31	0.6
84	85.0	79.8	"	5.20	"	1134	1.012	2.92	3.26	11.6
85	22.8	79.7	"	2.30	"	304	1.018	1.19	1.39	16.8
86	22.8	79.8	"	2.45	"	304	1.012	1.27	1.39	9.4
88	23.5	79.7	"	2.45	"	314	1.021	1.29	1.41	9.3
89	24.3	79.9	"	2.40	"	324	1.006	1.23	1.45	17.9

Table 5E (Continued)

Run No.	Air, lb-mol/hr-ft	Temp °F	Δθ, min	-ΔW, mg	-ΔW$_o$ mg	D_pG/μ	C_T	Rate x 10^4 lb-mols/hr-ft^2 Exper.	Eqn 36	% Dev.
1591	39.9	80.5	2.0	4.15	0.60	532	0.965	2.04	2.00	2.0
92	39.9	80.5	"	3.90	"	532	0.965	1.89	2.00	5.8
94	39.9	80.5	"	3.90	"	532	0.968	1.90	2.00	5.3
95	39.1	80.1	"	4.10	"	522	0.991	2.07	1.97	4.8
96	151.9	79.7	"	8.10	0.50	2026	1.021	4.62	4.76	3.0
97	144.0	79.3	"	7.70	"	1921	1.045	4.48	4.60	2.7
99	150.9	79.5	"	7.35	"	2013	1.033	4.22	4.74	12.3
1600	147.9	79.6	"	7.10	"	1973	1.027	4.04	4.68	15.8
									Ave.	7.5
2-in. depth, 0-in. radius; 1 pellet per run										
2015	22.0	78.7	5.0	1.35	0.25	2935	1.086	1.13	1.54	36.3
16	22.0	79.4	"	1.65	"	293	1.042	1.39	1.54	10.8
18	22.0	79.4	"	2.00	"	293	1.039	1.73	1.54	11.0
19	22.0	79.9	"	1.80	"	293	1.006	1.49	1.54	3.4
20	38.3	80.1	"	2.75	"	511	0.994	2.28	2.20	3.5
21	38.3	80.8	"	2.70	"	511	0.950	2.12	2.20	3.8
23	38.3	79.0	"	2.60	"	511	1.067	2.29	2.20	3.9
24	36.7	79.0	"	2.40	"	490	1.067	2.09	2.14	2.4
26	85.0	77.5	3.0	1.90	0.05	1134	1.178	3.46	3.70	6.9
27	88.9	79.6	"	2.10	"	1186	1.027	3.35	3.85	14.9
29	85.9	78.9	"	2.35	"	1146	1.077	3.94	3.72	5.6
30	85.9	79.6	"	2.30	"	1146	1.027	3.67	3.72	1.4
31	152.8	81.0	"	3.55	"	2038	0.940	5.22	5.41	3.6
32	156.8	80.2	"	3.55	"	2092	0.988	5.49	5.50	0.2
34	153.8	80.2	"	3.60	"	2052	0.988	5.57	5.44	2.3
35	147.9	81.3	"	3.60	"	1973	0.918	5.18	5.30	2.3
									Ave.	7.0
2-in. depth, 1/2-in. radius; 2 pellets per run										
2037	143.0	79.3	2.0	4.65	0.40	1908	1.049	5.31	4.93	7.2
38	142.0	80.0	"	4.50	"	1894	1.000	4.88	4.91	6.2
40	148.9	79.5	"	4.80	"	1986	1.030	5.40	5.06	6.3
41	153.8	80.2	"	5.00	"	2052	0.985	5.40	5.17	4.3
42	88.9	79.5	"	3.35	0.60	1186	1.036	3.39	3.62	6.8
43	86.9	80.0	"	3.65	"	1159	1.003	3.64	3.57	1.9
55	86.9	79.6	"	3.45	"	1159	1.027	3.49	3.57	2.3
56	88.9	80.0	"	3.70	"	1186	1.000	3.69	3.62	1.9
58	22.8	79.6	3.0	2.05	0.20	304	1.024	1.50	1.49	0.7
59	24.3	80.1	"	2.10	"	324	0.994	1.50	1.59	6.0
61	24.3	79.4	"	2.00	"	324	1.042	1.49	1.59	6.7
62	24.3	79.5	"	1.95	"	324	1.030	1.43	1.59	11.2
63	40.7	79.6	"	2.90	0.30	543	1.024	2.11	2.18	3.3
64	39.9	80.5	"	3.10	"	532	0.971	2.16	2.15	0.5
66	39.9	80.2	"	3.10	"	532	0.988	2.20	2.15	2.2
67	40.7	81.2	"	3.30	"	543	0.926	2.21	2.18	1.4
									Ave.	4.3

Table 5E (Continued)

Run No.	Air, lb-mol/hr-ft^2	Temp °F	$\Delta\theta$, min	$-\Delta W$, mg	$-\Delta W_o$ mg	$\frac{D_p G}{\mu}$	C_T	Rate x 10^4 lb-mols/hr-ft^2 Exper.	Eqn 36	% Dev.
2-in. depth, 1-in. radius; 4 pellets per run										
3525	142.0	80.9	1.5	6.30	0.70	1894	0.942	4.19	4.86	16.0
26	140.1	81.1	"	6.70	"	1869	0.929	4.42	4.81	8.8
28	138.1	81.1	"	4.60	"	1842	0.932	5.11	4.77	6.7
29	130.2	81.4	"	7.50	"	1736	0.915	4.94	4.59	7.1
31	42.3	81.3	2.5	5.75	"	564	0.918	2.21	2.21	0.0
32	43.1	80.6	"	6.25	"	575	0.959	2.53	2.24	12.3
34	44.7	81.5	"	6.40	"	596	0.904	2.45	2.29	6.5
35	43.9	81.5	"	6.05	"	586	0.909	2.32	2.26	2.6
36	22.0	86.7	3.0	5.40	0.65	293	0.648	1.22	1.45	18.9
37	25.0	86.8	"	6.50	"	334	0.646	1.50	1.57	4.7
39	25.8	86.6	"	6.35	"	344	0.652	1.48	1.60	8.1
40	24.3	86.4	"	5.90	"	324	0.651	1.36	1.54	13.2
41	81.0	82.4	2.0	8.00	"	1081	0.858	3.76	3.37	10.4
42	87.9	80.7	"	7.90	"	1173	0.953	4.11	3.56	13.4
44	71.2	82.1	"	7.50	"	950	0.870	3.55	3.10	12.7
45	81.0	81.2	"	7.00	"	1081	0.923	3.49	3.37	3.4
									Ave.	9.1
2-in. depth, 2-in. radius; 4 pellets per run										
1759	39.9	79.5	2.0	3.95	0.40	532	1.030	2.18	2.13	2.3
60	40.7	79.7	"	3.85	"	543	1.021	2.10	2.16	2.9
62	39.9	79.5	"	3.65	"	532	1.033	2.00	2.13	6.5
63	39.9	80.2	"	4.00	"	532	0.988	2.12	2.13	0.5
64	22.0	80.0	"	2.60	0.45	293	1.003	1.29	1.45	12.4
65	22.0	79.5	"	2.75	"	293	1.030	1.41	1.45	2.8
67	22.0	78.9	"	2.75	"	293	1.074	1.52	1.45	4.6
68	22.0	78.4	"	2.50	"	293	1.109	1.31	1.45	10.7
70	90.9	78.2	"	6.40	"	1213	1.127	4.00	3.64	9.0
71	83.0	77.9	"	5.90	"	1107	1.150	3.72	3.43	7.8
73	85.0	79.0	"	6.80	"	1134	1.067	4.04	3.48	13.9
74	87.9	78.8	"	6.35	"	1173	1.080	3.78	3.56	5.8
75	142.0	80.6	"	9.75	0.50	1894	0.959	5.28	4.86	8.0
76	155.8	80.0	"	9.10	"	2078	0.993	5.10	5.16	1.2
78	147.9	79.2	"	8.80	"	1973	1.052	5.20	4.82	7.3
79	153.8	79.7	"	8.80	"	2052	1.021	5.04	5.12	1.6
									Ave.	6.1

Table 5

F. 1-inch orifice, 1/2-inch pellets

Run No.	Air, lb-mol / hr-ft^2	Temp °F	$\Delta\theta$, min	$-\Delta W$, mg	$-\Delta W_o$ mg	$\frac{D_p G}{\mu}$	C_T	Rate x 10^4 lb-mols/hr-ft^2 Exper.	Eqn 36	% Dev.
2-inch depth, 1-in. radius; 1 pellet per run										
3480	31.1	80.4	2.5	4.15	0.05	972	0.974	1.30	1.34	3.1
81	31.1	80.4	"	4.10	"	972	0.974	1.28	1.34	4.7
83	30.4	80.1	"	4.15	"	950	0.991	1.32	1.32	0.0
84	30.4	80.1	"	4.15	"	950	0.991	1.32	1.32	0.0
85	117.4	80.0	1.5	6.05	"	3670	1.003	3.26	3.19	2.1
86	117.4	80.0	"	5.80	"	3670	1.003	3.13	3.19	1.9
88	115.5	79.3	"	6.00	"	3610	1.049	3.38	3.15	6.8
89	115.5	79.3	"	5.55	"	3610	1.049	3.13	3.15	0.6
91	171.5	79.7	"	7.50	0.25	5361	1.021	4.01	4.08	1.7
92	171.5	79.7	"	7.55	"	5361	1.021	4.03	4.08	1.2
94	161.7	80.5	"	7.45	"	5055	0.968	3.77	3.92	4.0
95	161.7	80.5	"	7.25	"	5055	0.968	3.67	3.92	6.8
96	56.4	79.8	2.5	6.35	0.30	1763	1.015	2.00	1.98	1.0
97	56.4	79.8	"	6.30	"	1763	1.015	1.98	1.98	0.0
99	56.4	79.9	"	6.75	"	1763	1.006	2.11	1.98	6.2
3500	56.4	79.9	"	6.50	"	1763	1.006	2.03	1.98	2.5
									Ave.	2.7

Table 5

G. 2-inch orifice, 1/8-inch pellets

Run No.	Air, lb-mol/hr-ft^2	Temp °F	Δθ, min	$-\Delta W$, mg	$-\Delta W_o$ mg	D_pG/μ	C_T	Rate x 10^4 lb-mols/hr-ft^2 Exper.	Eqn 36	% Dev.
1/16-in. depth, 1/2-in. radius; 4 pellets per run										
3340	155.8	80.3	1.5	2.05	0.30	1114	0.979	4.15	5.21	25.5
41	155.8	80.4	"	2.25	"	1114	0.976	4.62	5.21	1.3
43	154.8	80.3	2.0	2.80	"	1107	0.982	4.48	5.12	8.0
44	154.8	80.2	"	2.70	"	1107	0.988	4.32	5.12	18.5
46	86.9	80.3	"	1.90	0.10	621	0.979	3.21	3.57	11.2
47	85.9	80.0	"	1.70	"	614	0.997	2.92	3.54	21.2
49	86.9	80.0	"	1.95	"	621	1.000	3.37	3.57	5.9
50	85.9	79.9	"	2.00	"	614	1.006	3.48	3.54	1.7
3469	43.1	81.6	2.5	2.55	0.55	308	0.898	2.63	2.26	14.0
70	43.9	80.4	"	2.35	"	314	0.974	2.55	2.25	11.8
72	43.9	79.3	"	2.15	"	314	1.045	2.44	2.25	7.8
73	43.9	78.9	"	2.25	"	314	1.074	2.67	2.25	15.7
74	24.3	80.1	3.0	2.00	"	174	0.991	1.75	1.56	10.9
75	24.3	80.4	"	1.85	"	174	0.976	1.54	1.56	1.3
77	24.3	79.8	"	1.90	"	174	1.012	1.67	1.56	6.6
78	24.3	79.9	"	1.85	"	174	1.009	1.59	1.56	1.9
									Ave.	10.2
1/16-in. depth, 1-in. radius; 4 pellets per run										
3266	86.9	80.0	2.0	3.60	0.15	621	0.997	6.27	6.68	6.5
67	87.9	80.4	"	3.80	"	628	0.976	6.49	6.73	3.7
69	86.9	80.0	"	4.40	"	621	0.997	7.73	6.68	13.6
70	88.9	80.0	"	3.30	"	636	1.003	5.76	6.77	17.5
71	20.5	79.5	3.0	2.00	"	147	1.030	2.32	2.61	12.5
72	20.5	79.5	"	2.05	"	147	1.033	2.38	2.61	9.7
74	20.5	78.0	"	2.10	"	147	1.137	2.70	2.61	3.3
75	20.5	79.2	"	1.90	"	147	1.055	2.25	2.61	16.0
77	39.9	80.1	2.5	3.10	0.40	285	0.994	3.91	4.03	3.1
78	39.9	80.9	"	3.45	"	285	0.942	4.19	4.03	3.8
80	39.9	81.1	"	3.30	"	285	0.929	3.92	4.03	2.8
81	39.9	81.1	"	3.60	"	285	0.932	4.35	4.03	7.4
82	156.8	79.6	1.5	4.45	0.35	1121	1.027	10.23	9.80	4.2
83	157.8	79.9	"	3.80	"	1128	1.006	8.44	9.85	16.7
85	159.7	80.2	"	3.90	"	1142	0.988	8.53	9.92	16.3
86	158.8	79.4	"	3.95	"	1135	1.042	9.12	9.88	8.3
									Ave.	9.1

Table 5G (Continued)

Run No.	Air, lb-mol/hr-ft²	Temp °F	Δθ, min	-ΔW, mg	-ΔW₀ mg	D_pG/μ	C_T	Rate x 10^4 lb-mols/hr-ft² Exper.	Rate x 10^4 lb-mols/hr-ft² Eqn 36	% Dev.
1/16-in. depth, 1-1/2-in. radius; 4 and 6* pellets per run										
3392	149.9	80.0	1.5	2.55	0.00	1072	0.997	6.17	6.52	5.7
93	153.8	80.3	"	2.65	"	1100	0.979	6.30	6.63	5.2
95	153.8	80.0	"	2.25	"	1100	1.000	5.47	6.63	21.2
96	151.9	79.8	"	2.10	"	1086	1.015	5.18	6.58	27.0
98	43.9	79.8	2.5	1.95	0.15	314	1.015	2.67	2.93	9.7
99	43.1	79.7	"	1.85	"	308	1.018	2.52	2.90	15.1
3401	42.3	79.9	"	1.95	"	302	1.009	2.65	2.87	8.3
02	42.3	79.5	"	1.90	"	302	1.036	2.64	2.87	8.7
03	25.0	79.9	3.0	2.10	"	179	1.006	2.31	2.03	12.1
04	25.0	79.2	"	1.90	"	179	1.055	2.25	2.03	9.8
06	25.0	78.1	"	1.15	-0.30	179	1.134	1.99	2.03	2.0
07	24.3	78.2	"	1.10	"	174	1.123	1.91	2.00	4.7
09	88.9	80.9	2.0	4.45	0.20	636	0.945	4.89	4.64	5.1
10	90.9	79.0	"	4.20	"	650	1.067	5.19	4.71	9.2
12	89.9	78.5	"	4.35	"	643	1.099	5.54	4.68	15.5
13	90.9	78.6	"	3.90	"	650	1.096	4.93	4.71	4.5
									Ave.	10.2
3/16-in. depth, 1/2-in. radius; 4 pellets per run										
3351	86.9	80.1	2.0	2.90	0.20	621	0.991	4.89	5.21	6.5
52	86.9	80.1	"	3.00	"	621	0.994	5.07	5.21	2.8
54	86.9	80.2	"	2.95	"	621	0.988	4.96	5.21	5.0
55	86.9	80.4	"	3.15	"	621	0.976	5.25	5.21	7.6
56	153.8	80.6	1.5	3.30	"	1100	0.962	7.24	7.56	4.4
57	154.8	80.8	"	2.90	"	1107	0.950	6.25	7.59	21.4
59	153.8	80.6	"	3.25	"	1100	0.962	7.12	7.56	6.2
60	153.8	80.6	"	2.90	"	1100	0.962	6.32	7.56	19.6
61	39.9	80.7	2.5	2.90	0.40	285	0.953	3.47	3.15	9.2
62	39.9	80.6	"	3.10	"	285	0.959	3.78	3.15	16.7
64	39.9	80.9	"	3.30	"	285	0.942	3.98	3.15	20.9
65	39.9	80.8	"	3.90	"	285	0.947	4.83	3.15	34.7
66	21.2	80.2	3.0	2.40	0.65	152	0.988	2.10	2.08	1.0
67	22.0	80.0	"	2.60	"	157	1.003	2.38	2.14	10.1
69	22.0	79.9	"	2.50	"	157	1.006	2.26	2.14	5.3
70	22.8	80.2	"	3.05	"	163	0.988	2.88	2.18	24.3
									Ave.	12.2
3/16-in. depth, 1-in. radius; 4 pellets per run										
3288	39.1	79.7	2.5	2.65	0.40	280	1.021	3.35	3.81	13.7
89	39.1	80.3	"	3.05	"	280	0.982	3.79	3.81	0.5
91	39.9	79.9	"	3.30	"	285	1.009	4.27	3.86	9.6
92	39.9	80.3	"	3.45	"	285	0.982	4.38	3.86	11.9

* Runs 3409-13

Table 5 G (Continued)

Run No.	Air, lb-mol/hr-ft^2	Temp °F	Δθ, min	$-\Delta W$, mg	$-\Delta W_o$ mg	$\frac{D_p G}{\mu}$	C_T	Rate x 10^4 lb-mols/hr-ft^2 Exper.	Eqn 36	% Dev.
3/16-in. depth, 1-in. radius; 4 pellets per run										
3293	22.0	81.5	3.0	2.40	0.40	157	0.906	2.20	2.62	19.1
94	21.2	82.0	"	2.45	"	152	0.875	2.18	2.56	17.4
96	22.0	79.3	"	2.15	"	157	1.045	2.22	2.62	18.0
97	22.0	78.0	"	2.10	"	157	1.171	2.42	2.62	8.3
98	87.9	78.1	2.0	3.60	"	628	1.134	6.62	6.45	2.6
99	87.9	77.8	"	3.75	"	628	1.157	7.07	6.45	8.8
3301	88.9	77.0	"	3.50	"	636	1.218	6.89	6.50	5.7
02	88.9	77.6	"	3.45	"	636	1.168	6.49	6.50	0.2
03	153.8	78.6	1.5	5.05	0.25	1100	1.093	12.76	9.28	27.3
04	154.8	78.3	"	4.60	"	1107	1.120	11.84	9.33	21.2
06	155.8	78.8	"	4.30	"	1114	1.080	10.62	9.35	12.0
07	154.8	78.0	"	4.20	"	1107	1.144	10.99	9.33	15.1
									Ave.	12.0
3/16-in. depth, 1-1/2-in. radius; 6 pellets per run										
3414	90.9	80.1	2.0	3.35	0.10	650	0.991	3.91	4.61	17.9
15	90.9	80.9	"	3.45	"	650	0.945	3.85	4.61	19.7
17	90.9	80.4	"	3.50	"	650	0.976	4.04	4.61	14.1
18	90.9	80.5	"	3.30	"	650	0.971	3.78	4.61	22.0
20	25.0	79.2	3.0	2.10	"	179	1.055	1.71	2.00	17.0
21	25.0	78.9	"	2.05	"	179	1.074	1.69	2.00	18.3
23	25.8	79.1	"	2.20	"	184	1.061	1.81	2.04	12.7
24	25.8	79.0	"	2.15	"	184	1.064	1.77	2.04	15.3
58	39.9	80.0	2.5	2.80	0.35	285	0.997	2.37	2.70	13.9
59	39.9	80.6	"	2.65	"	285	0.962	2.15	2.70	25.6
61	39.9	80.0	"	3.20	"	285	1.003	2.78	2.70	2.9
62	39.9	79.5	"	3.30	"	285	1.036	2.98	2.70	9.4
63	152.8	79.8	1.5	3.35	0.50	1093	1.015	4.68	6.47	38.2
64	153.8	79.4	"	3.40	"	1100	1.039	4.88	6.50	33.2
66	153.8	80.3	"	3.50	"	1100	0.982	4.78	6.50	37.0
67	155.8	81.6	"	4.60	"	1114	0.901	5.25	6.55	24.8
									Ave.	20.1
5/16-in. depth, 1/2-in. radius; 4 pellets per run										
3371	22.0	79.3	3.0	2.25	0.40	157	1.042	2.35	2.59	10.2
72	22.0	79.0	"	2.10	"	157	1.067	2.20	2.59	17.7
74	22.8	81.2	"	2.50	"	163	0.926	2.36	2.64	11.9
75	22.0	81.2	"	2.35	"	157	0.923	2.19	2.59	18.3
76	87.9	80.0	2.0	3.85	0.10	628	1.000	6.84	6.36	7.0
77	88.9	80.0	"	3.15	"	636	1.000	5.56	6.40	15.1
79	90.9	80.5	"	3.10	"	650	0.968	5.29	6.50	22.9
80	90.9	80.2	"	3.35	"	650	0.985	5.83	6.50	10.8

Table 5 G (Continued)

Run No.	Air, lb-mol / hr-ft^2	Temp °F	Δθ, min	-ΔW, mg	-ΔW$_o$ mg	D_pG/μ	C_T	Rate x 10^4 lb-mols/hr-ft^2 Exper.	Eqn 36	% Dev.
5/16-in. depth, 1/2-in. radius; 4 pellets per run										
3381	39.9	80.9	2.5	2.70	0.15	285	0.942	3.50	3.81	8.9
82	39.9	81.1	"	2.90	"	285	0.932	3.73	3.81	2.1
84	39.9	81.6	"	3.45	"	285	0.898	4.32	3.81	11.8
85	39.9	80.4	"	3.15	"	285	0.974	4.26	3.81	10.6
87	153.8	80.0	1.5	3.80	"	1100	0.997	8.85	9.15	3.4
88	153.8	80.0	"	3.20	"	1100	1.000	7.41	9.15	10.0
90	153.8	80.5	"	3.85	"	1100	0.971	8.73	9.15	4.8
91	151.9	80.4	"	3.75	"	1086	0.974	8.53	9.07	6.3
									Ave.	10.7
5/16-in. depth, 1-in. radius; 4 pellets per run										
3308	156.8	78.9	1.5	4.25	0.25	1121	1.074	10.45	9.06	13.3
09	157.8	79.6	"	4.50	"	1128	1.024	10.57	9.10	13.9
11	155.8	79.2	"	3.80	"	1114	1.052	9.07	9.02	0.6
14	88.9	77.5	2.0	3.25	"	636	1.182	6.47	6.26	3.2
15	88.9	79.8	"	3.80	"	636	1.012	6.55	6.26	4.4
17	88.9	79.8	"	3.75	"	636	1.015	6.47	6.26	3.2
18	86.9	79.3	"	3.90	"	621	1.049	6.98	6.17	11.6
19	25.0	79.5	3.0	2.65	0.25	179	1.036	3.03	2.75	9.2
20	25.8	79.4	"	2.75	"	184	1.042	3.16	2.81	11.1
22	26.6	79.5	"	3.00	"	190	1.033	3.45	2.86	17.1
23	26.6	79.6	"	3.15	"	190	1.024	3.61	2.86	20.8
25	43.1	80.3	2.5	2.75	0.20	308	0.979	3.65	3.92	7.4
26	43.1	79.7	"	2.85	"	308	1.018	3.94	3.92	0.5
28	43.1	79.9	"	3.15	"	308	1.009	4.35	3.92	9.9
29	43.1	79.5	"	3.05	"	308	1.036	4.30	3.92	8.8
									Ave.	9.0
5/16-in. depth, 1-1/2-in. radius; 6 pellets per run										
3431	24.3	78.1	3.0	1.95	0.10	174	1.130	1.69	1.96	16.0
32	24.3	79.8	"	1.90	"	174	1.012	1.47	1.96	33.3
33	24.3	80.8	"	2.10	"	174	0.950	1.54	1.96	27.3
35	24.3	80.5	"	2.10	"	174	0.965	1.56	1.96	25.6
43	86.9	78.7	2.0	2.90	0.20	621	1.086	3.56	4.48	25.8
44	86.9	79.0	"	2.90	"	621	1.033	3.39	4.48	32.2
46	86.9	78.7	"	3.10	"	621	1.086	3.83	4.48	17.0
47	86.9	78.8	"	3.00	"	621	1.083	3.68	4.48	21.7
48	39.1	79.1	2.5	2.60	0.15	280	1.058	2.52	2.66	5.6
49	39.1	79.1	"	2.55	"	280	1.061	2.48	2.66	7.3
51	38.3	79.4	"	2.50	"	274	1.042	2.38	2.63	10.5
52	38.3	79.2	"	2.70	"	274	1.055	2.62	2.63	0.4

Table 5G (Continued)

Run No.	Air, lb-mol/hr-ft^2	Temp °F	Δθ, min	-ΔW, mg	-ΔW$_o$ mg	D_pG/μ	C_T	Rate x 10^4 lb-mols/hr-ft^2 Exper.	Eqn 36	% Dev.
5/16-in. depth, 1-1/2-in. radius; 6 pellets per run										
3453	154.8	80.2	1.5	3.45	0.20	1107	0.988	5.20	6.53	21.7
54	155.8	80.4	"	3.10	"	1114	0.973	4.54	6.55	44.3
56	154.8	80.0	"	3.05	"	1107	1.003	4.64	6.53	40.7
57	156.8	79.9	"	3.10	"	1121	1.006	4.73	6.58	39.1
									Ave.	23.0
1/2-in. depth, 1-in. radius; 6 pellets per run										
2350	41.5	81.6	3.0	5.15	0.20	297	0.898	3.24	3.59	10.8
51	40.7	81.9	"	5.35	"	291	0.886	3.34	3.54	6.0
53	42.3	80.4	"	5.35	"	302	0.976	3.68	3.64	1.1
54	41.5	80.8	"	5.70	"	297	0.950	3.85	3.59	6.8
55	21.2	80.5	"	3.00	0.35	152	0.965	2.07	2.32	12.1
56	21.2	79.9	"	3.20	"	152	1.009	2.33	2.32	0.4
58	21.2	80.3	"	2.95	"	152	0.982	2.07	2.32	12.1
59	21.2	79.9	"	3.05	"	152	1.006	2.20	2.32	5.5
60	86.9	80.5	"	7.20	0.70	621	0.965	5.08	5.81	14.4
61	88.9	80.0	"	7.65	"	636	1.000	5.63	5.89	4.6
63	87.9	79.4	"	7.85	"	628	1.039	6.02	5.85	2.8
64	88.9	78.7	"	7.10	"	636	1.086	5.75	5.89	2.4
2445	154.8	79.4	1.5	4.85	0.15	1107	1.039	7.91	8.46	7.0
46	155.8	80.5	"	4.90	"	1114	0.971	7.47	8.48	13.5
48	153.8	80.3	"	4.65	"	1100	0.982	7.16	8.41	17.5
49	154.8	80.5	"	4.95	"	1107	0.965	7.50	8.46	12.8
									Ave.	8.1
1/2-in. depth, 2-in. radius; 6 pellets per run										
2310	161.7	80.6	3.0	5.70	0.45	1188	0.962	4.09	5.63	37.7
11	161.7	80.3	"	5.30	"	1188	0.982	3.86	5.63	45.9
13	159.7	79.9	"	5.25	"	1142	1.009	3.92	5.64	43.9
14	157.8	79.7	"	5.45	"	1128	1.018	4.12	5.60	35.9
15	21.2	81.0	"	2.35	"	152	0.934	1.55	1.52	1.9
16	21.2	81.1	"	2.25	"	152	0.932	1.47	1.52	3.4
18	21.2	80.4	"	1.90	"	152	0.974	1.26	1.52	20.6
19	21.2	80.4	"	1.95	"	152	0.974	1.30	1.52	16.9
20	41.5	79.3	"	3.15	0.60	297	1.045	2.16	2.35	8.8
21	40.7	80.2	"	3.15	"	291	0.985	2.03	2.32	14.3
23	42.3	80.5	"	3.15	"	302	0.968	2.00	2.38	19.0
24	41.5	80.4	"	3.30	"	297	0.976	2.14	2.35	9.8
25	86.9	79.7	"	4.30	"	621	1.021	3.06	3.80	24.2
26	86.9	78.9	"	4.15	"	621	1.074	3.09	3.80	23.0
28	86.9	80.4	"	4.30	"	621	0.976	2.93	3.80	30.0
29	87.9	80.3	"	3.90	"	628	0.979	2.62	3.82	45.8
									Ave.	23.8

Table 5

H. 2-inch orifice, 1/4-inch pellets

Run No.	Air, lb-mol/hr-ft^2	Temp °F	$\Delta\theta$, min	$-\Delta W$, mg	$-\Delta W_o$ mg	D_pG/μ	C_T	Rate x 10^4 lb-mols/hr-ft^2 Exper.	Eqn 36	% Dev.
1/8-in. depth, 0-in. radius; 1 pellet per run										
1322	79.0	79.7	5.0	3.80	0.50	1054	1.018	3.20	3.32	3.8
23	71.2	79.8	"	3.95	"	950	1.012	3.33	3.10	6.9
25	70.2	79.4	"	4.15	"	936	1.039	3.61	3.07	15.0
26	70.2	79.7	"	3.75	"	936	1.018	3.15	3.07	2.5
50	189.3	79.2	"	6.00	0.05	2525	1.055	5.98	5.85	2.2
51	187.3	78.7	"	5.05	"	2499	1.090	5.19	5.82	12.1
53	185.3	77.7	"	7.15	"	2472	1.065	7.20	5.78	8.1
54	186.3	79.0	"	6.70	"	2485	1.070	6.78	5.80	14.5
55	43.1	80.0	"	2.30	"	575	0.997	2.13	2.24	5.2
56	41.5	80.2	"	1.95	"	554	0.985	1.78	2.18	22.5
58	41.5	80.0	"	2.60	"	554	1.003	2.44	2.18	10.7
59	40.7	80.2	"	2.50	"	543	0.982	2.30	2.16	6.1
60	23.5	80.0	"	1.45	"	314	0.997	1.33	1.51	13.5
61	23.5	80.0	"	1.50	"	314	1.003	1.38	1.51	9.4
63	25.0	79.7	"	1.60	"	334	1.018	1.51	1.57	4.0
64	25.0	79.8	"	1.50	"	334	1.012	1.40	1.57	12.1
									Ave.	9.3
1/8-in. depth, 1/4-in. radius; 1 pellet per run										
1901	85.0	79.5	2.0	2.05	0.40	1134	1.033	4.05	3.48	14.1
02	85.9	79.2	"	1.50	"	1146	1.055	2.76	3.50	26.8
04	86.9	79.4	"	1.85	"	1159	1.042	3.60	3.53	1.9
05	87.9	79.5	"	1.75	"	1173	1.033	3.43	3.56	3.8
06	189.3	80.9	"	2.70	0.15	2525	0.942	5.72	5.85	2.3
07	189.3	81.3	"	2.70	"	2525	0.917	5.57	5.85	5.0
09	188.3	81.0	"	2.70	"	2512	0.940	5.72	5.83	1.9
10	189.3	81.5	"	2.80	"	2525	0.904	5.72	5.85	2.3
12	25.8	79.1	"	0.75	0.10	344	1.036	1.60	1.60	0.0
13	25.0	79.7	"	0.70	"	334	1.049	1.50	1.55	3.3
15	25.0	79.2	"	0.80	"	334	1.055	1.76	1.55	11.9
16	25.0	79.1	"	0.75	"	334	1.061	1.64	1.55	5.5
17	42.3	79.4	"	1.20	0.15	564	1.039	2.60	2.21	15.0
18	41.5	79.0	"	1.10	"	554	1.067	2.51	2.18	13.1
20	41.5	79.3	"	1.00	"	554	1.045	2.12	2.18	2.8
21	41.5	79.6	"	1.10	"	554	1.024	2.31	2.18	5.6
									Ave.	7.2

Table 5H (Continued)

Run No.	Air, lb-mol/hr-ft^2	Temp °F	Δθ, min	-ΔW, mg	-ΔW$_o$ mg	$\frac{D_p G}{\mu}$	C_T	Rate x 10^4 lb-mols/hr-ft^2 Exper.	Eqn 36	% Dev.
1/8-in. depth, 1/2-in. radius; 2 pellets per run										
1219	40.7	78.6	2.0	1.95	0.10	543	1.096	2.42	2.20	9.1
20	40.7	77.0	"	1.65	"	543	1.218	2.25	2.20	2.2
22	41.5	71.1	"	1.45	"	554	1.815	2.92	2.23	23.6
23	41.5	72.0	"	1.30	"	554	1.697	2.43	2.23	8.2
25	22.0	80.5	"	1.50	"	293	0.965	1.61	1.48	8.1
27	22.0	80.0	"	1.05	"	293	1.003	1.13	1.48	31.0
28	22.8	80.2	"	0.95	"	304	0.988	1.00	1.51	51.0
29	79.0	79.8	"	2.55	"	1054	1.012	2.95	3.39	14.9
30	79.0	79.2	"	2.50	"	1054	1.039	2.97	3.39	14.1
32	79.0	78.7	"	2.45	"	1054	1.090	3.05	3.39	11.1
33	79.0	78.6	"	2.25	"	1054	1.093	2.80	3.39	21.1
34	189.3	79.8	"	3.80	0.20	2525	1.015	4.35	5.98	37.5
35	189.3	80.1	"	3.70	"	2525	0.981	4.09	5.98	46.2
37	187.3	80.4	"	4.45	"	2499	0.974	4.93	5.94	20.5
38	187.3	80.8	"	4.40	"	2499	0.950	4.63	5.94	28.3
									Ave.	21.8
1/8-in. depth, 1-in. radius; 2 pellets per run										
1239	185.3	78.9	2.0	5.80	0.05	2472	1.077	7.37	8.60	16.7
40	185.3	79.1	"	6.25	"	2472	1.061	7.84	8.60	9.7
42	186.3	77.8	"	5.95	"	2485	1.154	8.11	8.63	6.4
43	187.3	79.6	"	6.30	"	2499	1.024	7.62	8.66	13.6
45	81.0	79.7	"	4.15	0.00	1081	1.018	5.03	5.02	0.2
46	83.0	79.5	"	3.40	"	1107	1.036	4.19	5.11	22.0
48	81.0	79.0	"	3.65	"	1081	1.064	4.62	5.02	8.7
49	79.0	79.0	"	3.40	"	1054	1.067	4.32	4.94	14.4
50	38.3	80.3	"	2.85	"	511	0.982	3.33	3.09	7.2
51	38.3	80.5	"	2.30	"	511	0.971	2.66	3.09	16.2
52	39.1	80.2	"	2.50	"	522	0.988	2.94	3.13	6.5
54	39.1	79.5	"	2.55	"	522	1.030	3.13	3.13	0.0
55	23.5	82.6	"	2.60	0.15	314	0.843	2.47	2.25	8.9
56	24.3	80.5	"	2.15	"	324	0.971	2.31	2.30	0.4
58	24.3	79.3	"	1.85	"	324	1.045	2.12	2.30	8.5
59	24.3	82.8	"	1.80	"	324	1.120	2.19	2.30	5.0
									Ave.	9.0
1/8-in. depth, 1-1/2-in. radius; 3 and 4* pellets per run										
1273	72.2	78.7	2.0	5.30	0.45	963	1.086	4.18	3.23	22.7
74	71.2	79.0	"	5.50	"	950	1.070	4.29	3.20	25.4
76	72.2	78.5	"	5.00	"	963	1.099	3.97	3.23	18.6
77	71.2	78.6	"	4.40	"	950	1.093	3.47	3.20	7.8

* Runs 1286-95

Table 5H (Continued)

Run No.	Air, lb-mol/hr-ft	Temp °F	Δθ, min	-ΔW, mg	-ΔW$_o$ mg	D_pG/μ	C_T	Rate x 10^4 lb-mols/hr-ft^2 Exper.	Rate x 10^4 lb-mols/hr-ft^2 Eqn 36	% Dev.
1/8-in. depth, 1-1/2-in. radius; 3 and 4* pellets per run										
1279	41.5	80.2	2.0	3.75	0.70	554	0.985	2.38	2.25	5.5
80	41.5	80.6	"	4.10	"	554	0.959	2.59	2.25	13.1
82	41.5	79.7	"	3.20	"	554	1.018	2.02	2.25	11.4
83	41.5	80.2	"	3.70	"	554	0.988	2.35	2.25	4.3
86	22.0	77.0	"	2.70	0.75	293	1.222	1.41	1.49	5.7
87	22.0	76.9	"	2.80	"	293	1.228	1.50	1.49	0.7
89	22.0	78.0	"	2.95	"	293	1.141	1.49	1.49	0.0
90	22.0	77.2	"	3.35	"	293	1.204	1.86	1.49	19.9
91	192.2	80.2	"	11.05	"	2564	0.985	6.04	6.10	1.0
92	192.2	79.5	"	11.25	"	2564	1.036	6.48	6.10	5.9
94	190.2	79.3	"	12.70	"	2537	1.049	7.47	6.06	18.9
95	188.3	79.4	"	12.05	"	2512	1.042	7.01	6.02	14.1
									Ave.	10.9
1/8-in. depth, 2-in. radius; 4 pellets per run										
1297	22.8	79.2	2.0	2.15	0.30	304	1.052	1.16	1.17	0.9
98	23.5	79.0	"	2.10	"	314	1.067	1.14	1.19	4.4
1300	24.3	78.5	"	2.45	"	324	1.106	1.42	1.22	14.1
01	24.3	79.0	"	2.15	"	324	1.070	1.18	1.22	3.4
02	41.5	79.9	"	3.25	0.45	554	1.006	1.68	1.73	3.0
03	41.5	80.1	"	4.20	"	554	0.991	2.22	1.73	22.1
05	41.5	80.3	"	3.43	"	554	0.979	2.04	1.73	15.2
06	41.5	80.5	"	3.20	"	554	0.968	1.58	1.73	9.5
07	77.1	80.5	"	4.60	"	1029	0.971	2.40	2.58	7.5
08	84.0	80.9	"	5.10	"	1121	0.942	2.61	2.73	4.6
10	84.0	78.8	"	5.70	"	1121	1.083	3.39	2.73	19.5
11	84.0	78.9	"	4.70	"	1121	1.077	2.73	2.73	0.0
12	183.4	79.9	"	9.15	0.65	2447	1.006	5.09	4.54	10.8
13	183.4	80.0	"	9.10	"	2447	1.000	5.03	4.54	12.1
15	181.4	79.6	"	8.70	"	2420	1.024	4.91	4.51	8.1
16	181.4	80.3	"	8.70	"	2420	0.982	4.71	4.51	4.2
									Ave.	8.7
3/8-in. depth, 0-in. radius; 1 pellet per run										
865	21.2	79.4	5.0	2.75	0.30	283	1.039	2.43	2.23	8.2
66	22.8	79.5	"	2.50	"	304	1.033	2.16	2.34	8.3
68	21.2	79.3	"	2.65	"	283	1.049	2.35	2.23	5.1
69	22.8	79.4	"	2.60	"	304	1.039	2.28	2.34	2.6
80	39.9	79.6	"	3.80	0.45	532	1.027	3.28	3.37	2.7
81	39.1	79.7	"	3.90	"	522	1.021	3.35	3.32	0.9
83	39.9	79.7	"	4.00	"	532	1.021	3.45	3.37	2.3
84	39.9	80.1	"	4.60	"	532	0.991	3.92	3.37	14.0

* Runs 1286-95

Table 5 H (Continued)

Run No.	Air, lb-mol/hr-ft^2	Temp °F	Δθ, min	-ΔW, mg	-ΔW$_o$ mg	$\frac{D_p G}{\mu}$	C_T	Rate x 10^4 lb-mols/hr-ft^2 Exper.	Eqn 36	% Dev.
3/8-in. depth, 0-in. radius; 1 pellet per run										
885	82.0	81.5	5.0	6.70	0.40	1094	0.909	5.46	5.38	1.5
86	86.9	81.3	"	6.10	"	1159	0.920	4.99	5.59	12.0
88	85.9	77.1	"	5.20	"	1146	1.211	5.54	5.55	0.2
89	88.9	81.0	"	7.10	"	1186	0.940	6.00	5.67	5.5
90	196.1	84.2	"	11.10	0.30	2616	0.761	7.83	9.49	21.2
91	195.2	85.5	"	12.20	"	2604	0.699	7.93	9.45	19.2
93	193.2	83.7	"	11.75	"	2577	0.785	8.57	9.39	9.6
94	195.2	86.1	"	12.70	"	2604	0.673	7.96	9.45	18.7
									Ave.	8.3
3/8-in. depth, 1/2-in. radius; 2 pellets per run										
1875	75.1	78.2	2.0	3.70	0.10	1002	1.127	4.84	4.98	2.9
76	84.0	78.4	"	4.00	"	1121	1.113	5.17	5.36	3.7
78	83.0	79.0	"	3.90	"	1107	1.070	4.85	5.32	9.7
79	85.0	78.9	"	4.35	"	1134	1.077	5.45	5.40	0.9
95	40.7	79.9	"	3.40	0.10	543	1.006	3.95	3.35	15.2
96	39.9	80.0	"	3.45	"	532	0.997	3.98	3.30	17.1
98	40.7	79.7	"	3.10	"	543	1.018	3.63	3.35	7.7
99	39.9	80.3	"	3.05	"	532	0.982	3.45	3.30	4.3
1927	185.3	80.3	"	8.85	0.50	2472	0.979	9.73	8.96	7.9
28	185.3	80.3	"	8.85	"	2472	0.982	9.77	8.96	8.3
30	185.3	80.0	"	9.05	"	2472	1.000	10.18	8.96	12.0
31	186.3	80.7	"	8.70	"	2485	0.953	9.30	8.99	3.3
38	24.3	78.9	"	2.90	1.10	324	1.074	2.30	2.39	3.9
39	24.3	78.7	"	2.95	"	324	1.086	2.39	2.39	0.0
41	24.3	78.3	"	2.95	"	324	1.120	2.47	2.39	3.2
42	24.3	78.1	"	2.95	"	324	1.141	2.51	2.39	4.8
									Ave.	6.6
3/8-in. depth, 1-in. radius; 2 pellets per run										
905	24.3	78.3	2.0	2.10	0.50	324	1.120	2.13	2.12	0.5
06	24.3	78.9	"	2.25	"	324	1.074	2.24	2.12	5.4
08	24.3	78.6	"	2.40	"	324	1.093	2.48	2.12	14.5
09	24.3	79.1	"	2.60	"	324	1.061	2.66	2.12	20.3
10	38.3	80.1	"	1.75	-0.95	511	0.994	3.19	2.85	10.7
11	37.5	78.9	"	1.45	"	500	1.077	3.07	2.81	8.5
13	37.5	78.2	"	1.10	"	500	1.123	2.74	2.81	2.6
14	37.5	79.4	"	1.20	"	500	1.042	2.67	2.81	5.2
15	80.0	80.0	"	3.70	"	1067	1.000	5.54	4.60	17.0
16	81.0	79.9	"	2.95	"	1081	1.003	4.66	4.64	0.4
18	81.0	79.7	"	2.90	"	1081	1.018	4.67	4.64	0.6
19	81.0	79.7	"	2.90	"	1081	1.021	4.68	4.64	0.8

Table 5H (Continued)

Run No.	Air, lb-mol/hr-ft^2	Temp °F	Δθ, min	-ΔW, mg	-ΔW$_o$ mg	D_pG/μ	C_T	Rate x 10^4 lb-mols/hr-ft^2 Exper.	Eqn 36	% Dev.
3/8-in. depth, 1-in. radius, 2 pellets per run										
920	196.1	79.7	2.0	6.90	-1.40	2616	1.018	10.06	8.24	18.1
21	197.1	79.8	"	9.95	"	2629	1.012	13.68	8.26	39.6
23	197.1	80.0	"	8.70	"	2629	1.003	12.06	8.26	31.5
24	195.2	80.3	"	6.05	"	2604	0.982	8.72	8.21	5.8
									Ave.	11.3
3/8-in. depth, 1-1/2-in. radius; 2* and 3 pellets per run										
955	23.5	75.6	2.0	2.75	1.70	314	1.335	1.67	1.52	9.0
56	21.2	77.0	"	2.85	"	283	1.218	1.67	1.43	14.4
58	21.2	76.5	"	3.15	2.20	283	1.262	1.43	1.43	0.0
59	21.2	76.9	"	3.05	"	283	1.225	1.24	1.43	15.3
60	39.9	80.3	"	3.90	0.85	532	0.982	2.38	2.15	9.7
61	39.9	80.3	"	3.55	"	532	0.982	2.10	2.15	2.4
63	39.9	80.1	"	4.30	"	532	0.994	2.72	2.15	21.0
64	40.7	80.0	"	4.90	"	543	0.997	2.41	2.18	9.5
65	79.0	79.3	"	6.85	1.85	1054	1.049	4.17	3.35	19.7
66	79.0	78.8	"	5.20	"	1054	1.080	2.90	3.35	15.5
68	79.0	78.3	"	5.55	"	1054	1.120	3.29	3.35	1.8
69	197.1	79.5	"	10.70	"	2629	1.030	7.24	6.07	16.2
70	82.0	79.1	"	4.75	0.50	1094	1.058	3.57	3.43	3.9
71	197.1	80.5	"	10.00	"	2629	0.971	7.32	6.07	17.1
73	199.1	80.2	"	8.20	"	2656	0.985	6.02	6.12	1.7
74	197.1	80.5	"	7.75	"	2629	0.971	5.59	6.07	8.6
									Ave.	10.4
3/8-in. depth, 2-in. radius; 4 pellets per run										
1015	70.2	80.6	2.0	5.65	0.90	936	0.962	2.72	2.59	4.8
16	70.2	80.8	"	5.35	"	936	0.947	2.51	2.59	3.2
18	71.2	80.3	"	5.50	"	950	0.982	2.69	2.62	2.6
20	195.2	83.5	"	10.50	0.40	2604	0.795	4.78	5.04	5.4
21	194.2	83.1	"	9.90	"	2591	0.818	4.63	5.02	8.4
23	193.2	82.5	"	11.10	"	2577	0.853	5.44	5.01	7.9
24	189.3	83.2	"	10.00	"	2525	0.811	4.64	4.94	6.5
45	40.7	79.1	"	3.40	0.90	543	1.058	1.58	1.82	15.2
46	39.9	79.8	"	4.05	"	532	1.012	1.90	1.80	5.3
48	40.7	79.0	"	4.40	"	543	1.067	2.22	1.82	18.0
49	40.7	79.5	"	4.10	"	543	1.036	1.98	1.82	8.1
50	22.8	75.5	"	2.90	"	304	1.347	1.60	1.25	21.9
51	22.8	75.3	"	2.45	"	304	1.355	1.25	1.25	0.0
53	22.8	75.9	"	2.50	"	304	1.307	1.24	1.25	0.8
54	23.5	76.0	"	2.40	"	314	1.303	1.16	1.27	9.5
									Ave.	7.8

* Runs 955-59

Table 5 H (Continued)

Run No.	Air, lb-mol/hr-ft^2	Temp °F	Δθ, min	-ΔW, mg	-ΔW$_o$ mg	D_pG/μ	C_T	Rate x 10^4 lb-mols/hr-ft^2 Exper.	Eqn 36	% Dev.
5/8-in. depth, 0-in. radius; 1 pellet per run										
1502	43.1	80.5	2.0	1.20	0.0	575	0.971	2.79	3.38	21.1
03	43.1	80.6	"	1.50	"	575	0.959	3.43	3.38	1.5
05	42.3	80.6	"	1.35	"	564	0.959	3.07	3.34	8.8
06	42.3	80.6	"	1.55	"	564	0.959	3.55	3.34	5.9
30	25.8	76.0	5.0	1.95	0.10	344	1.299	2.29	2.42	5.7
31	25.8	78.4	"	2.20	"	344	1.109	2.22	2.42	9.0
33	25.8	77.9	"	2.40	"	344	1.147	2.52	2.42	4.0
34	26.6	78.1	"	2.40	"	354	1.134	2.49	2.47	0.8
2009	185.3	80.4	"	10.35	-0.05	2472	0.976	9.67	8.72	9.8
10	186.3	80.8	"	9.75	"	2485	0.950	8.87	8.75	1.4
12	185.3	79.2	"	9.15	"	2472	1.055	9.25	8.72	5.7
13	186.3	79.3	"	9.00	"	2485	1.045	9.01	8.75	2.9
2168	79.0	80.3	"	5.30	"	1054	0.982	5.00	5.01	0.2
69	81.0	80.6	"	6.00	"	1081	0.959	5.53	5.09	8.0
71	84.0	80.5	"	5.25	"	1121	0.968	4.89	5.21	6.5
72	84.0	80.9	"	5.60	"	1121	0.942	5.07	5.21	2.8
									Ave.	5.9
5/8-in. depth, 1/2-in. radius; 2 pellets per run										
1971	41.5	79.3	2.0	3.10	0.30	554	1.049	3.50	3.25	7.1
74	41.5	80.0	"	2.95	"	554	1.000	3.16	3.25	2.8
75	40.7	80.1	"	3.20	"	543	0.994	3.43	3.21	6.4
76	24.3	79.2	"	1.75	0.20	324	1.055	1.95	2.30	17.9
79	24.3	78.8	"	2.05	"	324	1.080	2.38	2.30	3.4
80	24.3	79.1	"	2.05	"	324	1.058	2.33	2.30	1.3
82	85.9	78.7	"	4.80	0.30	1146	1.086	5.82	5.22	10.3
83	85.0	78.5	"	4.40	"	1134	1.103	5.38	5.19	3.5
85	85.0	78.4	"	4.45	"	1134	1.113	5.50	5.19	5.6
86	85.0	78.8	"	4.45	"	1134	1.080	5.34	5.19	2.8
87	185.3	79.7	"	7.65	0.25	2472	1.018	8.97	8.60	4.1
88	185.3	80.2	"	7.70	"	2472	0.988	8.77	8.60	1.9
90	183.4	80.2	"	7.85	"	2447	0.988	8.94	8.54	4.5
91	182.4	79.6	"	6.95	"	2433	1.024	8.17	8.52	4.3
									Ave.	5.4
5/8-in. depth, 1-in. radius; 2* and 4 pellets per run										
1370	39.9	80.4	2.0	3.45	0.50	532	0.974	3.42	2.77	19.0
71	39.9	81.0	"	3.45	"	532	0.937	3.29	2.77	15.8
73	39.9	80.0	"	2.90	"	532	1.000	2.86	2.77	3.1
74	39.9	80.5	"	3.00	"	532	0.965	2.87	2.77	3.5
1998	185.3	78.1	"	13.40	0.55	2472	1.134	8.68	7.40	14.7
99	185.3	80.5	"	15.60	"	2472	0.965	8.65	7.40	14.5
2001	185.3	80.4	"	14.60	"	2472	0.976	8.16	7.40	9.3
02	185.3	80.5	"	13.45	"	2472	0.971	7.46	7.40	0.8

* Runs 1370-74

Table 5H (Continued)

Run No.	Air, lb-mol/hr-ft^2	Temp °F	Δθ, min	-ΔW, mg	-ΔW$_o$ mg	D_pG/μ	C_T	Rate x 10^4 lb-mols/hr-ft^2 Exper.	Eqn 36	% Dev.
5/8-in. depth, 1-in. radius; 2* and 4 pellets per run										
2158	22.0	80.3	2.0	3.45	0.80	293	0.979	1.54	1.85	20.1
59	22.0	80.5	"	3.85	"	293	0.965	1.75	1.85	5.7
61	22.0	80.7	"	3.85	"	293	0.956	1.74	1.85	6.3
62	22.0	80.7	"	3.35	"	293	0.956	1.45	1.85	27.6
63	75.1	79.9	"	8.20	"	1002	1.006	4.43	4.11	7.2
64	84.0	80.0	"	7.50	"	1121	1.003	4.00	4.42	10.5
66	83.0	79.7	"	7.45	"	1107	1.018	4.03	4.39	8.9
67	83.0	79.7	"	7.40	"	1107	1.018	4.00	4.39	9.8
									Ave.	11.1
5/8-in. depth, 1-1/2-in. radius; 3 pellets per run										
1149	82.0	80.2	2.0	4.80	0.50	1094	0.985	3.37	3.40	0.9
50	76.1	80.4	"	4.50	"	1015	0.974	3.10	3.24	4.5
52	76.1	79.6	"	4.20	"	1015	1.027	3.02	3.24	7.3
53	75.1	80.3	"	5.00	"	1002	0.982	3.51	3.21	8.5
55	197.1	79.2	"	6.75	0.20	2629	1.055	5.49	6.01	9.5
56	197.1	79.5	"	6.90	"	2629	1.036	5.51	6.01	9.1
58	199.1	79.2	"	6.50	"	2656	1.052	5.26	6.05	15.0
59	201.1	79.5	"	6.70	"	2683	1.033	5.32	6.09	14.5
60	24.3	78.2	"	2.45	0.80	324	1.123	1.47	1.54	4.8
61	25.8	78.4	"	2.30	"	344	1.113	1.33	1.60	20.3
63	23.5	78.5	"	2.15	"	314	1.103	1.18	1.51	28.0
64	24.3	78.6	"	2.30	"	324	1.096	1.30	1.54	18.5
65	40.7	79.0	"	3.70	1.00	543	1.064	2.28	2.16	5.3
66	38.3	78.5	"	3.80	"	511	1.099	2.45	2.07	15.5
68	41.5	77.6	"	3.15	"	554	1.171	2.00	2.18	9.0
69	41.5	77.8	"	3.30	"	554	1.157	2.11	2.18	3.3
									Ave.	10.9
5/8-in. depth, 2-in. radius; 4 pellets per run										
4086	38.3	78.5	2.0	3.70	1.00	511	1.106	1.78	1.83	2.8
87	38.3	78.6	"	3.35	"	511	1.096	1.54	1.83	18.8
89	38.3	78.4	"	3.95	"	511	1.110	1.95	1.83	6.2
90	37.5	78.6	"	3.60	"	500	1.093	1.69	1.81	7.1
91	81.0	80.4	"	6.60	"	1081	0.976	3.26	2.99	8.3
92	74.1	80.6	"	5.60	"	988	0.962	2.64	2.82	6.8
94	75.1	80.3	"	5.55	"	1002	0.982	2.66	2.84	6.8
95	74.1	80.6	"	6.30	"	988	0.962	3.04	2.82	7.2
96	199.1	78.8	"	9.00	0.95	2653	1.083	5.19	5.34	2.9
97	196.1	77.9	"	8.55	"	2616	1.150	5.20	5.30	1.9
99	197.1	79.1	"	10.20	"	2629	1.058	5.83	5.32	8.7
1100	196.1	78.9	"	8.55	"	2616	1.077	4.88	5.30	10.7
2153	21.2	79.6	"	2.70	0.60	283	1.024	1.28	1.25	2.3
54	22.0	79.2	"	2.60	"	293	1.052	1.25	1.28	2.4
56	22.0	79.2	"	2.45	"	293	1.052	1.16	1.28	10.3
									Ave.	6.9

* Runs 1370-74

Table 5H (Continued)

Run No.	Air, lb-mol/hr-ft^2	Temp °F	Δθ, min	-ΔW, mg	-ΔW$_o$ mg	D_pG/μ	C_T	Rate x 10^4 lb-mols/hr-ft^2 Exper.	Rate x 10^4 lb-mols/hr-ft^2 Eqn 36	% Dev.
1-in. depth, 1/2-in. radius; 2 pellets per run										
1803	27.3	79.3	2.0	1.75	0.20	364	1.049	1.94	2.04	5.2
04	27.3	79.7	"	1.75	"	364	1.018	1.88	2.04	8.5
06	27.3	80.1	"	1.60	"	364	0.994	1.66	2.04	22.9
07	27.3	80.1	"	1.95	"	364	0.994	2.07	2.04	1.4
08	193.2	80.8	"	7.00	"	2577	0.950	7.69	7.29	5.2
09	191.2	80.6	"	5.90	"	2551	0.959	6.51	7.24	11.2
11	189.3	80.2	"	6.50	"	2525	0.988	7.41	7.20	2.8
12	191.2	79.6	"	6.00	"	2551	1.024	7.07	7.24	2.4
14	43.1	79.4	"	2.40	0.15	575	1.042	2.79	2.75	1.4
15	43.1	79.0	"	2.35	"	575	1.070	2.80	2.75	1.8
17	43.1	78.5	"	2.30	"	575	1.099	2.81	2.75	2.1
18	43.1	78.6	"	2.65	"	575	1.093	3.25	2.75	15.4
19	87.9	78.1	"	3.35	0.00	1173	1.130	4.51	4.37	3.1
20	88.9	78.0	"	3.60	"	1186	1.144	4.91	4.40	10.4
22	88.9	79.9	"	3.55	"	1186	1.009	4.26	4.40	3.3
23	90.9	80.1	"	3.65	"	1213	0.994	4.32	4.47	3.5
									Ave.	6.3
1-in. depth, 1-in. radius; 3 pellets per run										
1602	27.3	79.0	2.0	2.70	0.25	364	1.067	2.07	1.92	7.2
03	27.3	79.0	"	2.55	"	364	1.070	1.95	1.92	1.5
05	28.1	79.0	"	2.40	"	375	1.064	1.82	1.96	7.7
06	28.1	79.1	"	2.65	"	375	1.061	2.02	1.96	3.0
07	181.4	79.6	"	8.05	"	2420	1.024	6.34	6.58	3.8
08	181.4	79.5	"	8.20	"	2420	1.033	6.52	6.58	0.9
11	181.4	78.8	"	7.50	"	2420	1.080	6.22	6.58	5.8
21	86.9	80.2	"	5.55	0.45	1159	0.988	4.00	4.08	2.0
22	86.9	80.5	"	5.40	"	1159	0.971	3.82	4.08	5.2
24	87.9	79.7	"	5.55	"	1173	1.018	4.12	4.11	0.2
25	86.9	79.0	"	5.60	"	1159	1.067	4.37	4.08	6.6
26	39.9	79.7	"	3.60	0.80	532	1.018	2.26	2.46	9.3
27	39.9	80.1	"	3.90	"	532	0.991	2.44	2.46	0.8
29	39.9	80.0	"	3.95	"	532	1.000	2.50	2.46	1.6
30	39.9	79.8	"	3.60	"	532	1.012	2.25	2.46	9.3
									Ave.	4.3
1-in. depth, 1-1/2-in. radius; 4 pellets per run										
1693	187.3	80.3	2.0	9.75	0.45	2499	0.982	5.44	5.82	7.0
94	187.3	82.0	"	10.25	"	2499	0.878	5.12	5.82	13.6
96	187.3	79.8	"	9.80	"	2499	1.012	5.63	5.82	3.4
97	187.3	79.9	"	8.80	"	2499	1.006	5.00	5.82	16.4

Table 5H (Continued)

Run No.	Air, lb-mol/hr-ft	Temp °F	Δθ, min	-ΔW, mg	-ΔW$_o$ mg	D_pG/μ	C_T	Rate x 10^4 lb-mols/hr-ft^2 Exper.	Rate x 10^4 lb-mols/hr-ft^2 Eqn 36	% Dev.
1-in. depth, 1-1/2-in. radius; 4 pellets per run										
1698	86.9	79.2	2.0	5.55	0.30	1159	1.055	3.30	3.53	7.0
99	85.9	79.1	"	5.50	"	1146	1.061	3.29	3.50	6.4
1701	84.0	78.9	"	5.60	"	1121	1.074	3.39	3.45	1.8
02	84.0	78.7	"	5.35	"	1121	1.086	3.26	3.45	5.8
04	24.3	79.2	"	3.05	0.75	324	1.055	1.45	1.54	6.2
05	25.8	79.1	"	3.15	"	344	1.058	1.51	1.60	6.0
07	25.8	78.8	"	2.90	"	344	1.080	1.38	1.60	15.9
08	26.6	79.2	"	2.60	0.50	354	1.052	1.32	1.64	24.2
09	41.5	79.8	"	4.15	"	554	1.015	2.20	2.18	0.9
10	41.5	79.9	"	4.05	"	554	1.006	2.13	2.18	2.3
12	41.5	79.4	"	4.30	"	554	1.042	2.36	2.18	7.6
13	41.5	79.5	"	4.10	"	554	1.030	2.21	2.18	1.9
									Ave.	7.9
1-in. depth, 2-in. radius; 4 pellets per run										
1558	39.1	81.0	2.0	4.00	0.85	522	0.935	1.76	1.97	11.9
59	38.3	81.0	"	3.85	"	511	0.935	1.67	1.94	16.2
61	38.3	80.8	"	4.15	"	511	0.950	1.87	1.94	3.7
62	39.1	80.9	"	4.30	"	522	0.942	1.94	1.97	1.5
63	23.5	80.7	"	2.85	0.70	314	0.953	1.22	1.41	15.6
64	24.3	80.8	"	2.85	"	324	0.950	1.21	1.45	19.8
66	23.5	80.7	"	2.85	"	314	0.956	1.23	1.41	14.6
67	24.3	80.8	"	2.90	"	324	0.947	1.24	1.45	16.9
69	83.0	80.3	"	6.00	0.65	1107	0.979	3.12	3.21	2.8
70	83.0	80.3	"	5.75	"	1107	0.982	2.98	3.21	7.7
72	83.0	80.0	"	5.75	"	1107	0.997	3.03	3.21	5.9
73	83.0	80.0	"	5.70	"	1107	0.997	3.00	3.21	7.0
74	187.3	80.2	"	8.80	0.40	2499	0.985	4.92	5.45	10.8
75	185.3	80.1	"	9.10	"	2472	0.994	5.15	5.41	5.0
77	185.3	80.6	"	8.85	"	2472	0.962	4.84	5.41	11.8
78	185.3	80.4	"	9.65	"	2472	0.976	5.38	5.41	0.6
									Ave.	9.5
2-in. depth, 2-in. radius; 4 pellets per run										
1737	190.2	75.0	2.0	7.90	0.35	2537	1.384	6.22	5.88	5.5
38	190.2	76.3	"	8.50	"	2537	1.273	6.18	5.88	4.9
40	189.3	78.2	"	8.80	"	2525	1.123	5.65	5.86	3.7
41	189.3	79.5	"	9.25	"	2525	1.030	5.46	5.86	7.3
42	85.9	77.9	"	5.45	0.50	1146	1.147	3.38	3.50	3.6
43	86.9	76.9	"	4.95	"	1159	1.225	3.25	3.53	8.6
45	85.0	77.6	"	5.10	"	1134	1.171	3.21	3.48	8.4
46	84.0	79.0	"	5.25	"	1121	1.064	3.01	3.45	14.6

Table 5 H (Continued)

Run No.	Air, lb-mol / hr-ft^2	Temp °F	$\Delta\theta$, min	$-\Delta W$, mg	$-\Delta W_o$ mg	$\frac{D_p G}{\mu}$	C_T	Rate x 10^4 lb-mols/hr-ft^2 Exper.	Rate x 10^4 lb-mols/hr-ft^2 Eqn 36	% Dev.
1748	22.8	77.3	2.0	2.15	0.25	304	1.193	1.35	1.48	13.3
49	22.8	77.6	"	2.25	"	304	1.168	1.39	1.48	6.5
51	22.8	77.6	"	1.85	"	304	1.168	1.11	1.48	33.3
52	22.8	78.1	"	2.30	"	304	1.130	1.38	1.48	7.2
53	58.2	80.6	"	5.30	0.50	776	0.959	2.74	2.72	0.7
54	40.7	80.3	"	4.00	"	543	0.982	2.05	2.16	4.4
56	40.7	79.5	"	4.15	"	543	1.033	2.25	2.16	4.0
57	40.7	79.8	"	4.15	"	543	1.012	2.20	2.16	1.8
									Ave.	8.0

APPENDIX B

PELLET DIMENSIONS AND PROPERTIES

APPENDIX B

Pellet Dimensions and Bed Porosity

I. Glass Bead Dimensions

(Sample beads measured three times, orthogonally, to the nearest 0.001-inch.)

Table 6. 1/8-inch pellets

Min.	Mid.	Max.	Ave.	Min.	Mid.	Max.	Ave.
.128	.138	.142	.136	.130	.136	.138	.135
.117	.124	.125	.122	.123	.129	.133	.128
.133	.138	.138	.136	.128	.139	.139	.135
.126	.134	.134	.131	.123	.130	.131	.128
.129	.138	.138	.135	.123	.131	.132	.129
.123	.129	.131	.128	.126	.139	.140	.135
.123	.128	.130	.127	.128	.135	.136	.133
.128	.134	.134	.132	.129	.131	.135	.132
.130	.135	.136	.134	.128	.131	.134	.131
.113	.124	.126	.121	.127	.133	.133	.131
.128	.137	.138	.134	.125	.133	.134	.131
.131	.136	.137	.135	.120	.124	.129	.124
.122	.132	.133	.129	.121	.129	.132	.127
.127	.136	.136	.133	.120	.130	.131	.127
.126	.133	.134	.131	.131	.132	.137	.133
.122	.131	.131	.128	.110	.122	.123	.118
.124	.137	.137	.133	.124	.132	.133	.130
.109	.121	.121	.117	.128	.131	.138	.132
.122	.135	.136	.131	.126	.134	.137	.132
.127	.129	.129	.128	.117	.124	.126	.122
.122	.129	.131	.127	.122	.135	.135	.131
.126	.129	.130	.128	.120	.129	.133	.127
.119	.124	.126	.123	.119	.124	.127	.123
.118	.128	.130	.125	.122	.135	.138	.132
.125	.134	.136	.132	.122	.126	.128	.125
.136	.136	.143	.138	.128	.132	.135	.132
.128	.135	.138	.134	.116	.124	.124	.121
.121	.130	.133	.128	.118	.127	.129	.125
.125	.131	.133	.130	.118	.125	.126	.123
.130	.135	.135	.133	.129	.139	.139	.136
			Averages				
.125	.132	.133	.130	.123	.131	.133	.129
	Overall Averages:		.124	.131	.133	.1295	

Table 7. 1/4-inch pellets

Min.	Mid.	Max.	Ave.	Min.	Mid.	Max.	Ave.
.241	.241	.250	.244	.234	.244	.248	.242
.234	.237	.240	.237	.233	.239	.243	.238
.239	.240	.241	.240	.237	.237	.246	.240
.243	.243	.245	.244	.238	.239	.251	.243
.236	.236	.238	.237	.242	.248	.250	.247
.232	.235	.241	.236	.238	.242	.243	.241
.229	.234	.236	.233	.224	.236	.237	.232
.234	.242	.243	.240	.232	.240	.253	.242
.238	.239	.244	.240	.239	.241	.244	.241
.232	.243	.255	.243	.229	.244	.247	.240
.241	.244	.253	.246	.233	.239	.244	.239
.239	.240	.240	.240	.240	.244	.244	.243
.239	.245	.255	.246	.234	.234	.238	.235
.242	.245	.246	.244	.242	.243	.244	.243
.237	.241	.244	.241	.222	.239	.243	.235
.232	.234	.243	.236	.240	.243	.247	.243
.237	.239	.249	.242	.239	.243	.247	.243
.241	.243	.245	.243	.228	.235	.239	.234
.230	.236	.251	.239	.240	.247	.252	.246
.239	.244	.246	.243	.235	.237	.240	.237
.240	.245	.249	.245	.244	.244	.250	.246
.240	.241	.242	.241	.227	.234	.241	.234
.239	.240	.240	.240	.235	.241	.244	.240
.243	.245	.249	.246	.237	.238	.240	.238
.238	.239	.239	.239	.238	.240	.240	.239
.237	.238	.243	.239	.240	.241	.247	.243
.240	.243	.243	.242	.231	.239	.240	.237
.238	.241	.245	.241	.238	.240	.244	.240
.230	.240	.243	.238	.238	.243	.247	.243
.238	.243	.243	.241	.235	.238	.239	.237
.237	.241	.245	.241	.235	.240	.244	.240

Overall Averages: .236 .240 .245 .2405

Table 8. 1/2-inch pellets

Min.	Mid.	Max.	Ave.	Min.	Mid.	Max.	Ave.
.564	.565	.568	.566	.569	.569	.571	.570
.556	.557	.557	.557	.538	.539	.540	.539
.553	.554	.554	.554	.556	.558	.559	.558
.554	.555	.555	.555	.554	.555	.559	.556
.554	.557	.557	.556	.546	.548	.548	.547
.591	.593	.596	.593	.565	.566	.567	.566
.566	.567	.568	.567	.563	.564	.566	.564
.556	.559	.560	.558	.600	.601	.604	.602
.563	.564	.564	.564	.563	.563	.565	.564
.554	.556	.557	.556	.579	.579	.580	.579
.568	.572	.573	.571	.580	.581	.582	.581
.588	.589	.592	.590	.601	.602	.602	.602
.552	.552	.553	.552	.552	.553	.553	.553
.564	.566	.566	.565	.531	.531	.531	.531
.559	.559	.560	.559	.561	.561	.562	.561
.547	.550	.553	.550	.571	.572	.573	.572
.541	.544	.544	.543	.609	.609	.609	.609
.550	.550	.550	.550	.560	.561	.554	.558
.558	.559	.559	.559	.580	.580	.582	.581
.563	.565	.567	.565	.573	.573	.575	.574
.579	.582	.583	.581	.586	.588	.589	.588
.587	.589	.592	.589	.564	.564	.565	.564
.552	.552	.553	.552	.559	.560	.560	.560
.561	.561	.564	.562	.547	.548	.548	.548
.546	.550	.553	.550	.562	.562	.564	.563
.568	.570	.571	.570	.557	.559	.560	.559
.557	.560	.561	.559	.584	.586	.588	.586
.555	.555	.555	.555	.557	.558	.558	.558
.554	.554	.556	.555	.572	.574	.575	.574
.556	.556	.556	.556	.592	.593	.595	.593
			Averages				
.561	.562	.563	.562	.568	.569	.569	.568
		Overall Averages:		.564	.565	.566	.5652

II. p-Dibromobenzene Pellet Dimensions

1/8-inch pellets

200 pellets displace 4.02 cc of water;

Volume per pellet = 0.0201 cc;

D_p = 0.3375 cm. = 0.1328 in.

(Weight of 200 pellets = 8.7234 gm;

Specific gravity = 2.17 vs 2.26 for pure compound)

As a check, ten sample pellets were measured three times, orthogonally, to the nearest 0.001-inch:

Min.	Mid.	Max.	Ave.
.127	.131	.132	.130
.127	.132	.132	.130
.125	.130	.132	.129
.125	.130	.131	.129
.121	.131	.133	.128
.127	.131	.132	.130
.124	.131	.131	.129
.127	.132	.132	.130
.124	.131	.133	.129
.126	.132	.132	.130

Average diameter = 0.129 in. = 0.3275 cm.

Pellet surface area based on water displacement data,

A_p = 0.358 cm^2.

1/4-inch pellets

20 pellets displace 2.12 cc of water;

Volume per pellet = 0.106 cc;

D_p = 0.588 cm. = 0.2315 in.

(Weight of 20 pellets = 4.6489 gms;

Specific gravity = 2.19 vs 2.26 for pure compound)

Check measurements:

Min.	Mid.	Max.	Ave.
.227	.230	.234	.230
.231	.233	.233	.232
.228	.230	.233	.230
.230	.231	.233	.231
.228	.228	.232	.229
.231	.234	.237	.234
.227	.230	.233	.230
.228	.231	.234	.231
.230	.230	.232	.231
.225	.228	.230	.228

Average diameter = 0.231 in. = 0.587 cm.

Pellet surface area based on water displacement data,

$$A_p = 1.086 \text{ cm}^2.$$

1/2-inch pellets

20 pellets displace 30.5 cc of water;

Volume per pellet = 1.525 cc;

$D_p = 1.428$ cm. = 0.562 in.

(Weight of 20 pellets = 58.8997 gms;

Specific gravity = 1.93 vs 2.26 for pure compound)

Check measurements:

Min.	Mid.	Max.	Ave.
.556	.559	.563	.559
.559	.563	.565	.562
.561	.565	.565	.564
.562	.563	.567	.564
.555	.556	.556	.556
.561	.563	.566	.563
.561	.563	.563	.562
.561	.562	.564	.562
.555	.558	.564	.559
.556	.558	.563	.559

Average diameter = 0.561 in. = 1.425 cm.

Pellet surface area based on water displacement data,

$$A_p = 6.406 \text{ cm}^2.$$

III. Bed Porosity

1/8-inch pellets

$D_p = 0.1295$ in.; $V_p = 0.001137$ in.$^3 = 6.58 \times 10^{-7}$ ft.^{3}

400 pellets weigh 17.6327 gms = 0.0389 lbs.

$$\text{Pellet density} = \frac{0.0389}{(400)(6.58 \times 10^{-7})} = 147.8 \text{ lbs/ft}$$

Weight of pellets in bed = 4.00 lbs.

$$\text{Total pellet volume} = \frac{4.0}{147.8} = 0.02705 \text{ ft}^3.$$

Bed volume $= (\pi)(2)^2(6.125) = 76.95$ in.$^3 = 0.04455$ ft.^{3}

$$\therefore \text{Porosity} = \frac{0.04455 - 0.02705}{0.04455} \times 100$$

$$= 39.3 \text{ percent}$$

Alternate measurement by filling void space with water:

Void volume = 455.5 cc = 27.80 in.$^3 = 0.0161$ ft.^{3}

$$\therefore \text{Porosity} = \frac{0.0161}{0.04455} \times 100 = 36.15 \text{ per cent.}$$

1/4-inch pellets

$D_p = 0.2405$ in.; $V_p = 0.00728$ in.$^3 = 4.215 \times 10^{-6}$ ft.^{3}

200 pellets weigh 60.7331 gms = 0.1339 lbs.

$$\text{Pellet density} = \frac{0.1339}{(200)(4.215 \times 10^{-6})} = 158.8 \text{ lbs/ft}^3$$

Weight of pellets in bed = 4.46 lbs.

$$\text{Total pellet volume} = \frac{4.46}{158.8} = 0.0281 \text{ ft.}^3$$

$$\therefore \text{Porosity} = \frac{0.04455 - 0.0281}{0.04455} \times 100$$

$$= 36.9 \text{ per cent}$$

Alternate measurement by filling void space with water:

Void volume = 467 cc = 28.54 $in.^3$ = 0.01652 $ft.^3$

$\therefore$ Porosity = $\frac{0.01652}{0.04455}$ x 100 = 37.1 per cent.

1/2-inch pellets

D_p = 0.5652 in.; V_p = 0.0945 $in.^3$ = 5.47 x 10^{-5} $ft.^3$

20 pellets weigh 80.8235 gms = 0.1782 lbs.

Pellet density = $\frac{0.1782}{(20)(5.47 \times 10^{-5})}$ = 162.9 lbs/ft^3

Weight of pellets in bed = 4.164 lbs.

Total pellet volume = $\frac{4.164}{162.9}$ = 0.02556 $ft.^3$

$\therefore$ Porosity = $\frac{0.04455 - 0.02556}{0.04455}$ x 100

= 42.6 per cent.

Alternate measurement by filling void space with water:

Void volume = 526 cc = 32.10 $in.^3$ = 0.01858 $ft.^3$

$\therefore$ Porosity = $\frac{0.01858}{0.04455}$ x 100 = 41.7 per cent.

APPENDIX C

TEMPERATURE CORRECTION FACTOR DETERMINATION

APPENDIX C

Table 9

Temperature Correction Factor Data

Run No.	Air lb-mol/hr-ft^2	Temp. $^\circ$F	$\Delta\theta$ min	$-\Delta W$, mg	$-\Delta W_o$ mg	$\frac{10^3}{^\circ R}$	Rate mg/cm^2-hr
1-in. orifice, 5/8-in. depth, 2-in. radius; 3 and 4* pellets (1/4-in.) per run							
1117	36.7	68.68	2.0	3.55	1.70	1.8915	12.7
1118	39.9	69.59	2.0	3.40	1.70	1.8883	11.7
1120	39.9	70.73	2.0	3.50	1.70	1.8842	12.4
1121	39.9	71.68	2.0	3.35	1.70	1.8808	11.3
1122	39.9	73.55	2.0	3.45	1.40	1.8742	14.1
1123	39.1	75.41	2.0	3.80	1.40	1.8677	16.5
1125	39.9	76.68	2.0	3.90	1.40	1.8633	17.2
1126	39.9	78.50	2.0	4.35	1.40	1.8570	20.2
1193	39.9	84.91	2.0	4.35	2.00	1.8352	21.5
1194	40.7	84.36	2.0	5.25	2.00	1.8370	29.7
1196	39.1	82.64	2.0	4.40	2.00	1.8428	22.0
1197	39.9	81.91	2.0	4.75	2.00	1.8453	25.2
1198	39.9	81.05	2.0	5.10	2.60	1.8482	22.9
1201	40.7	78.09	2.0	5.05	2.60	1.8584	22.4
1203	39.9	76.00	2.0	3.75	2.00	1.8657	16.0
1204	40.7	75.05	2.0	3.70	2.00	1.8690	15.6
1206	40.7	73.41	2.0	3.60	2.00	1.8747	14.6
1207	40.7	70.36	2.0	2.95	2.00	1.8855	8.7
2-in. orifice, 1/8-in. depth, 1/2-in. radius; 2 pellets (1/4-in.) per run							
1208	41.5	91.41	2.0	2.55	0.05	1.8135	34.3
1209	41.5	88.23	2.0	2.90	0.05	1.8241	39.1
1211	41.5	84.23	2.0	2.30	0.05	1.8375	30.9
1212	41.5	82.00	2.0	1.85	0.05	1.8450	24.7
1213	42.3	79.86	2.0	1.65	0.05	1.8523	22.0
1215	41.5	76.05	2.0	1.50	0.05	1.8655	19.9
1217	41.5	67.86	2.0	1.25	0.05	1.8944	16.5
1219	40.7	78.59	2.0	1.95	0.10	1.8567	20.6
1220	40.7	77.00	2.0	1.65	0.10	1.8622	16.5
1222	41.5	71.05	2.0	1.45	0.10	1.8831	13.7
1223	41.5	72.00	2.0	1.30	0.10	1.8797	11.7

* Runs 1117-26

Table 10

Temperature Correction Factor Calculations

$$\log C_T = \log \left(\frac{\Delta W_{80^\circ}}{\Delta W_t} \right) = -8250 \left(\frac{1}{540} - \frac{1}{T} \right) = -15.28 + \frac{8250}{T}$$

T.C., mv	t, °F	t, °R	$\frac{8250}{T}$	$\log C_T$	C_T
0.80	68.36	528.36	15.614	0.3366	2.171
0.82	69.27	529.27	15.588	0.3097	2.040
0.84	70.18	530.18	15.561	0.2830	1.919
0.86	71.09	531.09	15.534	0.2563	1.804
0.88	72.00	532.00	15.508	0.2297	1.697
0.90	72.91	532.91	15.481	0.2032	1.597
0.92	73.82	533.82	15.455	0.1768	1.502
0.94	74.73	534.73	15.428	0.1505	1.414
0.96	75.64	535.64	15.402	0.1243	1.331
0.98	76.55	536.55	15.376	0.0982	1.254
1.00	77.45	537.45	15.350	0.0725	1.182
1.02	78.36	538.36	15.324	0.0465	1.113
1.04	79.27	539.27	15.298	0.0206	1.049
1.06	80.18	540.18	15.273	-0.0051	0.988
1.08	81.09	541.09	15.247	-0.0308	0.932
1.10	82.00	542.00	15.221	-0.0564	0.878
1.12	82.91	542.91	15.196	-0.0819	0.828
1.14	83.82	543.82	15.171	-0.1073	0.781
1.16	84.73	544.73	15.145	-0.1327	0.737
1.18	85.64	545.64	15.120	-0.1580	0.695
1.20	86.55	546.55	15.095	-0.1831	0.656
1.22	87.45	547.45	15.070	-0.2079	0.620
1.24	88.36	548.36	15.045	-0.2329	0.585
1.26	89.27	549.27	15.020	-0.2579	0.552
1.28	90.18	550.18	14.995	-0.2827	0.522
1.30	91.09	551.09	14.970	-0.3075	0.493

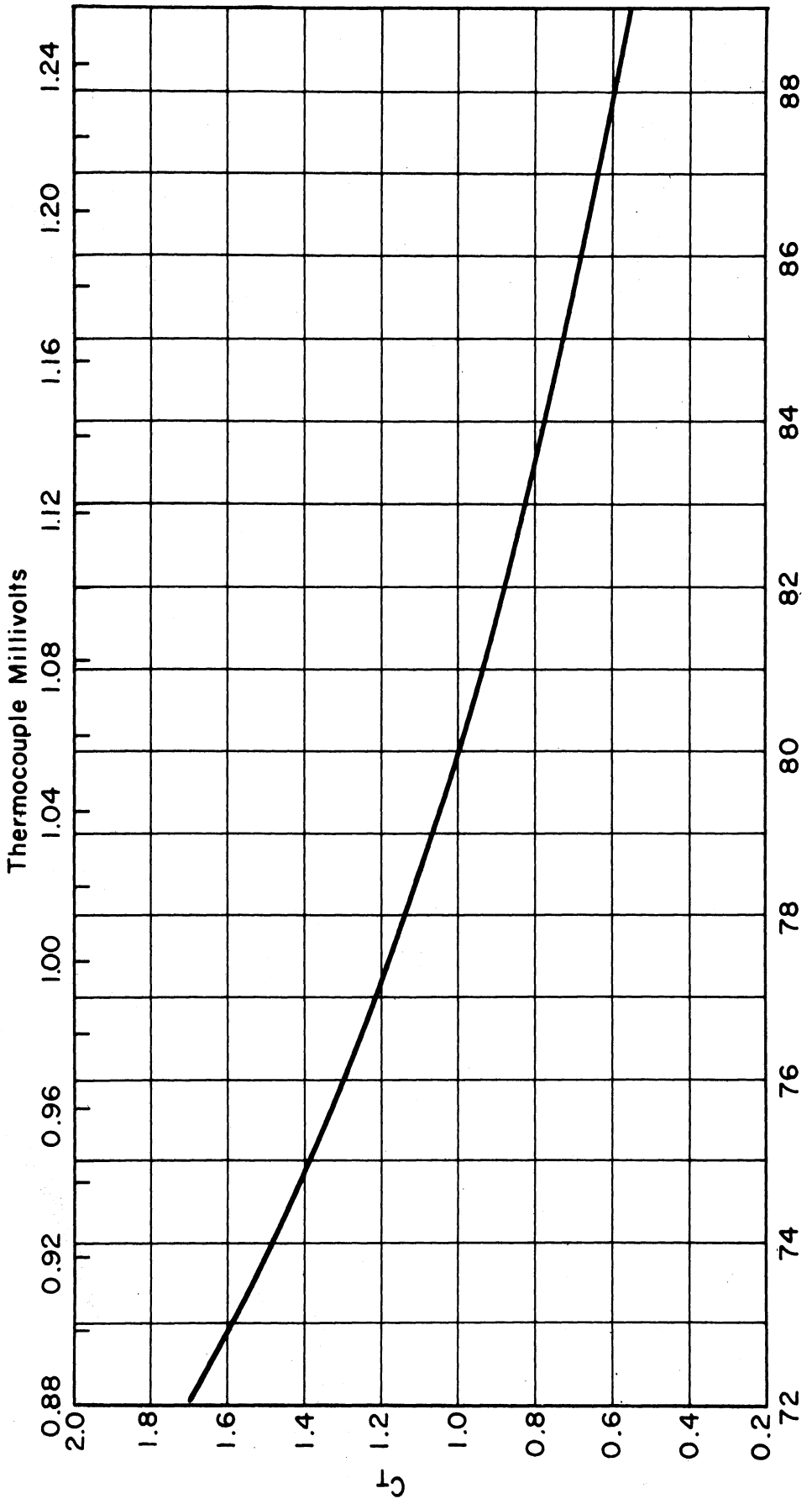

Fig.29. Temperature Correction Factor Plot.

APPENDIX D

DATA PROCESSING

APPENDIX D

Data Processing

The procedure used to process the raw data is outlined below, using data from Run No. 608 (see Figure 5, page 56).

A. The final weight is subtracted from the initial to obtain the uncorrected weight loss:

$$-\Delta W = W_i - W_f = 1071.40 - 1062.30 = 9.10 \text{ mg.}$$

B. The dry runs for the shift (Runs 610 and 615) are compared and seen to be consistent. A dry-run weight loss of 1.65 mg (Run 610) is therefore used for the run series 608-12.

C. The raw weight loss is corrected for the dry-run loss:

$$-\Delta W_d = -\Delta W - (-\Delta W_o) = 9.10 - 1.65 = 7.45 \text{ mg.}$$

D. The average thermocouple reading is found to be 1.022 millivolts, and the temperature correction factor, C_T, is obtained from Figure 29 (page 204)--1.106. Applying the temperature correction,

$$-\Delta W_t = (C_T)(-\Delta W_d) = (1.106)(7.45) = 8.24 \text{ mg.}$$

E. The pellet diameter used in this run was 1/4 inch, and four pellets were run for a period of two minutes (see top of data sheet, Figure 5). Taking the surface area of 1/4-inch active pellets as 1.086 cm^2 (Appendix B), the transfer rate is then calculated:

$$k'' = \frac{-\Delta W_t}{(n)(\theta)(A_p)} = \frac{8.24}{(4)(2/60)(1.086)} = 56.8 \text{ mg/cm}^2\text{-hr.}$$

F. k" is converted to lb-mols/ft^2-hr:

$$\frac{mg}{cm^2\text{-hr}} \left(\frac{gm}{mg}\right)\left(\frac{lb}{gm}\right)\left(\frac{1}{MW}\right)\left(\frac{cm}{in}\right)^2\left(\frac{in}{ft}\right)^2 = \frac{lb\text{-mol}}{ft^2\text{-hr}}$$

$$\therefore k' = 56.8 \left(\frac{1}{1000}\right)\left(\frac{1}{453.6}\right)\left(\frac{1}{236}\right)(2.54)^2(12)^2$$

$$= 4.93 \times 10^{-4} \text{ lb-mols/ft}^2\text{-hr.}$$

G. The rotameter reading of 80.5 corresponds to an air flow rate of 81.0 SCFM (60°F. and 1 atmosphere). This is converted to the superficial mass velocity:

$$\rho = 0.0765 \text{ lbs/ft}^3; \quad S = \pi r^2 = \pi(2/12)^2 = 0.0873 \text{ ft}^2.$$

$$\therefore G = \frac{(SCFM)(60)(\rho)}{S} = \frac{(81)(60)(0.0765)}{0.0873} = 4260 \frac{lb}{ft^2\text{-hr}}$$

$$\therefore G' = 4260/29 = 146.9 \text{ lb-mols/ft}^2\text{-hr.}$$

H. The Reynolds number is calculated, using D_p = 0.2405 in. (Appendix B) and μ = 0.0436 lbs/ft-hr (47):

$$Re = D_pG/\mu = \frac{(0.2405)(4260)}{(12)(0.0436)} = 1960$$

I. k' is divided by G' to obtain a dimensionless group which is plotted against the Reynolds number on log-log paper to yield the final correlation:

$$\frac{k'}{G'} = \frac{4.93 \times 10^{-4}}{146.9} = 3.35 \times 10^{-6}.$$

APPENDIX E

MISCELLANEOUS CALCULATIONS

APPENDIX E

Miscellaneous Calculations

I. Diffusivity and Schmidt number for p-dibromobenzene.

The diffusivity is calculated by use of the Gilliland equation (28):

$$D_G = 0.0166 \left[\frac{T^{3/2}}{P(V_a^{1/3} + V_b^{1/3})^2}\right] \sqrt{\frac{1}{M_a} + \frac{1}{M_b}}$$

Molecular weights: $p\text{-}C_6H_4Br_2 = 235.9$; $1/M = 0.00424$

$\text{Air} = 28.85$; $1/M = \underline{0.03465}$

0.03889

$$\sqrt{0.03889} = 0.1973$$

Molecular volumes: Air = 29.9;

$p\text{-}C_6H_4Br_2 = (6)(14.8) + (4)(3.7) + (2)(27) - 15 = 142.6$;

$$\sqrt[3]{29.9} + \sqrt[3]{142.6} = 3.10 + 5.225 = 8.325;$$

$$(8.325)^2 = 69.32$$

Temperature: $80°F. = 300.0°K.$; $(300)^{3/2} = 5200.$

$$\therefore D_G = \frac{(0.0166)(5200)(0.1973)}{(1)(69.32)} = \underline{\underline{0.2455 \text{ ft}^2/\text{hr}.}}$$

Schmidt number: $\mu_{air} = 0.0436$ lbs/ft-hr (47);

$$\rho_{air} \text{ at } 80°F = \left(\frac{28.85}{379}\right)\left(\frac{520}{540}\right) = 0.0735 \text{ lbs/ft}^3;$$

$$\therefore Sc = \frac{\mu}{\rho D_G} \quad \frac{0.0436}{(0.0735)(0.2455)} = \underline{\underline{2.41}}$$

II. Surface Temperature Calculation.

Since the heat needed to vaporize the solid p-dibromobenzene is transferred to the pellet from the air stream, an enthalpy balance may be written:

$$k_g(p_s^o - 0)\lambda = h(T_a - T_s) \ ,$$

where p_s^o is the vapor pressure of p-dibromobenzene at T_s. Rearranging this equation,

$$\frac{p_s{}^o}{T_a - T_s} = \frac{h}{k_g\lambda} \qquad (50)$$

h/k_g can be evaluated by applying the analogy between heat and mass transfer. Assuming the identity of the two j-factors,

$$\left(\frac{k_g M_m P}{G}\right)\left(\frac{\mu}{\rho D_G}\right)^{2/3} = j_d \cong j_h = \left(\frac{h}{C_p G}\right)\left(\frac{C_p \mu}{k}\right)^{2/3}$$

$$\therefore \frac{h}{k_g} = C_p M_m P \left(\frac{\mu}{\rho D_G}\right)^{2/3}\left(\frac{k}{C_p \mu}\right)^{2/3} = C_p M_m P (Sc)^{2/3}(Pr)^{-2/3} \qquad (51)$$

$$= (0.24)(29)(760)(1.80)(1.227) = 11{,}680 \ \frac{\text{BTU-mm Hg}}{\text{mol-}^\circ\text{F.}} \ ,$$

the values for C_p and Pr being taken from McAdams (47).

In the absence of actual data, the latent heat of sublimation of p-dibromobenzene can be approximated through the use of the Clapeyron Equation:

$$\frac{d(\ln P)}{dT} = \frac{\lambda}{RT^2} \qquad (52)$$

Using International Critical Table data for the vapor pressure, $p^\circ = 0.0158$ mm Hg at 21.0°C. and 0.0794 mm Hg at 32.8°C. Since the vapor pressure curve is essentially straight between these two points,

$$\frac{d(\ln P)}{dT} = \frac{\ln\left(\frac{0.0794}{0.0158}\right)}{(11.8)(1.8)} = \frac{1.615}{(11.8)(1.8)} = 0.076\ {}^\circ R^{-1}$$

$$\therefore \lambda = (0.076)(1.987)(540)^2 = 44{,}000 \text{ BTU/lb-mol.}$$

$$\therefore \frac{p_s^\circ}{T_a - T_s} = \frac{h}{k_g \lambda} = \frac{11{,}680}{44{,}000} = 0.2655 \frac{\text{mm Hg}}{{}^\circ R}$$

Using a vapor pressure at 80°F. of 0.038 mm Hg (37),

$$T_a - T_s = \frac{0.038}{0.2655} = \underline{\underline{0.143^\circ F}}$$

$\therefore$ The actual surface temperature is only negligibly different from the air temperature.

BIBLIOGRAPHY

BIBLIOGRAPHY

1. Aerov, M. E., and Umnik, N. N., Journal of Applied Chemistry (USSR), 23, 1071 (1950).

2. Argo, W. B., and Smith, J. M., Chemical Engineering Progress, 49, 443 (1953).

3. Arthur, J. R., and Linnett, J. W., Journal of the Chemical Society (London), 1947, 416.

4. Arthur, J. R., Linnett, J. W., Raynor, E. J., and Sington, E. P. C., Transactions of the Faraday Society, 46, 270 (1950).

5. Bedingfield, C. H., and Drew, T. B., Industrial and Engineering Chemistry, 42, 1164 (1950).

6. Bernard, R. A., and Wilhelm, R. H., Chemical Engineering Progress, 46, 233 (1950).

7. Brotz, W., Chemie-Ingenieur-Technik, 23, 408 (1951).

8. Bunnell, D. G., Irvin, H. B., Olson, R. W., and Smith, J. M., Industrial and Engineering Chemistry, 41, 1977 (1949).

9. Chernyshev, A. B., Farberov, I. L., and Pomeranchuk, A. A., Doklady Akademii Nauk, S.S.S.R., 56, 727 (1947).

10. Chilton, T. H., and Colburn, A. P., Industrial and Engineering Chemistry, 26, 1183 (1934).

11. Chilton, T. H., and Colburn, A. P., Industrial and Engineering Chemistry, 27, 255 (1935).

12. Chu, J. C., Kalil, J., and Wetteroth, W. A., Chemical Engineering Progress, 49, 141 (1953).

13. Coberly, C. A., and Marshall, W. R., Chemical Engineering Progress, 47, 141 (1951).

14. Colburn, A. P., Industrial and Engineering Chemistry, 22, 967 (1930).

15. Colburn, A. P., Transactions of the American Institute of Chemical Engineers, 29, 174 (1933).

16. Colburn, A. P., and Hougen, O. A., Industrial and Engineering Chemistry, 22, 522 (1930).

BIBLIOGRAPHY (Continued)

17. Cox, E. R., Transactions of the American Society of Mechanical Engineers, 50, 13 (1923).

18. Dreisbach, R. R., P-V-T Relationships of Organic Compounds, Handbook Publishers, Inc., Sandusky, Ohio (1952).

19. Ergun, S., Chemical Engineering Progress, 48, 89 (1952).

20. Ergun, S., Chemical Engineering Progress, 48, 227 (1952).

21. Evans, G. C., and Gerald, G. F., Chemical Engineering Progress, 49, 135 (1953).

22. Fick, A., Annalen der Physik, 94, 59 (1855).

23. Forstall, W., and Shapiro, A. H., Journal of Applied Mechanics, 17, 399 (1950).

24. Furnas, C. C., U. S. Bureau of Mines, Bulletin No. 307 (1929).

25. Gaffney, B. J., and Drew, T. B., Industrial and Engineering Chemistry, 42, 1120 (1950).

26. Gamson, B. W., Chemical Engineering Progress, 47, 19 (1951).

27. Gamson, B. W., Thodos, G., and Hougen, O. A., Transactions of the American Institute of Chemical Engineers, 39, 1 (1943).

28. Gilliland, E. R., Industrial and Engineering Chemistry, 26, 681 (1934).

29. Graton, L. C., and Fraser, H. J., Journal of Geology, 43, 785 (1935).

30. Hall, R. E., and Smith, J. M., Chemical Engineering Progress, 45, 459 (1949).

31. Hinton, A. G., quoted by H. M. Spiers, "World Power Conference, London, 1928, Technical Data on Fuel", p. 101, World Power Conference (1928).

32. Hobson, M., and Thodos, G., Chemical Engineering Progress, 45, 517 (1949).

33. Hobson, M., and Thodos, G., Chemical Engineering Progress, 47, 370 (1951).

34. Hsu, C., Dissertation Abstracts, 13, 207 (1953).

BIBLIOGRAPHY (Continued)

35. Hughes, M. L., Journal of the Iron and Steel Institute (London), 156, 371 (1947).

36. Hurt, D. M., Industrial and Engineering Chemistry, 35, 522 (1943).

37. International Critical Tables, Volume III, McGraw-Hill Book Company, New York (1928).

38. Ishino, T., and Otake, T., Technology Reports of the Osaka University, 2, 123 (1952).

39. Kaufman, D. J., and Thodos, G., Industrial and Engineering Chemistry, 43, 2582 (1951).

40. Kinney, S. P., U. S. Bureau of Mines, Technical Paper No. 442 (1929).

41. Linton, W. H., and Sherwood, T. K., Chemical Engineering Progress, 46, 258 (1950).

42. Maeda, S., Technology Reports of the Tohoku University, 16, No. 2, 1 (1952).

43. Maeda, S., and Kawazoe, K., Chemical Engineering (Japan), 17, 276 (1953).

44. Maisel, D. S., and Sherwood, T. K., Chemical Engineering Progress, 46, 131 (1950).

45. Maxwell, J. C., The Philosophical Magazine, 35, 199 (1868).

46. Mayo, F., Hunter, T. O., and Nash, A. W., Journal of the Society of Chemical Industry (London), 54, 376 (1935).

47. McAdams, W. H., Heat Transmission, McGraw-Hill Book Company, New York (1942).

48. McCune, L. K., and Wilhelm, R. H., Industrial and Engineering Chemistry, 41, 1124 (1949).

49. Morales, M., Spinn, C. W., and Smith, J. M., Industrial and Engineering Chemistry, 43, 225 (1951).

50. Morris, F. H., and Whitman, W. G., Industrial and Engineering Chemistry, 20, 234 (1928).

51. Perry, J. H., Chemical Engineers' Handbook, McGraw-Hill Book Company, New York (1950).

BIBLIOGRAPHY (Continued)

52. Powell, R. W., Transactions of the Institution of Chemical Engineers (London), 18, 36 (1940).

53. Prandtl, L., Zeitschrift für Physik, 11, 1072 (1910).

54. Pratt, H. R. C., Transactions of the Institution of Chemical Engineers (London), 28, 177 (1950).

55. Ranz, W. E., Chemical Engineering Progress, 48, 247 (1952).

56. Resnick, W., and White, R. R., Chemical Engineering Progress, 45, 377 (1949).

57. Reynolds, O., Papers on Mechanical and Physical Subjects, Volume I, Cambridge University Press (1900).

58. Saunders, O. A., and Ford, H., Journal of the Iron and Steel Institute (London), 141, 291P (1940).

59. Saunders, H. L., and Wild, R., Journal of the Iron and Steel Institute (London), 154, 73P (1946).

60. Schuler, R. W., Stallings, V. P., and Smith, J. M., Chemical Engineering Progress Symposium Series, 48, No. 4, Reaction Kinetics and Transfer Processes, 19 (1952).

61. Schwartz, C. E., and Smith, J. M., Industrial and Engineering Chemistry, 45, 1209 (1953).

62. Sherwood, T. K., and Petrie, J. M., Industrial and Engineering Chemistry, 24, 736 (1932).

63. Shulman, H. L., and DeGouff, J. J., Industrial and Engineering Chemistry, 44, 1915 (1952).

64. Stefan, J., Sitzungberichte der Akademie der Wissenschaften in Wein, 68, 403 (1873).

65. Taecker, R. G., and Hougen, O. A., Chemical Engineering Progress, 45, 188 (1949).

66. Taylor, G. I., British Advisory Committee for Aeronautics, Reports and Memoranda, No. 272 (1916).

67. Wilke, C. R., and Hougen, O. A., Transactions of the American Institute of Chemical Engineers, 41, 445 (1945).

68. Zil'berman-Granovskaya, A. A., and Shugam, E. A., Zhurnal Fizicheskoi Khimii, 14, 1004 (1940).

NOMENCLATURE

NOMENCLATURE

A	area, ft^2
a	square feet of transfer area per cubic foot of bed volume, ft^{-1}
B	variable in the correlating equations, dimensionless
C_p	heat capacity at constant pressure, BTU/lb-°F
C_T	temperature correction factor, dimensionless
D	diameter, ft
D_G	molecular diffusivity, ft^2/hr
f	friction factor, dimensionless
G	superficial mass velocity, based on empty cross-section, lbs/ft^2-hr
H	bed depth, ft
h	heat-transfer coefficient, BTU/ft^2-hr-°F
HTU	height of a transfer unit, ft
j	Colburn factor for heat and mass transfer = f/2, dimensionless
j_d	Colburn factor for mass transfer = $(k_g M_m P/G)(Sc)^{2/3}$, dimensionless
j_h	Colburn factor for heat transfer = $(St)(Pr)^{2/3}$, dimensionless
k	thermal conductivity, BTU/ft^2-hr-(°F/ft)
k'	mass-transfer rate, $lb\text{-}mols/ft^2$-hr
k''	mass-transfer rate, mg/cm^2-hr
k_g	mass-transfer coefficient, $lb\text{-}mols/ft^2$-hr-mm Hg
m	variable exponent in the correlating equations, dimensionless
M	molecular weight, dimensionless

N	mass-transfer rate, lbs/hr
n	number of active pellets per run; also number of transfer units in Equation 5
P	pressure, mm Hg
p	partial pressure, mm Hg
Pr	Prandtl number, $C_p\mu/k$, dimensionless
R	Gas Law Constant, consistent dimensions
r	radius, ft
Re	Reynolds number, D_pG/μ, dimensionless
S	cross-sectional area of bed, ft^2
Sc	Schmidt number, $\mu/\rho D_G$, dimensionless
St	Stanton number, h/C_pG, dimensionless
T	absolute temperature, ^oR
V	volume, ft^3
W	weight, lb_M
x	distance in the direction of transfer, ft
Δ	finite difference (state 2 minus state 1)
ϵ	fractional void volume or porosity, dimensionless
θ	time, minutes
λ	latent heat of sublimation, BTU/lb-mol
μ	viscosity, lbs/ft-hr
ρ	density, lbs/ft^3
φ	Gamson shape factor, dimensionless

Superscripts

'	molal units
^{o}	vapor pressure

Subscripts

a	air
d	corrected for "dry run"
f	final; also film conditions
g	non-transferring component
i	initial
lm	logarithmic mean
m	mean
o	zero velocity
p	pellet
s	surface
t	corrected for temperature
v	transferring component

Abbreviations

CFM	cubic feet per minute
lb_M	pound mass
ln	natural logarithm, base e
log	common logarithm, base 10
SCFM	standard cubic feet per minute (at 60°F and 1 atmosphere)
$<$	less than
$>$	greater than
$\geq$	equal to or greater than
$\cong$	approximately equal to